

https://dspace.org/

The effects of RU486, used as a postcoital contraceptive, on the rat uterus during early pregnancy

Theron, Kathrine Elizabeth

2011-03-09
http://hdl.handle.net/10539/9128

Downloaded from a DSpace repository. https://dspace.org/

CHAPTER 1

GENERAL INTRODUCTION

1.1 Emergency Contraception

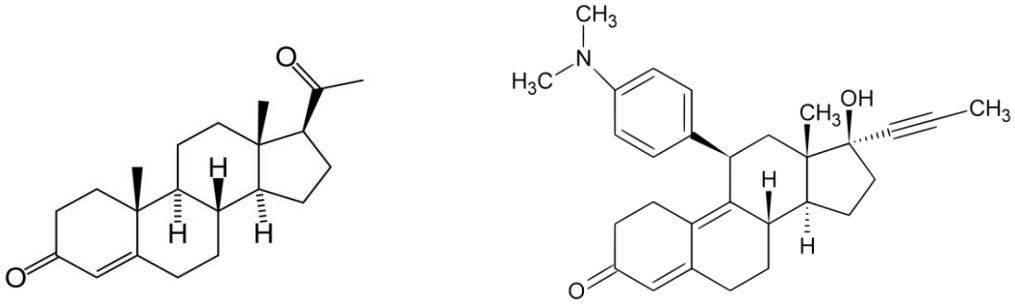
The term 'Emergency Contraception (EC)' is defined by The World Health Organisation (WHO) as 'those back-up methods for contraceptive emergencies which women can use within the first few days after unprotected sexual intercourse, or in the event of potential contraceptive failure to prevent an unwanted pregnancy (http://www.who.int/mediacentre/factsheets/fs244/en/index.html). These contraceptives include all methods acting after intercourse, but prior to implantation (Bastianelli *et al.*, 2008). Currently, the two most commonly used EC regimes are the Yuzpe regime, consisting of an initial dose of oestrogen followed by a dose of levonorgestrel 12 hours later (Yuzpe *et al.*, 1974), and the levonorgestrel regime, consisting of two doses of levonorgestrel taken 12 hours apart (World health organisation task force on postovulatory methods of fertility regulation, 1998; Devoto *et al.*, 2005). The efficacy of these regimes is highest 72 hours postcoitum and diminishes with an increase in the coitus-to-treatment interval up to 120 hours (von Hertzen *et al.*, 2002; Devoto *et al.*, 2005). The shortfall of these ECs, however, is that they are effective only prior to blastocyst implantation and are incapable of preventing the establishment of ongoing pregnancy (Cheng *et al.*, 2004; Ortiz *et al.*, 2004).

Alternatively, Progesterone Receptor Modulators (PRMs), modulate the cellular and physiological environment and interfere with implantation and early pregnancy (Banaszak *et al.*, 2000; Chabbert-Buffet *et al.*, 2005). Such antiprogestins include Mifepristone (RU486), Onapristone (ZK98299), Asoprisnil (J867) and Ulipristal (VA2914) (for a review see Chabbert-Buffet *et al.*, 2008). Recent clinical studies have demonstrated that a single dose of 600mg of RU486 administered within 72 hours postcoitum was more efficient at preventing pregnancy than the Yuzpe regime. In addition, the incidence of side-effects, such as nausea, vomiting and headaches, was lower with RU486 than the Yuzpe regime (Glasier *et al.*, 1992; Webb *et al.*, 1992). Further studies on RU486 indicate that a dose as low as 10mg is effective as an emergency contraceptive (Cheng *et al.*, 1999; Jin *et al.*, 2005). A small dose, 10mg, of Mifepristone was as effective as a 750mg dose of levonorgestrel and more effective than the Yuzpe regime in preventing pregnancy following unprotected intercourse (Jin *et al.*, 2005). In addition, RU486 was demonstrated to be consistently effective up to 120 hours after unprotected sexual intercourse, unlike the two previously described EC regimes which diminished in efficacy from 72 hours postcoitum (World health organisation task force on postovulatory methods of fertility regulation, 1999; Xiao *et al.*, 2002).

Mifepristone as an EC is not widely used due to its status as an abortion drug and the associated controversy. While it is currently only available in a few countries in this capacity, such as China (Chabbert-Buffet *et al.*, 2008), the WHO has contributed substantially to the development of RU486 as a hormonal EC throughout the world (World health organisation task force on postovulatory methods of fertility regulation, 1999; Jin *et al.*, 2005).

1.2 The Progesterone Receptor Modulator, RU486

RU486 or Mifepristone (marketed as Mifegyne or Mifeprex) (Snyman, 2006) is a synthetic, steroidal, progesterone receptor modulator (PRM) (Figure 1.1) first discovered in 1980 by researchers at the Roussel Uclaf Institute in France (Goldberg *et al.*, 1998). Initially RU486 was used for medical termination of intrauterine pregnancies. To date, RU486 is approved in several countries, including South Africa, for use in; medical termination of early pregnancy, softening and dilatation of the cervix prior to surgical termination of pregnancy, use in combination with the prostaglandin, gemeprost, for second trimester pregnancy termination and labour induction in foetal death during the third trimester. Although it has been shown to be highly effective as an EC, the mechanism of action of RU486 when used as an emergency contraceptive remains unknown. However, RU486 is able to inhibit the attachment of a human blastocyst to an *in vitro* endometrial three-dimensional cell culture model (Lalitkumar *et al.*, 2007). The inhibition of blastocyst implantation was not possible with the levonorgestrel emergency contraception regime (Lalitkumar *et al.*, 2007).



Progesterone RU486

Figure 1.1 Geometric isomers of the steroid hormone progesterone and the antagonist RU486 (Szyczewski *et al.*, 2004; Chabbert-Buffet *et al.*, 2008).

RU486 [1β-(4-dimethylamino phenyl)-17β-hydroxy-17α-(prop-1-ynyl)-estra-4, 9-diene-3-one], a derivative of norethindrone, is a potent progesterone (PR) and glucocorticoid receptor (GR) antagonist. It has a 10-fold higher affinity for the PR than progesterone itself. RU486 also binds weakly to the androgen receptor (AR). It is not able to bind to the mineralocorticosteroid receptors and was initially thought that it was unable to bind to the oestrogen receptor (ER) (Baulieu, 1991; Sarkar, 2002); however, recent reports have suggested weak binding of RU486 to ERs (Jeng *et al.*, 1993; Dibbs *et al.*, 1995).

1.2.1 Mode of action of RU486

1.2.1.1 Overview of the Progesterone Receptor (PR)

Progesterone (P) signalling is mediated by the progesterone receptors (PRs); ligand-activated transcription factors that are members of the superfamily of DNA-binding receptors, comprised of four well-defined functional domains: the N-terminal transcription domain, the centrally located DNA binding domain (DBD), the hinge region and the highly conserved C-terminal ligand binding domain (LBD) (Figure 1.2) (Baulieu, 1991; Leonhardt and Edwards, 2002; Sarkar, 2002). The PR exists in two different forms; namely, isoform PR-A, a 94kDa protein and isoform PR-B, a 120kDa protein (Conneely *et al.*, 1989; Kastner *et al.*, 1990; Kraus and Katzenellenbogen, 1993). Although the two forms of PR have similar steroid hormone and DNA binding activities, they have been shown to demonstrate different cell and gene specificities in their transcriptional activities (Mulac-Jericevic *et al.*, 2000; Mulac-Jericevic *et al.*, 2003).

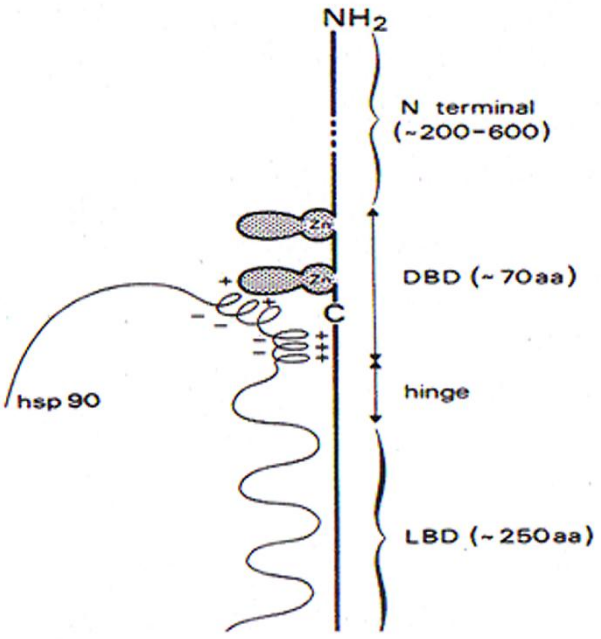


Figure 1.2 The four functional domains of the progesterone receptor. DBD: DNA binding domain; LBD: Ligand binding domain; hsp90: Heat shock protein 90. (Baulieu, 1991).

The DBD consists of approximately 70 amino acids that make up two type II 'zinc finger' structures of invariant cysteine repeats with four cysteines in each finger that facilitate binding of the receptor to specific DNA sequences. The LBD consists of approximately 250 amino acids at the C-terminal end of the molecule. The LBD contains an additional transactivation domain (AF2) which is not only responsible for binding to the hormone; but, is also responsible for interactions with the heat shock protein (hsp90), hormone-dependent transactivation and co-activator recruitment, as well as receptor dimerisation (Pratt *et al.*, 1988; Fawell *et al.*, 1990; Baulieu, 1991; Freedman, 1992; Vegeto *et al.*, 1992).

PRs are located in the cytosol of the target cells bound to a heat-shock protein of molecular weight 90kDa (hsp90). Once in the target cells, cytosolic P binds to PR, forming a complex (P + PR + hsp90). As this complex enters the nucleus of the cell, hsp90 binds to the nuclear protein p59 (forming a complex: P + PR + hsp90 + p59), which causes the receptor complex to become positively charged, resulting in detachment of the hsp90 + p59 complex from the receptor (Figure 1.3). This new hormone-receptor complex (P + PR) binds to the hormone response element in the promoter region of the regulated gene, via the DBD (Mahajan and London, 1997). Ultimately, this changes the nucleosomal conformation, with subsequent binding of a transcription factor and initiation of transcription (Mahajan and London, 1997).

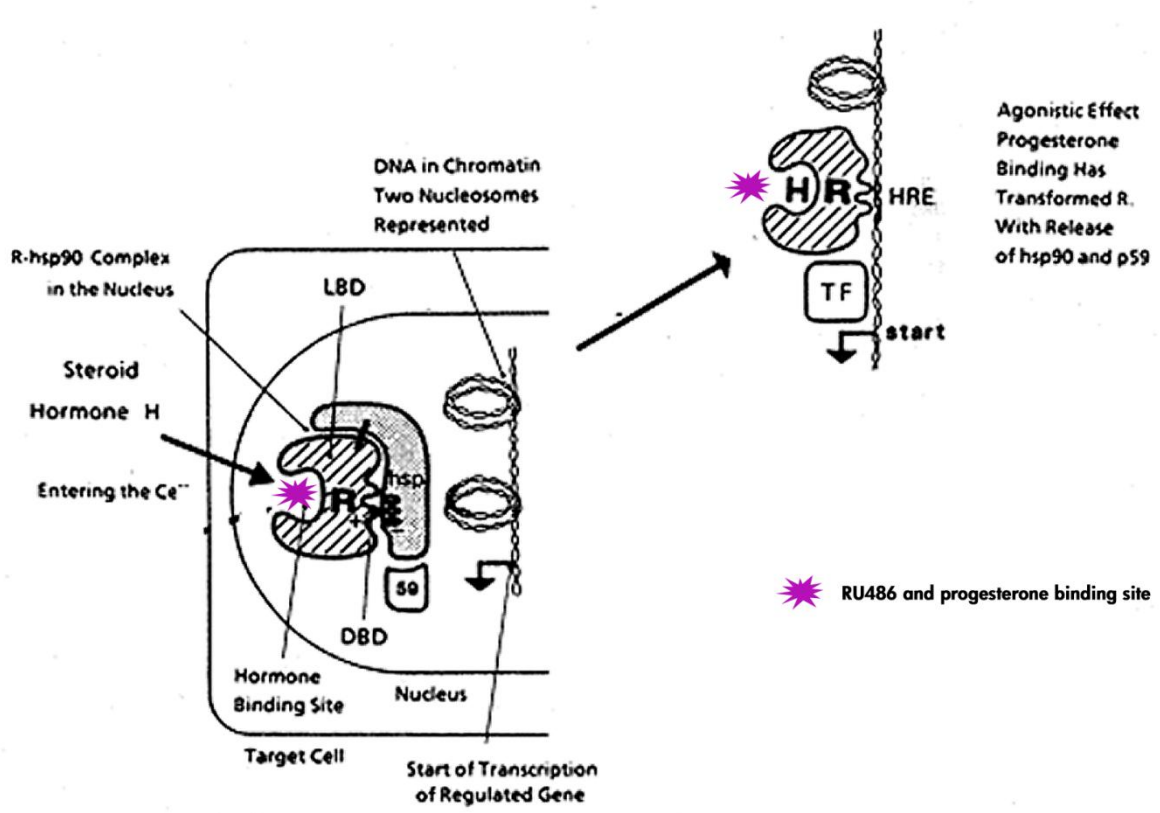


Figure 1.3 Activation of the progesterone receptor by progesterone (modified from Baulieu, 1991).

1.2.1.2 RU486 and the PR

Binding of both P and RU486 to PR generates conformational changes in PR that ultimately permits it to bind to DNA. Binding of P or RU486 and thus the activation of PR is associated with a loss of the heat shock proteins as described above, as well as dimerisation of the positively charged P + PR complex (Sarkar, 2002). The binding of P to PR increases the transcription of P-dependent genes, as the PR dimer is then able to bind to specific DNA sequences within the promoter region of genes responsive to progesterone, thus producing P-related effects. These regions are referred to as progesterone response elements (PREs). In contrast, a receptor complex activated by RU486 results in

an inhibitory function in the C-terminal region of the LBD (Figure 1.3). This inhibitory function renders the DNA-bound receptor transcriptionally inactive (Mahajan and London, 1997; Liu *et al.*, 2002; Sarkar, 2002).

PRMs are PR ligands that exhibit agonist, antagonist and mixed agonist/antagonist effects in progesterone target tissues in a cell- and tissue-specific dependent manner (Smith and O'Malley, 2004). RU486 was previously thought to be a pure progesterone antagonist (PA) because of the results obtained from the McPhail test, which determines a compound's progestational activity by assessing the degree of endometrial proliferation and transformation in immature rabbits primed with oestrogen, prior to administration of the substance to be tested (Elger *et al.*, 2000). Subsequent studies, however, have indicated that RU486 acts as a marginal agonist (Spitz and Chwalisz, 2000), for instance, in the MDA-MB-231 breast cancer cell line engineered to express the two forms of PR, PR-A or PR-B, or both. Here, RU486 demonstrated an agonist effect by inhibiting cell growth through PR-A and PR-B (Leo and Lin, 2008). With regards to cell morphology within this breast cancer cell line, RU486 exhibited an antagonist effect through PR-A and an agonist effect through PR-B (Leo and Lin, 2008). In addition, in the presence of protein kinase A activators, such as 8-Br-cAMP, RU486 was converted to a progesterone agonist in the T47D mammary tumour cell model (Attardi *et al.*, 2002).

It was previously thought that pure progesterone antagonists (PAs), which completely antagonise PR function, were unable to bind to the PREs, whereas PRMs were able to bind (Klein-Hitpass *et al.*, 1991). The current paradigm states that although pure PAs are able to bind to PREs, the conformational change that they promote is nevertheless distinct from that induced by the PRMs (Gass *et al.*, 1998). Liu *et al.* (2002) observed a difference in the action of RU486 within two cell lines, as RU486 acted as an agonist in T47D cells and as an antagonist in HeLa cells. This led them to investigate the molecular basis for this difference in RU486 effects using varying concentrations of co-activator and co-repressor ratios in a cell-free chromatin transcription system (Liu *et al.*, 2002); as well as the action of RU486 under these conditions and the hypothesis that the ability of RU486 to activate transcription in different cell and tissue types depends on the relative amount of co-activators or co-repressors within the specific environment (Figure 1.4) (Liu *et al.*, 2002).

RU486 has a prolonged metabolic half-life of approximately 20-30 hours in humans and 4 hours in rats and thus effectively excludes the corresponding agonist (progesterone) for receptor binding to the receptors. RU486 is metabolised by the liver and is eliminated primarily through the digestive tract. The resulting metabolites of RU486, like progesterone, are able to bind to the PR, effectively limiting, or preventing progesterone effects in the target cells. The agonist progesterone, if not quickly

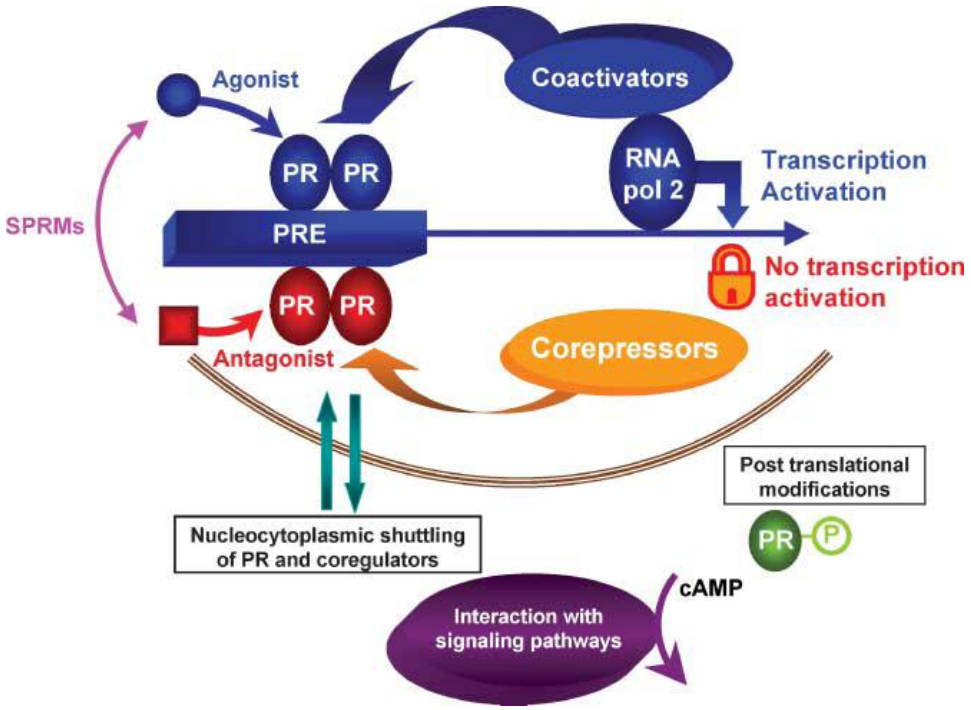


Figure 1.4 Progesterone receptor (PR) activation by progesterone receptor ligands. A conformational change on the inactive receptor complex is induced upon binding of progesterone. This leads to dissociation of the heat shock protein 90 (hsp90), dimerisation of the receptor, DNA binding and subsequent recruitment of co-activators, such as steroid receptor co-activator (SRC) and CBP, to aid in communication with the basal transcription apparatus RNA POL2 (RNA polymerase). Progesterone antagonists (PAs) compete for binding with the agonist for PR, promoting dimerisation and binding to the specific progesterone response element (PRE) of the target DNA. PAs result in an altered conformational change in PR, rendering it transcriptionally inactive and resulting in a non-productive interaction of the recptor with DNA. This is as a result of PR recruitment of co-repressors, such as nuclear receptor co-repressor (NcoR) and silencing mediator of retinoic acid and thyroid hormone receptor (SMRT), instead of co-activators (Chabbert-Buffet *et al.*, 2005).

bound to the PR, is either rapidly eliminated from the target cells, or metabolised *in situ* (Mahajan and London, 1997; Sitruk-Ware and Spitz, 2003).

1.2.1.3 RU486 Effects on the Endometrium

The efficacy of RU486 used as a postcoital contraceptive was established in a study in adolescents who had unprotected sexual intercourse, requested an emergency contraceptive and were administered 600mg of RU486 (Glasier *et al.*, 1992). Of the 402 adolescents treated with RU486, no pregnancies ensued as compared to 4 pregnancies out of 398 subjects treated with a combination of ethinyl oestradiol and norgestrel (Glasier *et al.*, 1992). Further studies have demonstrated that a low dose of RU486 (10mg) is as effective as an emergency contraceptive as the higher dose (World health organisation task force on postovulatory methods of fertility regulation, 1999; Xiao *et al.*, 2002).

Since PRs are predominantly found in the reproductive organs, RU486 exacts its effect mainly within the uterus (Weiss, 1993). By binding to PRs and blocking the effects of natural progesterone on the endometrium, RU486 administration during early pregnancy, post-implantation, halts the development of the secretory endometrium, leading to ultrastructural changes of the decidual capillaries in the endometrium, vascular damage, bleeding, decidual necrosis, detachment and exclusion of the implanted blastocyst (Van Look and Bygdeman, 1989). RU486 administration prior to blastocyst implantation results in the degeneration and shedding of the endometrial lining, thus preventing the implantation of the blastocyst (Couzinet *et al.*, 1986).

When administered during the follicular phase of the menstrual cycle, RU486 is able to effectively, although reversibly, suppress folliculogenesis and ovulation, but has no effect on the endometrial development during the implantation period (Stuenkel *et al.*, 1990). RU486 treatment following selection of the dominant follicle for release during ovulation is able to interrupt normal follicular development and prolong the menstrual cycle, significantly inhibiting endometrial development (Liu *et al.*, 1987; Shoupe *et al.*, 1987; Danielsson *et al.*, 1997).

1.3 Early Pregnancy

1.3.1 Blastocyst implantation

Although the mode of blastocyst implantation varies greatly among mammalian species, certain conditions, necessary for successful implantation, are common to all types of implantation: the fertilised ovum must have reached the blastocyst stage by this time and the precise preparation of the uterus by the ovarian hormones must have attained optimal receptivity. Thus, the accurate correlation between development of the blastocyst and receptivity of the endometrium is vital for successful implantation (Murphy, 1998).

In most mammalian species, the embryo arrives in the uterus at the morula stage and develops into a blastocyst within the uterus. In humans, this blastocyst stage is reached at around day 4 of pregnancy while in the rat this occurs at around day 3.5 of pregnancy (Enders and Schlafke, 1967). This development from the one cell stage to the blastocyst stage usually takes place within the non-adhesive zona pellucida, which surrounds the developing embryo. The non-adhesive nature of the zona pellucida most likely functions to ensure that the developing embryo is transported successfully through the uterine tube and into the uterus (Carson *et al.*, 2000). By around day 5 of pregnancy, just prior to implantation, most blastocysts lose their zona pellucidae, but remain unimplanted (Enders and Schlafke, 1967).

The subsequent implantation of the blastocyst occurs in three consecutive phases; including, apposition, adhesion and invasion (Carson *et al.*, 2000). In the rat, where the day of mating is designated day 0.5 of pregnancy, apposition of the trophectoderm to the luminal epithelium is accompanied by luminal closure of the uterus on day 4.5, irreversible blastocyst attachment on day 5.5, with penetration of the luminal epithelium beginning on day 6.5 of pregnancy (Carson *et al.*, 2000; Tassell *et al.*, 2000).

1.3.2 The window of receptivity

It is well-known that the blastocyst can attach to a number of sites outside the uterus, for example, the peritoneal membrane of the abdominal cavity, the ovary, the fimbria of the uterine tube and the uterine tube itself, as well as to various different artificial sites. However, the blastocyst is only able to attach to the endometrium of the uterus – the natural tissue of attachment – under highly specialised conditions (Carson *et al.*, 2000; Wang and Dey, 2006). This occurs during a very narrow range of time, known as the 'window of receptivity'. The term 'receptivity' describes the physiological and structural stage of the endometrium in which such specific attachment and implantation takes place (Psychoyos, 1986). Even though the uterus is the only site in which the blastocyst cannot attach ubiquitously, it is the only site in which a blastocyst can develop to form a fully formed complex organism (Murphy, 1995; Carson *et al.*, 2000).

1.3.3 Ovarian hormonal control

The 'window of receptivity' is under the strict control of the ovarian hormones, progesterone and oestrogen with oestrogen being the dominant ovarian hormone during oestrous and the first few days of pregnancy. This period is followed by at least 48 hours of progesterone control, at the end of which a very low dose of oestrogen initiates implantation of the blastocyst (Psychoyos, 1970).

The ovarian hormones act to initiate implantation by inducing an essential series of uterine epithelial cell changes necessary for successful implantation. These include ultrastructural changes as

demonstrated by Psychoyos, Ljungkvist, and Murphy, amoung others, over the last few decades (for a review see Murphy, 2000a); biochemical changes as reviewed by Paria *et al.* (2000; 2002), Lim *et al.* (2002), and Wang and Dey, (2006), and more recently, changes in patterns of gene expression (for a review see Reese *et al.*, 2008 and references within). In a novel study by Cowell (1969) it was found that the blastocyst of the mouse was able to implant at any stage of pregnancy provided the uterine epithelium was damaged, indicating that the uterine epithelial cells act as a barrier to ubiquitous attachment and implantation of the blastocyst within the uterus. Conversely, conditioning of the uterus by ovarian hormones was necessary for the successful implantation of a blastocyst when the uterine epithelium was intact (Murphy and Shaw, 1994). The main ovarian hormone acting on the endometrium during early pregnancy in order to establish this precise priming of the uterus for blastocyst implantation is progesterone (Psychoyos, 1970; Murphy, 2004).

1.4 RU486 and Early Pregnancy

As mentioned above, progesterone is the key hormone responsible for the establishment of the window of receptivity and since RU486 binds to PRs, it blocks progesterone binding and subsequent signalling to the uterine cells. It follows that the various stages of endometrial priming by progesterone will be inhibited by the PRM, RU486. RU486 is well established as an abortificant and an emergency contraceptive (for a review see Sarkar, 2002); however, the exact effects RU486 has on the endometrium by blocking this progesterone signalling during early pregnancy is currently under investigation.

The overall aim of this study was to better elucidate the mechanisms of the action of RU486, at a cellular and molecular level, used as a postcoital contraceptive to successfully prevent implantation of a viable blastocyst and subsequent pregnancy. In addition, the aim was to assess the effects of a PR partial blocker on the endometrium during early pregnancy and in so doing, evaluate the importance and define the function of progesterone and PR in the implantation of a viable blastocyst and subsequent pregnancy. More specifically:

i) Since RU486 binds to and prevents PRs from transducing its signals to the endometrium, the cellular transformations for implantation are disrupted. These effects of RU486 on the cells of the endometrial compartments are investigated here at an ultrastructural level;

ii) As the uterine epithelial cells are the target of progesterone signalling, the effects of RU486 treatment on both progesterone recptor localisation and gene expression are documented during early pregnancy;

iii) Normally, in preparation for implantation, the endometrium undergoes proliferation. However, as RU486 blocks progesterone binding to the uterine cells, this phase of cell growth is likely inhibited. Hence the susceptibility of the uterine epithelial cells to undergo apoptosis is investigated, specifically localisation and gene expression profiles of the apoptotic inducer, Bax, and apoptotic inhibitor, Bcl-2;

iv) The growth, development and regression of blood vessels are a fundamental part of implantation and the maintenance of pregnancy. Here, the role of RU486 as an anti-angiogenic agent is assessed with regards to the patterns of cellular localisation and gene expression of Vascular Endothelial Growth Factor (VEGF), basic Fibroblast Growth Factor (bFGF) and Platelet-derived Growth Factor (PDGF), respectively, these being critical mediators of the angiogenic cascade;

v) As RU486 inhibits the receptivity of endometrial cells to progesterone, this affects the normal molecular and cellular patterns of gene and protein expression required for uterine receptivity to implantation. Here, probable changes in the spatial localisation and gene expression levels of known the endometrial receptivity markers, Leukaemia Inhibitory Factor (LIF), Mucin 1 (Muc-1) and Calcitonin are evaluated after RU486 treatment.

CHAPTER 2

MATERIALS AND METHODS

2.1 Animals

The study was approved by the Animal Ethics Committee of the University of the Witwatersrand, clearance number: AEC2005/38/3). Thirty-six adult, virgin female inbred Hooded Wistar rats (12-14 weeks of age and weighing ± 200 g) were obtained from the Central Animal Unit at the University of the Witwatersrand. Animals were maintained in temperature-controlled quarters at 23 ºC, with a 12-hour light-dark cycle and received rat pellets (Epol, Pretoria West, RSA) and water *ad libitum.* Daily vaginal smears of each animal were used to confirm normal oestrous cycling and for the identification of the pro-oestrous stage of the oestrous cycle, for purposes of mating. The smears were fixed in alcohol and stained with Shorr's stain (Appendix A) (Humason, 1979), dehydrated through a graded series of alcohols and mounted in Entellan (Merck, Whitehouse Station, NJ, USA). Staging of the oestrous cycle was according to Gordon (1977). Pregnancy was achieved by overnight mating of pro-oestrous females with males of proven fertility. The presence of a vaginal plug, as well as sperm in the vaginal smear taken the following morning was used to confirm successful mating and this was designated as day 0.5 of pregnancy.

2.2 Treatment Regime

In order to examine the cellular and molecular, biological associated changes in uterine progesterone effects in response to the postcoital contraceptive drug, RU486 (Sigma-Aldrich, St. Louis, MO, USA), rats on day 3 of pregnancy were injected subcutaneously with either vehicle (peanut oil) (n=18), or RU486 (n=18) (Appendix A). Tissue was retrieved on day 4.5 (Group 1), 5.5 (Group 2) and 6.5 (Group 3) of pregnancy, respectively. Each group of 12 rats consisted of six control and six experimental animals chosen at random.

Animals were anaesthetised on the designated day of pregnancy with an intraperitoneal injection of Rompin-Ketamin (1:4) (Appendix A) (Centaur Labs, Bryanston, Johannesburg, RSA). Once the animals had been anaesthetised, and a ventral midline incision made, 1 ml of 1 % Pontamine Sky blue dye (Appendix A) (BDH Chemical Supplies, Poole, England, United Kingdom) solution, an indicator of decidualisation, was injected into the inferior vena cava, to aid in visualising tissue oedema (Psychoyos, 1973). After circulation through the bloodstream for approximately 15 minutes, both uterine horns were excised and the rats killed by exsanguination. One uterine horn was cut into implantation and non-implantation sites respectively, and processed for scanning electron microscopy, transmission electron microscopy, and light microscopy, respectively (see details below). Next, the other uterine horn was placed into a 1% saline solution (Appendix A) and the blastocysts flushed out

using a syringe filled with 1% saline solution. The uterine horn was then cut into implantation and non-implantation sites and these placed individually into RNAlater (Sigma-Aldrich, St. Louis, MO, USA), or flash frozen in liquid nitrogen for subsequent RNA extraction.

The implantation sites were distinguished from the non-implantation sites by prominent blue bands of the aforementioned Pontamine Sky blue dye solution. Such blue bands were, however, not always evident in the 4.5 day pregnant rats. In such cases, areas in which the blood vessels appeared aggregated were taken as implantation sites, while areas in which little vessel aggregation was visible were taken as non-implantation sites.

2.3 Characterisation of Surface Ultrastructural Changes in the RU486-Treated Rat Uterus

This section describes the use of Scanning Electron Microscopy (SEM) and Transmission Electron Microscopy (TEM) to assess any changes in the ultrastructure of the rat uterus at days 4.5, 5.5 and 6.5 of pregnancy in control pregnant and RU486-treated animals, respectively.

As mentioned above, uterine samples were divided into the implantation and non-implantation sites at days 4.5, 5.5 and 6.5 of pregnancy, following treatment with RU486 or vehicle and prepared for either SEM or TEM. These samples were then viewed under a Scanning Electron Microscope or a Transmission Electron Microscope.

2.3.1 Scanning electron microscopy

2.3.1.1 Tissue Preparation

The method used to prepare the tissue for scanning electron microscopy was adapted from (Adams *et al.*, 2002). A segment of the uterine horn containing two implantation and two non-implantation sites was placed in 2.5 % gluteraldehyde (SPI-Chem, West Chester, PA, USA) in phosphate buffer (PO_4 buffer), pH 7.2 (Appendix A) and pinned out to their *in vivo* length for 10 minutes. After this initial fixation step, the tissue was dissected along the mesometrial border and pinned open in the buffered 2.5 % gluteraldehyde for a further 50 minutes at room temperature. The uterine horn was then subsequently divided into implantation and non-implantation sites and rinsed in PO_4 buffer for 3 immersions of 5 minutes each and post-fixed in 2 % osmium tetroxide (SPI-Chem, West Chester, PA, USA) in PO_4 buffer for 1 hour at room temperature. The tissue was then rinsed in PO_4 buffer for 3 immersions of 5 minutes each and dehydrated though a graded series of ethanol (50 % - 70 % - 95 % - 100 %). Next, the tissue was critical point dried in liquid CO_2 in a Hitachi HCP-2 critical point dryer (Hitachi, Tokyo, Japan). Following this, the tissue was mounted onto standard aluminium stubs and sputter coated with gold-palladium in an E5100 Polaron Cool Sputter Coater (Quorum Technologies,

Kent, UK). The specimens were viewed using a LEO Field-Emission Electron Microscope (FE-SEM) scanning electron microscope (Carl Zeiss, Oberkochen, Germany), operating at 10 keV.

2.3.1.2 Data Collection

Secondary electron images were collected digitally at a dimension of 1024 x 768 pixels and 72 pixels per inch (PPI), using a series of magnifications; including, X40, X200, X2000, X5000, X10000, X15000, X20000, X50000.

2.3.1.3 Morphological Analysis of Tissue

Table 2.1 shows the six luminal epithelial surface characteristics and their descriptions used in the morphological analysis of the RU486-treated and control pregnant uterine tissue. To avoid any subjectivity, the morphological analysis of the electron micrographs (112 mm by 78 mm) was performed blind, that is, without prior knowledge of the treatment group a specific micrograph derived from. For the morphological analysis of the folding of the uterine horn, the X40 and X200 micrographs from each animal were used. With regards to the analysis of the cell borders and apices, the microvilli, and the secretions, the X5000, X10000, X15000, X20000 and X50000 micrographs from each animal were used.

Table 2.1 The micrographs of the implantation and non-implantation sites at day 4.5, 5.5 and 6.5 of pregnancy of the control animals and animals treated with RU486 at day 3 of pregnancy were analysed with regards to six uterine epithelial cell characteristics. The scoring system for each characteristic is described below.

Epithelial Characteristics		**Scoring**
Surface Folding	the extent to which the endothelium had folded	(1 – smooth, 2 – slightly folded, 3 – folded, 4 – very folded)
Cell Borders	whether they were obvious or recessed between the cells	(1 – sunken, 2 – flat, 3 – raised)
Cell Apices	whether they were flat or bulging into the lumen	(1 – flat, 2 – slightly raised, 3 – raised)
Microvilli Concentration	the relative number of microvilli seen per cell	(1 – sparse, 2 – medium density, 3 – dense)
Small Secretions	the number of small secretory droplets seen within the field	(0 – none, 1 – some, 2 – a lot)
Large Surface Protrusions	the number of large protrusions seen on the cell surface	(0 – none, 1 – some, 2 – a lot)

2.3.2 Transmission electron microscopy

2.3.2.1 Tissue Preparation

Two implantation and two non-implantation sites were placed into 2.5% gluteraldehyde (Appendix A) in PO_4 buffer for an hour at room temperature and rinsed in three changes of PO_4 buffer for 5 minutes each time. Following the rinses, the tissue was post-fixed in 2% osmium tetroxide in PO_4 buffer for

one hour and rinsed again in three changes of PO_4 buffer for 5 minutes each time. The tissue was dehydrated through a graded series of ethanol (50%-70%-95%-100%) and infiltrated with a graded series of Spurr's resin (Advanced Laboratory Solutions, Randburg, Gauteng, RSA) (50%-75%-100%) (Appendix A) for one hour each. The tissue was placed into fresh 100% Spurr's resin for an hour, following which it was blocked and cured in fresh 100% Spurr's resin for 24 hours at 60ºC. Semi-thin sections (1µm) of each implantation and non-implantation site were cut on an ultramicrotome (Leica Ultracut UCT; Leica Microsystems, Bannockburn, IL, USA) and stained with 0.5% Toluidine Blue (SPI-Chem, West Chester, PA, USA) (Appendix A) for 10-20 seconds, so as to orientate the epithelium. Ultra-thin (gold/silver) sections were then cut from properly orientated blocks using a diamond knife and picked up onto 200 mesh copper grids (Ted Pella, Redding, CA, USA). The grids were stained with a 5% aqueous uranyl acetate (Electron Microscopy Sciences, Hatfield, PA, USA) solution (Appendix A) for 3 minutes, rinsed in three changes of 50% methanol and allowed to dry for 10 minutes before being stained for a further 2 minutes in a 1% aqueous lead citrate (Electron Microscopy Sciences, Hatfield, PA, USA) solution in 4% concentrated sodium hydroxide (NaOH) (Appendix A) (ACE, Southdale, Gauteng, RSA). Following this, grids were rinsed in dilute NaOH followed by three changes of distilled water, and were then allowed to dry before storing in grid boxes. Sections were viewed and photographed in a Jeol JEM-100S transmission electron microscope (Jeol, Tokyo, Japan) operating at 80kV.

2.3.2.2 Data Collection

The Toluidine Blue semi-thin sections were viewed using a Zeiss Axioskop 2 plus microscope and photographed with a digital camera linked to the microscope (Zeiss AxioCam HRc; Carl Zeiss, Oberkochen, Germany). The images were captured using the AxioVision software 40 v 4.8.0.0 (Carl Zeiss Imaging Solution GmbH; Carl Zeiss, Oberkochen, Germany) at a dimension of 1388 x 1040 pixels and 150 PPI. Digital transmission images were collected of secondary electron microscopy images, at a dimension of 1376 x 1032 pixels and 72 PPI, using each of the following series of magnifications: X1200, X2000, X2500, X3000, X4000, X5000, X6000, X8000, X10000, X12000, X15000, X20000, X30000.

2.3.2.3 Morphological Analysis of Tissue

The transmission electron micrographs and the Toluidine Blue (1µm) sections were viewed and analysed according to specific criteria:

- Evidence of secretion by the luminal epithelial cells into the lumen
- The presence of large cell surface protrusions
- The shape of the luminal epithelial cells (cuboidal or columnar)
- The shape and position of the luminal epithelial cell nuclei
- The appearance of the uterine epithelial cell microvilli

- The apical epithelial surface structure with regards to the cell apices
- The number of small and large apical vesicles
- The number and position of the lipids within the uterine epithelial cells
- The appearance of the basal plasma membrane
- The appearance of the stromal/decidual cells and their nuclei
- The appearance of the glands with regards to the appearance of epithelium lining, as well as whether the luminae were open or closed and whether the glands were vesicular or not
- Evidence of apoptotic cells/activity

2.4 Characterisation of the Progesterone Receptor, Endometrial Biomarker, Angiogenic Pathway-Related and Apoptotic Pathway-Related Gene mRNA Expression in the RU486-Treated Rat Uterus

This section describes the use of quantitative reverse transcriptase real-time polymerase chain reaction (RT-qPCR) to study the expression of the Progesterone Receptor (PR), the endometrial biomarker genes; Leukaemia Inhibitory Factor (LIF), Mucin-1 (Muc-1) and Calcitonin; the angiogenic pathway-related genes; Vascular Endothelial Growth Factor (VEGF), basic Fibroblast Growth Factor (bFGF) and Platelet-derived Growth Factor (PDGF) and the apoptotic genes; Bax and Bcl-2 mRNA in the rat uterus at days 5.5 and 6.5 of pregnancy in both the control pregnant and RU486-treated animals. No animals at day 4.5 of pregnancy were used in the RT-qPCR study, as day 5.5 and day 6.5 of pregnancy represent the day of blastocyst implantation and invasion. As these two days are the most significant as far as any effect RU486 may have on the endometrium during early pregnancy in order to prevent implantation and subsequent pregnancy, it was decided that these two days were the most significant for the purpose of this study.

Total RNA was extracted from rat uterus samples at days 5.5 and 6.5 of pregnancy, following treatment with RU486 or vehicle, using the RNeasy Mini protocol for isolation of total RNA from animal tissues (Qiagen, Germantown, Maryland, USA). The RNA extracts were reverse transcribed to cDNA using MultiScribe Reverse Transcriptase (Applied Biosystems, Foster City, CA, USA) and cDNA representing portions of each of the genes for PR, LIF, Muc-1, Calcitonin, VEGF, bFGF, PDGF, Bax, and Bcl-2 cDNA were amplified with real-time qPCR. The effect of RU486 on the expression of these genes in the implantation and non-implantation sites of the rat uterus at days 5.5 and 6.5 of pregnancy was analysed by relative quantification reverse transcriptase real-time PCR.

2.4.1 RNA extraction

The RNA isolation method used in this study was adapted from the RNA extraction booklet supplied by Qiagen (2008). This kit uses a silica based minicolumn extraction procedure. Essentially, after the RNA, derived from the tissue source, has bound to the silica column, it is eluted with water. One

implantation and one non-implantation site was placed into sterile eppendorf tubes (Whitehead Scientific, Brackenfell, Western Cape, RSA), flash frozen in liquid nitrogen and stored in a -70ºC freezer until required for RNA extraction.

The working area was wiped down with 70% ethanol followed with RNase away (Qiagen, Germantown, Maryland, USA) prior to RNA extraction, to prevent transfer of RNA from any extraneous sources. The tissue was placed into a clean autoclaved glass Petri dish and weighed to ensure that the tissue piece was less than 30mg. The tissue was macerated using sterile autoclaved scissors and then placed into an autoclaved glass Dounce tissue homogeniser (Omni International, NW Kennesaw, GA, USA). For every 1ml of buffer RLT (Qiagen, Germantown, Maryland, USA) used from the kit, 10µl of β-mercaptoethanol (Sigma-Aldrich Co., St Louis, MO, USA) was added. Six hundred µl of the RLT buffer-BME solution (Appendix A) was added to the homogeniser and the tissue was homogenised until the cells had lysed sufficiently. The homogenate was passed through a 1000µl pipette tip (Whitehead Scientific, Brackenfell, Western Cape, RSA) several times to ensure homogeneity, before being pipetted directly onto a QIAshredder spin column (Qiagen, Germantown, Maryland, USA) placed in a 2ml collection tube, and centrifuged at maximum speed for 5 minutes in a HERMLE Z229 micro-centrifuge (BHG, Nordrhein-Westfalen, Germany). The resulting supernatant was transferred to a new autoclaved eppendorf by pipetting and the pellet discarded. Six hundred µl of 70% ethanol in RNase-free water (Qiagen, Germantown, Maryland, USA) was added to the clear lysate and mixed immediately by pipetting. Seven hundred µl of this sample, including any precipitate that may have formed, was added to an RNeasy mini column placed in a 2ml collection tube (Qiagen, Germantown, Maryland, USA) and centrifuged for 15 seconds. The flow-through was discarded. In the event that the total volume of the sample exceeded 700µl, the residual volume was added to the same RNeasy column and centrifuged for a further 15 seconds. The flow-through was discarded each time, but not the collection tube. Seven hundred µl of buffer RW1 (Qiagen, Germantown, Maryland, USA) was added to the RNeasy mini column, the tube was sealed and the sample centrifuged for 15 seconds at maximum speed to wash the column. The flow-through and the collection tube were discarded. The RNeasy column was transferred to a new 2ml collection tube and 500µl of buffer RPE (Qiagen, Germantown, Maryland, USA), to which 4 volumes of 100% ethanol had been added (Appendix A), was pipetted onto the RNeasy column. The tube was closed gently and centrifuged for 15 seconds at maximum speed to wash the column. The flow-through was discarded. A further 500µl of buffer RPE was added to the RNeasy column and centrifuged for 2 minutes to dry the silica gel membrane. To elute, the RNeasy column was transferred to a new 1.5ml collection tube and 50µl of RNase-free water was pipetted directly onto the RNeasy silica-gel membrane and centrifuged for 1 minute. The eluate was then pipetted directly onto the RNeasy silica-gel membrane again and centrifuged for a further minute to ensure the maximum RNA concentration. The RNA concentration of each sample was then established using the Thermo Scientific NanoDrop 3300

Fluorospectrometer (Thermo Scientific, Wilmington, DE, USA). The tubes containing the RNA were stored in the freezer at -80°C until required for RT-qPCR, to avoid degradation of the sample.

2.4.1.1 Total RNA Cleanup

To assess the purity of an RNA sample, the ratio of the absorbance of the sample at a wavelength of both 260nm and 280nm is used (Wilfinger *et al.*, 1997). For 'pure' RNA, a ratio of ~2.0 is considered acceptable. If this ratio is smaller then it may indicate the presence of contaminants (RNeasy Mini Protocol; Qiagen, Germantown, Maryland, USA). The ratio of absorbance at 230nm and 260nm is a secondary measure of nucleic acid purity, which indicates the presence of contaminants (RNeasy Mini Protocol; Qiagen, Germantown, Maryland, USA). In some cases the A230/260 ratio obtained from the fluorospectrometer was below the desired total of 1.8 and an RNA cleanup step (RNeasy Mini Protocol; Qiagen, Germantown, Maryland, USA) was applied to these samples. Prior to starting the RNA cleanup, the sample volume was adjusted to 100µl with RNase-free water (Qiagen, Germantown, Maryland, USA). Three hundred and fifty µl of buffer RLT was added to the diluted sample and mixed well by pipetting. A further 250µl of 100% ethanol was added to the mixture and mixed by pipetting up and down. The resulting 700µl of sample was transferred to an RNeasy Mini spin column placed into a 2ml collection tube and centrifuged for 15 seconds. The flow-through was discarded and the collection tube kept. Five hundred µl of buffer RPE was added to the spin column and centrifuged for a further 15 seconds to wash the column. The flow-through in the collection tube was discarded and the collection tube kept. A further 500µl of buffer RPE was added to the spin column and centrifuged for 2 minutes to wash the spin column membrane. The collection tube containing the flow-through was discarded and the spin column placed in a new 2ml collection tube. The spin column was then centrifuged for a further minute to ensure that all buffer RPE was removed from the silica membrane and the collection tube was discarded. The spin column was placed into a new 1.5ml microcentrifuge tube and 30µl of RNase-free (Qiagen, Germantown, Maryland, USA) water was added directly onto the spin column membrane. The water was left on the column membrane for 5 minutes prior to centrifuging for 1 minute to elute the RNA. This step was included to ensure that the maximum amount of RNA was solubilised in the water. The RNA eluate was then re-added to the column membrane and re-eluted by centrifugation for a further minute. The RNeasy spin column was then discarded and the tubes containing the RNA were stored in the freezer at -80°C until required for RT-qPCR to avoid degradation of the sample.

2.4.1.2 RNA Integrity and Concentration

To determine the integrity of the extracted RNA, the samples were loaded onto a 1% agarose (Whitehead Scientific, Brackenfell, Western Cape, RSA) gel (Appendix A). The gel trays, combs, equipment, Erlenmeyer flask and work surfaces were swabbed with RNase Away (Qiagen, Maryland, USA) to ensure no RNA contamination occurred during gel electrophoresis. One gram of agarose was

microwaved in 100ml of 1x TBE (Tris: Sigma-Aldrich Co., St Louis, MO, USA; EDTA: UnivAR Saarchem, Krugersdorp, RSA; Boric Acid: Saarchem Merck Chemicals, Gauteng, RSA) buffer (Appendix A) in a sterile Erlenmeyer flask, until the agarose had dissolved. Eight µl of 100µg/ml ethidium bromide (Sigma Chemical Co., St Louis, MO, USA) was added to the gel solution. When the gel solution had cooled to comfortable touch, it was poured into a horizontal mini electrophoresis unit (Sigma-Aldrich Co., St Louis, MO, USA) and allowed to set for 45 minutes. A small amount of each RNA sample was diluted to the same concentration with RNase free water. Two µl of loading dye (Promega, Madison, WI, USA) were added to each diluted RNA sample to a volume of 10µl. To denature the RNA, this mixture was incubated in a water bath for 10 minutes. The agarose gel was then removed from the casting apparatus and covered with cold 1x TBE buffer until the RNA samples were ready to load. Once the RNA samples had incubated for 10 minutes, they were placed on ice and allowed to chill for 2 minutes. The RNA samples were then mixed, centrifuged briefly, and loaded onto the agarose gel. The gel was run for 1 hour at a constant voltage of 65V and a current of 150mA. The gels were viewed with the Molecular Imager® Gel Doc^{TM} XR System (Bio-Rad Laboratories Inc., Hercules, CA, USA) under a UV light and an image recorded. Only samples showing two clear bands of the 18S and 28S ribosomal RNA (rRNA) with a faint smear representing mRNA in the background were included in the study. Figure 2.1 shows an example of an agarose gel containing RNA extracted using the RNeasy Mini Kit.

In order to determine the integrity and concentration of the extracted RNA, a NanoDrop 3300 Fluorospectrometer (Thermo Scientific, Wilmington, DE, USA) was used. One µl of each RNA sample was analysed on the NanoDrop and the A_{260} and A_{280} values and the concentration of the sample were recorded. The purity of the samples was determined by the A_{260}/A_{280} ratio and only those samples with a purity ratio of between 1.8 and 2.2 were used for the RT-qPCR process.

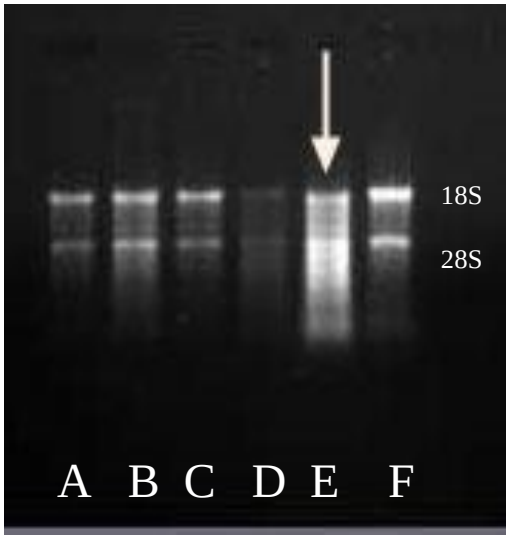


Figure 2.1 A 1% Agarose gel showing RNA samples extracted using the Qiagen RNeasy Mini Kit. The two bands represent 18S and 28S rRNA and the smear in the background represents the mRNA. Lane E shows a degraded sample, devoid of distinct bands (lane E, arrowed).

2.4.2 Primer design and synthesis

Specific primers were designed for the amplification of target DNA fragments for the angiogenic pathway-related and apoptotic genes. Gene expression assays for LIF, Muc-1 and Calcitonin were purchased predesigned and diluted from Applied Biosystems, so it was not necessary to design primers for these genes. The primers for the angiogenic pathway-related and apoptotic genes were not purchased directly from Applied Biosystems.

The first step was to find the entire gene sequence for the rat PR, VEGF, bFGF, PDGF, Bax and Bcl-2 genes, respectively, including, the endogenous control β-actin. The on-line databases, Ensembl Gene Browser (Ensembl, 2008) and the National Centre for Biotechnology Information (NCBI, 2008) were used for this purpose (Table 2.2).

Table 2.2 The Ensembl Identification numbers for the angiogenic pathway-related and apoptotic pathway-related gene transcripts and the Ensembl Identification number of the gene that the transcript is a product of.

Gene	Ensembl Transcript Identification Number	Ensembl Gene Identification Number
B-actin	ENSRNOT00000042459	ENSRNOG00000034254
PR	ENSRNOT00000038313	ENSRNOG00000006831
VEGF	ENSRNOT00000026637	ENSRNOG00000019598
bFGF	ENSRNOT00000023388	ENSRNOG00000017392
PDGF	ENSRNOT00000023196	ENSRNOG00000017197
Bax	ENSRNOT00000028328	ENSRNOG00000020876
Bcl-2	ENSRNOT00000003768	ENSRNOG00000002791

The exon sequences for each gene (Appendix B) were uploaded into Primer Express 2.0 (Applied Biosystems, Foster City, CA, USA) primer design software. The following guidelines were followed when designing the primers (Dieffenbach *et al.*, 1995): The GC content should be 50-60%; the size of the PCR product or amplicon should be 17-28 bases in length; the melting temperature (Tm) should be between 50-65°C; runs of three or more C's or G's at the 3' end should be avoided so as not to promote mispriming; the 3' end should end with a G or a C or CG GC to increase the efficiency of the primer. A list of possible primer pairs was then generated by the Primer Express 2.0 software. Each primer pair was analysed for primer compatibility, hairpins, primer dimers and nucleotide runs using PRIMERW (Scientific & Educational Software, version 2.0). The chosen primer pair was further checked in the online programs BLAST (http://blast.ncbi.nlm.nih.gov/Blast.cgi) and BLAT (http://genome.ucsc.edu/cgi-bin/hgBlat?command=start) to ensure that the primer sequence was specific for the desired gene. The primers (Table 2.3) were synthesised by the MCB Synthetic DNA Unit, University of Cape Town, Department of Molecular and Cellular Biology, RSA. The primer sequences for each gene are listed in table 2.3 along with their product size.

Table 2.3 Primers used and product size

mRNA	PRODUCT SIZE (bps)	PRIMER SEQUENCE
B-actin	112	F primer 5'-CCTAAGGCCAACCGTGAAAA-3' R primer 5'-TGGTACGACCAGAGGCATACAG-3'
PR	105	F primer 5'-TGCTCTTCTCTCGGTCCTGC-3' R primer 5'-CGGCTTCGACTCCAGAGAAA-3'
VEGF	101	F primer 5'-CGAAAGCGCAAGAAATCCC-3' R primer 5'-TTACACGTCTGCGGATCTTGG-3'
bFGF	103	F primer 5'-CACCCTATCCCTTCACAGCCT-3' R primer 5'-GCCTTCCACCCAAAGCAGTA-3'
PDGF	104	F primer 5'-GGAGTCGAGTCGGAAAGCTCAT-3' R primer 5'-AACACCTCTGTACGCGTCTTGC-3'
Bax	102	F primer 5'-AGTGTCTCAGGCGAATTGGC-3' R primer 5'-CACGGAAGAAGACCTCTCGG-3'
Bcl-2	108	F primer 5'-ACTGAGTACCTGAACCGGCATC-3' R primer 5'-GGAGAAATCAAACAGAGGTCGC-3'

F – Forward primer, **R** – reverse primer.

2.4.3 Complimentary DNA (cDNA) synthesis

Synthesis of cDNA from total RNA is the first step in the two-step RT-qPCR gene expression quantification experiment. In this step, oligo $d(T)_{16}$, from the TaqMan Reverse Transcription Reagents (Applied Biosystems, Foster City, CA, USA) primes total RNA samples for reverse transcription using MultiScribe Reverse Transcriptase. The reverse transcription protocol was adapted from the

SYBR Green PCR Master Mix and RT-qPCR Reagents protocol (Applied Biosystems, Foster City, CA, USA, 2006). The concentration and integrity of the RNA samples were rechecked on the day of reverse transcription, using the NanoDrop 3300 Fluorospectrometer (Thermo Scientific, Wilmington, DE, USA). The samples were then diluted with RNase-free water to a concentration of 70ng/µl. The reverse transcription kit reagents were allowed to thaw on ice at room temperature and then vortexed and centrifuged for a few seconds to mix. The enzymes were kept at -20°C until needed and were not vortexed, as shredding of the enzymes can occur. The RT Reaction Mix solution was made up as set out in Table 2.4. The diluted RNA samples were then added to the RT Reaction Mix solution and reverse transcription (RT) was performed according to the parameters in Table 2.5.

Table 2.4 RT Reaction mix for the synthesis of cDNA from total RNA

Component	Volume/Reaction	Final Concentration
10x TaqMan Buffer - 500 mM KCl, 100 mM Tris-HCl, pH 8.3	1µl	1x
25mM $MgCl_2$	2.2µl	5.5mM
Deoxynucleotide Mix (dNTPs) - 2.5 mM each dATP, dCTP, dTTP, dGTP	2 µl	500µM per dNTP
Oligo $d(T)_{16}$ - 50 µM oligodeoxynucleotide of sequence d(T)16 in 10 mM Tris-HCl, pH 8.3	0.5 µl	2.5µM
RNase Inhibitor - 20 U/µL of RNase Inhibitor in 20 mM HEPES-KOH, pH 7.6, 50 mM KCl, 8 mM DTT, and 50% (v/v) glycerol	0.2 µl	0.4 U/µl
MultiScribe Reverse Transcriptase - 50 U/µL of recombinant Moloney Murine Leukemia Virus (MuLV) Reverse Transcriptase in 20 mM Tris-HCl, pH 7.5, 0.1 mM Na_2EDTA, 1 mM DTT, 0.01% (v/v) NP-40, and 50% (v/v) glycerol	0.25 µl	1.25 U/µl
RNA diluted in RNase-free water	3.85 µl	-
TOTAL	**10 µl**	

A No Template Control (NTC) was included where the RNA was substituted with RNase-free water. A negative RT (–RT) control was also included, where the MultiScribe Reverse Transcriptase (Applied Biosystems, Foster City, CA, USA) was replaced with RNase-free water (Qiagen, Germantown, Maryland, USA) to ensure that no genomic DNA contamination existed in the samples.

Table 2.5 Thermal cycling parameters for reverse transcription.

Step	Rationale	Temperature	Time
Incubation	To maximise primer-RNA template binding	25°C	10 min
Reverse Transcription	cDNA synthesis by Reverse Transcription	48°C	30 min
Reverse Transcriptase Inactivation	Inactivation of the reverse transcription enzymes	95°C	5 min

At this point, the samples were stored at 4°C until proceeding to the PCR reaction step.

2.4.4 Real-time quantitative reverse transcription polymerase chain reaction (real-time RT-qPCR)

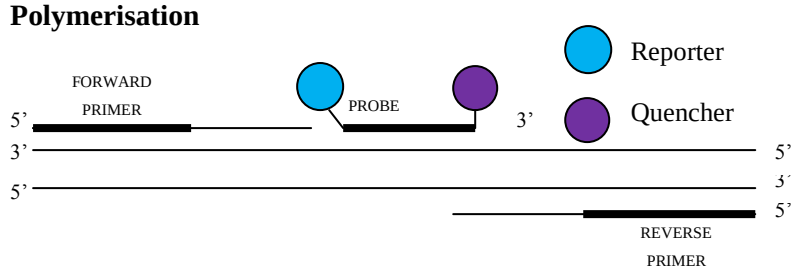
PCR is a technique utilised for the successful amplification of a desired fragment of DNA, via repetitive cycling of DNA synthesis. PCR amplification utilises two oligonucleotide primers which anneal to the complimentary strands of target DNA with their 3' ends co-aligned. Extension of the annealed primers is achieved with the enzyme AmpliTaq DNA polymerase, which catalyses the addition of the relevant nucleotides. Repeated cycling of heat denatured template, annealing of primers to their complimentary sequences and the extension of annealed primers with AmpliTaq DNA Polymerase results in the amplification of the target DNA. In addition to the standard PCR reaction mix of nucleotides, Taq polymerase and other reagents, real-time PCR requires the presence of fluorescent probes, most of which are designed to emit a signal for every amplified DNA strand (TaqMan Gene Expression Master Mix Protocol; Applied Biosystems, Foster City, CA, USA).

In real-time qPCR the amplification and detection of mRNAs occur within the same tube, allowing results to be monitored on-line and thus in real time. Gene expression is quantified precisely by coupling the polymerase chain reaction with fluorescent reporter probes to specific messenger RNA species. As the PCR product is amplified, there is a proportionate increase in the fluorescent signal (TaqMan Gene Expression Master Mix Protocol; Applied Biosystems, Foster City, CA, USA). The cycle threshold (CT) is the cycle in which there is the first detectable significant increase in fluorescence. This is the value used for the relative quantification of the RT-qPCR product.

2.4.4.1 TaqMan Gene Expression Assays

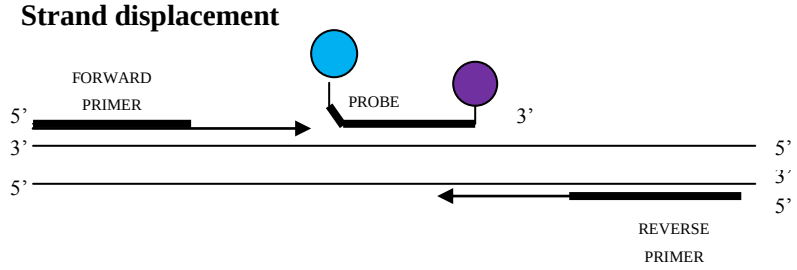
TaqMan gene expression assays were used for the endometrial biomarkers gene expression determination. The assay ID for LIF is Rn00573491_g1 (Applied Biosystems, Foster City, CA, USA), for Calcitonin this is Rn00569199_m1 (Applied Biosystems, Foster City, CA, USA) and for Muc-1 this is Rn01462585_m1 (Applied Biosystems, Foster City, CA, USA). The TaqMan gene expression assays are made up of two unlabelled primers and a FAM® dye-labelled TaqMan® MGB probe. The endogenous control, β-actin (Applied Biosystems, Foster City, CA, USA) contained a VIC® dye-labelled TaqMan® MGB probe and two unlabelled primers.

Polymerisation



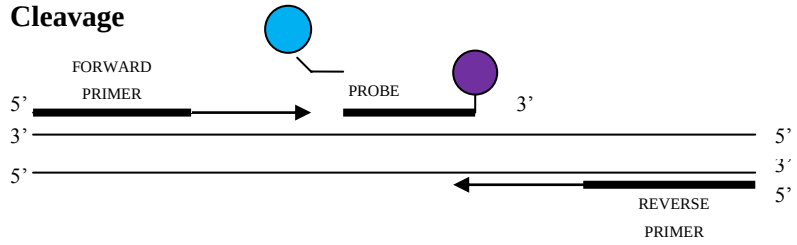
Step 1: A reporter (R) and a quencher (Q) are attached to the 5' and 3' ends of a TaqMan probe.

Strand displacement



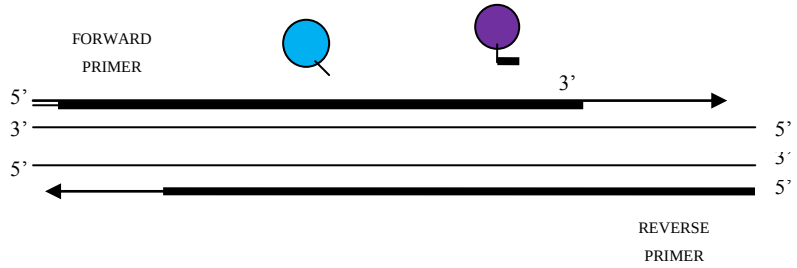
Step 1 (continued)**:** When both dyes are attached to the probe, reporter dye emission is quenched

Cleavage



Step 2: During each extension cycle, the AmpliTaq Gold ® DNA polymerase cleaves the reporter dye from the probe

Polymerisation Completed



Step 3: After being separated from the quencher, the reporter dye emits its characteristic fluorescence.

Figure 2.2 The 5' nuclease assay process that takes place during TaqMan real-time PCR. (Getting Started Guide: Relative Quantification, Applied Biosystems 7300/7500/7500 Fast Real-Time PCR System, page 19; Applied Biosystems, Foster City, CA, USA, 2006)

The TaqMan gene expression assays consist of two unlabelled primers for amplifying the sequence of interest and one TaqMan MGB probe (6-FAM dye-labelled) for detecting the target sequence. The TaqMan MGB probe contains a reporter dye (6-FAM) linked to the 5'end of the probe, a minor groove binder (MGB) as well as a nonfluorescent quencher (NFQ) at the 3' end of the probe.

During each cycle of the PCR amplification, the 5' nuclease assay process occurs (Figure 2.2). The TaqMan MGB probe anneals specifically to a complementary sequence between the reverse and forward primer sites. When the probe is intact, the proximity of the reporter dye to the quencher dye results in suppression of the reporter fluorescence primarily by fluorescent resonance energy transfer (FRET) (Figure 2.2, step 1). The DNA polymerase cleaves only probes that are hybridised to the target. Cleavage separates the reporter dye from the quencher dye, resulting in increased fluorescence by the reporter. If the target sequence is complimentary to the probe and amplified during PCR, then there is an increase in the fluorescent signal, as a result nonspecific amplifications are not detected (Figure 2.2, step 2). Polymerisation of the strand continues; but, the 3' end of the probe is blocked to prevent extension of the probe during PCR (Figure 2.2, Step 3; PN 4333458B: TaqMan Gene Expression Assays Protocol, Applied Biosystems, Foster City, CA, USA).

2.4.4.1.1 TaqMan gene expression assay real-time RT-qPCR optimisation

A real-time qPCR standard curve was performed to establish the optimal cDNA concentration. The RNA concentrations chosen for the standard curve were 50ng/µl, 10ng/µl, 2ng/µl, 400pg/µl and 80pg/µl. A NTC was also included without the addition of RNA to the RT Reaction Mix. Reverse Transcription was then carried out as described in section 2.4.3, followed by the step as described in section 2.4.4.1.2. The results were unsatisfactory in that the samples amplified at a threshold cycle too late. An extra step of 70°C for 1 minute was added to the end of each PCR cycle; however, this was also unsuccessful. The number of PCR cycles was then increased from 40 to 60, without success. Finally, the amount of cDNA added to the PCR reaction mix was increased, thus increasing the cDNA concentration. This finally resulted in satisfactory amplification of the target cDNA at 40 PCR cycles.

2.4.4.1.2 TaqMan gene expression assay real-time RT-qPCR

In the real-time PCR step, the cDNA encoding LIF, Muc-1 and Calcitonin was amplified using TaqMan Gene Expression PCR Master Mix (Applied Biosystems, Foster City, CA, USA). To prepare the PCR reaction mix, the TaqMan Gene Expression PCR Master Mix, the TaqMan gene expression assays and the endogenous control components were thawed on ice before vortexing and then centrifuging to concentrate the tube contents. All of the components (Table 2.6) were added together and then mixed thoroughly by vortexing.

Table 2.6 TaqMan gene expression PCR reaction mix.

Reagent	Volume/Sample	Final Concentration
2X TaqMan Gene Expression PCR Master Mix - AmpliTaq Gold® DNA Polymerase, UP (Ultra Pure), Uracil-DNA glycosylase, dNTPs with dUTP, ROX™ Passive Reference and optimized buffer components	12.5µl	1X
20X TaqMan Gene Expression Assay Mix - unlabelled PCR primers (900nM) and TaqMan® MGB probe (FAM™ dye-labelled) (250nM)	1.25µl	1X
cDNA template	11.25µl	-
TOTAL	**25µl**	

The RT-qPCR plates were prepared by placing 13.75µl of the PCR reaction mix into each well followed by 11.25µl of the corresponding cDNA to make a final volume of 25µl. Next, the plate was placed into the Applied Biosystems 7500 Real-Time PCR System (Applied Biosystems, Foster City, CA, USA). A Relative Quantitative (RQ) plate document was set up for each RQ run from a single plate. On each RQ plate document the detectors, endogenous controls and detector tasks were specified. Wells that contained PCR reagents for the amplification of target sequences were labelled Target (T) and those that contained reagents for the amplification of the endogenous control sequence were labelled Endogenous Control (E). The thermal cycling conditions were set up as shown in Table 2.7.

Table 2.7 Thermal cycling parameters for TaqMan real-time qPCR

Step	UNG Incubation	AmpliTaq Gold Activation	PCR	
	HOLD	HOLD	CYCLE (40 cycles)	
			Denature	Anneal/Extend
Temperature	50°C	95°C	95°C	60°C
Time	2 min	10 min	15 sec	1 min

Following the PCR amplification, the RQ plate data was then analysed and viewed using SDS software (Applied Biosystems 7500 Real-Time PCR System User Guide, 2005).

2.4.4.2 SYBR Green RT-qPCR Optimisation

The primer pairs were optimised both to ensure they were binding correctly and to ascertain the correct annealing temperature for each pair. The optimisation was carried out on two separate samples and included a NTC, wherein no cDNA was added to the PCR Reaction Mix and a negative (–) RT control, in which the MultiScribe Reverse Transcriptase enzyme was omitted from the RT Reaction Mix when performing the reverse transcription. RT-qPCR was then performed at a range of temperatures; including, 50°C, 55°C, 60°C and 65°C, respectively, in order to determine the optimal annealing temperature for each primer pair. The optimal annealing temperature for VEGF, PDGF, Bax, Bcl-2 and PR was determined to be 60°C and that for bFGF was 65°C.

2.4.4.2.1 PCR product gel electrophoresis

The PCR product was then run out on a 1.5% agarose gel, refer to section 2.4.1.2, to ensure that the primers were working specifically and also that no product appeared in the controls. Five µl of DNA ladder was pipetted into the first and last well of the gel. For each PCR product sample, 5µl of PCR product and 1µl of loading dye (Promega, Madison, WI, USA) was pipetted into each well. The gel apparatus was connected to a power pack and set to run for 1.5 hours at a constant 85V and 150mA. Following electrophoresis, the gel was viewed and imaged on the Molecular Imager® Gel Doc™ XR System (Bio-Rad Laboratories Inc., Hercules, CA, USA) under UV transillumination.

2.4.4.2.2 SYBR green RT-qPCR analysis

In the real-time PCR step, the cDNA encoding PR, VEGF, bFGF, PDGF, Bax, and Bcl-2, respectively was amplified using SYBR Green PCR Master Mix (Applied Biosystems, Foster City, CA, USA). To prepare the PCR reaction mix, the SYBR Green Master Mix, the AmpErase UNG (Applied Biosystems, Foster City, CA, USA) and the primers were thawed on ice before vortexing and then centrifuging the tube contents. The components (Table 2.8) were all added together in sequence and mixed thoroughly by vortexing.

Table 2.8 SYBR Green PCR reaction mix.

Reagent	Volume/Sample	Final Concentration
2X SYBR Green PCR Master Mix – SYBR Green 1 Dye, AmpliTaq Gold® DNA Polymerase, dNTPs with dUTP, Passive Reference 1, and optimized buffer components	4.9µl	1X
AmpErase UNG - 1 U/µL uracil-N-glycosylase in 30 mM Tris-HCl, pH 7.5, 1 mM EDTA, 150 mM NaCl, 1 mM DTT,5% (v/v) glycerol, and 0.05% (w/v)Tween 20	0.1µl	0.01 U/µl
PR/VEGF/bFGF/PDGF/Bax/Bcl-2 Forward Primer – 2mM stock	1µl	1X
PR/VEGF/bFGF/PDGF/Bax/Bcl-2 Reverse Primer – 2mM stock	1µl	1X
cDNA template	3µl	-
TOTAL	**10µl**	

The RT-qPCR plates were prepared by placing 7µl of the PCR reaction mix into each well, followed by 3µl of the corresponding cDNA to make a final volume of 10µl. The plate was then placed into the Applied Biosystems 7500 Real-Time PCR Instrument. A Relative Quantitative (RQ) plate document was then set up for each RQ run from a single plate. On each RQ plate document the detectors, endogenous controls and detector tasks were specified. Wells that contain PCR reagents for the amplification of target sequences were labelled Target (T) and those that contain reagents for the amplification of the endogenous control sequence were labelled Endogenous Control (E). The thermal cycling conditions were set up as per Table 2.9.

Table 2.9 Thermal cycling parameters for SYBR Green real-time qPCR

Step	UNG Incubation	AmpliTaq Gold Activation	PCR	
	HOLD	HOLD	CYCLE (40 cycles)	
			Denature	Anneal/Extend
Temperature	50°C	95°C	95°C	60°C - VEGF and PDGF 65°C - bFGF
Time	2 min	10 min	15 sec	1 min

After the completion of the PCR run, dissociation curves were run for each plate to detect non-specific amplification. The melting temperature for a DNA double helix depends on the base composition, thus all primer pairs should have the same melting temperature unless there is contamination, mispriming or primer dimers (SYBR Green PCR Master Mix and RT-PCR; Applied Biosystems, Foster City, CA, USA, 2002). Next, the RQ plate data was analysed and viewed using SDS software (Applied Biosystems 7500 Real-Time PCR System User Guide, 2005).

2.4.4.3 Data Collection

Using the Applied Biosystems Sequence Detection Software version 1.2.3 7500 System SDS Software, the RQ plates for each group of genes were added into a RQ study to determine the threshold cycle (CT) values for each sample. The threshold and baseline for each gene was set automatically using the Applied Biosystems SDS software. The CT values were then imported into an Excel spreadsheet for analysis. An average CT value for the endogenous control β-actin was obtained and this value was used to normalise the data from each gene.

An average CT value was obtained for both the implantation and non-implantation sites at days 5.5 and 6.5 of the control pregnant and the RU486-treated animals for each of the genes LIF, Muc-1, Calcitonin, VEGF, bFGF, PDGF, Bax, Bcl-2, and PR. The change in CT (ΔCT) for each day of pregnancy was obtained by normalising the data using the endogenous control average CT value. The equation used was:

$CT_{(target)} - CT_{(endogenous\ control)} = \Delta CT$ (Livak and Schmittgen, 2001).

In order to carry out relative quantification, a calibrator sample is required. In this study, the calibrator sample chosen was the implantation sites at day 5.5 of pregnancy in the control pregnant animals, as this is the site and day of blastocyst implantation. The change in gene expression levels relative to the site of blastocyst implantation is of most importance and relevance to this study. The ΔCT values were then calibrated using the chosen calibration sample, using the equation,

$\Delta CT_{(target)} - \Delta CT_{(calibrator)} = \Delta\Delta CT$.

The up-regulation of gene expression, as compared to the calibrator, for each day of pregnancy was then established using the equation $2^{-\Delta\Delta CT}$. Down-regulation of gene expression relative to the calibrator sample was established using the inverse ($2^{\Delta\Delta CT}$). The fold change was then used for graphical representation.

2.5 Immunofluorescence (IF)

This section describes the use of immunofluorescence (IF) to study the expression of the Progesterone Receptor (PR) protein; the apoptotic proteins, Bax and Bcl-2; the angiogenic pathway-related proteins, Vascular Endothelial Growth Factor (VEGF), basic Fibroblast Growth Factor (bFGF) and Platelet-derived Growth Factor (PDGF); and the endometrial biomarkers, Leukaemia Inhibitory Factor (LIF), Mucin-1 (Muc-1) and Calcitonin, in the rat uterus, at days 4.5, 5.5 and 6.5 of pregnancy in each of the control pregnant and RU486-treated animals.

2.5.1 Tissue preparation for IF

The light microscopy method used in this study was adapted from Kramer *et al.* (1993). Two implantation and non-implantation sites were placed into 10% buffered formalin fixative (Appendix A) for no less than 24hrs. Following fixation, the tissue was placed in an automatic tissue processor (Shandon Citadel 1000; Thermo Scientific, Wilmington, DE, USA) where it was dehydrated through a graded series of ethanol (70%-95%-95%-95%-100%-100%-100%), cleared in chloroform and embedded in paraffin wax, such that transverse sections could be cut from each tissue block.

2.5.1.1 IF Section Preparation

The IF method used in this study was adapted from the Protocols and Support Products insert supplied by Santa Cruz Biotechnology (Santa Cruz, CA, USA). Five μm thick sections were cut using a Jung Biocut 2035 microtome (Leica Instruments, Nussloch, Germany) and heat adhered onto silane slides (Appendix A) at 60°C overnight. On the day of incubation the sections were deparaffinised in xylene, rehydrated through a graded series of ethanol (100%-95%-70%) and placed into distilled water for 1 minute.

IF sections requiring antigen retrieval were placed into a plastic container and covered with tris-ethylenediamine tetraacetic acid (EDTA) (Sigma-Aldrich Co., St. Louis, MO, USA) buffer (pH 9.0; Appendix A) or sodium citrate (BDH Laboratory Chemicals, Poole, England, UK) (pH 6.0; Appendix A) depending on which solution provided the best results for each antibody. Sections were heated in a microwave at medium heat (720W) for 5 minutes for antigen unmasking. The container was topped up with fresh buffer and heated at medium heat for a further 5 minutes. The slides were allowed to cool in the buffer for 20 minutes. The sections were aspirated and circled with a DAKO pen (DAKO, Carpinteria, CA, USA) and rinsed in one change of PBS for 5 minutes, following antigen unmasking

and covered with 0.1% Triton-X100 (Sigma-Aldrich Co., St. Louis, MO, USA) in 0.1% BSA (Sigma-Aldrich Co., St. Louis, MO, USA)/PBS to permeabilise the cells. Following cell permeabilisation, all sections were rinsed in three changes of 0.1% BSA/PBS for 5 minutes each and incubated with 25µl primary antibody overnight at 4°C in a Tupperware container lined with damp blotting paper to prevent evaporation and drying out. The primary antibodies were diluted with 0.1% BSA/PBS. The following morning the slides were washed three times in 0.1% BSA/PBS for 5 minutes each and then incubated in a dark chamber with 25µl of secondary antibody conjugated to a fluorescent dye for 1 hour at room temperature.

Table 2.10 IF tissue section preparation for the endometrial biomarkers, and the apoptotic and angiogenic pathway-related proteins.

	Endometrial Biomarkers			**Apoptotic Pathway-Related Proteins**			**Angiogenic Pathway-Related Proteins**		
Protein	Muc-1	LIF	Calcitonin	PR	Bax	Bcl-2	PDGF	bFGF	VEGF
Antigen retrieval	-	medium heat in microwave 720W 5 minutes X 2; cool 20 minutes in buffer						-	-
Solution	-	EDTA pH 9.0					Na citrate pH 6	-	-
Wash	1 X 5 minutes in PBS								
Permeabelise	Triton-X 100 in 1% BSA/PBS								
Duration	20 minutes	10 minutes							
Wash	3 X 5 minutes in 1%BSA/PBS								
1° Ab 25 µl overnight at 4°C	Goat anti-Muc-1	Goat anti-LIF	Rabbit anti-Calcitonin	Rabbit anti-PR	Rabbit anti-Bax	Mouse anti-Bcl-2	Rabbit anti-PDGF	Rabbit anti-bFGF	Goat anti-VEGF
	Diluted in 1%BSA/PBS								
Concentration	1:100	1:75	1:100	1:50	1:50	1:50	1:75	1:50	1:50
Wash	3 X 5 minutes in 1% BSA/PBS								
2º Ab 25 µl for 1hr at RT	Donkey anti-goat IgG Alexa Flour 488		Goat anti- rabbit IgG Alexa Flour 594			Donkey anti-mouse IgG AF 594	Goat anti-rabbit IgG Alexa Flour 594		Donkey anti-goat IgG AF 488
	Diluted in PBS								
Concentration	1:50	1:100	1:150	1:200	1:200	1:200	1:200	1:200	1:200
Wash	3 X 5 minutes in PBS								
DAPI	DAPI in PBS (1:10 000) for 10 minutes								
Wash	3 X 5 minutes in PBS								
Mount with GelMount, coverslip and view									

EDTA – tris-ethylenediamine tetraacetic acid (pH 9.0); **Na citrate** – sodium citrate (pH 6.0); **BSA** – bovine serum albumin; **PBS** – phosphate buffered saline (pH 7.6); **1° -** primary; **Ab** – antibody; **2° -** secondary; **RT** – room temperature.

The secondary antibodies were diluted in PBS. Table 2.10 shows primary and secondary antibody concentrations for each protein. All primary antibodies were purchased from Santa Cruz Biotechnology, Inc. (Santa Cruz, CA, USA) and all Alexa Fluor secondary antibodies from Molecular Probes (Invitrogen, Carlsbad, CA, USA). The slides were washed in a foil covered glass dish with

PBS for three changes of 5 minutes each and then incubated with DAPI (Cambrex, East Rutherford, NJ, USA) diluted in PBS at a concentration of 1:10 000 for 10 minutes (Appendix A). The sections were then rinsed three times in PBS for 5 minutes each and mounted and coverslipped with GelMount (Biomeda Corporation, Foster City, CA, USA) aqueous mounting medium with antifade. The sections were viewed using an Olympus fluorescent microscope (Olympus IX71; Olympus, Centre Valley, Pennsylvania, USA) with appropriate filters linked via a colour camera (Olympus XM10; Olympus, Centre Valley, Pennsylvania, USA) to a personal computer (HP Compaq XD7400 Core 2 Duo microtower running Windows Vista Basic).

2.5.2 Negative controls

Negative controls were used to ensure that the secondary antibodies were specific for their respective primary antibodies. The primary antibodies were substituted with 0.1% BSA\PBS and the normal protocol continued. In a second negative control, the tissue was treated in the same way as the experimental slides, except the secondary antibodies were substituted with PBS. These controls were done to ensure that cross-reactivity between tissue constituents was not occurring. For a positive control, antibodies were applied to tissue with a known positive reaction to the specific primary antibody. Colon was the positive control for anti-Muc-1, lung for anti-LIF and thyroid for anti-Calcitonin. Breast adenocarcinoma, a kind gift from Mrs Nalini Pather, was used for the other antibodies, as apoptosis and angiogenesis are known to be prevalent in such tumours. The tissue was treated in the same way as that of the experimental slides. These controls were carried out to ensure that the IF technique and antibodies were working properly.

2.5.3 Data collection

The tissue sections from each animal were incubated with a primary antibody raised against LIF, Muc-1, Calcitonin, VEGF, bFGF, PDGF, Bax, Bcl-2 or PR followed by incubation with a secondary antibody bound to a fluorophore. Quantification of stained sections was performed using a x40 objective lens and microscope (Olympus IX71; Olympus, Centre Valley, Pennsylvania, USA) linked via a colour video camera (Olympus XM10; Olympus, Centre Valley, Pennsylvania, USA) to a personal computer (HP Compaq XD7400 Core 2 Duo) with image analysis software (Olympus Soft Imaging Solutions; Olympus, Centre Valley, Pennsylvania, USA). The microscope settings remained constant for each exposure. Micrographs were taken of the epithelium and the glands of each section. Micrographs of the blood vessels were taken from the angiogenic pathway-related sections. Using the image analysis software, analySIS Life Science Research program FIVE – Digital imaging Solutions (Olympus Soft Imaging Solutions; Olympus, Centre Valley, Pennsylvania, USA), the intensity of the fluorescence of the x40 micrographs was analysed. This was done by first using the software to define the regions of interest (ROIs); namely, the epithelium, the subepithelial stroma, the glands and the glandular stroma. The blood vessels and the stroma surrounding the blood vessels were also defined

as ROIs in the angiogenic pathway-related proteins study. The mean intensity of each ROI was then analysed using the image analysis software. The results of this analysis was placed into the statistics program JMP version 8 (SAS Institute Inc., Cary, North Carolina, USA) according to the group (day 4.5, 5.5 and 6.5 of pregnancy; treated with RU486 or untreated), as well as the ROI (epithelium, subepithelial stroma, glands, glandular stroma, blood vessels and stroma surrounding the blood vessels) for statistical analysis.

2.5.4 Statistical analysis

The following statistics tests were performed to determine whether there was any significant difference between the means of the different treatment groups and within the treatment groups, with regards to the expression of each protein within the regions of interest. Summaries of these statistical tests can be found in Appendix C.

The O'Brien's, Brown-Forsythe's, Levene's and Bartlett's tests where used to test whether the variances within each treatment group for LIF, Muc-1, Calcitonin, VEGF, bFGF, PDGF, Bax, Bcl-2 and PR were equal.

If the variances of the protein expression of a particular group were found to be equal ($p<0.05$) then this test was followed by a one-way Analysis of Variance (ANOVA), to test for a significant difference between the means within a particular treatment group or the means between the different treatment groups for the expression of that protein. If there was a significant difference between the means ($p<0.05$) then a Tukey-Kramer *post hoc* analysis was performed to determine which treatment groups were significantly different from each other for the expression of that protein.

If the variances in the different treatment groups for the expression of a particular protein were not equal ($p>0.05$) according to the O'Brien's, Brown-Forsythe's, Levene's and Bartlett's tests, then a Welch ANOVA was performed. The Welch ANOVA tests whether there is a significant difference between the means, whilst allowing the variances to be unequal. This test is based on the ANOVA F test and uses weighted means and does not require the variances to be equal (JMP statistics program version 8; SAS Institution Inc., USA). The Welch ANOVA was also followed by a Tukey-Kramer *post hoc* analysis, where a significant difference between the means was found ($p<0.05$), to determine which groups were significantly different to each other.

CHAPTER 3

THE EFFECTS OF RU486 ON THE WINDOW OF RECEPTIVITY

3.1 INTRODUCTION

Subsequent to fertilisation, the embryo develops into a blastocyst for implantation, specifically, into the uterine wall (Carson *et al.*, 2000). In addition to embryo maturation and development, the endometrium itself has to undergo certain changes in order to be receptive to the implanting blastocyst, this to ensure successful pregnancy. These changes in the endometrium are under the regulation of the ovarian hormones, progesterone and oestrogen, which act together to prime the uterus and establish the 'window of receptivity', during which time a viable blastocyst is able to implant (Wang and Dey, 2006).

3.1.1 Increased Vascular Permeability

In the rat and mouse, one of the first uterine responses to the presence of implanting blastocysts is that of a localised increase in vascular permeability, restricted to the regions in the uterus where blastocysts adhere to the uterine wall. Such areas are referred to as implantation sites (Psychoyos, 1986; Carson *et al.*, 2000). After an intravenous injection of a macromolecular blue dye, Pontamine Sky blue, at around day 5 of pregnancy, the increase in vascular permeability at the implantation sites can be visualised. The dye binds to albumin in the blood and then leaks into the endometrium from the endometrial blood vessels exhibiting increased vascular permeability. Macroscopically visible distinct blue bands are formed in the uterine horns at the implantation sites (Psychoyos, 1961;1986; Tung *et al.*, 1986; Carson *et al.*, 2000). As the occurrence of increased vascular permeability coincides with the attachment reaction between the blastocyst and the uterine epithelial cells, it has been suggested that this response may be important in meeting the early metabolic needs of the developing, implanted blastocyst as well as those of the endometrium (Psychoyos, 1961;1986).

3.1.2 The Plasma Membrane Transformation of Early Pregnancy

During attachment of the blastocyst, the first site of contact between maternal and foetal cells is the plasma membrane of the surface epithelial cells of the uterus. As this epithelial cell layer has been shown to be a major barrier to the attachment and subsequent implantation of the blastocyst, it was suggested that the plasma membrane of these uterine epithelial cells has a crucial role in the implantation process (Murphy and Shaw, 1994).

Compared with their individual effects, when the ovarian hormones, progesterone and oestrogen, act in sequence, as they do during early pregnancy to prime the uterus for attachment, the plasma membrane of the uterine epithelial cells undergo remarkable changes in structure. These changes have

been collectively referred to as the 'plasma membrane transformation' of early pregnancy and have been shown to be under the direct control of progesterone and oestrogen (Murphy, 1993; Murphy and Shaw, 1994). The term 'plasma membrane transformation' was conceived and introduced by Murphy (1993) and Murphy and Shaw (1994) to emphasise the fact that these changes are not confined to the apical plasma membrane, but extend to the lateral and basal plasma membranes as well, and that these membrane changes are not only apparent during the period of attachment, but are ongoing during early pregnancy (Murphy, 2000a). The plasma membrane transformation extends to molecular and biochemical events of early pregnancy such as loss of the anti-adhesive molecule, Muc-1, from the apical surface of the uterine epithelial cells at the time of implantation (DeSouza *et al.*, 1998) as well as the decrease in the amount of the apical glycocalyx of the luminal epithelial cells (Schlafke and Enders, 1975).

3.1.3 Apical Surface Changes

In rats and mice, the long, thin, regular microvilli on the apical plasma membrane of the uterine epithelial cells, typical of the oestrous cycle and early pregnancy, undergo structural changes (Terry *et al.*, 1996; Murphy, 2000a). As pregnancy progresses, the microvilli are gradually replaced by shorter, more irregular microvilli. When blastocyst implantation begins, by days 5-6 of pregnancy, the apical surface of the uterine epithelial cells is almost completely devoid of microvilli (Murphy, 2000a). This process may be related to the observed disruption of the terminal web (Luxford and Murphy, 1989;1992). Previous studies have indicated that in order for the blastocyst to come into close apposition with the maternal tissue, in order for implantation to occur, this flattening of the apical surface is crucial (Nilsson, 1966; Ljungkvist and Nilsson, 1971; Ljungkvist, 1972a). The observation that this re-organisation of the apical surface of the uterine epithelial cells occurs in the pseudopregnant animals and can be induced in ovariectomised rats treated with progesterone and oestrogen, suggests that this early pregnancy event is a maternal response not dependent on the presence of a blastocyst (Pollard and Finn, 1974; Luxford and Murphy, 1992; Png and Murphy, 2000). By this stage of pregnancy, the apical membrane of the uterine epithelial cells consists of irregular, rounded cytoplasmic projections, referred to as pinopods due to their possible pinocytosis of uterine fluid and endocytosis of macromolecules (Psychoyos and Martel, 1985; Lessey, 2000; Murphy, 2000b). In the human endometrium, these cytoplasmic projections are referred to as uterodomes due to the lack of pinocytotic function as evident by the inability of these projections to take up a tracer (Adams *et al.*, 2002). The exact function of these pinopods is unknown and it has also been hypothesised that they are the first contact site between the embryonic and maternal tissue as they tower over the rest of the uterine surface (Martel *et al.*, 1991).

Apposition of the blastocyst is usually accompanied by luminal closure said to provide firmer adhesion. The lumen of the uterus begins to narrow and the uterine epithelial cells from opposing

sides of the lumen adhere to one another or, in the presence of a blastocyst, to the trophoblast. This process is thought to function to "hold" the blastocyst in place, as well as to bring the blastocyst in close contact with the uterine epithelial cells in preparation for implantation (Hyland *et al.*, 1998; Murphy, 1998). Png and Murphy (2000) indicated that this closure of the lumen occurs in the pseudopregnant rat endometrium and is not restricted to the implantation sites, suggesting a regulatory role for the ovarian hormones in this early pregnancy event.

3.1.4 Cellular Changes

In addition to the plasma membrane changes, which occur prior to implantation, the uterine epithelial cells undergo a transition from simple columnar cells, with oval basal nuclei, to simple cuboidal cells, with round central nuclei (Ljungkvist, 1972a). This displacement of the nuclei to a more central location is as a result of increased lipid and glycogen accumulation in the basal portion of the luminal epithelial cells (Poteat and Bo, 1971). The lipid accumulation is reported to be under the control of progesterone and oestrogen. In ovariectomised animals lacking hormonal therapy, lipid droplets are found below the nucleus with some located in other regions of the cytoplasm (Ljungkvist, 1971b; Hosie, 1997). Oestrogen administration results in a decrease in lipid accumulation (Ljungkvist, 1971a; Hosie, 1997), whereas progesterone markedly increases lipid accumulation (Ljungkvist, 1971c; Hosie, 1997).

Another characteristic change in cellular structure of the uterine epithelial cells is the appearance of electron-lucent apical vesicles around day 4.5 of pregnancy. The appearance of these small apical vesicles coincides with the formation of the pinocytotic pinopods (Parr and Parr, 1982). It has thus been suggested that these apical vesicles act to restore the plasma membrane internalised during pinocytotic/endocytotic activity, or to facilitate the transport of secretions to the uterine lumen (Nilsson and Lundkvist, 1979; Parr and Parr, 1982). These electron lucent apical vesicles develop in ovariectomised animals in response to progesterone alone, but not oestrogen and are at their greatest number when progesterone treatment is followed by initial priming of the endometrium by oestrogen. In addition, they are most numerous in the pregnant endometrium just prior to blastocyst implantation (Parr and Parr, 1982).

3.1.5 The Basal Plasma Membrane Transformation

During early pregnancy the basal plasma membrane has been reported to become more folded with a more tortuous outline with the progression of pregnancy from day 1 to day 6 (day 1 designated day of sperm in vaginal smear) (Shion and Murphy, 1995). There are discrepancies in the literature with regards to the hormonal control of the appearance of the basal plasma membrane. Shion and Murphy (1995) report that in both the ovariectomised rat uterus lacking hormonal replacement and that treated with oestrogen, the basal plasma membrane remained relatively smooth and uncomplicated. However,

Ljungkvist (1971a; 1971b) and Williams and Rogers (1980) described a folded basement membrane of the epithelial cells in the ovariectomised and oestrogen treated animals. Hosie (1997) indicated a convoluted basal plasma membrane in the ovariectomised animals with a smooth appearance in the oestrogen treated animals. Treatment with progesterone displayed a basal plasma membrane much more tortuous in appearance with numerous well-developed projections towards the subepithelial stromal compartment, suggesting that the transformation of the basal plasma membrane during early pregnancy is under the influence of the ovarian hormone progesterone (Ljungkvist, 1971c; Shion and Murphy, 1995; Hosie, 1997). The investigators suggested that the resultant increase in surface area may facilitate blastocyst implantation by providing a larger surface area for interaction with the implanting blastocyst prior to invasion into the stromal layer by breaching the basal plasma membrane (Shion and Murphy, 1995).

3.1.6 Decidualisation

Another consequence of the 'plasma membrane transformation' is that of the decidual cell reaction. This decidual cell reaction is thought to result by signal transduction from the uterine epithelial cells (Murphy, 1995). The transformation of the small, elongated stromal cells into large, round decidual cells is as a result of both structural and biochemical alterations of these cells (Shaw *et al.*, 1998) and is a maternal response rather than one induced by the blastocyst (Kramer *et al.*, 1993). Decidual cells are believed to function in the nourishment of the developing blastocyst (Shaw *et al.*, 1998) and restriction of endometrial invasion by the blastocyst (Loke *et al.*, 1995).

The prevention of blastocyst attachment and subsequent early pregnancy failure results if the crucial events of early pregnancy are not initiated and synchronised during the 'window of receptivity' (Carson *et al.*, 2000). It is hypothesised that one of the mechanisms through which the PRM, RU486, inhibits blastocyst implantation is by disrupting the precise priming of the endometrium for blastocyst implantation by the ovarian hormones oestrogen and progesterone.

In the rhesus monkey, a single dose of RU486 was described to alter the endometrial morphology, as evident by loss of the luminal microvilli and pinopods, smoothing of the uterine surface and reduction in the height of the luminal epithelial cells with marked changes in the shape and size of the nuclei (Sengupta *et al.*, 2003). Localised apoptosis in the luminal epithelial cells was also observed (Sengupta *et al.*, 2003). Rumpel *et al.* (1993) conducted a morphological study on the effects on long-term progesterone antagonists. Their study described increased apoptosis observed in both the luminal and glandular epithelia as a result of progesterone antagonism (Rumpel *et al.*, 1993). Most of the morphological changes they observed could be attributed to the inhibitory action of the anti-progestins (Rumpel *et al.*, 1993).

The lack of research on the morphological effects of RU486 on the endometrium prompted the current investigation.

3.2 RESULTS

3.2.1 Characterisation of Surface Ultrastructural Changes in the RU486-Treated Rat Uterus

All animals were injected intravenously with the high molecular weight dye, Pontamine Sky blue, prior to sacrificing. This dye localises to the implantation sites due to increased vascularisation and vascular permeability that occurs during early pregnancy (Psychoyos, 1973;1986). In the control pregnant animals, there were on average 5-7 implantation sites observed as prominent blue bands in each uterine horn. In animals treated with RU486, an average of 0-2 blue bands was localized in each uterine horn. The blue bands of the implantation sites in the RU486-treated animals were considerably narrower and more lightly stained than those in the control pregnant animals. The uterine horns of the treated animals that had a reduced number of implantation sites generally appeared similar to those of the control pregnant animals, as the horns were long, thin and rounded. The horns in the RU486-treated animals in which no implantation sites were observed, were contracted in length, expanded in width and also appeared oedematous (Scholtz *et al.*, 2008).

Table 3.1 provides an overview of the results obtained from the morphological analysis of the scanning electron micrographs with regards to each of the 6 characteristics used for comparison. Although dominant characteristics were apparent in the implantation and non-implantation sites of each group, some variations were observed (Scholtz *et al.*, 2008). Table 3.2 provides an overview of the results obtained from the morphological analysis of the transmission electron micrographs as set out in section 2.3.2.3.

3.2.1.1 Folding of the uterine surface

At the light microscopy level, using the Toluidine Blue semi-thin sections for analysis, the luminae of the control pregnant and RU486-treated animals generally displayed a smooth luminal surface within the implantation sites at all three days of pregnancy (Figure 3.1A). In the non-implantation sites the luminae were more irregular in appearance with folding of the uterine surface evident (Figure 3.1B). This irregular folding was also observed on an ultrastructural level, using scanning electron microscopy. The implantation sites, localised by Pontamine Sky blue, of each group were seen as smooth areas devoid of, or having very few small folds (Figure 3.1C). The non-implantation sites of both the control and treated animals showed similar deep transversal folds crossing the entire width of the uterine lumen (Figure 3.1D). In the uterine horns of animals treated with RU486 without localised implantation sites, low power micrographs revealed a more or less smooth endometrial surface,

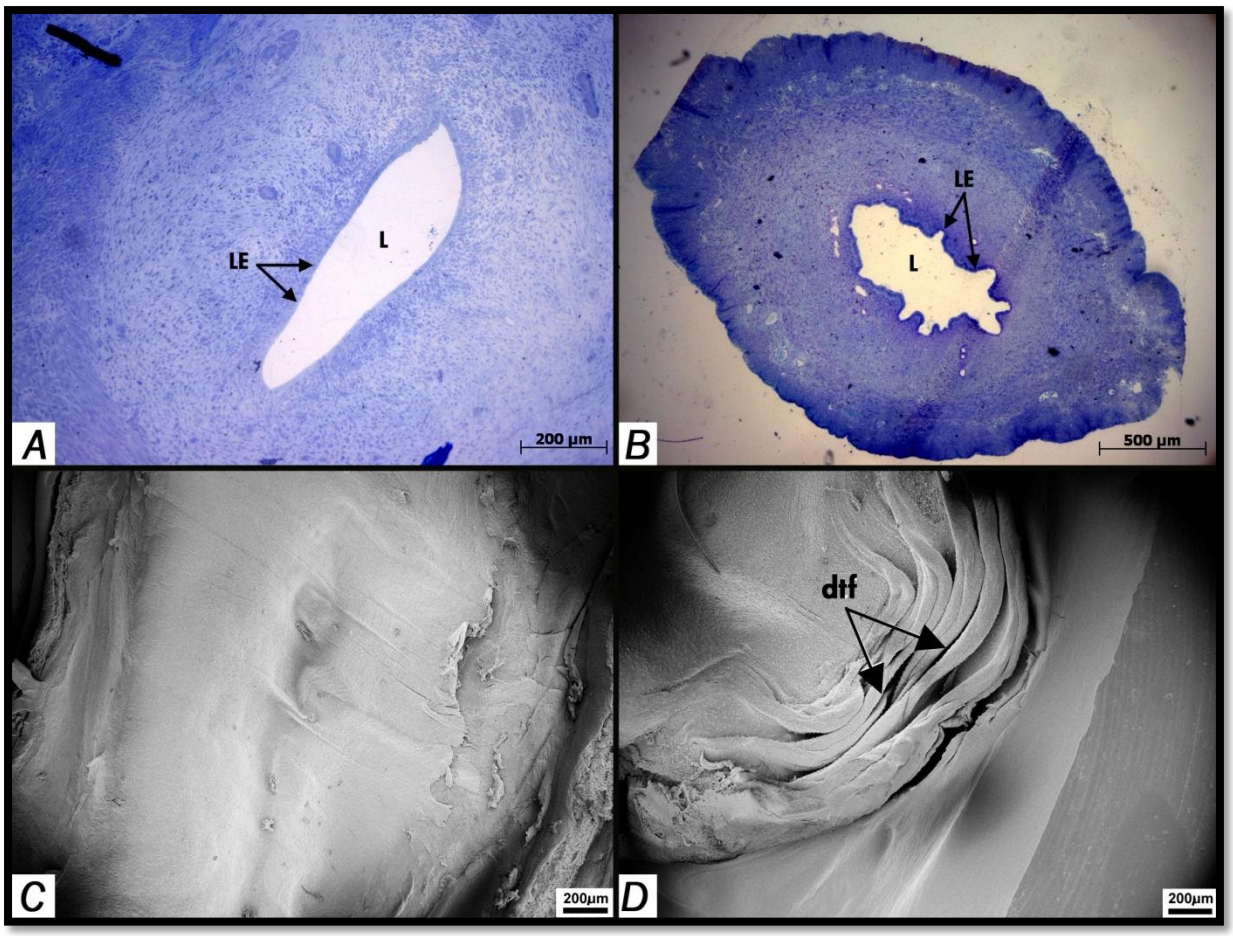


Figure 3.1 Morphology of the uterine surface of the pregnant rat uterus. (A and C) The smooth and regular uterine surface indicative of the implantation sites of the pregnant rat uterus. This smooth surface of the implantation sites was observed in both the control and RU486-treated animals. **(B and D)** The highly folded uterine surface indicative of the non-implantation sites of the pregnant rat uterus with visible deep transversal folds. This folding was seen in the non-implantation sites of both the control and RU486-treated animals. **L –** lumen; **LE –** luminal epithelium; **dtf –** deep transversal folds.

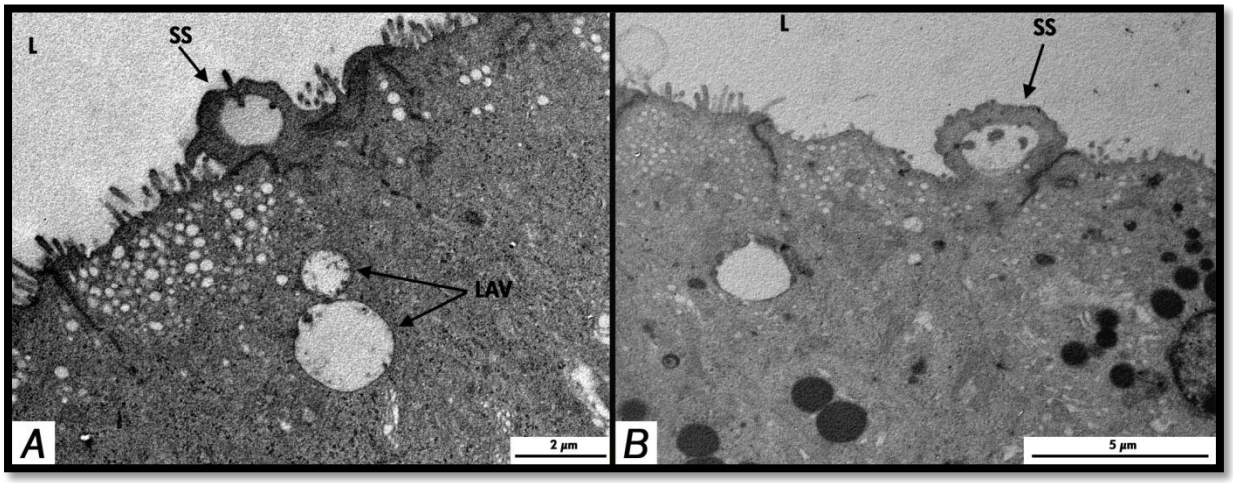


Figure 3.2 Ultrastructure of the small secretory droplets. (A and B) These small secretory droplets are observed at the periphery of the uterine epithelial cells. **L –** lumen; **SS –** small secretory droplets; **LAV –** large apical vesicle.

similar to those of the implantation sites of the control groups. In summary, if there was any localisation of Pontamine Sky blue, however faint, then folding of the uterine surface in the non-implantation sites was observed. If no localisation occurred, then the uterine surface was smooth in its entirety.

Table 3.1 Results table of the scanning electron microscopy analysis. The six luminal epithelial characteristics are as described in section 2.3.1.3, in both the implantation and non-implantation sites of the control pregnant (UT) and the RU486-treated animals (T) at days 4.5, 5.5 and 6.5 of pregnancy.

Treatment	Folding	Cell borders	Apices of cells	Microvilli concentration	Small secretions	Cell surface protrusions
4.5 UT IS	Smooth/ Few Folds	Flat/ Raised	Flat	Medium	Some	None
4.5 UT NIS	Folded	Flat	Flat	Medium/ Dense	Some/ Many	None
4.5 T IS	Smooth/ Few folds	Raised	Flat	Sparse/ Medium	Some	Few
4.5 T NIS	Few Folds	Raised	Flat	Medium	None	None
5.5 UT IS	Smooth	Flat	Flat/ Slightly Raised	Sparse/ Medium	None	None
5.5 UT NIS	Folded	Flat	Flat/ Slightly Raised	Medium/ Dense	Some	None
5.5 T IS	Smooth	Raised	Flat	Medium	Some/ Many	Some
5.5 T NIS	Very Folded	Flat	Slightly Raised	Medium/ Dense	Some	None/Some
6.5 UT IS	Smooth	Flat	Slightly Raised	Medium	Some	None
6.5 UT NIS	Few Folds/ Folded	Sunken/ Flat	Slightly Raised	Medium/ Dense	Many	None
6.5 T IS	Smooth/ Few folds	Flat/ Raised	Flat	Medium	Some	Few
6.5 T NIS	Very Folded	Flat	Flat	Medium	Some	Some

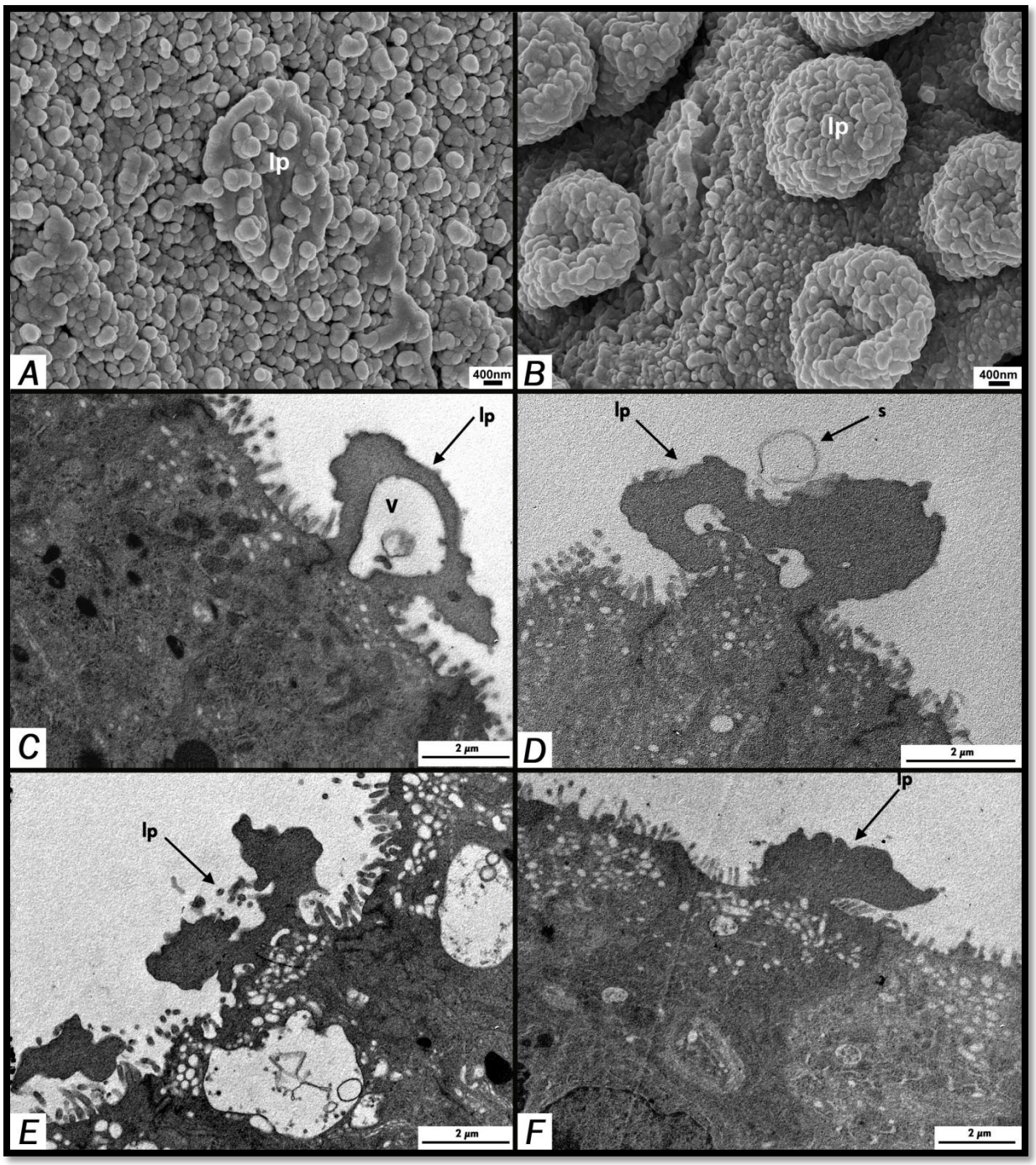


Figure 3.3 Electron micrographs of the large cell surface protrusions of the pregnant animals treated with RU486 at day 3.0 of pregnancy. (A and B) Scanning electron micrographs of the large cell surface protrusions that are raised above the uterine epithelial cell layer and have a surface covered by small microvilli-like projections. Scale bar 400nm. **(C)** Transmission electron micrograph of a large cell surface protrusion containing a vacuole **(v)**. **(D)** Transmission electron micrograph of a large cell surface protrusion releasing a vacuole into the luminal space **(s) (E)** Transmission electron micrograph of a large cell surface protrusion having released a vacuole into the luminal space **(arrow)**. **(F)** Transmission electron micrograph of a large cell surface protrusion cut through a different plane and thus not displaying an enclosed vacuole. **lp –** large cell surface protrusion; **v-** vacuole; **s –** secretion.

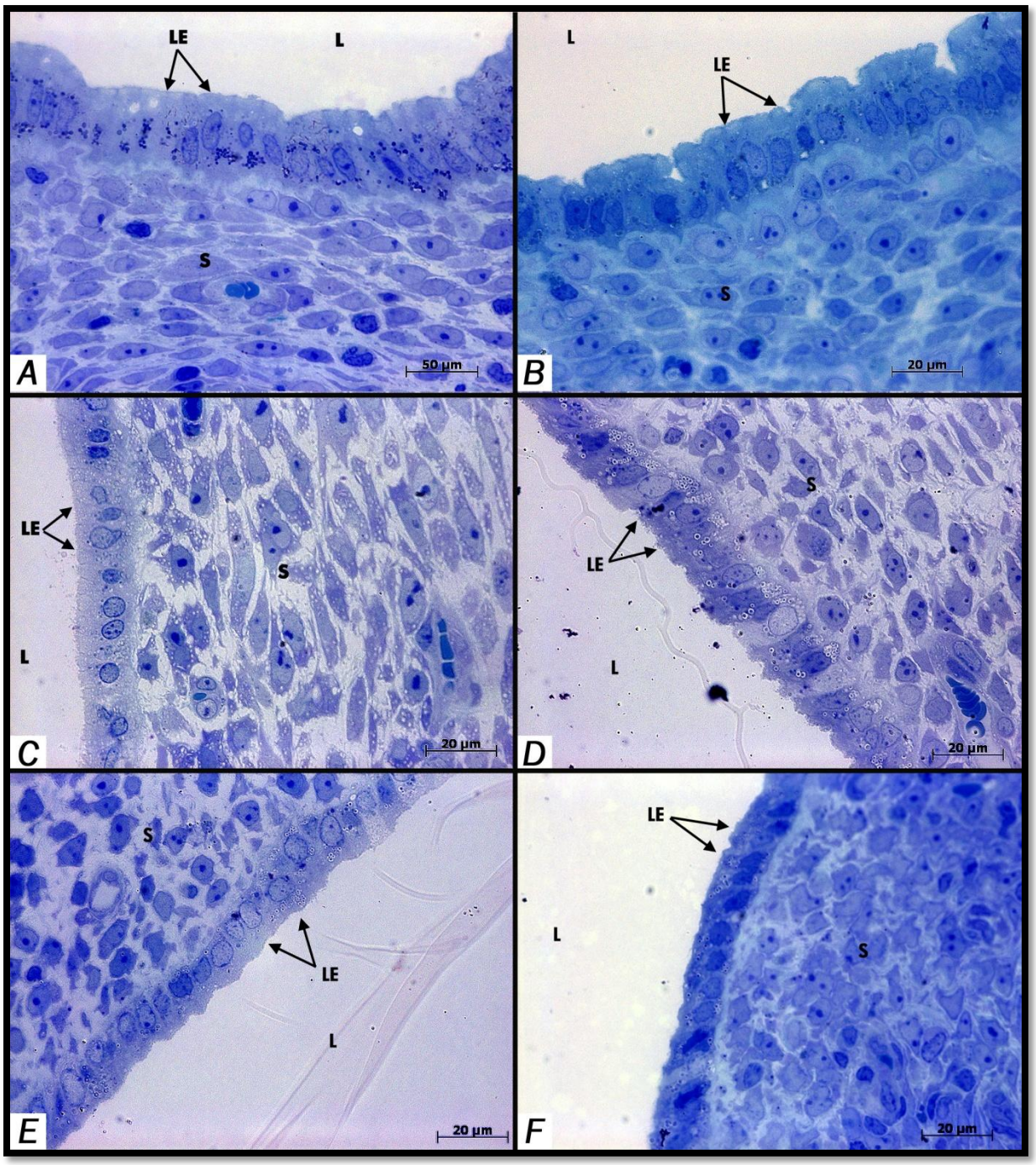


Figure 3.4 Toluidine Blue semi-thin sections of the control pregnant animals. (A) Implantation site at day 4.5 of pregnancy. **(B)** Non-implantation site at day 4.5 of pregnancy. **(C)** Implantation site at day 5.5 of pregnancy. **(D)** Non-implantation site at day 5.5 of pregnancy. **(E)** Implantation site at day 6.5 of pregnancy. **(F)** Non-implantation site at day 6.5 of pregnancy. **L –** lumen; **LE –** luminal epithelium; **S –** stroma.

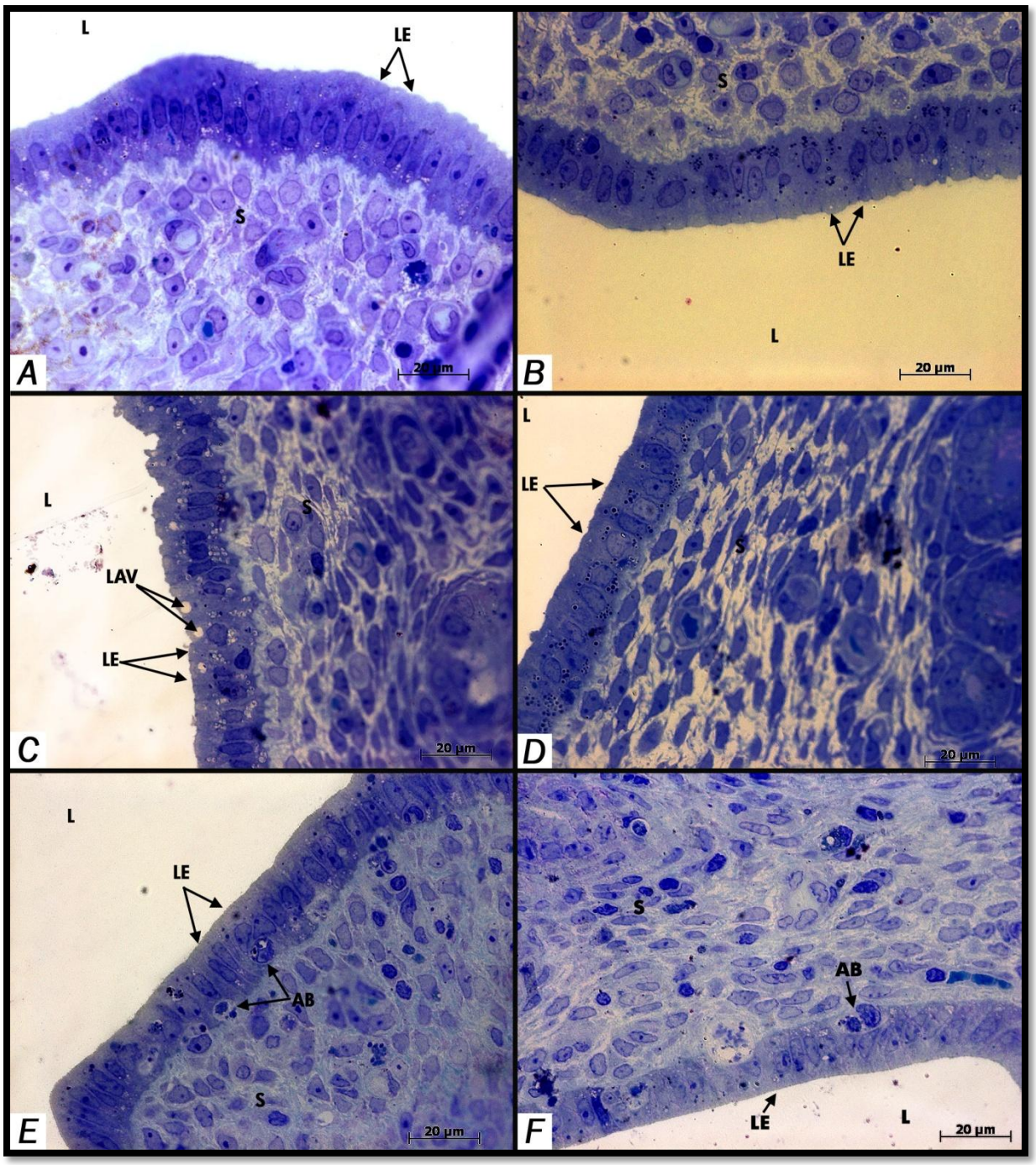


Figure 3.5 Toluidine Blue semi-thin sections of the RU486-treated animals. (A) Implantation site at day 4.5 of pregnancy. **(B)** Non-implantation site at day 4.5 of pregnancy. **(C)** Implantation site at day 5.5 of pregnancy. **(D)** Non-implantation site at day 5.5 of pregnancy. **(E)** Implantation site at day 6.5 of pregnancy. **(F)** Non-implantation site at day 6.5 of pregnancy. **L –** lumen; **LE –** luminal epithelium; **AB** – apoptotic bodies; **S –** stroma.

3.2.1.2 Luminal secretions

Analysis of the appearance of small, round, smooth secretory droplets seen near the periphery of the uterine epithelial cells by means of scanning electron microscopy revealed that in the implantation sites of the control pregnant animals, these small secretions were absent at day 5.5 of pregnancy (Figure 3.8C). At the same day of pregnancy in the RU486-treated animals, many of these secretions were seen in the implantation sites (Figure 3.9C). In all other groups, while these small secretions occurred, they were, most abundant in the implantation sites of the RU486-treated animals at day 5.5 of pregnancy, suggesting that RU486 results in a more secretory endometrium. These small secretory droplets located near the periphery of the luminal epithelial cells were also observed by transmission electron microscopy (Figure 3.2A and B). The secretion pattern of these droplets could not be analysed using this microscopy technique as the ultra thin sections are less than 1µm thick and are thus not indicative of the uterine luminal surface as a whole. As a result, these small secretory droplets were not observed in all transmission electron micrographs.

In addition to the small secretory droplets, large apical vesicles were observed in the apical portion of the luminal epithelial cells, as depicted in Figure 3.2A. These secretions were more abundant in both the implantation and non-implantation sites of the RU486-treated animals relative to the control pregnant animals at day 5.5 of pregnancy, the day of blastocyst implantation, suggesting a more secretory endometrium as a result of RU486 administration.

3.2.1.3 Large cell surface protrusions

Large cell surface protrusions were observed on the uterine epithelial cell surface in the treated groups by both scanning electron microscopy and transmission electron microscopy, but were absent in the control animals. These large cell surface protrusions appeared to be similar in composition to the rest of the apical membrane of the uterine epithelial cells and displayed small microvilli-like projections on their surfaces (Figure 3.3A and B).

Morphological analysis by scanning electron microscopy indicated that in the implantation sites of the RU486-treated animals, these large cell protrusions were generally not observed at day 4.5 of pregnancy. By day 5.5 of pregnancy there was an increase in the number of these protrusions, followed by a decrease by day 6.5 of pregnancy. In the non-implantation sites these large cell surface protrusions were present at days 4.5 to 6.5 of pregnancy. While this pattern was similar in the transmission electron microscopy analysis, in the implantation sites at day 6.5 of pregnancy, the number of these large cell surface protrusions did not appear to decrease. Using scanning electron microscopy, a large portion of the uterine surface can be observed, whereas with transmission electron microscopy only a thin section through the endometrium is analysed. This could account for the

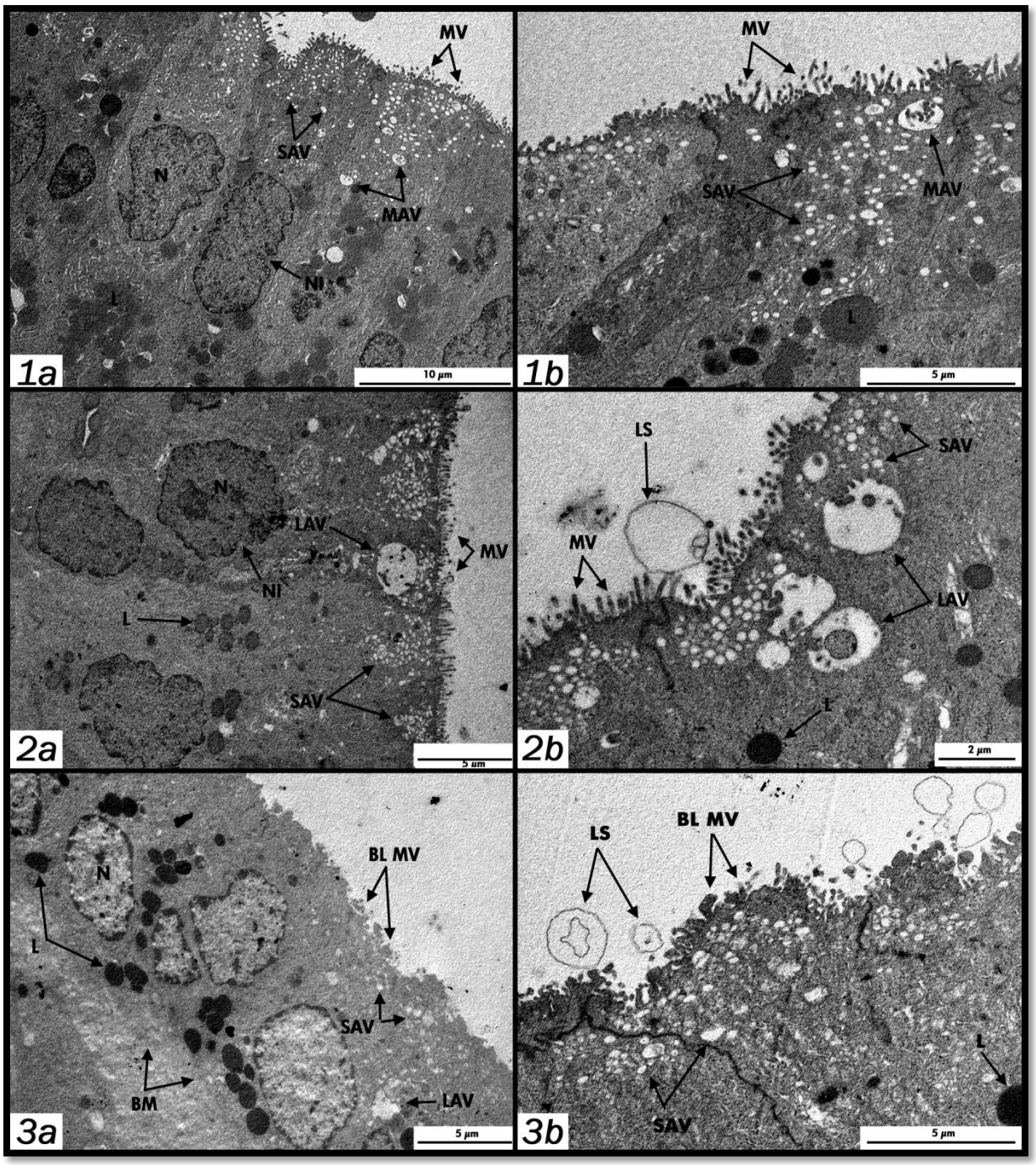


Figure 3.6 Low and high power micrographs of the control pregnant rat uterus. (1a and b) A low and high power micrograph of an implantation site at day 4.5 of pregnancy. **(2a and b)** A low and high power micrograph of a non-implantation site at day 4.5 of pregnancy. **(3a and b)** A low and high power micrograph of an implantation site at day 5.5 of pregnancy. **MV** – microvilli; **BL MV** – bleb-like microvilli; **LS** – luminal secretion; **SAV** – small apical vesicles; **LAV** – large apical vesicles; **N** – nucleus; **NI** – nuclear indentation; **L** – lipid droplets; **BM** – basal plasma membrane.

discrepancy observed in the abundance of the large cell surface protrusions observed between the two electron microscopy techniques.

Interestingly, in some transmission electron micrographs, these large cell surface protrusions appeared to contain large vacuoles enclosing a secretion (Figure 3.3C), whereas in others the secretion was being (Figure 3.3D) or had been released into the luminal space (Figure 3.3E). In other micrographs, these large cell surface protrusions did not appear to have a vacuole; possibly due to the plane of section, and the enclosed vacuole not being bisected (Figure 3.3F).

These large cell surface protrusions have previously been suggested to be resultant of an increase in apoptosis following RU486 administration (Scholtz *et al.*, 2008). In the RU486-treated animals, large vacuoles were observed that were dissimilar to those described in the previous section (Figure 3.11F). Combined with the identification of vacuoles in the large cell surface protrusions, it is suggested here that these large vacuoles are possibly secondary lysosomes and further that these apical protrusions are a functional cell surface modification serving to release lysosomal content into the lumen. Moreover, these surface protrusions may form in response to the RU486-induced increase in apoptosis.

3.2.1.4 Luminal epithelial cells

Analysis of the shape of the luminal epithelial cells by both transmission electron microscopy and Toluidine Blue light microscopy demonstrated columnar epithelial cells with centrally located, round to elongated, large nuclei in the implantation and non-implantation sites of the control pregnant animals at day 4.5 of pregnancy (Figure 3.4A and B; Figure 3.6.1a and Figure 3.6.2a). By day 5.5 of pregnancy, the epithelial cells had reduced in height and were low columnar in the implantation sites and low columnar to cuboidal in the non-implantation sites, with round, large, basally located nuclei (Figure 3.4C and D; Figure 3.6.3a and Figure 3.6.4a). With the progression of pregnancy, the epithelial cells continued to reduce in height and were low columnar to cuboidal with basally located, round, large nuclei in both the implantation and non-implantation sites at day 6.5 of pregnancy (Figure 3.4E and F; Figure 3.6.5a and Figure 3.6.6a).

RU486 administration appeared to inhibit this loss of epithelial cell height with the progression of pregnancy as the epithelial cells remained columnar at all three days of pregnancy, with the exception of within the implantation sites at day 5.5 of pregnancy, where the epithelial cells were columnar to low columnar in appearance. The nuclei of the epithelial cells in the RU486-treated animals moved to a basal location with the progression of pregnancy (Figure 3.5A-F; Figure 3.7.1a, .2a, .3a, .4a, .5a, .6a).

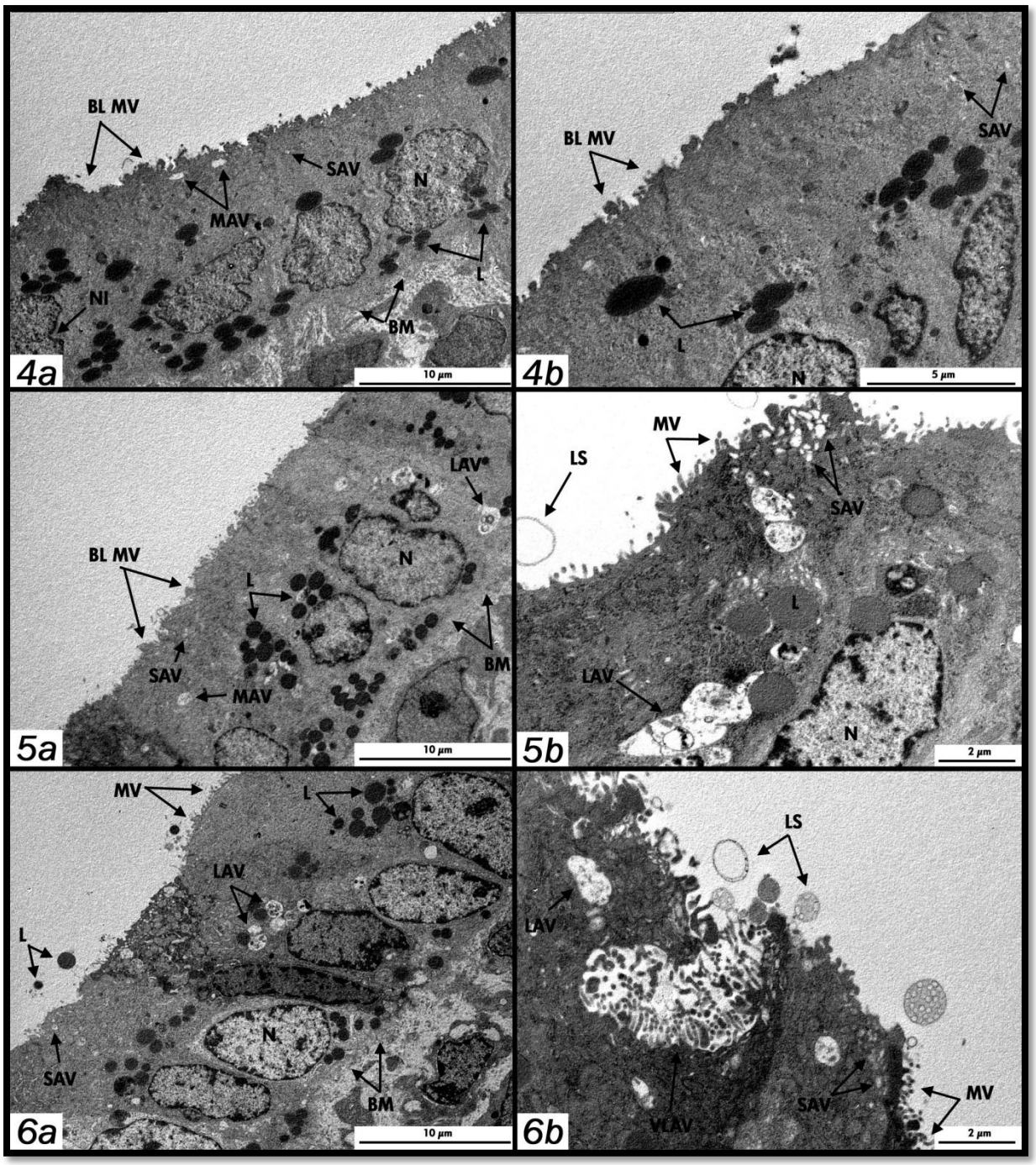


Figure 3.6 cont. Low and high power micrographs of the control pregnant rat uterus. (4a and b) A low and high power micrograph of a non-implantation site at day 5.5 of pregnancy. **(5a and b)** A low and high power micrograph of an implantation site at day 6.5 of pregnancy. **(6a and b)** A low and high power micrograph of a non-implantation site at day 6.5 of pregnancy. **MV** – microvilli; **BL MV** – bleb-like microvilli; **LS** – luminal secretion; **SAV** – small apical vesicles; **MAV –** medium apical vesicle; **LAV** – large apical vesicles; **VLAV –** very large apical vesicles; **N** – nucleus; **NI** – nuclear indentation; **L** – lipid droplets; **BM** – basal plasma membrane.

3.2.1.5 Microvilli concentration and appearance

The microvilli of both the control pregnant and RU486-treated animals were generally short in length at all days of pregnancy as revealed by scanning electron microscopy. While not much variation was seen in microvilli length from group to group, variation was observed in microvilli concentration. In the control animals the implantation sites displayed microvilli that were generally medium in concentration (Figure 3.8A and E), except at day 5.5 of pregnancy, when the microvilli were sparse to medium in concentration (Figure 3.8C). In contrast, within the non-implantation sites of the control animals, the microvilli were observed to be medium to dense (Figure 3.8B, D and F).

In the implantation sites of the treated animals, the microvilli were sparse at day 4.5 (Figure 3.9A) of pregnancy progressing to a medium concentration by day 5.5 (Figure 3.9C) and 6.5 (Figure 3.9E). In the non-implantation sites of the treated animals, the microvilli were generally medium in concentration (Figure 3.9B, D and F) (Scholtz *et al.*, 2008).

Transmission electron microscopy analysis indicated long, thin, regular microvilli in both the implantation and non-implantation sites at day 4.5 of pregnancy in the control pregnant animals (Figure 3.6.1b and Figure 3.6.2b). By day 5.5 of pregnancy, these microvilli were lost and had been replaced by irregular, short, bleb-like microvilli in both the implantation and non-implantation sites (Figure 3.6.3b and Figure 3.6.4b). As pregnancy progressed to day 6.5, this uneven, bleb-like appearance continued (Figure 3.6.5b and Figure 3.6.6b). In contrast, in the implantation sites the microvilli appeared longer relative to those at day 5.5 of pregnancy, as reported previously by Png and Murphy (1997) (Figure 3.6.3b and Figure 3.6.5b).

Following treatment with RU486, the microvilli remained thin and regular in both the implantation and non-implantation sites with the progression of pregnancy from day 4.5 to day 5.5; however, at day 5.5 of pregnancy the microvilli were shorter relative to those at day 4.5 of pregnancy in the RU486-treated animals (Figures 3.7.1b; .2b; .3b; .4b). By day 6.5 of pregnancy, the microvilli in the implantation sites remained long and thin (Figure 3.7.5b); being longer than those at day 5.5 of pregnancy, but somewhat shorter than those at day 4.5 of pregnancy. In the non-implantation sites, the microvilli had a more irregular, bleb-like appearance (Figure 3.7.6b).

3.2.1.6 Cell borders of the uterine epithelial cells

Scanning electron microscopy analysis delineated the cell borders of the implantation sites at day 4.5 of pregnancy in the control pregnant animals to be well defined and raised (Figure 3.8A). In a few sections, the cell borders did appear flat and indistinct. In the non-implantation sites at this day of pregnancy, the cell borders were generally flat and indistinct (Figure 3.8B). By day 5.5 of

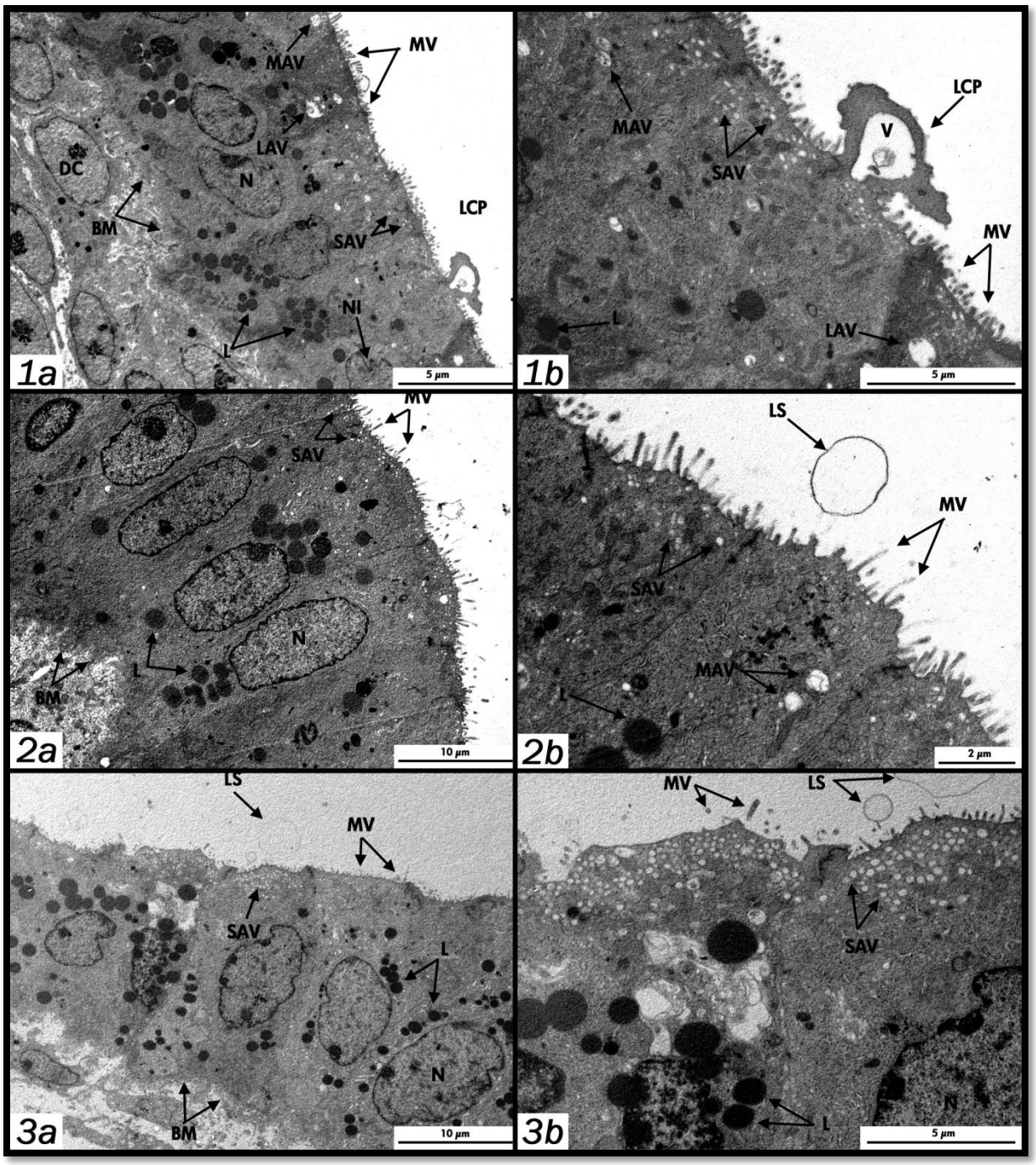


Figure 3.7 Low and high power micrographs of the RU486-treated pregnant rat uterus. (1a and b) A low and high power micrograph of an implantation site at day 4.5 of pregnancy. **(2a and b)** A low and high power micrograph of a non-implantation site at day 4.5 of pregnancy. **(3a and b)** A low and high power micrograph of an implantation site at day 5.5 of pregnancy. **MV** – microvilli; **LS** – luminal secretion; **LCP –** large cell surface protrusions; **SAV** – small apical vesicles; **MAV –** medium apical vesicles; **LAV** – large apical vesicles; **N** – nucleus; **NI** – nuclear indentation; **L** – lipid droplets; **BM** – basal plasma membrane.

pregnancy, the cell borders of both the implantation (Figure 3.8C) and non-implantation (Figure 3.8D) sites were generally more flat with some cells displaying more sunken cell borders. At day 6.5 of pregnancy, the cell borders of the implantation sites were observed to be flat and indistinct (Figure 3.8E), while in the non-implantation sites, the cell borders were quite flat to sunken (Figure 3.8F).

In the RU486-treated animals, the cell borders at day 4.5 of pregnancy were seen to be raised in both the implantation (Figure 3.9A) and non-implantation (Figure 3.9B) sites. By day 5.5 of pregnancy, the cell borders in the implantation sites were noted to be well defined and raised (Figure 3.9C), whereas those in the non-implantation sites were more flat and indistinct (Figure 3.9D). At day 6.5 of pregnancy, the cell borders were flat and indistinct to raised and well defined in the implantation sites (Figure 3.9E) and flat and indistinct in the non-implantation sites (Figure 3.9F) (Scholtz *et al.*, 2008).

3.2.1.7 Cell apices of the uterine epithelial cells

The uterine epithelial cells of all groups were generally hexagonal to oval in shape, when viewed from above by scanning electron microscopy. At day 4.5 in the control pregnant animals the cell apices were flat in both the implantation (Figure 3.8A) and non-implantation sites (Figure 3.8B). By day 5.5 of pregnancy, the cell apices were flat to slightly raised in both the implantation (Figure 3.8C) and non-implantation (Figure 3.8D) sites; and by day 6.5, they were slightly raised in both the implantation (Figure 3.8E) and non-implantation (Figure 3.8F) sites (Scholtz *et al.*, 2008). Transmission electron microscopy and light microscopy analysis indicated flat to slightly raised cell apices of the columnar luminal epithelial cells in the implantation sites at day 4.5 of pregnancy, with flat cell apices in the non-implantation sites (Figure 3.4A and B; Figure 3.6.1a and Figure 3.6.2a). By day 5.5 of pregnancy the cell apices of the columnar to cuboidal epithelial cells were flat to slightly raised in both the implantation and non-implantation sites (Figure 3.4C and D; Figure 3.6.3a and Figure 3.6.4a). As pregnancy progressed to day 6.5, the apices of the low columnar to cuboidal uterine epithelial cells were more raised to slightly raised in appearance in both the implantation and non-implantation sites (Figure 3.4E and F; Figure 3.6.5a and Figure 3.6.6a).

In the RU486-treated animals, the cell apices in the implantation (Figure 3.9A) and non-implantation (Figure 3.9B) sites at day 4.5 of pregnancy were flat as observed by scanning electron microscopy. By day 5.5 of pregnancy, the cell apices were flat in the implantation (Figure 3.9C) sites and slightly raised in the non-implantation (Figure 3.9D) sites. At day 6.5 of pregnancy, the cell apices were flat in both the implantation (Figure 3.9E) and non-implantation (Figure 3.9F) sites (Scholtz *et al.*, 2008). Transmission electron microscopy and light microscopy analysis indicated flat to slightly raised cell

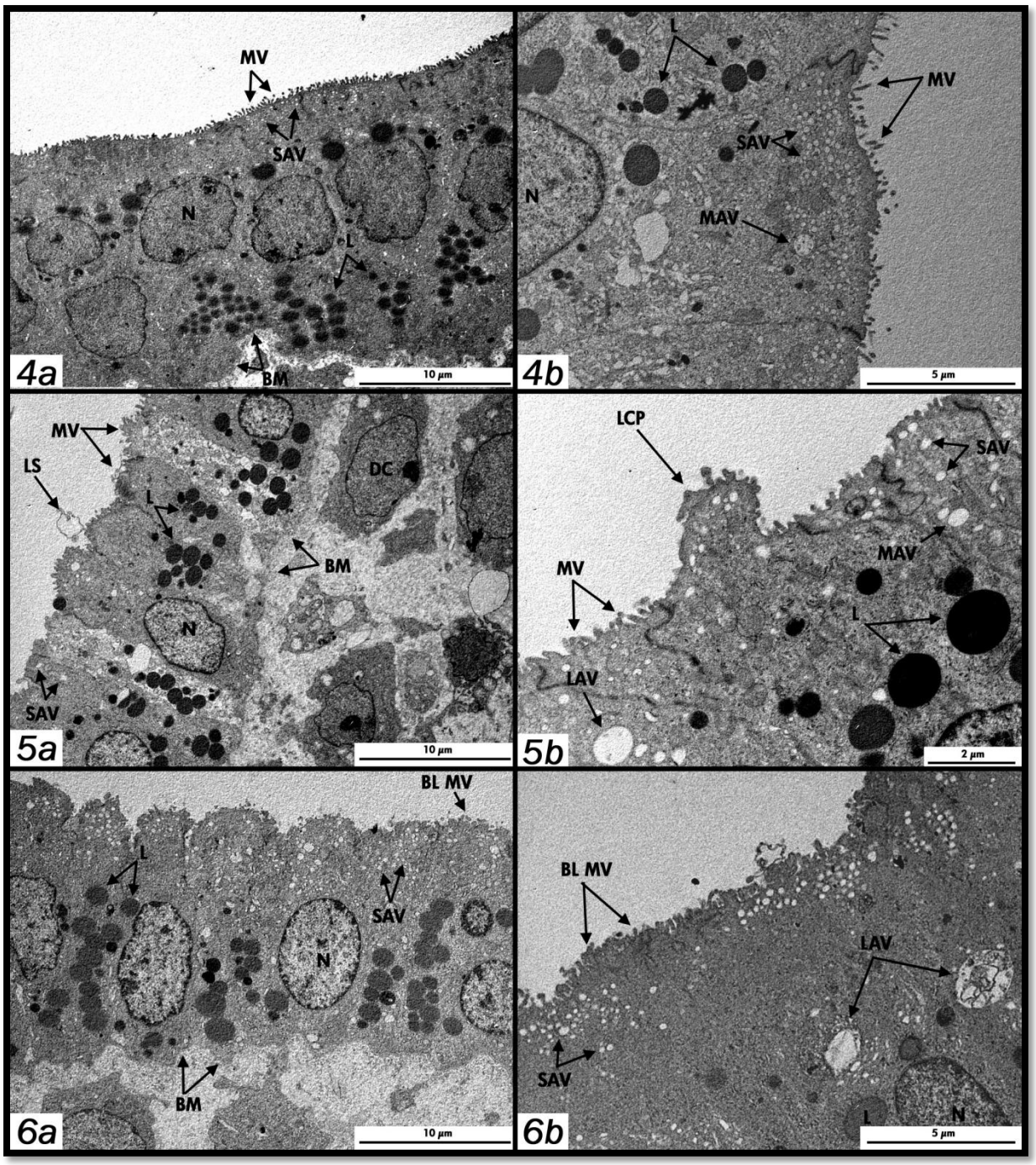


Figure 3.7 cont. Low and high power micrographs of the RU486-treated pregnant rat uterus. (4a and b) A low and high power micrograph of a non-implantation site at day 5.5 of pregnancy. **(5a and b)** A low and high power micrograph of an implantation site at day 6.5 of pregnancy. **(6a and b)** A low and high power micrograph of a non-implantation site at day 6.5 of pregnancy. **MV** – microvilli; **BL MV –** bleb-like microvilli; **LS** – luminal secretion; **LCP –** large cell surface protrusions; **SAV** – small apical vesicles; **MAV –** medium apical vesicles; **LAV** – large apical vesicles; **N** – nucleus; **L** – lipid droplets; **BM** – basal plasma membrane; **DC –** decidual cell.

apices of the columnar epithelial cells in the implantation sites of the RU486-treated animals at day 4.5 of pregnancy and raised to slightly raised cell apices in the non-implantation sites (Figure 3.5A and B; Figure 3.7.1a and Figure 3.7.2a). By day 5.5 and 6.5 of pregnancy, the cell apices of the columnar epithelial cells were mostly flat in both the implantation and non-implantation sites with a few slight apical bulges (Figure 3.5C-F; Figure 3.7.3a; Figure 3.7.4a; Figure 3.7.5a and Figure 3.7.6a).

3.2.1.8 Uterine epithelial cell lipids

Electron dense lipid droplets were observed by transmission electron microscopy within the uterine epithelial cells. At day 4.5 of pregnancy in the control pregnant animals, these lipid droplets were mostly observed in the basal and central portion of the uterine epithelial cells in both the implantation and non-implantation sites (Figure 3.6.1a and 3.6.2a). By day 5.5 of pregnancy, these electron dense lipid droplets had increased in number and were located in a perinuclear pattern in the low columnar to cuboidal uterine epithelial cells (Figure 3.6.3a and Figure 3.6.4a). As pregnancy progressed to day 6.5, these lipid droplets decreased in number and were mostly situated in the apical and basal portions of the uterine epithelial cells (Figure 3.6.5a and Figure 3.6.6a), suggesting that a number of these lipid droplets had migrated to the apical portion of the uterine epithelial cells. In some cases, lipid droplets could be seen within the luminal space (Figure 3.6.6a).

In the RU486-treated animals the lipid droplets were fewer and smaller relative to those observed in the control pregnant animals (Figures 3.7.1a, .2a, .3a, .4a, .5a, .6a). In addition, they were more scattered and sparse and not clustered as they were in the control pregnant animals with lipid droplets secreted into the luminal space in some cases. With the progression of pregnancy, the lipid droplets became more numerous in the RU486-treated animals (Figures 3.7.1a, .2a, .3a, .4a, .5a, .6a).

3.2.1.9 The Basal plasma membrane of uterine epithelial cells

At day 4.5 of pregnancy in the control pregnant animals, the basal plasma membrane of the uterine epithelial cells was irregular and wavy in appearance, with projections into the stroma as depicted in Figure 3.4A and B. With the progression of pregnancy, the basal plasma membrane became more and more regular (Figure 3.4C and D; Figure 3.4E and F). In the RU486-treated animals, a similar pattern was also observed. The basal plasma membrane was, however, more irregular in appearance, relative to the control pregnant animals at all three days of pregnancy (Figure 3.5A-F).

3.2.1.10 Decidual cells

In the control pregnant animals at all three days of pregnancy, the stromal cells had differentiated into large, fat, round cells indicative of the decidual response. This decidual layer was evident in both the implantation and non-implantation sites at all three days of pregnancy, with the exception of the non-

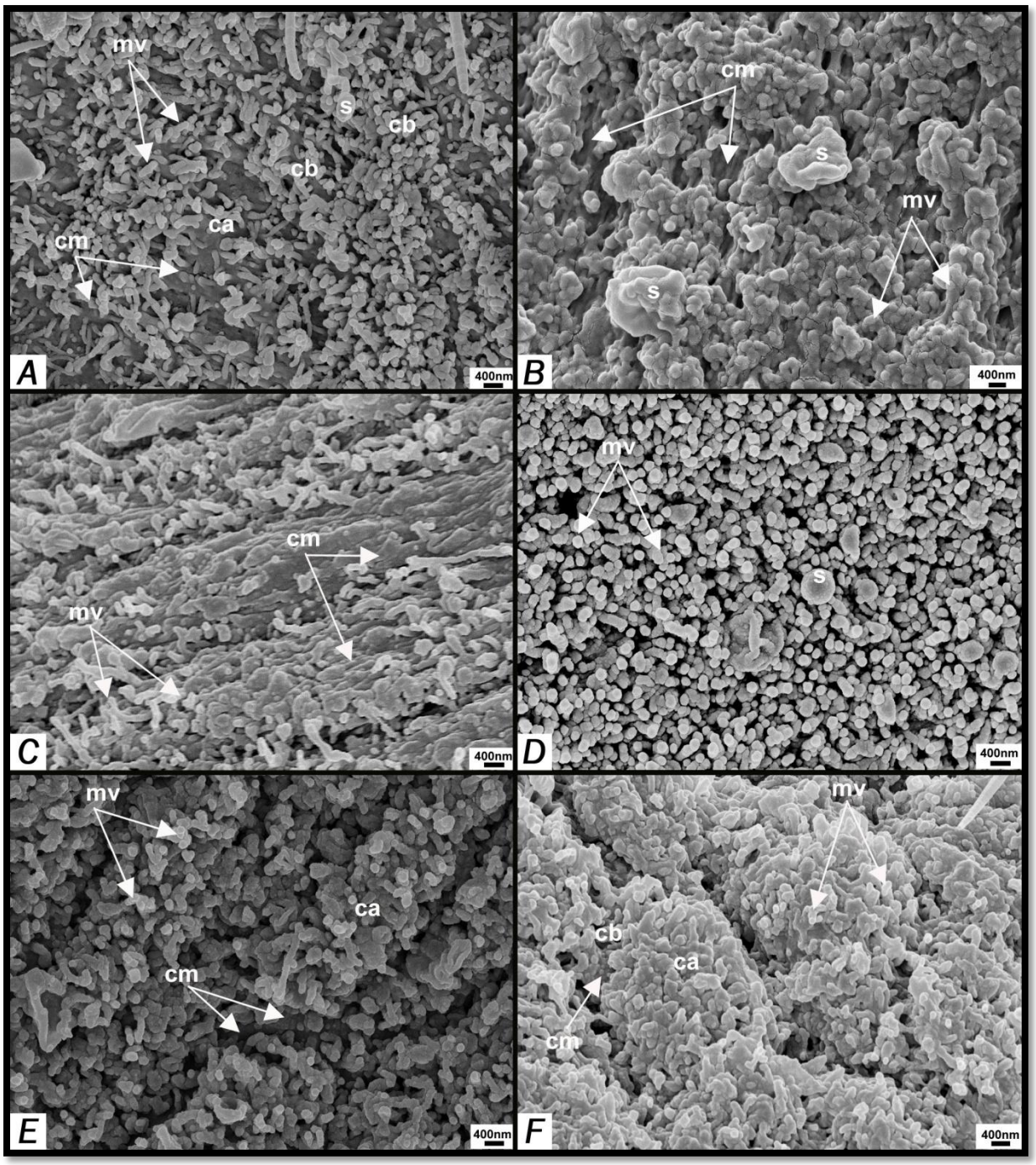


Figure 3.8 Scanning electron micrographs of the uterine epithelial cells at days 4.5, 5.5 and 6.5 of pregnancy in the rat uterus. (A) An implantation site at day 4.5 of pregnancy. **(B)** A non-implantation site at day 4.5 of pregnancy. **(C)** An implantation site at day 5.5 of pregnancy. **(D)** A non-implantation site at day 5.5 of pregnancy **(E)** An implantation site at day 6.5 of pregnancy. **(F)** A non-implantation site at day 6.5 of pregnancy. **ca –** cell apex; **cb –** cell border; **cm -** cell membrane; **mv –** microvilli; **s –** secretory droplet**.**
Scale bar = 400nm.

implantation sites at day 4.5 of pregnancy, where some elongated fibroblast stromal cells were still apparent (Figures 3.4A-F). At day 5.5 of pregnancy, the decidual cells appeared to be larger and rounder in the implantation sites relative to the non-implantation sites (Figures 3.4C and D).

In the RU486-treated animals, the decidual response was less pronounced. The small and indistinct decidual layer was comprised of small, round to elongated cells (Figures 3.5A-F).

3.2.1.11 Morphology of the glands

In the control pregnant animals the endometrial glands were analysed using Toluidine Blue semi-thin sections and were generally observed to be lined by a high cuboidal epithelium and displayed lumens that were closed or very small. At all three days of pregnancy, small vesicles were observed in the apical region of the glandular epithelial cells, giving the glands a vesicular appearance (Figures 3.10A, B and C).

In the RU486-treated animals at day 4.5 of pregnancy, the glands were more vesicular when compared to the control pregnant animals, lined by a low cuboidal epithelium and displayed large open luminae in both the implantation and non-implantation sites (Figure 3.10D). By day 5.5 of pregnancy, the luminae of the glands were less dilated and lacked the large apical vesicles in both the implantation and non-implantation sites observed at day 4.5 of pregnancy, but still contained smaller vesicles (Figure 3.10E). By day 6.5 of pregnancy, the diameter of the luminae of the glands had begun to reduce in both the implantation and non-implantation sites, becoming more like those observed in the control pregnant animals (Figure 3.10F).

3.2.1.12 Apoptotic bodies

One of the most striking observations in the transmission electron microscopy and light microscopy analysis was the marked increase in apoptotic cells, as evident by apoptotic bodies, within the luminal and glandular epithelial cells (Figures 3.11A-F). In the control pregnant animals, while a few apoptotic cells were observed, in the RU486-treated animals, a marked increase in apoptotic activity was noted with the progression of pregnancy, with the most apoptotic cells observed in the implantation sites at day 6.5 of pregnancy. This distinct increase in apoptotic activity, though mainly restricted to the luminal and glandular epithelial cells, was, nevertheless, observed in the stromal compartment.

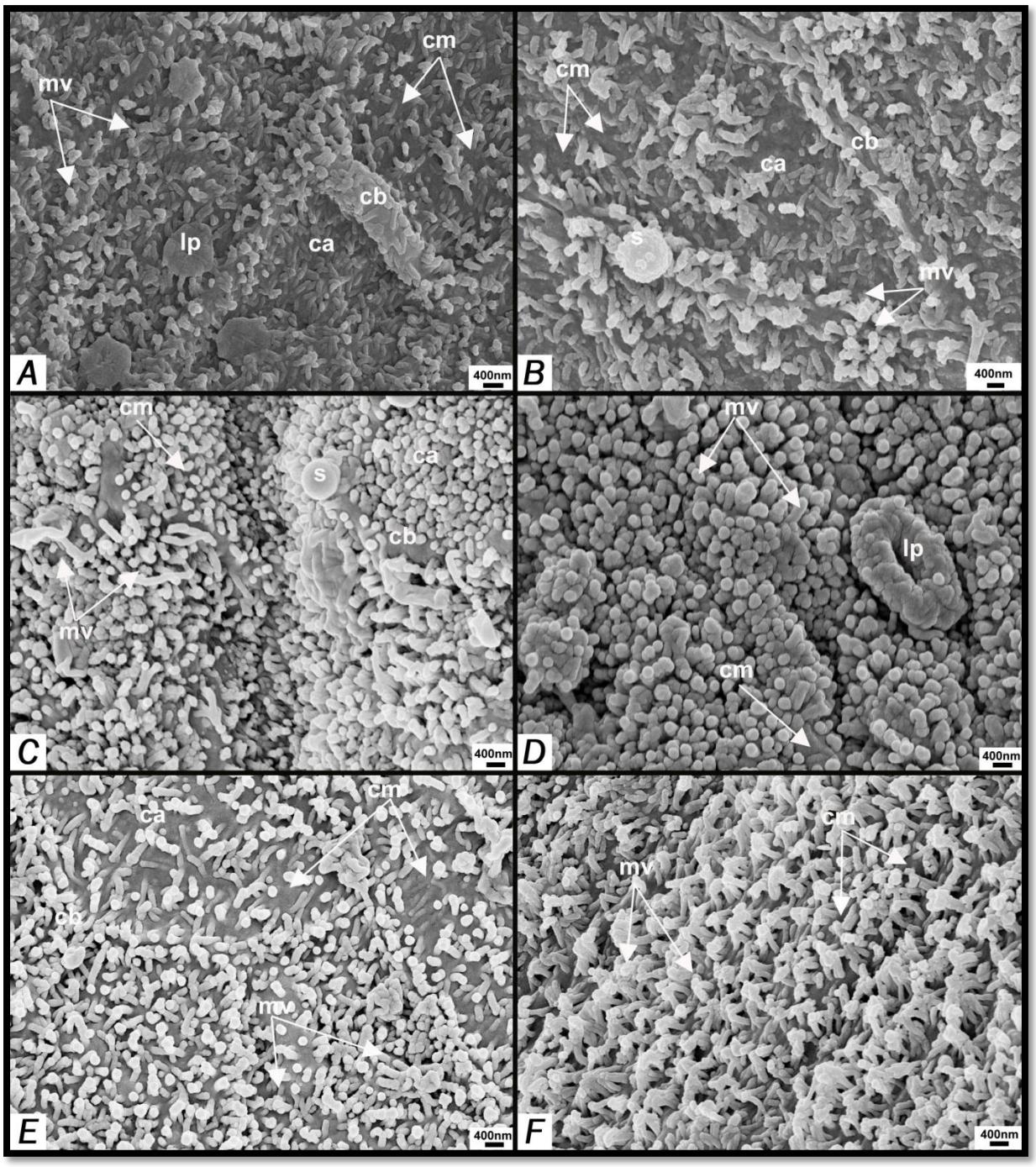


Figure 3.9 Scanning electron micrographs of the uterine epithelial cells at days 4.5, 5.5 and 6.5 of pregnancy, following treatment with RU486 at day 3 of pregnancy. (A) An implantation site at day 4.5 of pregnancy. **(B)** A non-implantation site at day 4.5 of pregnancy. **(C)** An implantation site at day 5.5 of pregnancy. **(D)** A non-implantation site at day 5.5 of pregnancy. **(E)** An implantation site at day 6.5 of pregnancy. **(F)** A non-implantation site at day 6.5 of pregnancy. **ca –** cell apex; **cb –** cell border; **cm -** cell membrane; **mv –** microvilli; **s –** secretory droplet; **lp** – large cell surface protrusion**.** Scale bar = 400nm.

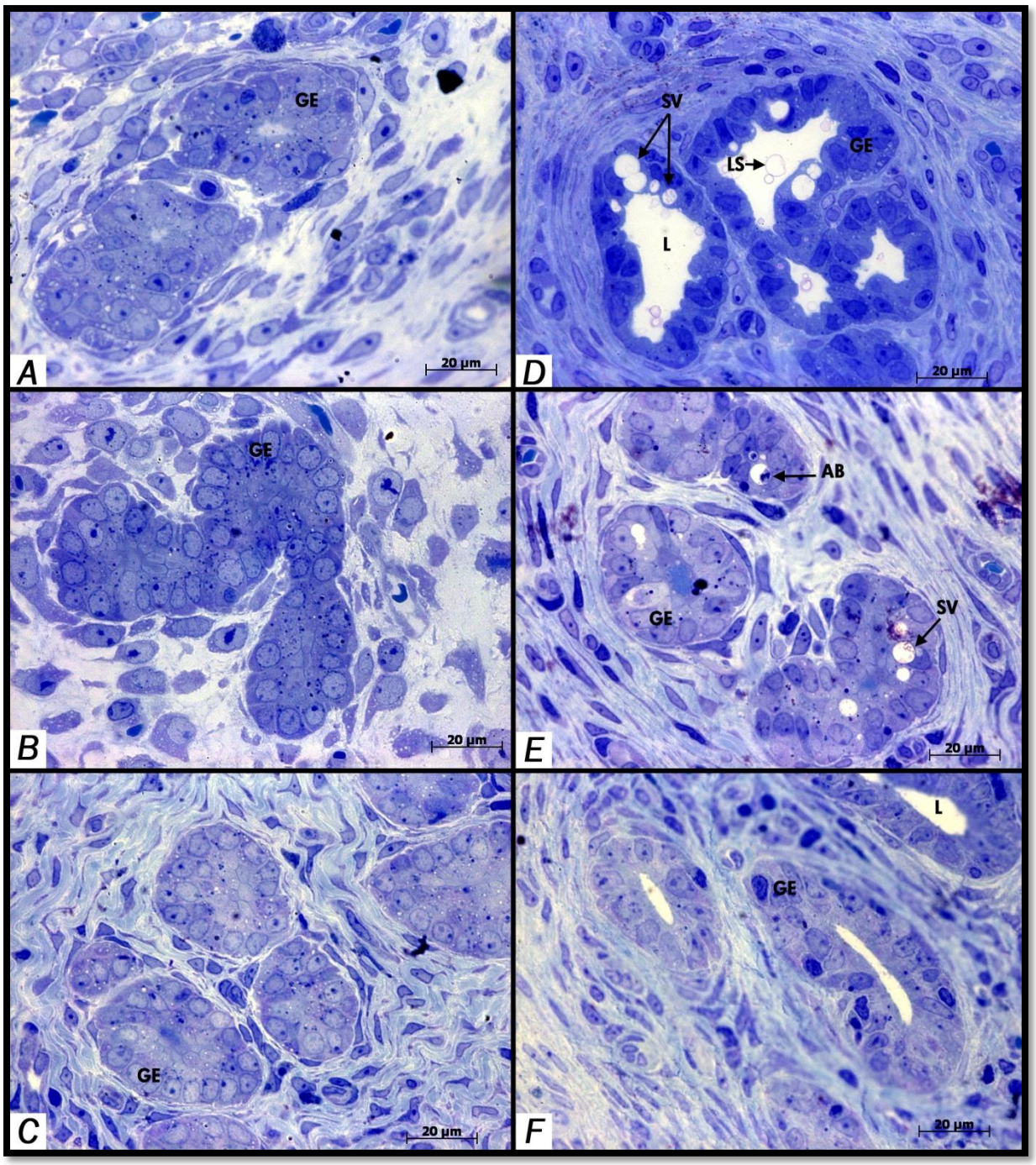


Figure 3.10 Toluidine Blue light microscopy images of the glandular epithelium in the control pregnant and RU486-treated endometrium. (A) Closed to slightly open, vesicular glands indicative of the control pregnant animals at day 4.5 of pregnancy. **(B)** Closed, slightly vesicular glands on the control pregnant animals at day 5.5 of pregnancy. **(C)** Closed, vesicular glands indicative of the control pregnant animals at day 6.5 of pregnancy. **(D)** Open, very vesicular glands of the RU486-treated animals at day 4.5 of pregnancy. **(E)** Slightly open, vesicular glands indicative of the RU486-treated animals at day 5.5 of pregnancy. **(F)** Open, slightly vesicular glands of the RU486-treated animals at day 6.5 of pregnancy. **GE –** glandular epithelium; **L -** lumen; **LS –** luminal secretion; **SV –** secretory vesicles; **AB –** apoptotic body.

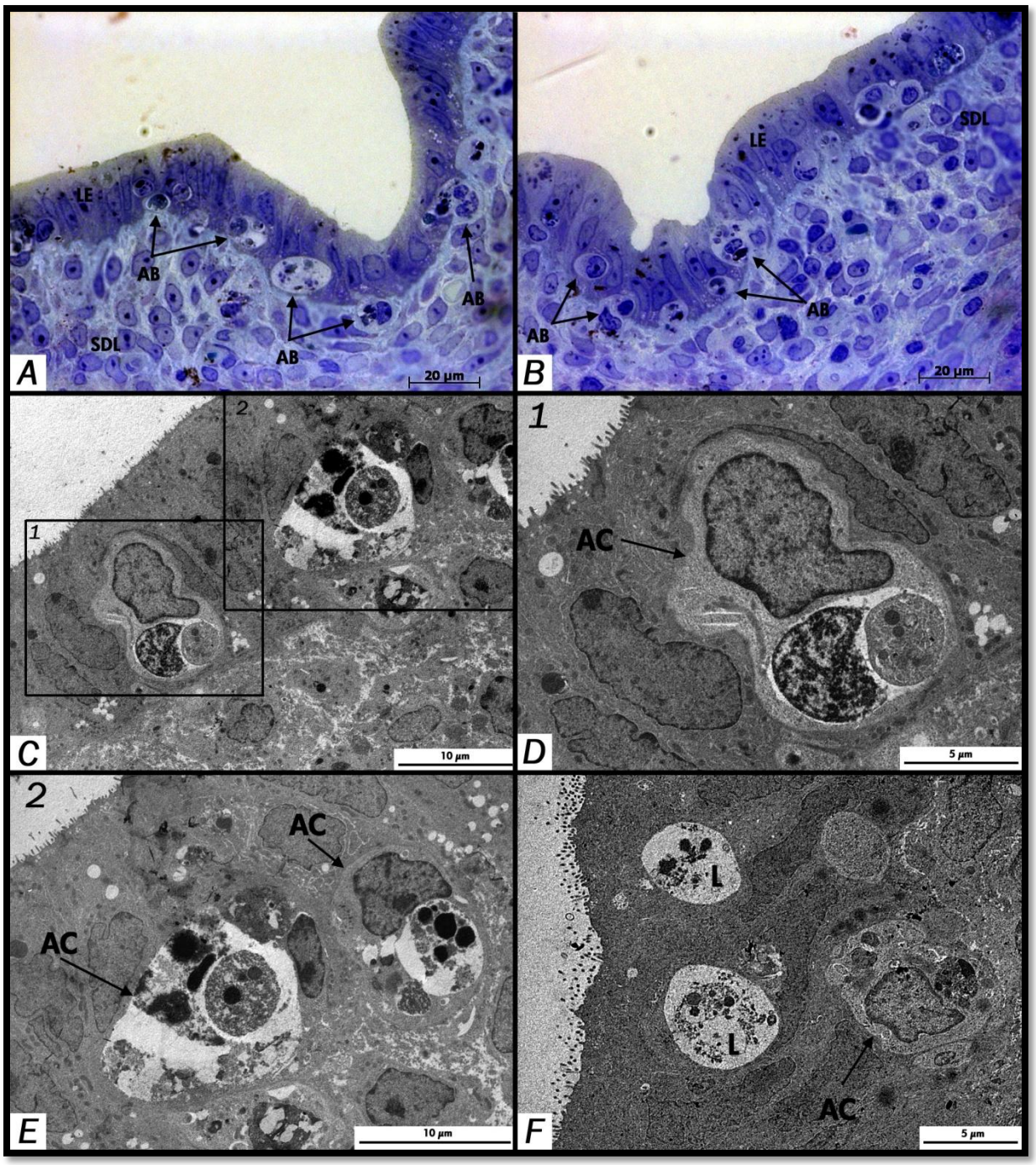


Figure 3.11 Light and transmission electron micrographs depicting the RU486-induced increase in apoptotic activity. (A and B) Toluidine Blue light micrographs of the luminal epithelial cells undergoing apoptosis as a result of RU486 administration. **(C, D and E)** Two cells at different stages of apoptosis. **(F)** Lysosomes containing apoptotic bodies moving towards the luminal surface, possibly to form large cell surface protrusions; indicative of the RU486-treated animals, as evident by bulging of the uterine surface above the lysosomes. **AB** – apoptotic body; **LE** – luminal epithelium; **SDL** – small decidual layer; **AC** – apoptotic cell; **L -** lysosome.

3.3 DISCUSSION

The process of blastocyst apposition and implantation fundamentally depends on the secretion of the ovarian hormones in a precise ratio at the right time (Psychoyos, 1973). Previous studies have shown that the partial progesterone blocker RU486 disrupts the implantation of the blastocyst in both the human and the rat endometrium (Psychoyos and Prapas, 1987; Bygdeman *et al.*, 1997; Marions *et al.*, 1998; Marions *et al.*, 2002; Danielsson *et al.*, 2003).

3.3.1 The Effects of RU486 on Vascular Permeability

Pontamine Sky blue localisation of the implantation sites, by prominent blue bands due to increased vascularisation of the implantation sites, is a well-documented process in rodents (Psychoyos, 1970;1973). This specific localisation of the implantation sites is only apparent from day 4.5 onwards, which coincides with the folding of the surface of the non-implantation sites (Winkelmann and Spornitz, 1997). The increased vascularisation and tissue permeability is reported to be under oestrogenic control (Curtis *et al*., 1999; Tan *et al*., 1999). In support of this, animals ovariectomised on day 4 of pregnancy failed to increase uterine vascularity within 24 hours, unless injected with oestrogen on the afternoon of day 4 (Psychoyos, 1970).

In the present study, the uterine tissue treated with RU486 prior to the implantation of the blastocyst showed morphological differences relative to the uterine tissue of normal pregnancy. Injection with Pontamine Sky blue prior to sacrificing of the animals revealed fewer and very faint blue bands of the implantation sites than in the control pregnant animals, with some uterine horns showing no blue bands. It appears that these animals did not develop, to the same extent, the increased vascularisation and permeability of early pregnancy and were thus unreceptive to blastocyst implantation (Scholtz *et al.*, 2008).

It is well-known that RU486 is able to bind to the PR, thus, at least partially blocking progesterone binding and subsequent progesterone effects on the endometrium (Sarkar, 2002). However, additional research has established the ability of RU486 to bind to the ER (Chwalisz *et al.*, 1995) and that it blocks oestrogen action with almost 80% efficacy, relative to the pure oestrogen antagonist ICI 164382 (McDonnell and Goldman, 1994). These results, combined with the reports that the increase in vascular permeability is under the control of the ovarian hormone oestrogen (Curtis *et al.*, 1999; Tan *et al.*, 1999), provide an explanation for the decrease in vascular permeability observed in the RU486-treated animals. The lack of this vascular response in ovariectomised animals (Psychoyos, 1970) supports the overall hypothesis of this study that RU486 results in a hormonally under-stimulated endometrium rather than an endometrium characteristic of unopposed oestrogen.

That the occurrence of the increase in vascular permeability coincides with an increase in progesterone signalling in the endometrium (Psychoyos, 1961;1973), suggests that progesterone plays an important role in the increase in vascular permeability of early pregnancy. Previous reports indicate that this vascular event is under the control of the ovarian hormone oestrogen (Curtis *et al.*, 1999; Tan *et al.*, 1999; Ma *et al.*, 2001) and that progesterone has little effect on this event (Ma *et al.*, 2001). However, it is well-known that progesterone and oestrogen are closely intertwined in effecting the changes necessary for blastocyst implantation to occur (Feil *et al.*, 1972; Leavitt *et al.*, 1977; Graham and Clarke, 1997; Curtis *et al.*, 1999; Hewitt and Korach, 2000a). It can thus be postulated that the oestrogenic-regulation of the increase in vascular permeability observed around day 5 of pregnancy is possibly triggered by progesterone signalling. If this is the case, then blocking progesterone signalling by RU486 may, in turn, inhibit this triggering of oestrogen-induced vascular permeability, resulting in the observed lack of this vascular event subsequent to RU486 administration.

3.3.2 The Effects of RU486 on Uterine Folding

A study by Winkelmann and Spornitz (1997) reported the occurrence of deep transversal folds seen specifically in the surface of the non-implantation sites of the endometrium. Moreover, the folding of the uterine endometrial surface was not evident in tissue fixed by immersion, but only in tissue fixed by perfusion. It was therefore suggested that perfusion fixation probably represented a functional state maintained *in vivo* by myometrial action (Winkelmann and Spornitz, 1997). However, the results of the present study contradict these findings, as the folding of the uterine surface was present, despite the use of immersion fixation of the tissue. With respect to hormonal signalling, as this folding was observed in both the RU486-treated and control pregnant animals, it can be concluded that surface folding of the endometrium is not influenced by progesterone or oestrogen alone, as ERs are also partially occupied by RU486 (Chwalisz *et al.*, 1995).

Treatment of ovariectomised rats with oestradiol alone has previously been shown to stimulate prominent folding of the uterine surface (Hosie and Murphy, 1992;1995b;a). However, additional studies have established a co-relationship between progesterone and oestrogen, wherein signalling from both hormones during early pregnancy function to establish a receptive uterus (Feil *et al.*, 1972; Graham and Clarke, 1997; Curtis *et al.*, 1999; Tan *et al.*, 1999; Hewitt and Korach, 2000a). It is interesting to note that in the uterine horns in which blue bands were absent, surface folding was not evident, supporting the hypothesis that the oestrogenic action resulting in the uterine surface folding at the non-implantation sites is dependant on interaction with, or priming by progesterone, or regulation by a down-stream event. It is important to note that the prominent folding of the uterine surface following oestradiol treatment of ovariectomised animals is not restricted to specific areas, such as in the pregnant animals, but rather appears along the entire length of the uterine horn (Hosie and Murphy, 1992;1995b;a).

Alternatively, the lack of surface folding in the RU486-treated animals could be due to a lack of oestrogen stimulation as a result of the ability of RU486 to bind to ERs and partially block oestrogen effects (see McDonnell and Goldman, 1994; Chwalisz *et al.*, 1995; Chwalisz *et al.*, 1998). The appearance of folding in the areas of the uterine horns of the RU486-treated animals in which faint blue bands were seen can be attributed to the inability of RU486 to completely block oestrogen action (McDonnell and Goldman, 1994; Chwalisz *et al.*, 1995; Chwalisz *et al.*, 1998). Ovariectomised animals display a uterine surface that is smooth in appearance (Hosie and Murphy, 1992;1995b;a) suggesting that RU486 results in a uterus under-stimulated by hormones rather than an oestrogen-stimulated uterus. These results suggest that the folding of the uterine horn is another pathway that RU486 disrupts, and is possibly one of the mechanisms responsible for the ability of RU486 to effectively prevent pregnancy.

3.3.3 The Effects of RU486 on the Plasma Membrane Transformation of Early Pregnancy

The well-documented plasma membrane transformation (PMT) of early pregnancy has been reported to be an integral part of successful priming of the uterus for blastocyst implantation (Enders and Schlafke, 1967; Cowell, 1969; Tachi *et al.*, 1970; Ljungkvist, 1972a;b; Murphy and Shaw, 1994; Murphy, 2004). The changes that occur in the apical plasma membrane comprise a flattening of the uterine epithelial cells with regards to the cell apices and cell borders, a change in microvilli length and density as pregnancy progresses and a loss of small secretory droplets seen near the periphery of the uterine epithelial cells. When progesterone and oestrogen act together to prime the uterus for blastocyst implantation the long, thin regular microvilli characteristic of oestrogen predominance during oestrous and the first days of pregnancy are gradually replaced by shorter more irregular microvilli as progesterone becomes the predominant ovarian hormone (Enders and Schlafke, 1967; Tachi *et al.*, 1970; Murphy and Shaw, 1994). It has been clearly shown that these changes are necessary to ensure the blastocyst comes into close appositional contact with the maternal endometrium (Psychoyos, 1973;1986) and for subsequent implantation to occur (Ljungkvist, 1972a;b; Murphy and Shaw, 1994).

In the present study the results obtained in the control pregnant animals were in accordance with these earlier studies. By day 6.5 of pregnancy in the control pregnant animals, the irregular, bleb-like microvilli of the day 5.5 pregnant uterine epithelial cells appeared to be slightly longer, suggesting that with the progression of pregnancy, these bleb-like microvilli are replaced again by the long, thin, regular microvilli of the pre-implantation stage. In agreement with this observation, Png and Murphy (1997) showed that the microvilli appear on the apical surface soon after blastocyst implantation has occurred and the window of receptivity is lost. This reformation of the microvilli has been described

in pseudopregnant animals, suggesting a role for the ovarian hormones rather than the blastocyst itself (Png and Murphy, 2000).

In the animals treated with RU486, the uterine epithelial cells were generally morphologically similar to that of a hormonally under-stimulated uterus. The cellular features described here, include a smooth uterine surface, flat cell apices, clearly defined cell borders, sparse, short, blunt microvilli and a few secretory droplets seen at the periphery of the uterine epithelial cells (Hosie and Murphy, 1992; Luxford and Murphy, 1992; Hosie and Murphy, 1995b;a).

As, in the present study, such features were clearly present in the uteri of the drug treated animals on day 4.5 of pregnancy, it is hypothesized that at this time point, RU486 inhibits progesterone signaling due to its marked affinity for binding to the PR and thus exclusion of progesterone binding. In relation to the lack of oestrogen effects, two hypotheses can be postulated. Either oestrogen is unable to exact its effect at such a small dose without initial priming of the uterus by progesterone, as oestrogen and progesterone are closely intertwined to effect the changes in the uterus necessary for implantation to occur (Feil *et al.*, 1972; Leavitt *et al.*, 1977; Graham and Clarke, 1997; Curtis *et al.*, 1999; Hewitt and Korach, 2000a). Alternatively, RU486 has been reported to block oestrogen effects within the endometrium (McDonnell and Goldman, 1994; Chwalisz *et al.*, 1995; Chwalisz *et al.*, 1998), which would account for the hormonally under-stimulated endometrium observed within the current study.

By days 5.5 and 6.5 of pregnancy in the treated animals, the uterus had a more progesterone stimulated appearance, with flat cell apices, raised cell borders, short dense microvilli and many small secretions, especially at day 5.5 of pregnancy. These features observed here, are quite typical of a progesterone-stimulated uterus (Hosie and Murphy, 1992; Luxford and Murphy, 1992; Hosie and Murphy, 1995a;b).

It is suggested that the appearance of this progesterone-stimulated uterus relates to the half-life of RU486. As RU486 has a half-life of 4h, it can be postulated that by day 5.5 of pregnancy, some progesterone would be able to bind to those PR not occupied by RU486. This would then lead to a more progesterone-stimulated uterus, rather than a hormonally under-stimulated uterus.

3.3.4 The Effects of RU486 on the Luminal Epithelial Cells

In the normal cycling control pregnant rat endometrium, the luminal epithelial cells were low columnar to cuboidal in shape; however, following long-term treatment with the progesterone antagonist, the luminal epithelial cells became high columnar in shape (Rumpel *et al.*, 1993). The increase in luminal epithelial height as a consequence of progesterone antagonist administration was also observed in the present study; where the luminal epithelial cells were more columnar in

appearance in the RU486-treated animals relative to the low columnar to cuboidal epithelial cells observed in the control pregnant animals.

Rumpel *et al.*(1993) hypothesised that this increase in cell height was due to unopposed oestrogen-regulated proliferation of the luminal epithelial cells, since progesterone regulates this increase in proliferation due to oestrogen action (Clarke and Sutherland, 1990). However, the results of the present study led to the formulation of the hypothesis that RU486 results in a hormonally under-stimulated endometrium rather than an unopposed oestrogen-regulated endometrium due to the similarities in appearance of the RU486-treated endometrium and the endometrium of ovariectomised animals lacking hormone replacement (Ljungkvist, 1971a;b; Hosie and Murphy, 1992; Luxford and Murphy, 1992; Hosie and Murphy, 1995a;b; Hosie, 1997).

An additional hypothesis to consider for the ultrastructural differences in the RU486-treated animals is the decrease in LIF protein and mRNA levels following treatment with RU486. In LIF-null mice at days 4 to 5 of pregnancy the luminal epithelial cells were observed to be columnar in shape, similar to wild-type animals at days 2 to 3 of pregnancy, but with a more domed apical surface. The luminal epithelial cells in the LIF-null mice also remained microvillous up to day 7 of pregnancy (Fouladi-Nashta *et al.*, 2005).

3.3.5 The Effects of RU486 on the Lipid Droplets

In the ovariectomised animal model, lipid droplets have been described in the cytoplasm of the uterine epithelial cells (Ljungkvist, 1971b; Hosie, 1997). Treatment with oestrogen is reported to decrease this accumulation and progesterone to increase it (Ljungkvist, 1971a; Hosie, 1997). Thus the decrease in lipid droplets observed in the RU486-treated animals can be attributed to the loss of progesterone stimulation of the uterine epithelial cells as a result of the inability of progesterone to bind to its receptor. In agreement with this finding, long-term treatment with a progesterone antagonist reduced the lipid content considerably in the rat endometrium (Rumpel *et al.*, 1993).

With the progression of pregnancy in the RU486-treated animals, the lipid droplets increased in number, most likely as a result of the half-life of RU486, as described previously, and the subsequent re-establishment of progesterone signalling in the endometrium.

3.3.6 The Effects of RU486 on the Basal Plasma Membrane

Surprisingly, in the RU486-treated animals the basal plasma membrane was observed to be highly convoluted with numerous finger-like projections into the stromal compartment. The expected result was to observe a smooth basal plasma membrane as the transformation of this membrane is regulated by progesterone (Ljungkvist, 1971c; Shion and Murphy, 1995; Hosie, 1997).

This discrepancy can possibly be attributed to the hypothesis that RU486 results in an endometrium hormonally under-stimulated (Scholtz *et al.*, 2008), as Ljungkvist (1971b) and Hosie (1997) report a convoluted basal plasma membrane in the ovariectomised animal model. This is in contrast to Shion and Murphy (1995) who reported a smooth basal plasma membrane in the ovariectomised rat.

3.3.7 The Effects of RU846 on the Large Cell Surface Protrusions

A particularly interesting finding of this study was the occurrence of large cell surface protrusions, seen only in the tissue treated with RU486. Further, these protrusions increased in frequency as pregnancy progressed to day 5.5. Such structures have not previously been documented and further, no studies of progesterone administration to ovariectomised animals have mentioned such apical protrusions. Moreover, these protrusions were morphologically dissimilar to and larger than pinopods described by Adams *et al.* (2002).

While it would seem that RU486 plays a role in the presence of these protrusions on the endometrial surface, their possible function, if any, is unknown. They may, however, be an indication of increased epithelial apoptosis or necrosis due to the inhibition of progesterone binding, or may relate to a toxic effect of RU486 (Scholtz *et al.*, 2008). In partial support of this view, RU486 induced apoptosis, while progesterone suppressed it in rabbit uterine epithelial cells (Rotello *et al.*, 1992). However, as this study did not perform scanning electron microscopy morphological studies, it is unknown whether these apical protrusions were present or not. Nevertheless, Rotello *et al.* (1992) noted an increase in apoptosis of the uterine epithelium of pseudopregnant rabbits following RU486 administration. Thus, the observed increase in the cell surface protrusions seen in the present study, with the progression of pregnancy to day 5.5, could well be explained by an increase in apoptosis. This premise would, however, clearly require investigation of the expression of apoptotic markers, other than Bax and Bcl-2 at this time (see Chapter 5).

3.3.8 The Effects of RU486 on Glandular Morphology

The glands in the RU486-treated animals were highly secretory with dilated luminae at day 4.5 of pregnancy. This increase in lumen diameter has previously been described as a direct consequence of long-term treatment with progesterone antagonists; however, no explanation was provided (Rumpel *et al.*, 1993). The endometrial glands play an important role in the establishment of early pregnancy, as evident by peri-implantation pregnancy loss in the uterine gland knockout (UGKO) ewe model (Gray *et al.*, 2000; Gray *et al.*, 2001; Gray *et al.*, 2002). It is postulated that the endometrial glands synthesise, secrete or transport substances that are necessary for the survival and development of a viable blastocyst during the first stages of early pregnancy, prior to implantation (for a review see Carson *et al.*, 2000).

Glandular morphology was altered as a result of RU486 administration in the current research. It is unclear as to what the consequences of these changes in glandular morphology are; however, it can be postulated that this change in morphology can result in a change in the glandular synthesis, secretion or transport of regulatory factors necessary to facilitate blastocyst implantation. Molecules such as Leukaemia Inhibitory factor, Calcitonin and Osteopontin, which act on the luminal epithelial cells to facilitate development and implantation of a viable blastocyst (Carson *et al.*, 2000; Johnson *et al.*, 2001) have been reported to be secreted by the endometrial glands during early pregnancy; thus this disruption of the glandular morphology could have an impact on the secretion of such molecules.

Dilation of the glands has previously been reported in woman treated with 1mg/day of RU486 for 150 days (Croxatto *et al.*, 1998) as well as in monkeys treated with different antiprogestins and was attributed to altered glandular fluid outflow rather than to endometrial hyperplasia (Chwalisz *et al.*, 1998). This would account for the increase in secretory vesicles seen in the endometrial glands of the RU486-treated animals in the present study. Alternatively, the large vesicles observed at days 4.5 and 5.5 in the RU486-treated animals could be secondary lysosomes resulting from the increase in apoptosis observed within the glandular epithelium as a result of RU486 administration.

3.3.9 The RU486-Induced Increase in Apoptotic Activity within the Endometrium during Early Pregnancy

The increase in apoptotic activity observed within the present study concurs with previous research on the long-term effects of progesterone antagonists on the normal cycling rat endometrium (Rumpel *et al.*, 1993). In both the current study and this previous research (Rumpel *et al.*, 1993) the extent of glandular epithelial cells undergoing apoptosis was never close to the high numbers observed in the luminal epithelial cells. This increase in apoptosis as a result of RU486 administration can be attributed to the decrease in progesterone signalling as Rotello *et al.* (1992) have previously shown that in the rabbit endometrium progesterone suppresses apoptosis, whereas RU486 induces apoptosis.

3.3.10 The Effects of RU486 on Decidualisation

Another aspect of the plasma membrane transformation of early pregnancy is the potential effect this transformation has on the underlying stromal cells. In the present study it was observed that the stromal cells beneath the uterine epithelial cells began to undergo decidualisation around day 4.5 of pregnancy in both the implantation and non-implantation sites. No apparent difference was noted between the decidual cells of the implantation sites and those of the non-implantation sites.

The initial belief was that this decidual reaction was induced by the blastocyst itself via contact with the endometrium during implantation (Lundkvist *et al.*, 1979). However, more recent studies have artificially induced this decidual reaction in both virgin ovariectomised animals receiving

progesterone injections and in pseudopregnant animals. This evidence suggests that differentiation of the stromal cells into large decidual cells is a maternal response rather than one induced by the blastocyst. It has thus been suggested that this differentiation into large decidual cells, by the time membrane transformation occurs, may rather depend on signal transduction from the uterine epithelial cells (Murphy, 1995).

It is believed that this specialised decidualised tissue functions in embryo nourishment (Shaw *et al.*, 1998). Studies in which trophoblast invasion was increased in areas deficient in decidua, such as in the fallopian tubes or over a Caesarean scar, suggested that the decidual cells also play a role in the restriction of invasion of the uterus by the trophoblast cells of an implanting blastocyst (Loke *et al.*, 1995).

In the present research, RU486 enormously reduced the spontaneous decidualisation of the stromal cells. Previous studies have reported a complete loss of the decidual response following treatment with RU486 (Rider and Psychoyos, 1994; Piva *et al.*, 1996); however, results from the current study show a small decidual layer below the luminal epithelial cells at all three days of pregnancy analysed. This discrepancy can be explained by the half-life of RU486, as in the present study, the first time point analysed was 36 hours after RU486 administration. As the half-life of RU486 in the rat is 4 h, it can be postulated that by day 4.5 of pregnancy, the metabolism of RU486 had commenced, thus a partial progesterone response was observed in differentiation of the stromal cells into decidual cells. To test this hypothesis, a decidualisation marker, such as intermediate filament protein (IFP) (Glasser and Julian, 1986), would be beneficial to establish whether a decidual response does in fact occur in the RU486-treated animals or not.

Psychoyos (1961) reported a lack of endometrial decidualisation in the endometrium deprived of hormonal regulation. This observation combined with the lack of a decidual response in the RU486-treated animals concurs with the hypothesis of the current research that RU486 results in a hormonally under-stimulated endometrium.

In summary, the blocking of progesterone binding and subsequent signalling by RU486 has an overall ahormonal or ovariectomised effect on the uterus and the plasma membrane transformation of early pregnancy. While this may well be the mode of action of RU486 in preventing or disrupting blastocyst implantation, additional studies need to be carried out to better elucidate the cellular and molecular nature of the changes seen in the endometrium.

CHAPTER 4

THE EFFECTS OF RU486 ON PROGESTERONE RECEPTOR LOCALISATION AND EXPRESSION IN THE RAT UTERUS DURING EARLY PREGNANCY

4.1 INTRODUCTION

4.1.1 The Structure and Function of the Progesterone Receptor (PR)

The steroid hormone progesterone plays a pivotal role in the priming of the uterus for blastocyst attachment and implantation. The partial antiprogestin, RU486, binds to PR thus effectively blocking almost all progesterone effects essential to the development of an endometrium receptive to an implanting blastocyst. These experiments, therefore, investigate the potential effects that RU486 may have on the localisation and expression of this receptor during early pregnancy.

4.1.1.1 The PR isoforms

Most of the actions of progesterone are mediated by the PR, which exists in two different forms; namely, isoform PR-A, a 94kDa protein and isoform PR-B, a 120kDa protein (Figure 4.1) (Conneely *et al.*, 1989; Kastner *et al.*, 1990; Kraus and Katzenellenbogen, 1993). Although the two forms of PR have similar steroid hormone and DNA binding activities, they have been shown to demonstrate different cell and gene specificities in their transcriptional activities (Mulac-Jericevic *et al.*, 2000; Mulac-Jericevic *et al.*, 2003).

Knockout studies better elucidate some of these functions. PRAKO (PR-A knockout) (-/-) mice were shown to be infertile due to a reduction in oocytes production as a well as defective uterine implantation, as a decidual response in the stromal cells could not be induced by traumal stimulation (Ledford *et al.*, 1976; Lydon *et al.*, 1995; Mulac-Jericevic *et al.*, 2000). This data confirms an important role for PR-A in the decidualisation response and in the implantation process (Mulac-Jericevic *et al.*, 2000; Mulac-Jericevic *et al.*, 2003). In addition, analysis of uterine function in the PRBKO (PR-B knockout) (-/-) mouse indicated PR-A expression is sufficient to mediate the antiproliferative and implantation-associated responses seen in normal pregnancy (Mulac-Jericevic *et al.*, 2003).

The defective implantation process observed in PRAKO mice has been attributed to loss of the P-regulated expression of a subset of genes associated with receptivity, including the biomarker Calcitonin, and importantly to PR-B alone being unable to regulate this subset of genes (Mulac-Jericevic *et al.*, 2000). It is necessary to note that the differential target gene regulation by PR-B is not

as a result of differences in the spatiotemporal expression of PR-B relative to PR-A as the expression of PR-B in PRAKO mice displayed a similar expression pattern and regulation by oestrogen as in the wild-type mice (Mulac-Jericevic *et al.*, 2000). Uterine defects observed in these mice can thus be attributed to the differences in PR-B transcription factor activity rather than to differences in protein expression relative to PR-A (Conneely *et al.*, 2002). Selective activation of PR-B by progesterone in the PRAKO mice led to an abnormal progesterone-dependent induction of epithelial cell proliferation, dissimilar to the oestrogen-induced proliferation of early pregnancy (Mulac-Jericevic *et al.*, 2000), suggesting a role for PR-A and not PR-B in the inhibition of oestrogen-dependent hyperplasia of the uterus, in addition to limiting the potentially adverse implantation effects of the PR-B isoform (Mulac-Jericevic and Conneely, 2004).

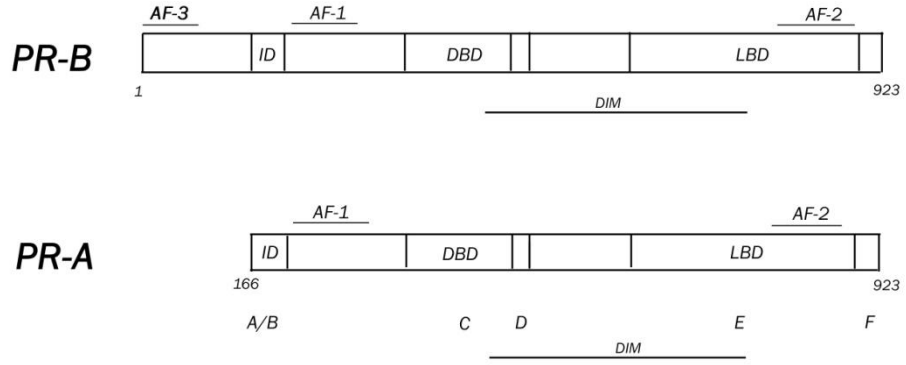


Figure 4.1 Schematic representation of the structural organisation of the two main PR isoforms, PR-A and PR-B. PR-B is situated from the amino acid position 1 to 923, whereas PR-A is situated from the amino acid position 166 to 923. AF-1, -2 and -3 represent the activation domains with AF-3 only present in the PR-B isoform. DBD – DNA binding domain; LBD – ligand binding domain; ID – inhibitory domain; DIM – the important sequences for dimerisation of the receptor (Mulac-Jericevic and Conneely, 2004).

4.1.1.2 PR activation

The PRs belong to a large family of structurally related gene products known as the nuclear receptors (NR) superfamily of transcription factors (Mangelsdorf *et al.*, 1995). The NR superfamily are able to regulate gene transcription by selective binding to DNA regulatory sequences and specific interaction with co-activator and/or co-repressor proteins to regulate the activity of the RNA polymerase complex (McKenna and O'Malley, 2001).

The binding of progesterone to PRs induces a significant conformational change within the receptor proteins, resulting in dimerisation of two ligand receptor complexes into three species: A:A or B:B homodimers or A:B heterodimers (Tsai *et al.*, 1988; Conneely *et al.*, 2003). This in turn leads to increased receptor phosphorylation (Weigel *et al.*, 1995), binding of the receptor dimers to specific hormone responsive DNA elements located in the promoter regions of target genes (Gronemeyer, 1991; Tsai and O'Malley, 1994), and subsequently the interaction of the receptor complex with

specific co-activator proteins and general transcription factors, to form a productive transcription initiation complex on specific target gene promoters (Oñate *et al.*, 1995; Kamei *et al.*, 1996).
The PRs are comprised of four well-defined functional domains: the N-terminal transcription domain, the central DNA binding domain (DBD), the hinge region and the C-terminal ligand binding domain (LBD) (Baulieu, 1991; Leonhardt and Edwards, 2002; Sarkar, 2002). The difference between PR-A and PR-B is demonstrated at the N-terminal or amino terminal of the PRs. This region is also referred to as the A/B region and contains the transcription domains (AF1 and AF3) which recruit co-activator proteins to the recptor to modulate the level and promoter specificity of target gene activation (Tora *et al.*, 1988; Dobson *et al.*, 1989; Meyer *et al.*, 1992; Sartorius *et al.*, 1994). The inhibitory domain (ID) located within this region is responsible for the recruitment of transcriptional inhibitory co-repressor proteins (Figure 4.1) (Giangrande *et al.*, 1997).

The ratio of PR-A to PR-B within a target cell under certain physiological conditions is likely to alter the relative complement of dimeric complexes and exert a significant impact on the overall cellular responses to progesterone (Conneely *et al.*, 2003). In support of this statement, PR-B has been shown to function as a strong activator of transcription of several PR-dependent promoters in a variety of cell types in which PR-A is inactive (Giangrande and McDonnell, 1999). Studies have also reported different progesterone antagonist responses in that antagonist bound PR-A is rendered inactive, whereas antagonist bound PR-B can be converted into a strongly active transcription factor by modulating intracellular phosphorylation pathways (Beck *et al.*, 1993; Musgrove and Sutherland, 1993; Sartorius *et al.*, 1994). In addition, the ability of PR-A to inhibit transcriptional responses induced by both the PR-B and the ERs suggests that PR-A may have the capacity to diminish overall progesterone responsiveness in certain tissues, as well as contribute to the anti-oestrogenic activities of progesterone previously reported by Lydon *et al.* (1995) within the uterus. Studies using PR knockout (PRKO) models have demonstrated the tissue specific roles of PRs within the reproductive tissues. The PRKO mouse model in which both PR isoforms were inhibited by a null mutation within the PR gene demonstrated impaired sexual behaviour and neuroendocrine gonadotropin regulation, anovulation, uterine dysfunction and impaired pregnancy-associated morphogenesis of the mammary glands (Lydon *et al.*, 1995; Mani *et al.*, 1996; Chappell *et al.*, 1999; Tibbetts *et al.*, 1999).

4.1.1.3 The role of PR during early pregnancy

Not only is progesterone essential during early pregnancy for uterine preparation for blastocyst implantation as well as in differentiation of the endometrial stroma into the decidual layer in order to support the development of the implanting embryo, but progesterone has also been shown to be a potent antagonist against the oestrogen-induced proliferation of the uterine epithelium during early pregnancy and within the oestrous and menstrual cycles (Lydon *et al.*, 1995; Tan *et al.*, 1999). The importance of progesterone during early pregnancy is further established by reports from PRKO mice

studies in which blastocyst implantation was unable to be supported following embryo transfer with unsuccessful stimulation of the decidual response (Lydon *et al.*, 1995). In addition, the uterine epithelial cells became hyperplastic as a result of unopposed proliferative oestrogen action (Lydon *et al.*, 1995).

4.1.1.3.1 Ovarian Hormonal Regulation of PR in the Endometrium

Studies have indicated that PRs are expressed in the epithelial, stromal and myometrial compartments of the uterus under the control of both ovarian hormones progesterone and oestrogen (Tibbetts *et al.*, 1998). Oestrogen increases the expression of PRs, whereas progesterone decreases PR expression in most target cells. In support of this, PR expression is increased during pro-oestrous, or as a result of exogenous administration of oestrogen (Feil *et al.*, 1972; Milgrom *et al.*, 1973; Leavitt *et al.*, 1977). Treatment with progesterone is able to oppose the oestrogen induction of PR expression (Milgrom *et al.*, 1973). The spatiotemporal pattern of PRs are dramatically changed during both the oestrous cycle and early pregnancy (Tan *et al.*, 1999). The PR is undetectable in the glandular epithelium during the window of implantation, although it is expressed in the stroma. Thus, if progesterone is to regulate the glandular products involved in the process of implantation, this regulation is likely to occur as a result of paracrine interactions from the progesterone-responsive stroma and not directly from the glandular epithelium (Giudice, 1999). This loss of PR expression within the glandular epithelial compartment of the sheep endometrium is thought to be required for the onset of differentiated functions in terms of the production of secretory proteins such as uterine milk proteins (UTMPs) and osteopontin (OPN) (Spencer and Bazer, 2002). Around the time of blastocyst implantation, PR expression has also been shown to be lost in the uterine epithelial compartment in numerous animals such as rhesus monkeys (Okulicz and Scarrell, 1998), human (Lessey *et al.*, 1988) and mice (Tan *et al.*, 1999).

4.1.1.3.2 Function of the PR Isoforms in the Endometrium

Analysis of the effects of PR ablation on the expression of several genes previously implicated in progesterone-dependent uterine implantation indicated that defects observed in PRKO mice are associated with the inhibition of the expression of several known epithelial markers of uterine receptivity, one of which is the endometrial biomarker of receptivity, Calcitonin (Mulac-Jericevic *et al.*, 2000). This data further elucidates an essential role for progesterone and its receptors in the establishment and maintenance of pregnancy, both directly and indirectly.

Subsequent to the PRKO mice studies, Mulac-Jericevic *et al.* (2000; 2003) additionally analysed the effect of a null mutation of each separate isoform of the PR gene on uterine function and early pregnancy. Analysis of progesterone-dependent uterine function in both the PRAKO and PRBKO mice further clarified the distinct functions of PR-A and PR-B within the endometrium (Mulac-Jericevic *et al.*, 2000; Mulac-Jericevic *et al.*, 2003). In these studies, it was reported that the

progesterone-induced differentiation of the endometrial cells into decidual cells was inhibited in the PRAKO mice, suggesting a key role for PR-A in the decidualisation response to progesterone, prior to blastocyst implantation (Mulac-Jericevic *et al.*, 2000). In addition, the PRAKO females were infertile, an observation similar to that within the PRKO females (Mulac-Jericevic *et al.*, 2000). Further research indicated that this infertility was not due entirely to the inability of the females to ovulate, indicating the infertility observed was also associated with defective uterine implantation (Mulac-Jericevic *et al.*, 2000). Analysis of the PRBKO mouse uterine function revealed that PR-A expression is sufficient to mediate both the antiproliferative- and implantation-associated responses of normal pregnancy (Mulac-Jericevic *et al.*, 2003).

In the present study the partial antiprogestin, RU486, was used as a postcoital contraceptive to better elucidate the requirements of the 'window of receptivity' in early pregnancy, as well as to clarify the mode of action of RU486 in the successful restriction of blastocyst implantation. RU486, when bound to the PR isoform PR-A, forms a functionally silent homodimer, whereas when bound to PR-B, such homodimers nevertheless can still activate transcription of certain P-dependent genes. In contrast, RU486, when bound to the heterodimers of PR-A:B, acts to suppress transcriptional activity, and it is this suppression that is characteristically seen in progesterone responsive cells (Sartor and Figg, 1996) typical of those located in the endometrium; where both PR-A and PR-B isoforms have been found (Tibbetts *et al.*, 1998).

4.2 RESULTS

4.2.1 Immunofluorescence Analysis of PR Protein Spatiotemporal Expression Pattern in the RU486-Treated Rat Endometrium.

Immunofluorescence was performed on each tissue section with primary antibodies raised against the PR, in order to determine the spatiotemporal expression pattern of the receptor during early. Following treatment with RU486 at day 3.0 of pregnancy, the spatiotemporal pattern of PR expression was analysed to observe what effect, if any, this PRM may have on both receptor localisation and expression.

4.2.1.1 The Spatiotemporal expression pattern of the PR protein in the control pregnant animals

In the implantation sites of the control pregnant animals, PR protein levels were extremely high at day 4.5 of pregnancy in all endometrial compartments analysed. The highest levels of PR protein expression were observed in the luminal and glandular epithelia respectively, followed by the subepithelial stroma and lastly the glandular stroma (Graph 4.1A-D; Figure 4.2A; Figure 4.3A; Table 4.1). By day 5.5 of pregnancy, PR protein levels in the luminal epithelium and subepithelial stroma had decreased significantly (Graph 4.1A and B; Figure 4.2C; Table 4.1), whereas in both the glandular epithelium and glandular stroma PR protein levels were increased significantly (Graph 4.1C and D; Figure 4.3C; Table 4.1). At day 6.5 of pregnancy, PR protein levels in the implantation sites were significantly increased in the luminal epithelium and the subepithelial stroma (Graph 4.1A and B; Figure 4.2E; Table 4.1) and decreased significantly in the glandular epithelium and glandular stroma (Graph 4.1C and D; Figure 4.3E; Table 4.1). In the implantation sites, while levels in the luminal epithelium and the subepithelial stroma mirror each other, the PR levels were lower in the stromal compartment. This was also valid for the glandular epithelium and the glandular stroma.

In the non-implantation sites of the control pregnant animals, PR protein levels at day 4.5 of pregnancy were not as intense as those of the implantation sites (Graph 4.1A-D; Figure 4.2A and B; Figure 4.3A and B; Table 4.1). PR protein levels were highest in the glandular epithelium and luminal epithelium of the non-implantation sites respectively, followed by the subepithelial stroma and then the glandular stroma (Graph 4.1A-D; Figure 4.2B; Figure 4.3B; Table 4.1). By day 5.5 of pregnancy, PR protein levels in the non-implantation sites had increased markedly in the luminal epithelium, the glandular epithelium and the glandular stroma (Graph 4.1A, C and D; Figure 4.2D; Figure 4.3D; Table 4.1). The increase in the subepithelial stroma was not as large despite it being significant (Graph 4.1B; Figure 4.2D; Table 4.1). By day 6.5 of pregnancy, PR protein levels remained stable in the luminal and glandular epithelium (Graph 4.1A and C; Figure 4.2F; Figure 4.3F; Table 4.1),

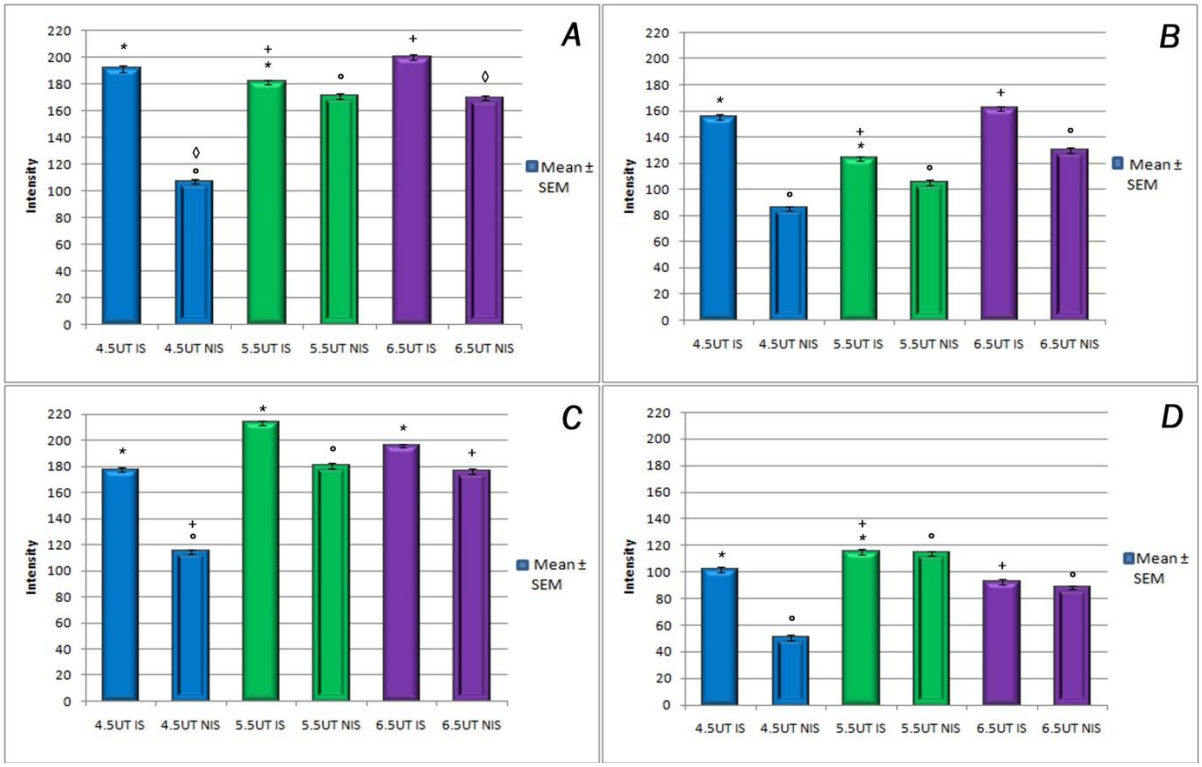
Table 4.1 One-way ANOVA and Tukey Kramer *post hoc* analysis of PR protein expression in the luminal epithelium, the subepithelial stroma, the glandular epithelium and the glandular stroma of the implantation (IS) and non-implantation (NIS) sites between days 4.5, 5.5 and 6.5 in the control pregnant (UT) and RU486-treated (T) animals showing groups that are significantly different ($p \leq 0.05$). Groups not connected by the same letter are significantly different.

Group								Mean
Luminal Epithelium								
6.5UT IS	A							**199.72**
4.5UT IS	A							**191.265**
5.5UT IS		B						**181.452**
5.5UT NIS			C					**170.548**
6.5UT NIS			C					**169.419**
5.5T NIS				D				**159.485**
6.5T IS				D				**154.268**
5.5T IS					E			**131.325**
6.5T NIS						F		**108.368**
4.5T IS						F		**107.482**
4.5UT NIS						F		**106.87**
4.5T NIS							G	**81.375**
Subepithelial Stroma								
6.5UT IS	A							**161.76**
4.5UT IS	A							**155.371**
6.5UT NIS		B						**129.804**
5.5UT IS		B						**123.465**
6.5T IS			C					**108.99**
5.5UT NIS			C					**105.363**
5.5T NIS				D				**87.908**
4.5UT NIS				D				**85.41**
5.5T IS					E			**73.812**
6.5T NIS					E			**70.357**
4.5T IS						F		**58.638**
4.5T NIS							G	**38.608**
Glandular Epithelium								
5.5UT IS	A							**213.401**
6.5UT IS		B						**195.89**
5.5UT NIS			C					**180.455**
4.5UT IS			C					**177.481**
6.5UT NIS			C					**176.476**
5.5T NIS				D				**151.365**
4.5T IS					E			**126.525**
5.5T IS					E			**124.69**
4.5UT NIS						F		**114.777**
6.5T NIS							G	**104.685**
6.5T IS							G	**102.78**
4.5T NIS							H	**84.623**
Glandular Stroma								
5.5UT IS	A							**115.217**
5.5UT NIS	A							**114.053**
4.5UT IS		B						**101.595**
6.5UT IS		B	C					**92.466**
6.5UT NIS			C	D				**88.2**
6.5T IS				D	E			**79.737**
5.5T IS				D	E			**78.857**
5.5T NIS					E			**72.218**
6.5T NIS						F		**62.271**
4.5T IS						F	G	**55.52**
4.5UT NIS							G	**50.618**
4.5T NIS							G	**47.35**

whereas it was increased significantly in the subepithelial stroma (Graph 4.1B; Figure 4.2F; Table 4.1) and decreased significantly in the glandular stroma (Graph 4.1D; Figure 4.3F; Table 4.1).

PR protein levels in the non-implantation sites were consistently lower in all the endometrial compartments analysed relative to that of the implantation sites (Graph 4.1A-D; Figure 4.2A-F; Figure 4.3A-F; Table 4.1).

In the non-implantation sites, PR expression pattern in the luminal epithelium and the subepithelial stroma mirrored each other with the progression of pregnancy from day 4.5 to day 5.5. This was also true for the glandular epithelium and the glandular stroma. At day 6.5 of pregnancy, while levels in the epithelial compartments remained stable, those in the stromal compartments did not.



Graph 4.1 Graphical representation of the Mean ± SEM (Standard Error of the Mean) of PR protein expression in the luminal epithelium (A), the subepithelial stroma (B), the glandular epithelium (C) and the glandular stroma (D) of the implantation (IS) and non-implantation (NIS) sites in day 4.5, day 5.5 and day 6.5 pregnant rat uteri treated with vehicle (UT) at day 3.0 of pregnancy, as obtained from image analysis of fluorescent intensities. *, °, ◊, + = significantly different ($p \leq 0.05$) using the Tukey-Kramer *post hoc* analysis.

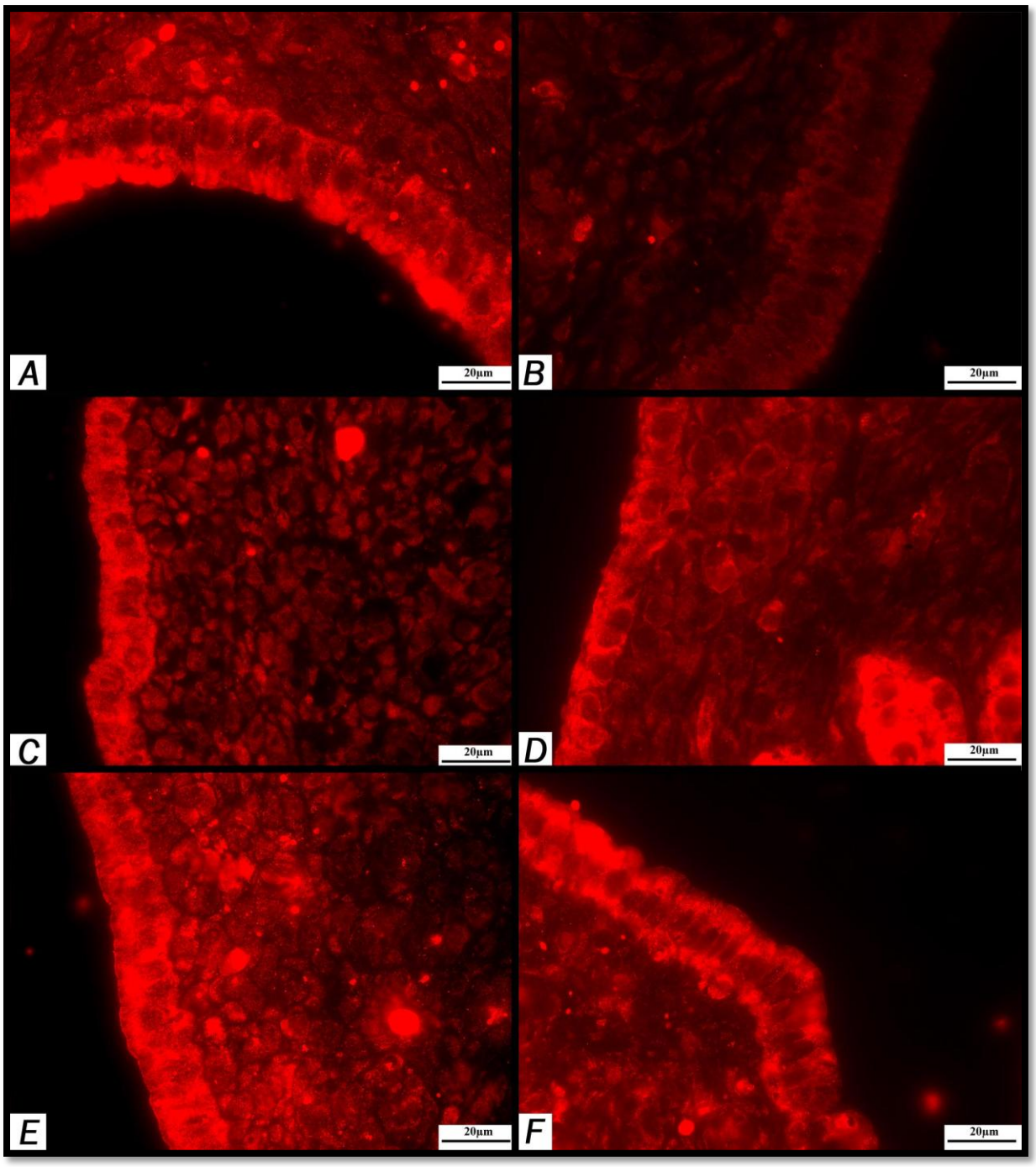


Figure 4.2 Immunofluorescent images illustrating PR protein localisation in the luminal epithelium and the subepithelial stroma of the implantation and non-implantation sites in the uteri of control pregnant rats. A: Implantation site at day 4.5 of pregnancy, **B:** Non-implantation site at day 4.5 of pregnancy, **C:** Implantation site at day 5.5 of pregnancy, **D:** Non-implantation site at day 5.5 of pregnancy, **E:** Implantation site at day 6.5 of pregnancy, **F:** Non-implantation site at day 6.5 of pregnancy. Scale = 20µm.

4.2.1.2 The effects of RU486 on the spatiotemporal expression pattern of the PR protein during early pregnancy

Overall, in the RU486-treated animals, PR protein levels increased significantly in the luminal epithelium and the subepithelial stroma of the implantation sites, with the progression of pregnancy from day 4.5 through to day 6.5 (Graph 4.2A and B; Figure 4.4A, C and E; Table 4.1). In the non-implantation sites, PR levels in these endometrial compartments increased significantly as pregnancy progressed from day 4.5 to day 5.5 and then decreased significantly by day 6.5 of pregnancy, to a level significantly higher than that at day 4.5 of pregnancy (Graph 4.2A and B; Figure 4.4B, D and F; Table 4.1).

In the glandular epithelial compartment, PR levels in the RU486-treated animals remained stable in the implantation sites and increased significantly in the non-implantation sites from day 4.5 to day 5.5 of pregnancy (Figure 4.2C; Figure 4.5A-D; Table 4.1). In the glandular stromal compartment, PR levels increased significantly in both the implantation and non-implantation sites (Graph 4.2D; Figure 4.5A-D; Table 4.1). By day 6.5 of pregnancy, PR levels in the glandular epithelium had decreased significantly in both the implantation and non-implantation sites (Graph 4.2C; Figure 4.5E and F; Table 4.1). In the glandular stroma, PR levels remained stable in the implantation sites and decreased significantly in the non-implantation sites (Graph 4.2D; Figure 4.5E and F; Table 4.1).

Following treatment with RU486, PR protein levels were radically reduced in all the endometrial compartments of both the implantation and non-implantation sites at day 4.5 of pregnancy relative to the control pregnant animals at this day of pregnancy (Graph 4.3A-D; Figure 4.2A-F; Figure 4.3A and B; Figure 4.4A and B; Figure 4.5A and B; Table 4.1). This decrease was more pronounced in the implantation sites as PR protein levels in the implantation sites of the control pregnant animals were significantly higher relative to the non-implantation sites. By day 5.5 of pregnancy, PR protein levels were significantly lower in the RU486-treated animals relative to the control pregnant animals, although not as drastically reduced as at day 4.5 of pregnancy (Graph 4.3A-D; Figure 4.2A-D; Figure 4.3A-D; Figure 4.4A-D; Figure 4.5A-D; Table 4.1).

At day 6.5 of pregnancy, despite the increase in PR protein levels in the luminal epithelium and subepithelial stroma of the implantation sites in the treated animals, PR levels remained significantly lower in the RU486-treated animals relative to the control pregnant animals at the same day of pregnancy (Graph 4.3A and B; Figure 4.2E; Figure 4.4E; Table 4.1). With regards to the non-implantation sites, PR levels in these endometrial compartments decreased in the RU486-treated animals at day 6.5 of pregnancy. Thus, PR levels remained significantly lower in the RU486-treated

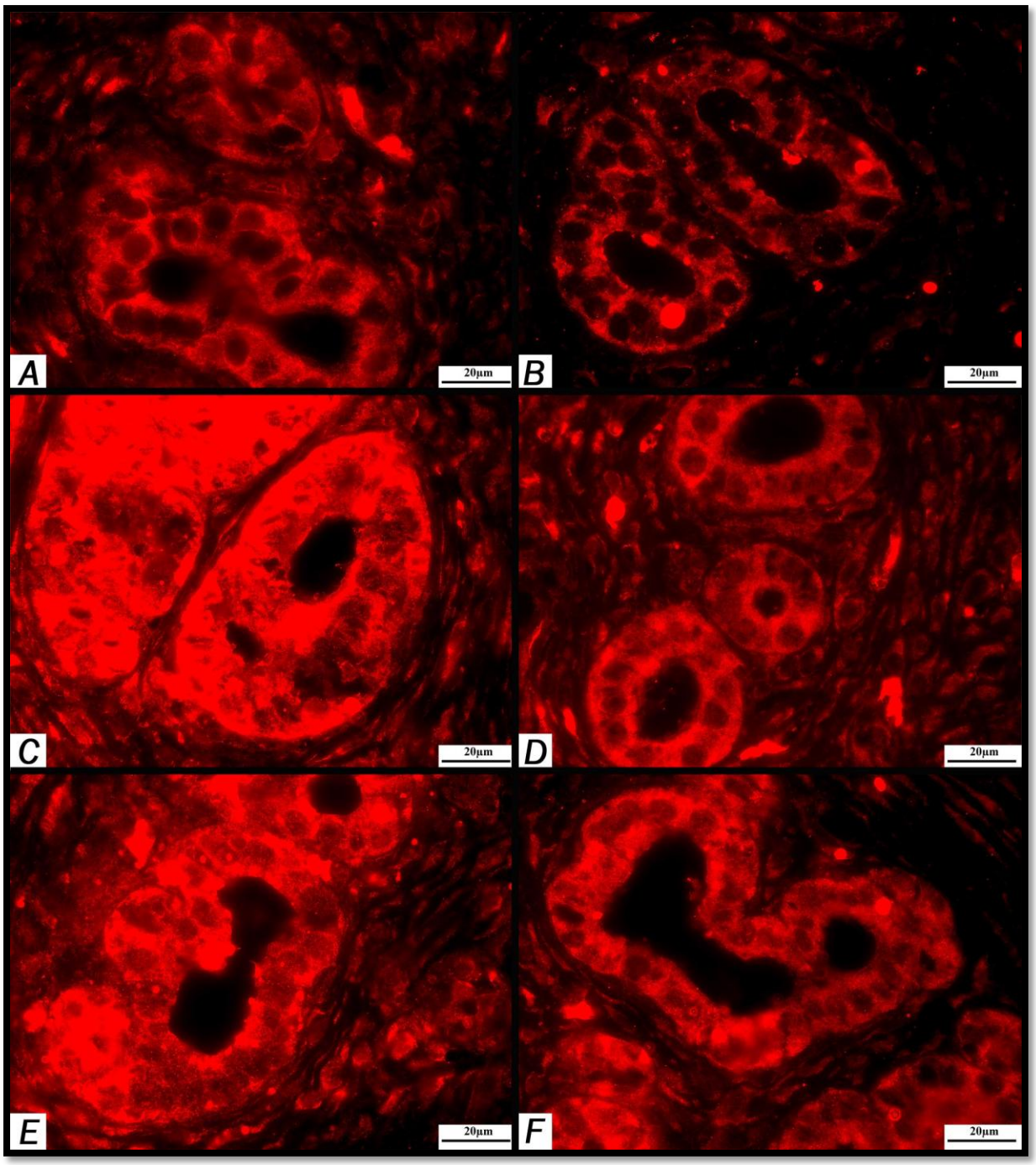
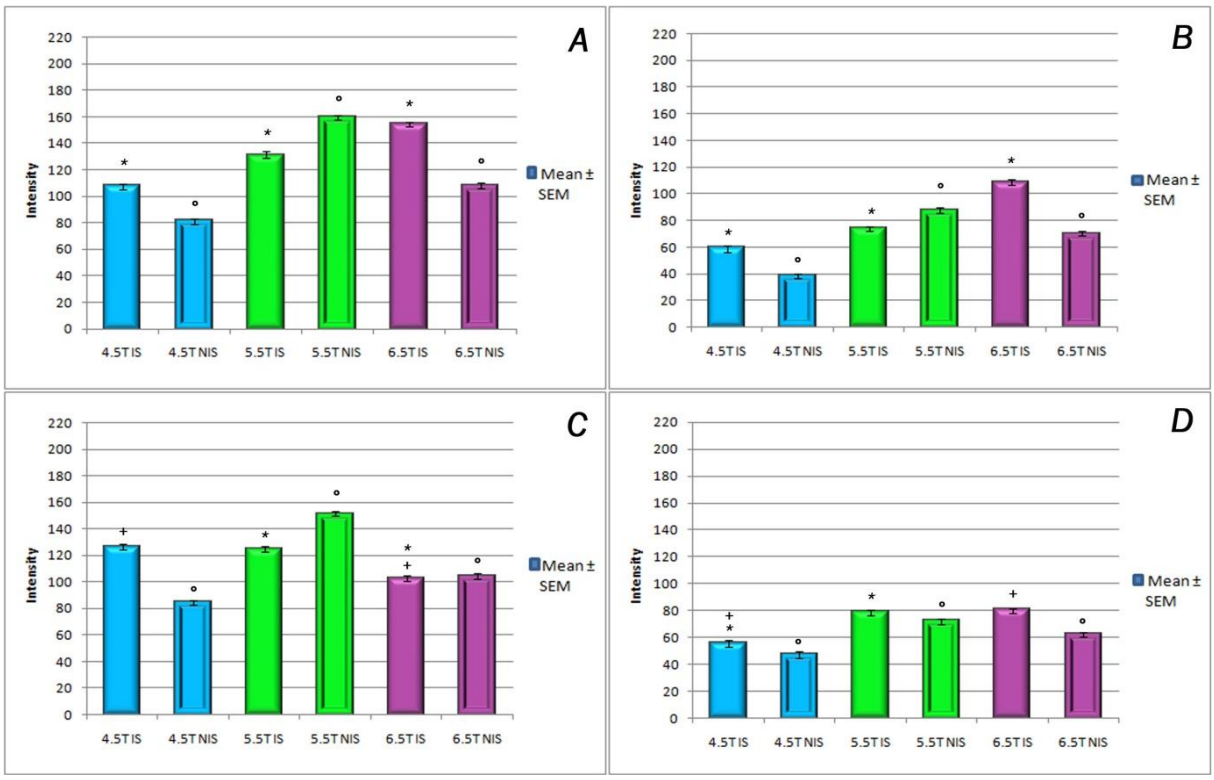


Figure 4.3 Immunofluorescent images illustrating PR protein localisation in the glandular epithelium and the glandular stroma of the implantation and non-implantation sites in the uteri of control pregnant rats. A: Implantation site at day 4.5 of pregnancy, **B:** Non-implantation site at day 4.5 of pregnancy, **C:** Implantation site at day 5.5 of pregnancy, **D:** Non-implantation site at day 5.5 of pregnancy, **E:** Implantation site at day 6.5 of pregnancy, **F:** Non-implantation site at day 6.5 of pregnancy. Scale = 20µm.

animals relative to the control pregnant animals (Graph 4.3A and B; Figure 4.2F; Figure 4.4F; Table 4.1).

In the glandular epithelium, PR protein levels decreased in both the implantation and non-implantation sites in the RU486-treated animals at day 6.5 of pregnancy, resulting in markedly reduced PR protein levels in this compartment relative to the control pregnant animals (Graph 4.3C; Figure 4.3E and F; Figure 4.5E and F; Table 4.1). PR levels in the glandular stroma remained significantly lower in the RU486-treated animals relative to the control pregnant animals at day 6.5 of pregnancy, however, to a lesser degree than observed in the other endometrial compartments (Graph 4.3D; Figure 4.3E and F; Figure 4.5E and F; Table 4.1).



Graph 4.2 Graphical representation of the Mean ± SEM of PR protein expression in the luminal epithelium (A), the subepithelial stroma (B), the glandular epithelium (C) and the glandular stroma (D) of the implantation (IS) and non-implantation (NIS) sites in day 4.5, day 5.5 and day 6.5 pregnant rat uteri treated with RU486 (T) at day 3.0 of pregnancy, as obtained from image analysis of fluorescent intensities. *, °, +, = significantly different ($p \leq 0.05$) using the Tukey-Kramer *post hoc* analysis.

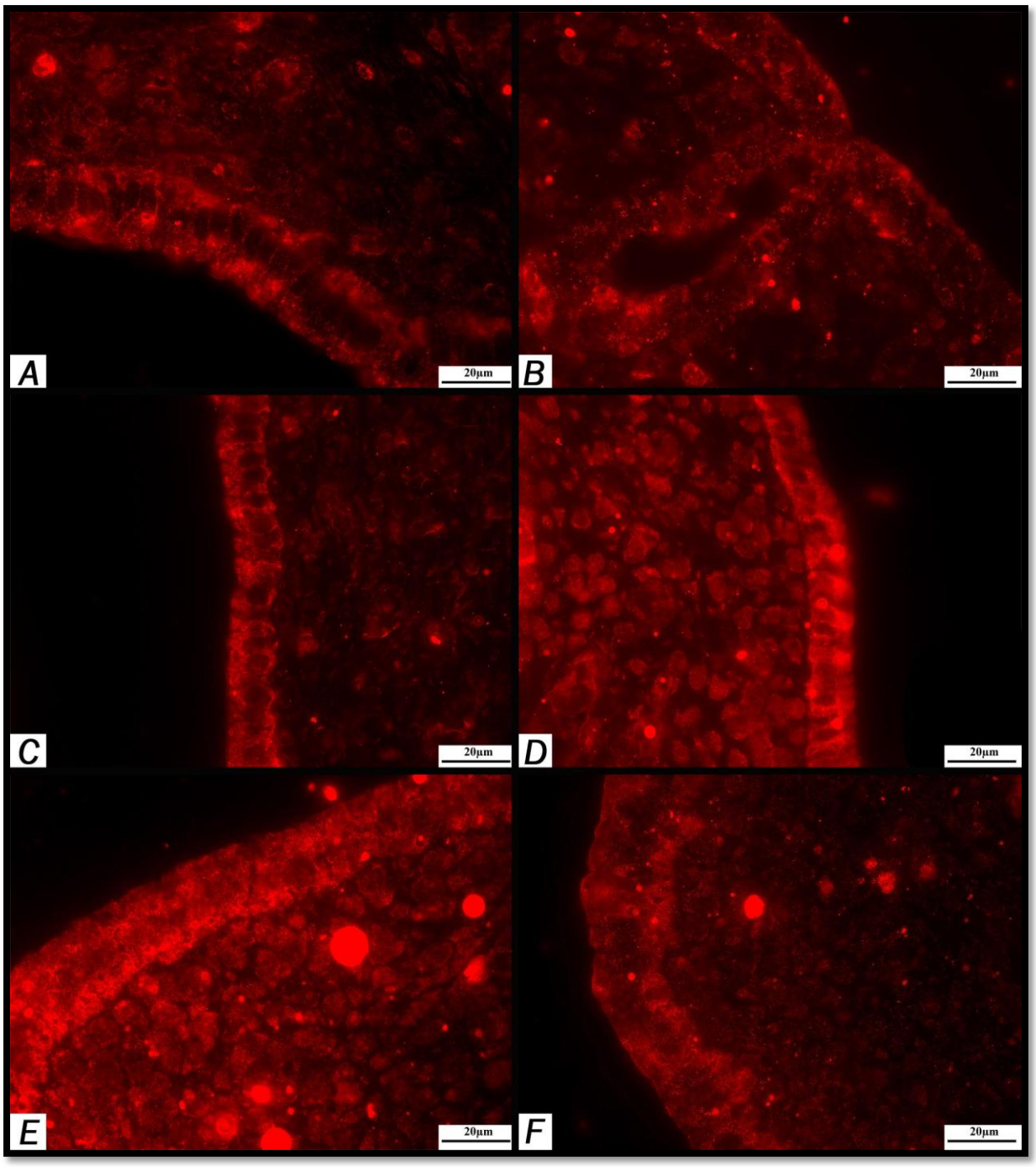
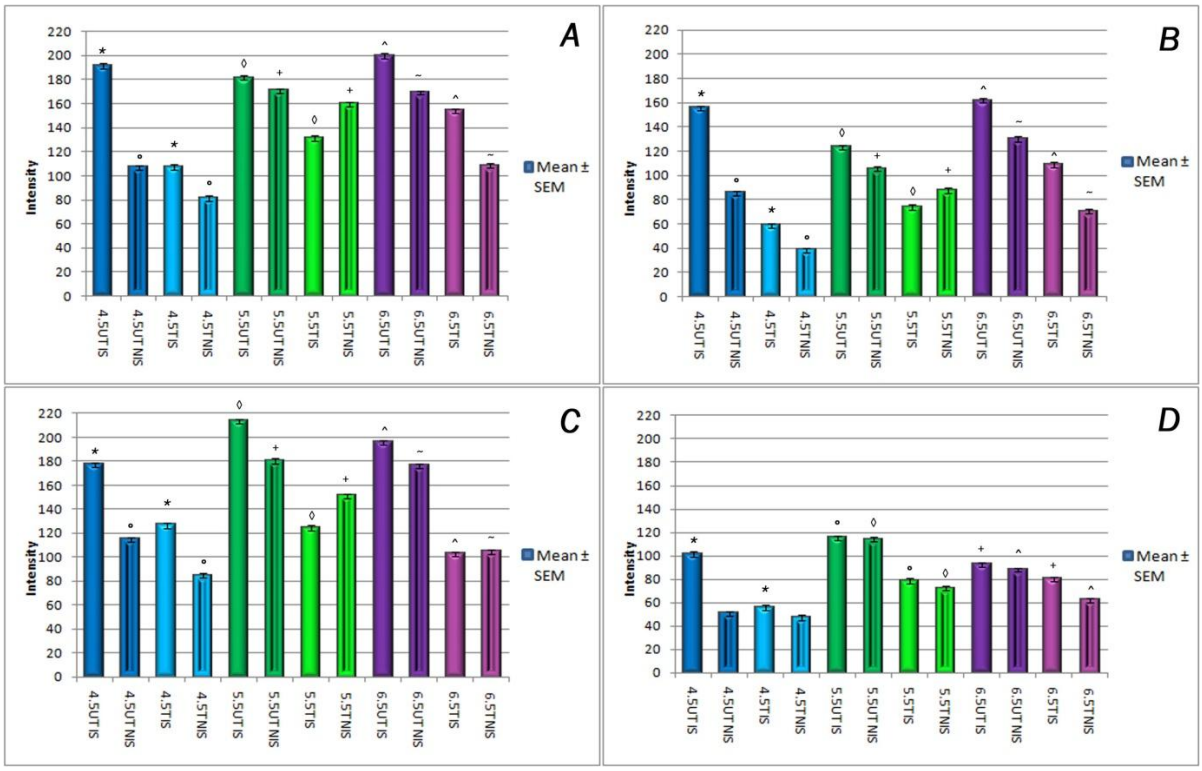


Figure 4.4 Immunofluorescent images illustrating PR protein localisation in the luminal epithelium and the subepithelial stroma of the implantation and non-implantation sites in the uteri of RU486-treated pregnant rats. A: Implantation site at day 4.5 of pregnancy, **B:** Non-implantation site at day 4.5 of pregnancy, **C:** Implantation site at day 5.5 of pregnancy, **D:** Non-implantation site at day 5.5 of pregnancy, **E:** Implantation site at day 6.5 of pregnancy, **F:** Non-implantation site at day 6.5 of pregnancy. Scale = 20µm.



Graph 4.3 Graphical representation of the Mean ± SEM of PR protein expression in the luminal epithelium (A), the subepithelial stroma (B), the glandular epithelium (C) and the glandular stroma (D) of the implantation (IS) and non-implantation (NIS) sites in day 4.5, day 5.5 and day 6.5 pregnant rat uteri treated with vehicle (UT) or RU486 (T) at day 3.0 of pregnancy, as obtained from image analysis of fluorescent intensities. *, °, ◊, +, ^,~ = significantly different ($p \leq 0.05$) using the Tukey-Kramer *post hoc* analysis.

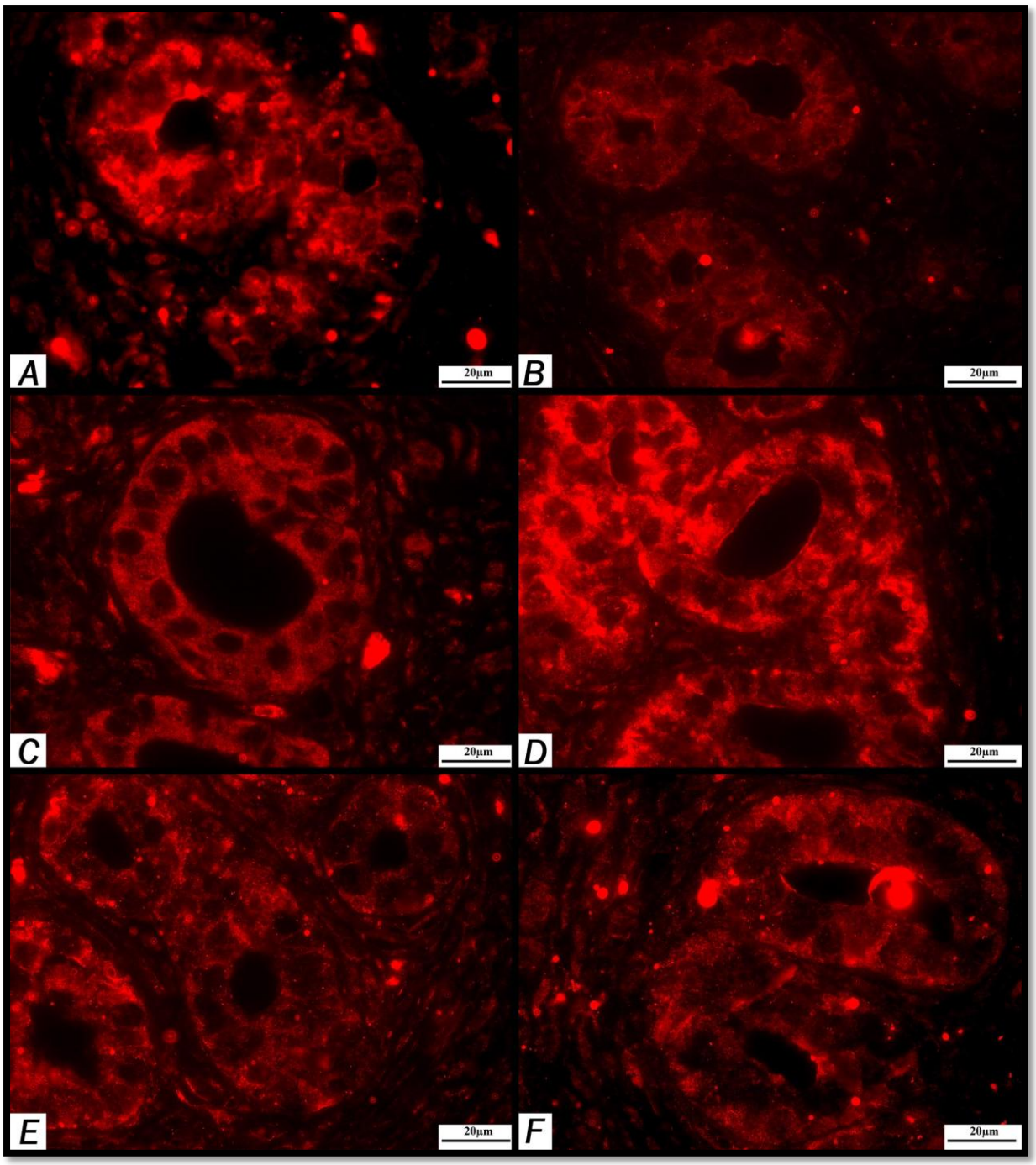


Figure 4.5 Immunofluorescent images illustrating PR protein localisation in the glandular epithelium and the glandular stroma of the implantation and non-implantation sites in the uteri of RU486-treated pregnant rats. A: Implantation site at day 4.5 of pregnancy, **B:** Non-implantation site at day 4.5 of pregnancy, **C:** Implantation site at day 5.5 of pregnancy, **D:** Non-implantation site at day 5.5 of pregnancy, **E:** Implantation site at day 6.5 of pregnancy, **F:** Non-implantation site at day 6.5 of pregnancy. Scale = 20µm.

4.2.2 The Effects of RU486 on PR Gene Expression in the Rat Uterus during Early Pregnancy

4.2.2.1 Relative quantification (RQ) analysis of PR gene expression in the control pregnant animals

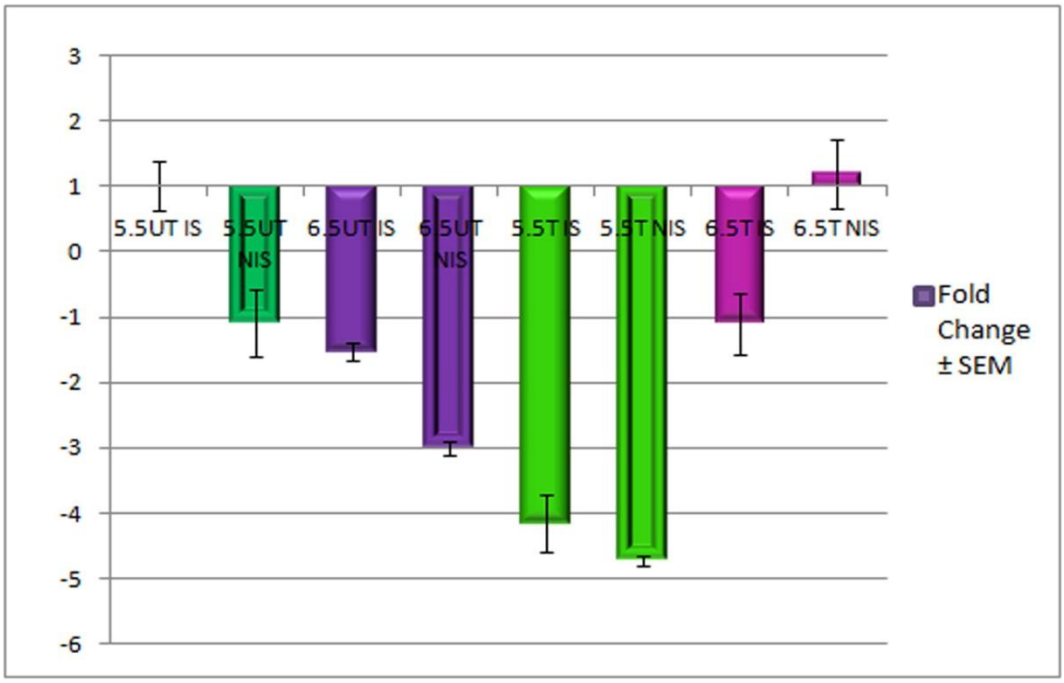
In the control pregnant animals at day 5.5 of pregnancy PR gene expression remained fairly similar (1.1-fold decrease) in the non-implantation sites relative to the implantation sites (Graph 4.4; Table 4.2). By day 6.5 of pregnancy, PR gene expression was decreased slightly by 1.5-fold in the implantation sites and 3-fold in the non-implantation sites relative to the calibrator sample, the implantation sites at day 5.5 of pregnancy (Graph 4.4; Table 4.2). PR gene expression between days 5.5 and 6.5 of pregnancy was down-regulated slightly by 1.5-fold in the implantation sites and down-regulated by 2.8-fold in the non-implantation sites. These results indicate an overall decrease in PR protein expression with the progression of pregnancy (Graph 4.4). At both days of pregnancy, PR levels were higher in the implantation sites relative to the non-implantation sites (Graph 4.4)

4.2.2.2 Relative quantification (RQ) Analysis of the effects of RU486 on PR gene expression

As a result of RU486 treatment, PR gene expression was reduced 4.2-fold in the implantation sites and 4.7-fold in the non-implantation sites at day 5.5 of pregnancy, relative to the implantation sites at day 5.5 of pregnancy in the control pregnant animals, the calibrator sample (Graph 4.4; Table 4.2). It was slightly higher in the implantation sites as compared to the non-implantation sites at this day of pregnancy (Graph 4.4).

By day 6.5 of pregnancy in the RU486-treated animals, PR gene expression had increased by 3.8-fold in the implantation sites and 5.7-fold in the non-implantation sites as compared to day 5.5 of pregnancy in the RU486-treated animals (Graph 4.4). PR gene expression in the implantation sites (1.1-fold decrease) and the non-implantation sites (1.2-fold increase) were fairly similar as compared to the calibrator sample (Graph 4.4; Table 4.2). The non-implantation sites at this day of pregnancy showed a higher expression of PR as compared to the implantation sites (Graph 4.4).

In general, RU486 decreased PR gene expression in both the implantation and non-implantation sites of the rat uterus at day 5.5 of pregnancy. At day 6.5 of pregnancy, PR gene expression in both the implantation and non-implantation sites of the RU486-treated animals was up-regulated relative to day 6.5 in the control pregnant animals. In the RU486-treated animals, PR gene expression increased significantly by day 6.5 of pregnancy while in the control pregnant animals PR gene expression decreased at day 6.5 of pregnancy (Graph 4.4; Table 4.2).



Graph 4.4 Graphical representation of PR gene expression as compared to day 5.5 in the control pregnant animals, the calibrator sample. The data is expressed as Fold Change ± SEM.
UT – untreated, **T** – treated, **IS** – implantation site, **NIS** – non-implantation site.

Table 4.2 RQ analysis of PR gene expression in the implantation (IS) and non-implantation (NIS) sites at day 5.5 and 6.5 of pregnancy in the control pregnant (UT) and RU486-treated (T) animals. A fold change of 2 or more denotes a significant difference in gene expression.

PR Gene Expression								
Day of Pregnancy	**Avg. C_T**	**SEM**	**ΔC_T**	**SEM**	**$\Delta\Delta C_T$**	**$2^{-\Delta\Delta Ct}$**	**$Log_{10}(2^{-\Delta\Delta Ct})$**	**Fold Change ($2^{\Delta\Delta Ct}$)**
B-actin *	19.65	0.67	-	-	-	-	-	-
5.5UT IS **	24.57	0.29	4.91	0.38	0	1	0	1
5.5UT NIS	24.70	0.15	5.04	0.52	0.13	0.91	-0.04	-1.09
6.5UT IS	25.18	0.80	5.53	0.13	0.62	0.65	-0.19	-1.54
6.5UT NIS	26.15	0.78	6.50	0.11	1.59	0.33	-0.48	-3.01
5.5T IS	26.62	0.22	6.97	0.45	2.06	0.24	-0.62	-4.17
5.5T NIS	26.81	0.60	7.15	0.07	2.24	0.21	-0.67	-4.72
6.5T IS	24.70	0.20	5.05	0.47	0.13	0.91	-0.04	-1.09
6.5T NIS	24.31	0.14	4.66	0.53	-0.25	1.19	0.08	1.19

UT - untreated, **T** - treated, **IS** - implantation site, **NIS** - non-implantation site, **C_T** - threshold cycle, **SEM** - standard error of the mean, ***** - endogenous control, ****** - calibrator sample. **ΔC_T** = C_T (Target) - C_T (Endogenous control). **$\Delta\Delta C_T$** = ΔC_T (Target) - ΔC_T (Calibrator).

4.3 DISCUSSION

4.3.1 The Effects of RU486 on Progesterone Receptor Expression and Localisation within the Rat Endometrium

The reported low pregnancy rates (~ 27%) (Navot *et al.*, 1994) during a normal reproductive cycle is probably due, in part, to a viable blastocyst only being able to implant during the 'window of receptivity' (Murphy, 1995; Carson *et al.*, 2000). This window is established by the priming of the endometrium by the ovarian hormones progesterone and oestrogen (Psychoyos, 1986). In the rat endometrium, implantation occurs on day 5.5 of pregnancy (with day 0.5 designated the day of the vaginal plug and spermatozoa within the vaginal secretions). In ovariectomised animals, an extremely low level of oestrogen is required to initiate this process in a progesterone-primed uterus (Psychoyos, 1986).

The findings of the current study during early pregnancy indicate high PR immunofluorescence staining in the implantation sites at day 4.5 of pregnancy and a decrease in the luminal epithelium and decidual compartments at day 5.5 of pregnancy, the day of blastocyst implantation, this being in confirmation with previous reports regarding PR immunolocalisation in the mouse (Tan *et al.*, 1999), sheep (Spencer and Bazer, 1995), cow (Kimmins and MacLaren, 2001), pig (Geisert *et al.*, 1994), western spotted skunk (Mead and Eroschenko, 1995), rhesus monkey (Okulicz and Scarrell, 1998) and human (Lessey *et al.*, 1988) endometrium. In contrast to previous reports in the mouse endometrium (Tan *et al.*, 1999), which is closet in species similarities to the rat, PR immunofluorescence staining in the present study increased in the glandular epithelium and glandular compartments at day 5.5 of pregnancy, or the day of blastocyst implantation. However, in an immunohistochemical study of PR staining in ovariectomised wild-type mice, oestrogen treatment resulted in complete loss of PR expression in the luminal epithelium while that in the glandular epithelium was preserved (Tibbetts *et al.*, 1998). These data suggest a differential regulation of PR by oestrogen in these epithelial compartments (Tibbetts *et al.*, 1998). PR expression is dually controlled by oestrogen and progesterone, which act sequentially to regulate the cellular concentration of PR. In most target cells PR mRNA and protein synthesis is increased by oestrogen and decreased by high serum progesterone levels (Tibbetts *et al.*, 1998; Tan *et al.*, 1999). The higher levels of PR protein in the glands at day 5.5 of pregnancy suggest a progesterone-dependent role for the glands at this day of pregnancy. As discussed later, a number of growth factors and cytokines are found in uterine flushings around this day of pregnancy (Carson *et al.*, 2000; Gray *et al.*, 2001; Gray *et al.*, 2002; Brayman *et al.*, 2004), suggesting a secretory role for the endometrial glands at this time. It is possible that this is the reason that PR protein expression is not decreased at day 5.5 of pregnancy despite high circulating levels of progesterone.

In accordance with other studies (Tan *et al.*, 1999), PR mRNA levels were decreased by day 6.5 of pregnancy in both the implantation (1.55-fold) and non-implantation sites (2.77-fold). *In situ* hybridisation indicated that the PR mRNA at this stage of pregnancy was no longer detectable in the epithelial compartments, but had shifted to the decidual bed (Tan *et al.*, 1999). The current study did not analyse PR mRNA levels in the various endometrial cell compartments and thus the overall down-regulation observed in PR mRNA levels within the entire uterus is due to the dilution of individual compartments effects by the decrease in PR expression in most endometrial compartments. Immunolocalisation of PR protein in the present study concur with the overall decrease in PR mRNA levels as pregnancy progresses from day 5.5 to day 6.5 and with the decrease being more pronounced in the non-implantation sites.

PR protein and mRNA levels were lower in all regions of the non-implantation sites when compared to those of the implantation sites at all three days of pregnancy analysed. This is consistent with previous reports (Logeat *et al.*, 1980; Hertogh *et al.*, 1986). Logeat *et al.* (1980) suggested that this increase in PR expression in the implantation sites is due to steroid hormone secretion by the implanting blastocyst. They reported stable levels of PR in ovariectomised rats in which decidualisation had been artificially stimulated by trauma. This finding led them to suggest that the presence of an embryo causally increases PR levels in the implantation sites. In further support of their hypothesis, pregnant animals that were ovariectomised on day 5 of pregnancy, in which implantation is still able to occur, maintained this 2-fold difference in PR levels between the implantation and non-implantation sites (Logeat *et al.*, 1980). No additional recent studies could be found to substantiate these claims.

The localised increase in PR within the implantation sites could be of importance in ensuring that the blastocysts implant in a precisely spaced pattern (Enders and Schlafke, 1967). The higher level of PR in the implantation sites is also likely to ensure that progesterone action within the implantation sites is sufficient in this area. While, the idea of a local effect of steroid hormone regulation by the blastocyst is a tidy hypothesis, a further premise is that PR levels are also regulated by a non-steroid hormone-mediated pathway. It is possible that an additional factor/s regulates PR levels and that this factor exists at higher levels within the implantation sites. In support of this statement, in ovariectomised hamsters, progesterone implants resulted in lower levels of uterine PR; however, the concentration of PR did not progressively decrease with increasing duration of exposure to progesterone (Okulicz, 1986). Okulicz interpreted this by stating that the maintenance of a PR steady-state is a consequence of constitutive PR replenishment, despite the high progesterone (Okulicz, 1986). This PR replenishment mechanism was also previously postulated in rabbits (Isotalo *et al.*, 1981). More recent studies have shown that PR levels in the endometrium of ovariectomised mice without hormonal treatment are high in the luminal and glandular epithelium (Parczyk *et al.*, 1997;

Tibbetts *et al.*, 1998). Parczyk *et al.* (1997) reported a 50% decrease in PR levels after ovariectomy, indicating PR regulation is not fully dependent on progesterone and oestrogen. Graham and Clarke (1997), however, reported that a decrease in circulating progesterone around the time of blastocyst fertilisation is sufficient to delay implantation.

In order to ascertain the function and importance of progesterone during early pregnancy, progesterone action and signalling needs to be antagonised. The simplest approach here is to effectively compete for binding of the physiological hormone ligand for progesterone with an inactive synthetic analogue (steroidal or nonsteroidal). RU486 is among the most widely used progestin antagonists (Leonhardt and Edwards, 2002).

Treatment with RU486 at day 3.0 of pregnancy resulted in a significant decrease in PR protein levels at all three days of pregnancy analysed, when compared to levels in the control pregnant animals. Importantly, at the day of blastocyst implantation, day 5.5 of pregnancy, treatment with RU486 resulted in significantly reduced PR protein and mRNA levels in both the implantation and non-implantation sites as compared to levels in the control pregnant animals. Due to the oestrogen and progesterone regulation of PR, it was initially hypothesised that treatment with RU486 would increase PR expression, the rationale being that the activation of this receptor is reportedly induced by oestrogen via the ER (Tan *et al.*, 1999). This, however, was not the case. A decrease in PR expression led to the exploration of the hypothesis that RU486 reduces oestrogen effects as well. Vinijsanun and Martin (1990) reported that the RU486-induced effects on the mouse endometrium were restricted to actions mediated by progesterone; however, in support of the hypothesis of the current study, PR levels reported in this study concur with reports in ovariectomised animals (Vinijsanun and Martin, 1990; Tibbetts *et al.*, 1998). Tibbetts *et al.* (1998) demonstrated that in the absence of hormonal treatment, PR immunostaining in ovariectomised wild-type mice was intense within the luminal and glandular epithelium. In contrast, the stroma and myometrium showed only trace levels of PR (Tibbetts *et al.*, 1998). In the present study, PR levels were not as great in the RU486-treated animals as compared to the control pregnant animals; however, PR expression was still high in both the luminal and glandular epithelium and was significantly lower in the decidual layer and the glandular stroma, in accordance with levels reported in a previous study (Parczyk *et al.*, 1997).

Parczyk *et al.* (1997) reported a decline in PR levels in whole tissue homogenates following ovariectomy. Treatment with the anti-oestrogen ZM 182780 to specifically block ER function in intact animals resulted in PR levels similar to that of the ovariectomised animals (Parczyk *et al.*, 1997). Treatment of ovariectomised animals with oestrogen, increased PR expression in all cell layers except the uterine epithelium where PR expression was repressed (Parczyk *et al.*, 1997). Ohta *et al.* (1993) reported an increase in PR within the uterine epithelium following ovariectomy (Ohta *et al.*,

1993). In accordance with this, other reports have indicated that oestrogen has dual effects on the expression of PR, in that it decreases levels in the luminal epithelium and increases levels in the myometrium and stroma (Tibbetts *et al.*, 1998; Tan *et al.*, 1999). Thus, an increase in the level of PR in the luminal epithelium of the ovariectomised and anti-oestrogen treated animals could be as a result of oestrogen ablation in these studies (Ohta *et al.*, 1993; Parczyk *et al.*, 1997). Neither Parczyk *et al.* (1997) nor Ohta *et al.* (1993) could exclude the possibility that the increase seen in PR was as a result of progesterone depletion, or another consequence of ovariectomy and not as a direct result of oestrogen depletion. In addition, that treatment with the pure anti-oestrogen ZM 182780 also resulted in an up-regulation of PR levels and that treatment with oestradiol resulted in a decrease in PR levels in the epithelium, led the investigators to suggest that this increase in PR is in fact an ER meditated effect (Parczyk *et al.*, 1997).

In the present study, PR levels in the RU486-treated animals were compared to control pregnant animals and not to ovariectomised animals or nonpregnant animals as in other studies (Ohta *et al.*, 1993; Parczyk *et al.*, 1997). PR levels are significantly increased during early pregnancy (Tibbetts *et al.*, 1998; Tan *et al.*, 1999) and as a result, in the present study a decrease in PR levels in all compartments of the endometrium, as a result of RU486 administration, is reported. In the current study, PR levels were still quite high after treatment with RU486; but, a comparison with PR levels after ovariectomy is necessary to establish whether RU486-treated and ovariectomised animals exhibit similar levels of PR expression. RU486 has been reported to have not only anti-progestin effects, but anti-oestrogenic effects as well, this since RU486 has been reported to show a very weak binding to both the human and rat ER (Chwalisz *et al.*, 1995). Progesterone has been shown to control oestrogen action in reproductive tracts, for example, by inhibiting the oestrogen-dependent cell proliferation during early pregnancy (Lydon *et al.*, 1995; Tan *et al.*, 1999), so it is not surprising that RU486 also interferes with various oestrogenic responses (McDonnell and Goldman, 1994). It has been hypothesised that this inhibition of oestrogen action is via the PR isoform PR-A as this isoform was demonstrated to inhibit human ER function, which could not be demonstrated by the PR-B isoform (McDonnell and Goldman, 1994). The researchers proposed that the mechanism of non-competitive inhibition of ER involves the sequestration by PR-A of a transcription factor required for ER transcriptional activity (McDonnell and Goldman, 1994).

In support of the theory that the endometrium is more hormonally under-stimulated as a result of RU486 treatment, rather than one exhibiting unopposed oestrogen action, relates to the increased vascular permeability of the implantation sites recognised as blue bands of Pontamine Sky blue staining, which is not observed in RU486-treated animals. As discussed previously in the ultrastructure section (see Chapter 3), this increased vascular permeability is under the control of the ovarian hormone oestrogen (Tan *et al.*, 1999) and thus a lack of this response in RU486-treated

animals, suggests that oestrogen action is reduced/inhibited by this antiprogestin. This visualisation of increased vascular permeability in the implantation sites by Pontamine Sky blue is also not demonstrated in ovariectomised animals lacking hormonal replacement (Psychoyos, 1970). However, upon treatment with oestrogen, this response can be induced in ovariectomised animals (Psychoyos, 1970). As described previously, it is possible that the oestrogen surge of early pregnancy, just prior to implantation, is not sufficient to initiate this increased vascular permeability response without prior priming of the endometrium with progesterone. However, given that RU486 can bind weakly to ER (Chwalisz *et al.*, 1995) and anti-oestrogenic reports of antiprogestins have been documented (Wolf *et al.*, 1989; Chwalisz *et al.*, 1991; Slayden and Brenner, 1994; Slayden and Brenner, 2004), it is postulated that it is more likely that RU486 induces a hormonally under-stimulated endometrium. Despite the weak binding of RU486 to ER, in the presence of PR-A in humans, McDonnell *et al.* (1994) reported that when compared to the pure anti-oestrogen ICI 164382, RU486 demonstrated an over 80% efficacy in its ability to reduce oestrogen action (McDonnell and Goldman, 1994).

In the present study, as pregnancy progressed from day 4.5 to day 6.5 in the RU486-treated animals, PR levels began to increase in all regions of both the implantation and non-implantation sites. This increase in PR expression can be attributed to the half-life of RU486, this being 4h in the rat (Mahajan and London, 1997; Sitruk-Ware and Spitz, 2003). It can thus be postulated that as RU486 is metabolised, progesterone is increasingly able to bind to its receptors and re-establish its effects on the endometrium. The decrease in RU486 would also result in increased oestrogen binding to ER and thus increased oestrogen effects on the endometrium. It is thus unclear as to which ovarian hormone is responsible for this increase in PR levels as RU486 is metabolised.

By day 6.5 of pregnancy, PR mRNA levels were significantly higher in the implantation and non-implantation sites as compared to that of the control pregnant animals at this day of pregnancy. This was not reflected in the PR protein levels, possibly because protein synthesis was not as yet sufficient for PR protein levels in the RU486-treated animals to have surpassed that of the control pregnant animals. Studies of protein levels in RU486-treated animals beyond day 6.5 of pregnancy are needed to substantiate this hypothesis. An additional explanation may relate to the limitation of protein expression being analysed in the luminal epithelium, subepithelial stroma, glandular epithelium and glandular stroma only, whereas in the RT-qPCR study, whole tissue homogenates were used, with a resultant dilution of measured PR expression. *In situ* hybridisation studies would be more beneficial to gene expression studies within the endometrium to better analyse expression patterns within the different endometrial compartments.

In the current study, immunolocalisation of PR indicated that levels were significantly reduced in the decidual area of the RU486-treated animals. Lydon *et al.* (1995) demonstrated that progesterone is

necessary for the induction of uterine decidualisation during early pregnancy as PRKO (-/-) mice did not display this response (Lydon *et al.*, 1995). Interestingly, this decidual response in ovariectomised animals is absent, this despite reported high levels of PR within the stroma surrounding the luminal epithelium within the ovariectomised animals (Parczyk *et al.*, 1997). This apparent discrepancy is most likely caused by a lack of circulating progesterone, thus possible factors responsible for directly inducing the decidual response are not able to be transcribed without the binding of progesterone to PR to induce progesterone-dependent gene transcription (Mahajan and London, 1997). The same hypothesis can be applied to RU486-treated animals in which PR levels are still detected within the decidual layer, even though they are lower than that seen within control pregnant animals.

Previous studies have reported a prevention of the decidual process by the antiprogestin RU486 (Crombie *et al.*, 1994). In the current study, however, the decidual response is reduced in the RU486-treated animals. A possible reason for this discrepancy could be that the decidual response in the Crombie *et al.* (1994) study was artificially stimulated in pseudopregnant mice, whereas the decidual response in the animals used in the present study was natural. The underlying mechanisms causing this difference between the naturally and artificially stimulated decidual response remains to be elucidated. The reported reduction in the extent of decidualisation following treatment with RU486 in the current study was visually assessed rather than with a specific decidualisation marker, such as prolactin, laminin or osteopontin (OPN). It would thus be beneficial to this work to revisit the effect of RU486 on decidualisation during early pregnancy using a carefully chosen marker.

It is interesting to note that in ER-α-deficient mice, the decidual response could be induced by progesterone and an increase in the level of PR, suggesting that oestrogen is not responsible for this increase in PR in the decidual bed. If this is the case, then the increase in PR levels could be regulated by a non-ER-mediated pathway (Paria *et al.*, 1999). Therefore, it would seem that the base level of PR seen not only in the decidual layer, but in the luminal and glandular epithelia and the glandular stroma may be as a result of a non-ER-mediated factor/s and pathway, and not as a result of a lack of oestrogen stimulation.

The decidual process is of vital importance in order to sustain a growing conceptus. Animals in which no decidual response was detected were unable to sustain a viable blastocyst (Rider *et al.*, 1985). It is thus feasible that the significant reduction of the decidual response in the rat uterus by RU486 could certainly be an explanation for the efficiency of RU486 in blocking implantation and subsequent pregnancy.

CHAPTER 5

ROLE OF RU486 IN INDUCING APOPTOSIS DURING EARLY PREGNANCY; ASSESSMENT USING THE BAX/BCL-2 INDEX

5.1 INTRODUCTION

5.1.1 Cell Death

The term apoptosis, derived from the Greek word for 'dropping off' of petals or leaves from plants or trees, is an active form of cellular suicide which follows specific pathways and is regulated by specific gene expression patterns and enzymic activation (Adapted from Gu *et al.*, 1994; Erickson, 1997). Apoptosis, as a normal physiological regulatory process, works in conjunction with mitosis to establish an adequate balance between cell division and cell death, serving to remove unneeded, or potentially dangerous cells (Erickson, 1997; Correia-da-Silva *et al.*, 2004). It is also implicated in pathological processes, such as tumour growth and recession, hyperthermia, and hypoxia (Thompson, 1995). In normal physiological processes, the importance of apoptosis can be seen embryonically in the deletion of interdigital webs between the fingers and toes and the formation of lumina in developing organs such as the heart and uterus, during foetal development (Erickson, 1997).

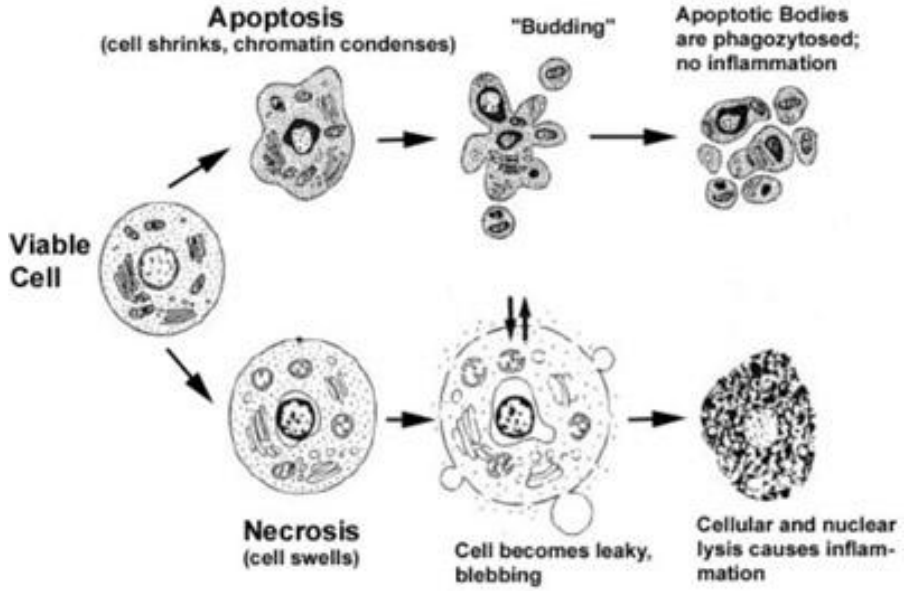


Figure 5.1 Schematic representation of the differences observed between the two major forms of cell death: apoptosis (programmed cell death) and necrosis.
(http://www.celldeath.de/encyclo/aporev/revfigs/rev_2.jpg)

Necrosis, the alternative form of cell death, is accidental and regulated by external factors (Erickson, 1997). Necrosis occurs in groups of cells and its single most common trigger is lack of oxygen or hypoxia; however, toxins such as insecticides and poisons can also trigger a necrotic response. When cells undergo necrosis, cell permeability increases which results in the bursting or rupturing of the cell

and the cellular organelles. The cytoplasmic and nuclear contents leak into the extracellular matrix, triggering an inflammatory response, whereby neutrophils and macrophages enter the necrotic area to phagocytose the necrotic tissue (Figure 5.1) (Walker *et al.*, 1988; Schwartzman and Cidlowski, 1993; Nelson, 1996; Erickson, 1997; Smith *et al.*, 1997). Alternatively, apoptosis is a sudden, rapid process, occurring in single cells, in which physiological stimuli trigger precise signal transduction pathways (Erickson, 1997; Smith *et al.*, 1997). Apoptotic cells shrink without swelling and are phagocytosed by surrounding cells, so negating inflammatory responses, as no toxic products are released into the surroundings (Figure 5.1) (Erickson, 1997; Smith *et al.*, 1997; Tassell *et al.*, 2000).

Apoptosis is characterised and identified by a number of known biochemical and molecular changes as well as a precise pattern of morphological changes (Figure 5.2) (Erickson, 1997; Tassell *et al.*, 2000). This series of changes includes, in order, disruption of the cellular metabolism, chromatin aggregation, detachment of the cell from the extracellular matrix, loss of specialised structures such as microvilli and junctional complexes, DNA coalescence and fragmentation, condensation and shrinkage of the cytoplasm, and the formation of blebs on the cell surface to form apoptotic bodies (Nelson, 1996; Erickson, 1997; Smith *et al.*, 1997; Tassell *et al.*, 2000). Both the fragmented DNA and cytoplasmic organelles are contained in membrane-bound apoptotic bodies; therefore, no materials causing inflammation are released. The apoptotic bodies are instead, engulfed by phagocytic neighbouring cells and macrophages (Figure 5.2) (Erickson, 1997).

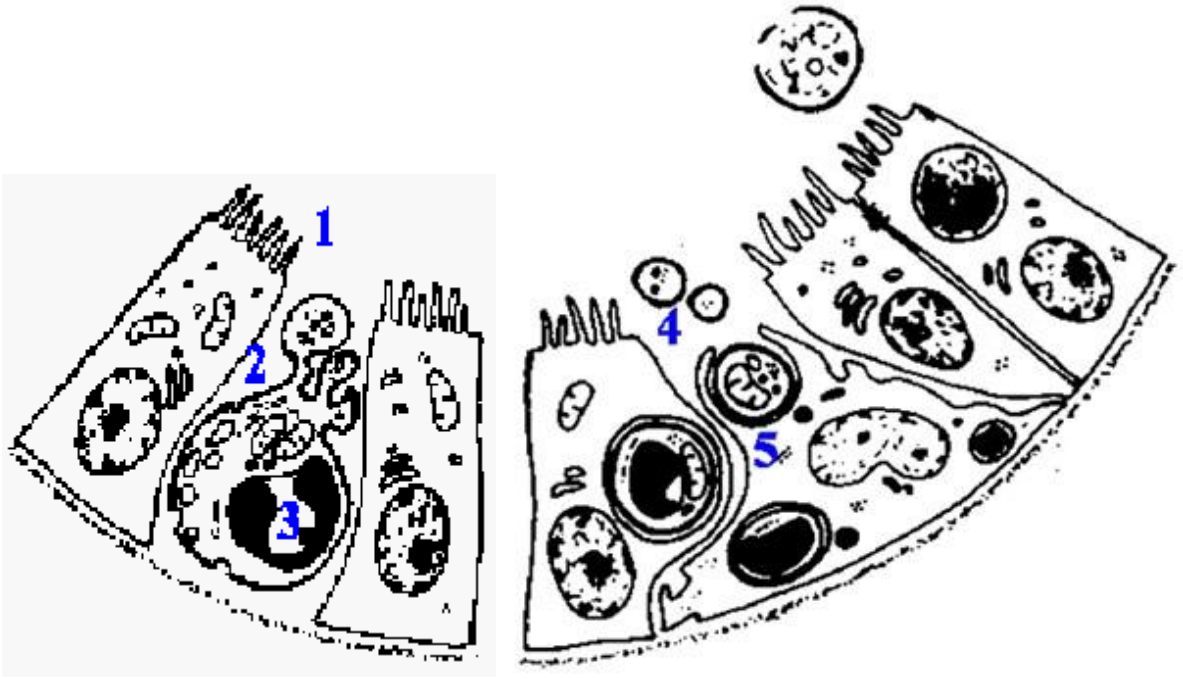


Figure 5.2 The characteristic cellular changes that occur during apoptosis. 1) Cell Shrinkage; 2) Loss of surface contact with neighbouring cells; 3) Condensation of the chromatin around the edge of the nucleus; 4) Fragmentation of the apoptotic cell into small apoptotic bodies; 5) Phagocytosis of the apoptotic bodies by neighbouring cells or macrophages.
(www.path.cam.ac.uk/part1B_pract/P01/image00.gif)

5.1.2 Progesterone Regulation of Apoptosis in the Endometrium

An important function of progesterone during early pregnancy is the regulation of apoptosis. The luminal epithelial cells within the endometrium act as a barrier to implantation (Murphy, 1998). Therefore, in order for a viable blastocyst to implant, it must first breach the luminal epithelium and burrow into the uterine wall. This inverse displacement of the luminal epithelium and the subsequent removal of the basement membrane, the extracellular matrix and the decidual cells is associated with apoptosis (Welsh and Enders, 1991; Welsh, 1993). Decidual cell death by apoptosis allows for remodelling of the implantation chamber to accommodate the growing embryo (Gu *et al.*, 1994; Akcali *et al.*, 1996; Galán *et al.*, 2000). Thus, apoptosis plays a crucial role in both placental implantation and the decidualisation process.

The uterine glands play an important role in the development of a receptive environment for successful blastocyst implantation and subsequent pregnancy, as evident by the loss of pregnancy in the uterine gland knockout (UGKO) ewe due to loss of the glandular secretory products (Gray *et al.*, 2001; Gray *et al.*, 2002). These secretory products include interferon γ (IFN-γ), Leukaemia Inhibitory Factor (LIF) and Calcitonin (Stewart *et al.*, 1992; Zhu *et al.*, 1998a; Gray *et al.*, 2002). The epithelium of the glands has been reported to undergo both apoptosis and proliferation during early pregnancy (Fei *et al.*, 2001; Selam *et al.*, 2001; Demir *et al.*, 2002), as well as during the menstrual cycle in humans and the oestrous cycle in rats (Burroughs *et al.*, 2000; Mendoza-Rodríguez *et al.*, 2002). This remodelling is thought to be necessary for acquisition of the secretory status of the glands (Murray, 1992).

To re-iterate, in the rat uterus, day 2.5 of pregnancy represents the pre-implantation phase, day 4.5, the day of blastocyst apposition against the uterine wall, day 5.5, irreversible adhesion of the blastocyst to the luminal epithelium and on day 6.5 of pregnancy, the blastocyst penetrates through the luminal epithelium into the maternal stromal layer by displacement penetration (Murphy, 1995; Carson *et al.*, 2000; Tassell *et al.*, 2000).

Initially, degradation of the luminal epithelial cells was thought to be as a result of an autolytic response (Schlafke and Enders, 1975; Welsh and Enders, 1985), or necrosis caused by the isolation of the epithelial cells from their oxygen and nutrients by the closely packed decidual cells (Parr *et al.*, 1987). Parr and colleagues (1987) showed that this degradation was by apoptosis. They presented electron micrographs of the mouse endometrium showing the characteristic surface blebbing and other features consistent with apoptotic cells (Parr *et al.*, 1987).

Further, Parr *et al.* (1987) suggested that this apoptosis of the uterine epithelial lining occurs only when the uterine epithelial cells are in close apposition with the trophoblasts. This, however, was shown to be erroneous by Welsh and Enders (1991) as the removal of three of the implantation barriers; namely, the epithelium lining the implantation site, the basal lamina of the epithelium, as well as the extracellular matrix below the epithelium, occurred before the presence of trophoblasts within the implantation site.

Invasion by the blastocyst also stimulates the stromal cells to further proliferate and continue to differentiate from fibroblast-like cells into decidual cells (Gu *et al.*, 1994; Shaw *et al.*, 1998; Carson *et al.*, 2000; Akcali *et al.*, 2003). Decidualisation of the stromal cells begins in the antimesometrial zone (Figure 5.3) around the time of blastocyst apposition at day 4.5 and then extends to the mesometrial zone (Figure 5.3). The decidual cells in the mesometrial region are smaller and less differentiated than those in the antimesometrial region (O'Shea *et al.*, 1983). When the blastocyst implants, extensive regression and remodelling of the decidual tissue takes place to accommodate the growing embryo (Gu *et al.*, 1994).

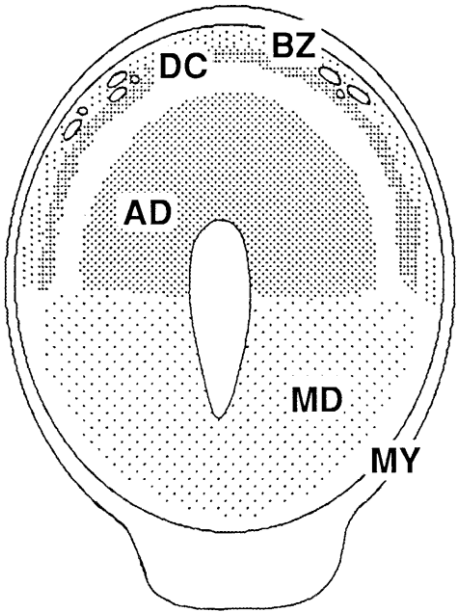


Figure 5.3 Schematic representation of the different regions within the mouse and rat uterus. AD – antimesometrial decidual region; MD – mesometrial decidual region; DC – decidua capsularis; BZ – basal zone; MY – myometrium. (From: Hirabayashi *et al.*, 1999)

The regression of the decidual cells by apoptosis also begins in the antimesometrial region, closest to the invading trophoblasts, and later in the mesometrial region (Gu *et al.*, 1994; Afonso *et al.*, 1997). Correia-da-Silva *et al.* (2004) showed that, in the rat, the regression of the decidua begins at day 10 in the antimesometrial area and on day 14 in the mesometrium. Interestingly, decidual tissue regresses in a similar manner whether the decidual response was induced by the implanting blastocyst, or by

artificial stimuli (Hirabayashi *et al.*, 1999), suggesting that the signals that promote or inhibit decidual cell death are intrinsic (Gu *et al.*, 1994; Tessier *et al.*, 2003).

During early pregnancy, glandular remodelling at approximately the time of the implantation window, has been reported in both the human and the rhesus monkey endometrium and is thought to occur to facilitate a change in function of the glands during the early stage of pregnancy to a more secretory state (Murray, 1992; von Rango *et al.*, 1998; Fei *et al.*, 2001; Gray *et al.*, 2001; Selam *et al.*, 2001). The apoptotic response during the menstrual and oestrous cycles is thought to be necessary for the maintenance of homeostasis during the proliferative phase as well as to facilitate sloughing off of the endometrium during the secretory phase (Johnson *et al.*, 2001).

In the menstrual cycle, apoptotic cells have been identified in the glands of both the basal and functional endometrium; however, the spatiotemporal pattern of apoptotic cells as reported in the literature is confused (Kokawa *et al.*, 1996; von Rango *et al.*, 1998). Von Rango *et al.* (1998) proposed that apoptosis begins in the glands of the basalis during the early secretory phase, spreading through the functionalis into the stroma and continuing through the peri-implantation phase. During the oestrous cycle of the rat, the highest apoptotic index of the both the luminal and glandular epithelial compartments is observed during the day of oestrous, whereas the lowest index is observed on the previous day, pro-oestrous (Burroughs *et al.*, 2000; Mendoza-Rodríguez *et al.*, 2002). Burroughs *et al.* (2000) also reported that maximal apoptosis occurred when oestrogen and progesterone levels were both low.

In general, progesterone has been shown to protect against apoptosis, whereas withdrawal of progesterone causes apoptosis to occur. The apoptotic cell death that occurs throughout the endometrium has been shown to be suppressed by progesterone in ovariectomised animals (Nawaz *et al.*, 1987).

5.1.3 Apoptosis Pathways

5.1.3.1 The tumour necrosis factor receptor (TNFR) gene superfamily

Extrinsic apoptosis signalling is mediated by the activation of cell surface receptors, so called "death receptors", which transmit apoptotic signals once bound to specific ligands. These receptors all belong to the TNFR gene superfamily and include TNFR-1, Fas/FasL and the TRAIL receptors (Sartorius *et al.*, 2001; Joswig *et al.*, 2003). Local concentrations of procaspase-8 in the vicinity of the death receptor signalling complex leads to activation of one of the initiator caspases, caspase-8, which in turn acts downstream to activate one of the effector caspases, such as caspase-3, which cleaves

cellular substrates essential for continued cell survival, thus ultimately resulting in cell death (Scaffidi, 1998).

5.1.3.2 The Bcl-2 family

The intrinsic apoptosis pathway involves apoptosome formation by the release of cytochrome c from the mitochondria. The pro-apoptotic Bcl-2 family members, such as Bax, induce the release of cytochrome c and other mitochondrial pro-apoptotic factors into the cytosol. Cytosolic cytochrome c then binds to the monomeric Apaf-1 to assemble the apoptosome (Figure 5.4). This complex triggers the activation of procaspase-9, which subsequently initiates a caspase cascade involving downstream effector caspases, such as caspase-3, -6 and -7; resulting in cell death (Luo *et al.*, 1998; Slee *et al.*, 1999; Acehan *et al.*, 2002; Joswig *et al.*, 2003). The anti-apoptotic Bcl-2 family members, such as Bcl-2, prevent cytochrome c release from the mitochondria, thus preventing the apoptotic pathway to progress (Akcali *et al.*, 1996).

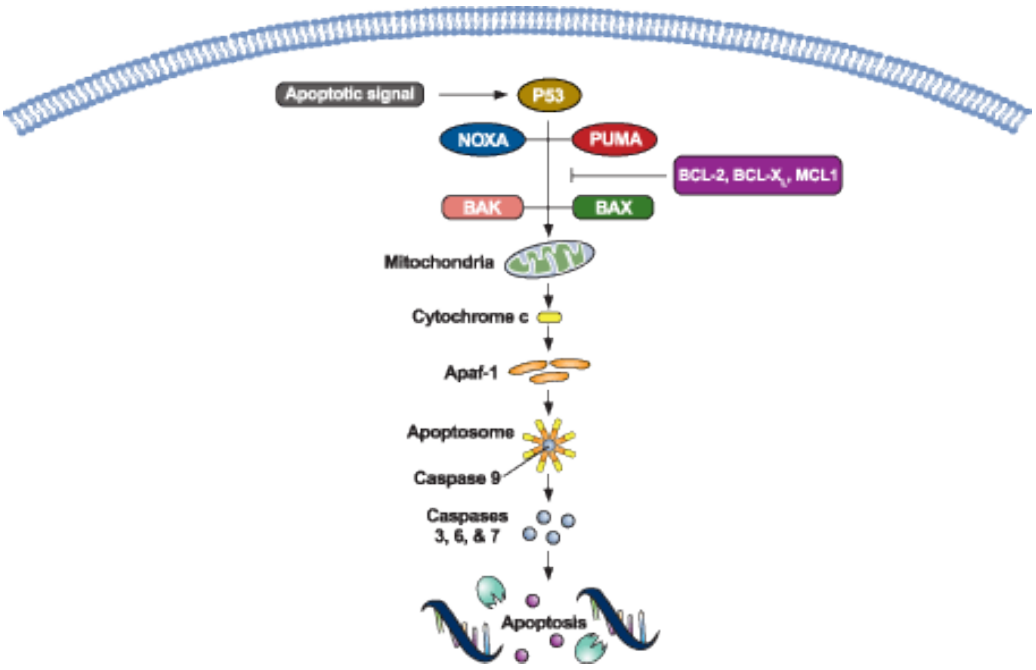


Figure 5.4 Schematic representation of the apoptosis cascade and the function of Bax and Bcl-2 in this pathway. Bax promotes release of cytochrome c by the mitochondria, which binds to Apaf-1, forming an apoptosome. This complex activates procaspase-9, resulting in the activation of the initiator caspase-9. This initiator caspase induces the effector caspases, such as caspase-3, -6 and -7, ultimately resulting in cell death (From: Ashkenazi, 2002).

5.1.3.2.1 Bax and Bcl-2

Apoptosis is regulated by various proteins, including the Bcl-2 protein family. This family of proteins consists of both pro-apoptotic (e.g. Bax, Bak, Bad, Bag and Bcl-x_s) and anti-apoptotic (e.g. Bcl-2, Bcl-x_L, Mcl-1) proteins (Erickson, 1997; Akcali *et al.*, 2003). Bcl-2 deficient mice exhibit extensive general apoptosis, while overexpression of Bcl-2 protects cells from apoptosis, providing evidence

that Bcl-2 inhibits the execution of apoptosis and is thus an anti-apoptotic protein (Akcali *et al.*, 1996; Erickson, 1997). Bax dimerises either with Bcl-2, or with itself to form functional cell death regulators (Akcali *et al.*, 1996).

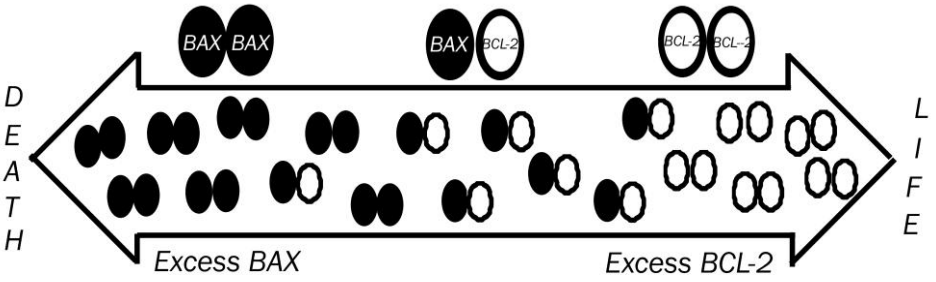


Figure 5.5 Schematic representation of the Bax/Bcl-2 ratio which determines cell survival or cell death following the apoptotic stimulus. The schematic indicates the dimerisation of the Bax and Bcl-2 proteins to form homodimers (Bax:Bax and Bcl-2:Bcl-2) and heterodimers (Bax:Bcl-2) (Adapted from: Erickson, 1997).

The ratio of Bcl-2/Bax heterodimers to Bax/Bax homodimers will determine whether or not a cell will undergo apoptosis, where excess Bax will promote cell death (Figure 5.5). When there is an excess of the Bcl-2 protein, it will bind to all the Bax proteins, thus neutralising Bax's pro-apoptotic effect. Excess Bcl-2 proteins will pair with each other resulting in an anti-apoptotic environment and cell survival. If there is an excess of Bax proteins, they bind all the Bcl-2 proteins forming Bax/Bcl-2 heterodimers. This results in a lack of bioavailable Bcl-2, allowing the excess Bax proteins to bind to each other to form homodimers which accelerate cell death following an apoptotic signal. A delicate cellular balance between anti-apoptotic and pro-apoptotic proteins ultimately controls the fate of the cell (Figure 5.5) (Oltvai *et al.*, 1993; Erickson, 1997; Akcali *et al.*, 2003).

The endometrial apoptosis of early pregnancy could be regulated by the Bax/Bcl-2 ratio, as Akcali *et al.* (1996) reported that decidual differentiation and eventual apoptosis was associated with a significant increase in Bax expression and decrease in Bcl-2 expression. The increase in Bax expression was first observed in the luminal and glandular epithelial compartments and then following this in the stroma directly below the luminal epithelium, which eventually progressed throughout the stromal compartment (Akcali *et al.*, 1996). Bax expression within the stroma was reported to occur simultaneously with the decidualisation process. Bcl-2 protein expression was only observed in the epithelial and glandular compartments and decreased as decidualisation progressed (Akcali *et al.*, 1996). The apoptotic process that occurs during the transition from pro-oestrous to oestrous in the rat uterus is also regulated in part by the Bax/Bcl-2 ratio (Mendoza-Rodríguez *et al.*, 2003). In the human endometrium, Bcl-2 expression is almost entirely inhibited during the secretory phase of the menstrual cycle, around the time of increased apoptosis, whereas Bax protein expression is highest at the end of the secretory phase (Critchley *et al.*, 1999; Castro *et al.*, 2002). An additional study reported that Bcl-2 protein is highly expressed during early pregnancy within the decidua of the rat

uterus, with expression dropping very quickly at day 9.5, when regression and remodelling of the decidual layer begins (Dai *et al.*, 2000). Immunostaining for Bax and Bcl-2 was not observed in the endometrium of nonpregnant animals, or during the preimplantation phase (Dai *et al.*, 2000).

The shift in the ratio or balance of Bcl-2 and Bax has been suggested to be responsible, at least in part, for the increased apoptosis observed within the glandular epithelium in both the menstrual and oestrous cycles (Tao *et al.*, 1997; Dmowski *et al.*, 2001; Mendoza-Rodríguez *et al.*, 2003). In the study by Tao and colleagues (1997), Bcl-2 protein levels were observed to be high in the basalis layer of the human endometrium during the proliferative phase. Bax protein expression was increased during the secretory phase of the menstrual cycle predominantly within the glands of the functionalis (Tao *et al.*, 1997). No studies on the apoptotic response during early pregnancy have suggested the mechanisms of control of the apoptotic pathway.

Studies by Dai *et al.* (2000) show that progesterone is an important modulator of the Bax/Bcl-2 balance in an endometrial cell line, as antiprogestins simultaneously suppressed Bcl-2 levels and enhanced Bax. This shift led to a six-fold increase in the Bax/Bcl-2 ratio, in favour of apoptosis (Dai *et al.*, 2000). In addition, a study by Vaskivuo *et al.*(2000) correlated the degree of apoptosis and the expression of Bax and Bcl-2 with cyclic changes in serum oestradiol and progesterone concentrations. Their study showed that while endometrial apoptosis was negatively correlated with serum oestradiol concentrations, it was most pronounced when both oestradiol and progesterone were removed. This data is in agreement with previous studies (Koh *et al.*, 1995; Pecci *et al.*, 1997).

The ultrastructural study here (see Chapter 3) morphologically indicated very high levels of apoptosis within the endometrium as a result of RU486 administration at day 3.0 of pregnancy. This suggested analysis of endometrial apoptosis and apoptotic factors, such as Bax and Bcl-2, would be beneficial to this research. In order for a blastocyst to implant in the rat endometrium, it must first breach the luminal epithelium and burrow into the uterine wall. This inverse displacement of the luminal epithelium, the basal lamina and the extracellular matrix (ECM) is accomplished by apoptosis, programmed cell death. Although an increase in apoptosis as a result of RU486 administration has been previously reported in rabbits (Rotello *et al.*, 1992), the specific apoptotic factors and pathways involved in driving this process have not yet been established. As the anti-apoptotic factor Bcl-2 and the pro-apoptotic factor Bax have been reported to be expressed in the endometrium during the menstrual (Critchley *et al.*, 1999; Castro *et al.*, 2002) and oestrous cycles (Mendoza-Rodríguez *et al.*, 2003), as well as in the decidua of the rat uterus during the post-implantation stage of early pregnancy, it was queried here whether Bax and Bcl-2, in response to RU486 could be crucial role players mediating apoptosis.

5.2 RESULTS

5.2.1 Immunofluorescence Analysis of Bax and Bcl-2 Protein Expression in the RU486-Treated Rat Endometrium

As different fluorescent secondary antibodies were used for localisation of Bax and Bcl-2 here, reliable quantitative analysis cannot be carried out due to the difference in the fluorescent intensities between the secondary antibodies. Thus the Bax/Bcl-2 index reported within this section was performed to show any trends in the change in the Bax/Bcl-2 ratio as pregnancy progressed from day 4.5 through to day 5.5 in both the control pregnant and RU486-treated animals, rather than definite shifts in the Bax/Bcl-2 ratio towards an anti- or pro-apoptotic environment. A decrease in Bax levels and/or an increase in Bcl-2 levels results in a decrease in the Bax/Bcl-2 index, suggesting a shift to a more anti-apoptotic environment. Conversely, an increase in Bax protein levels and/or a decrease in Bcl-2 protein levels results in an increase in the Bax/Bcl-2 ratio, suggesting a shift towards a more pro-apoptotic environment.

Immunofluorescence was performed on each tissue section with primary antibodies specific to the apoptotic factors, Bax and Bcl-2. It was of particular interest here to determine the spatiotemporal expression pattern of these factors during early pregnancy to access whether the apoptotic status of the endometrial compartments changed following treatment with RU486, using the aforementioned Bax/Bcl-2 index.

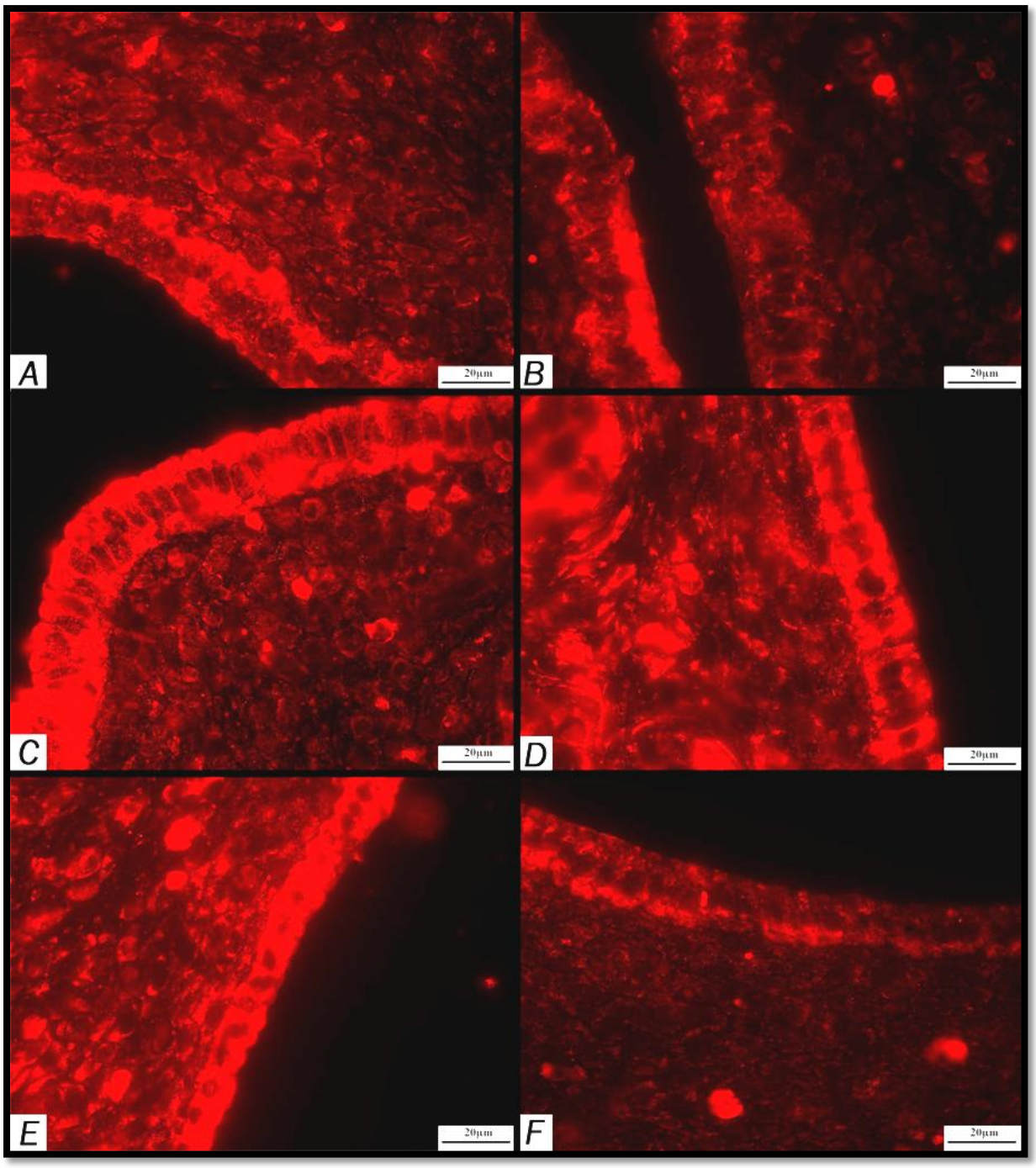


Figure 5.6 Immunofluorescent images illustrating Bax protein localisation in the luminal epithelium and the subepithelial stroma of the implantation and non-implantation sites in the uteri of control pregnant rats. A: Implantation site at day 4.5 of pregnancy, **B:** Non-implantation site at day 4.5 of pregnancy, **C:** Implantation site at day 5.5 of pregnancy, **D:** Non-implantation site at day 5.5 of pregnancy, **E:** Implantation site at day 6.5 of pregnancy, **F:** Non-implantation site at day 6.5 of pregnancy. Scale = 20µm.

Table 5.1 One-way ANOVA and Tukey Kramer *post hoc* analysis of Bax protein expression in the luminal epithelium, the subepithelial stroma, the glandular epithelium and the glandular stroma of the implantation (IS) and non-implantation (NIS) sites between days 4.5, 5.5 and 6.5 in the control pregnant (UT) and RU486-treated (T) animals showing groups that are significantly different ($p \leq 0.05$). Groups not connected by the same letter are significantly different.

Group										Mean
Luminal Epithelium										
6.5UT IS	A									**167.921**
5.5UT IS		B								**140.833**
5.5UT NIS			C							**132.435**
4.5UT IS				D						**116.919**
6.5T NIS					E					**104.375**
6.5T IS					E					**99.402**
4.5UT NIS						F				**91.486**
5.5T NIS						F	G			**87.222**
6.5UT NIS							G	H		**83.209**
5.5T IS							G	H		**80.174**
4.5T IS								H	I	**77.587**
4.5T NIS									I	**72.305**
Subepithelial Stroma										
6.5UT IS	A									**138.378**
4.5UT IS		B								**78.213**
5.5UT IS		B								**75.794**
5.5UT NIS			C							**60.185**
6.5T IS			C							**56.723**
6.5T NIS			C	D						**54.082**
6.5UT NIS				D	E					**49.449**
5.5T NIS				D	E					**48.673**
4.5T IS					E			F		**45.321**
4.5UT NIS					E			F		**44.832**
5.5T IS								F		**40.148**
4.5T NIS								F		**38.853**
Glandular Epithelium										
6.5UT IS	A									**195.443**
4.5UT IS		B								**182.52**
5.5UT IS		B								**180.705**
5.5UT NIS			C							**151.228**
6.5UT NIS				D						**102.518**
4.5UT NIS				D	E					**96.817**
6.5T IS					E	F				**92.733**
4.5T NIS						F	G			**87.733**
6.5T NIS							G			**85.303**
4.5T IS								H		**75.973**
5.5T NIS								H		**75.552**
5.5T IS									I	**62.807**
Glandular Stroma										
6.5UT IS	A									**90.7886**
5.5UT IS		B								**73.0129**
4.5UT IS			C							**64.7563**
5.5UT NIS				D						**54.2623**
6.5T NIS				D						**51.725**
6.5T IS					E					**44.0983**
4.5UT NIS					E					**43.3018**
6.5UT NIS					E					**42.0971**
5.5T NIS					E			F		**37.67**
4.5T NIS					E			F		**37.2068**
5.5T IS								F		**32.0588**
4.5T IS								F		**31.6938**

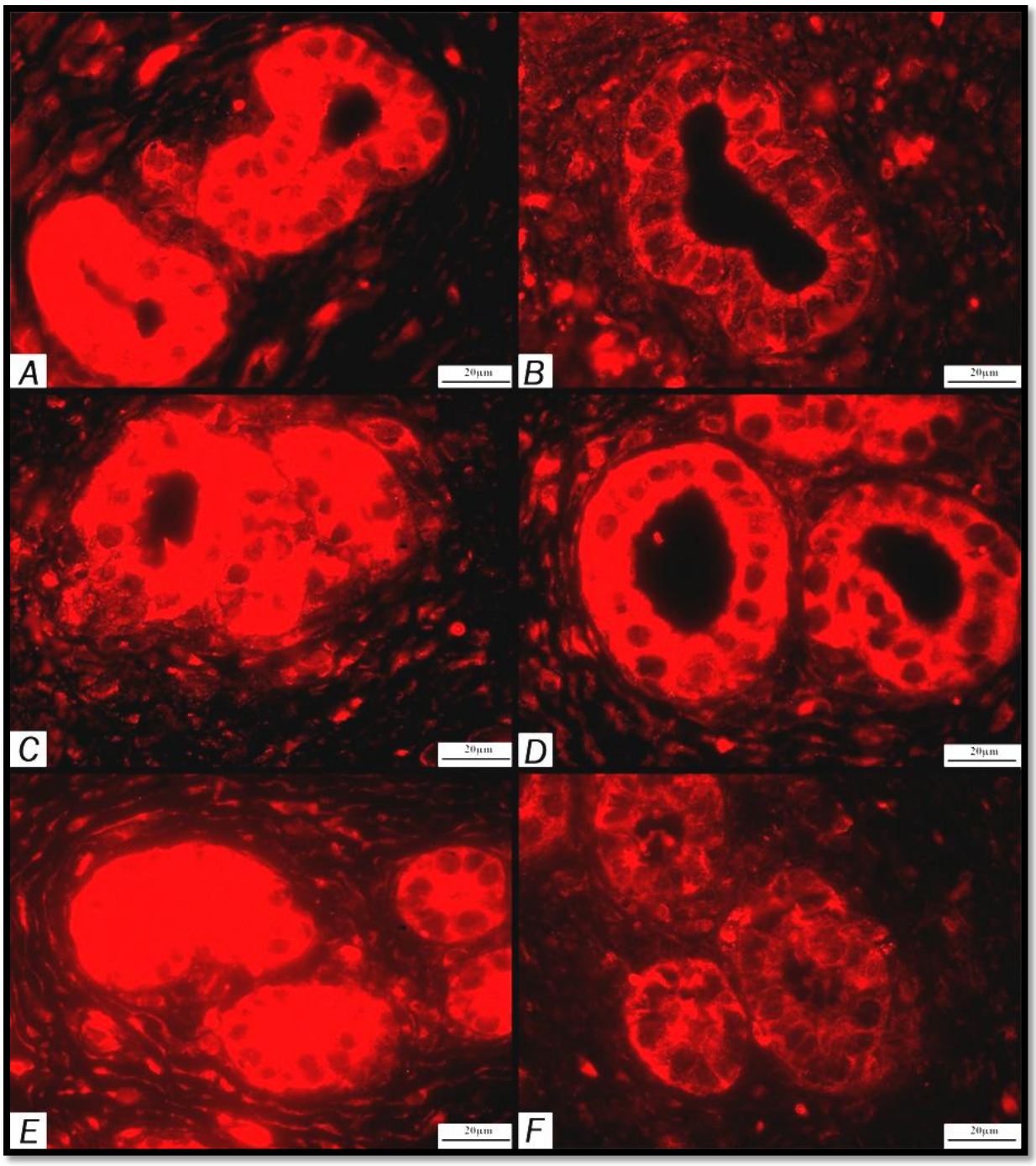


Figure 5.7 Immunofluorescent images illustrating Bax protein localisation in the glandular epithelium and the glandular stroma of the implantation and non-implantation sites in the uteri of control pregnant rats. A: Implantation site at day 4.5 of pregnancy, **B:** Non-implantation site at day 4.5 of pregnancy, **C:** Implantation site at day 5.5 of pregnancy, **D:** Non-implantation site at day 5.5 of pregnancy, **E:** Implantation site at day 6.5 of pregnancy, **F:** Non-implantation site at day 6.5 of pregnancy. Scale = 20µm.

Table 5.2 One-way ANOVA and Tukey Kramer *post hoc* analysis of Bcl-2 protein expression in the luminal epithelium, the subepithelial stroma, the glandular epithelium and the glandular stroma of the implantation (IS) and non-implantation (NIS) sites between days 4.5, 5.5 and 6.5 in the control pregnant (UT) and RU486-treated (T) animals showing groups that are significantly different ($p \leq 0.05$). Groups not connected by the same letter are significantly different.

Group							Mean
Luminal Epithelium							
6.5UT IS	A						98.6971
6.5T IS		B					71.12
5.5T NIS			C				62.8537
5.5T IS			C				62.0167
6.5T NIS			C				59.9533
5.5UT NIS				D			52.24
5.5UT IS					E		44.17
4.5UT IS					E	F	37.5465
4.5UT NIS						F	36.8017
6.5UT NIS						F	36.58
4.5T IS						F	35.53
4.5T NIS						F	33.3733
Subepithelial Stroma							
6.5UT IS	A						58.9414
5.5T IS		B					48.538
6.5T IS		B	C				43.025
5.5T NIS		B	C				42.7648
6.5T NIS			C	D			39.8217
5.5UT IS				D	E		34.7967
5.5UT NIS					E	F	31.9617
4.5UT IS					E	F	G 29.8983
6.5UT NIS					E	F	G 27.7329
4.5UT NIS						F	G 25.61
4.5T IS						F	G 25.3617
4.5T NIS							G 22.7017
Glandular Epithelium							
5.5T IS	A						42.3067
5.5T NIS	A						41.2983
5.5UT NIS	A	B					39.1067
6.5UT IS	A	B					39.0914
5.5UT IS	A	B	C				38.1917
6.5T NIS		B	C	D			33.695
4.5UT IS			C	D	E		31.801
6.5T IS				D	E		29.945
6.5UT NIS					E	F	26.7814
4.5UT NIS					E	F	26.3677
4.5T NIS						F	22.6017
4.5T IS						F	21.405
Glandular Stroma							
6.5T NIS	A						33.245
6.5UT IS	A	B					32.3629
5.5T NIS	A	B	C				28.24
5.5UT IS	A	B	C				27.7033
5.5UT NIS	A	B	C				27.1383
5.5T IS		B	C	D			26.0933
4.5UT IS			C	D			25.608
4.5UT NIS			C	D			25.1122
6.5T IS			C	D		E	24.64
6.5UT NIS			C	D		E	23.644
4.5T NIS				D		E	19.22
4.5T IS						E	17.82

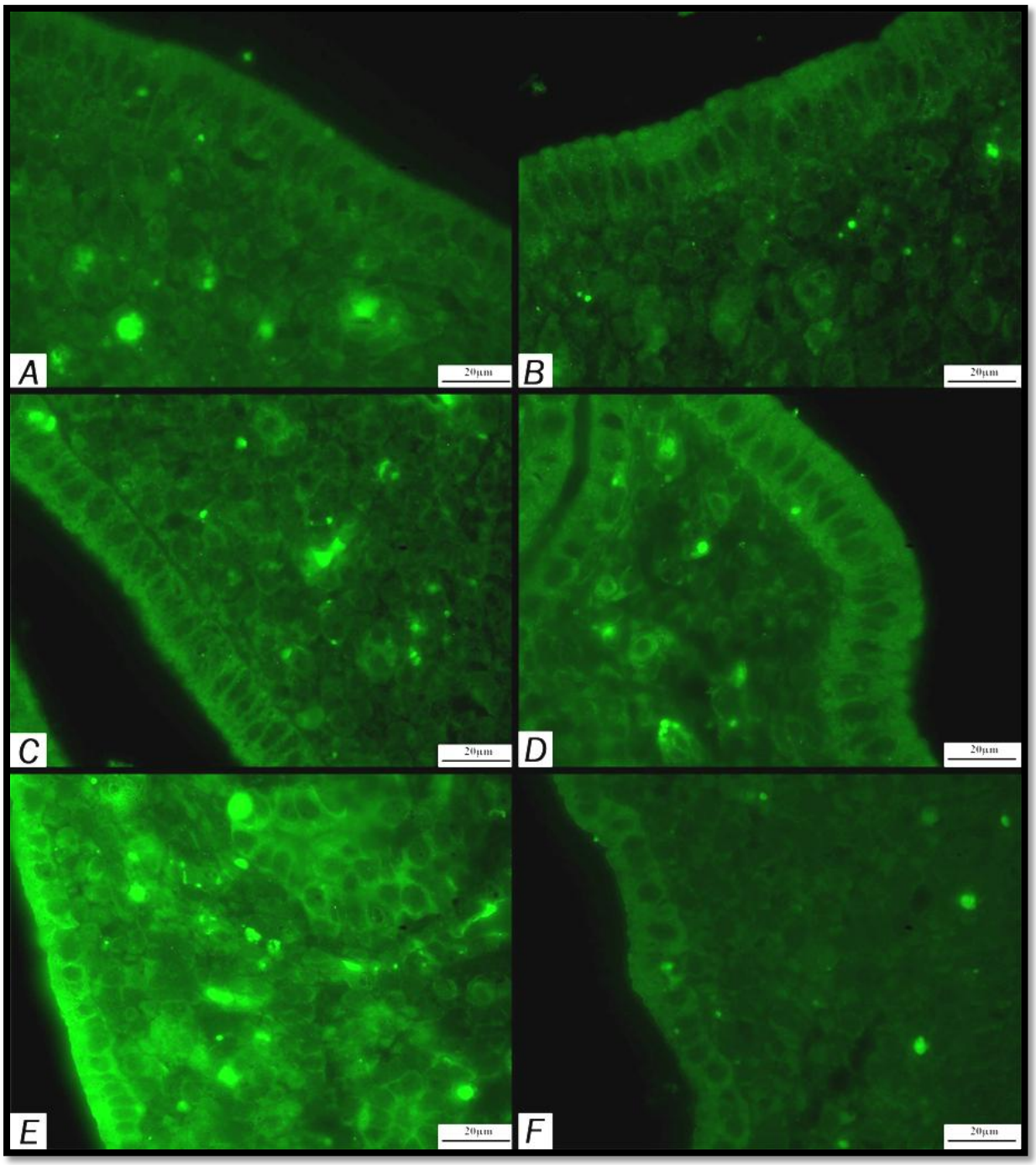


Figure 5.8 Immunofluorescent images illustrating Bcl-2 protein localisation in the luminal epithelium and the subepithelial stroma of the implantation and non-implantation sites in the uteri of control pregnant rats. A: Implantation site at day 4.5 of pregnancy, **B:** Non-implantation site at day 4.5 of pregnancy, **C:** Implantation site at day 5.5 of pregnancy, **D:** Non-implantation site at day 5.5 of pregnancy, **E:** Implantation site at day 6.5 of pregnancy, **F:** Non-implantation site at day 6.5 of pregnancy. Scale = 20µm.

5.2.1.1 The spatiotemporal expression pattern of the Bax and Bcl-2 proteins and analysis of the Bax/Bcl-2 index in the control pregnant animals

In the implantation sites of the control pregnant animals, Bax protein expression was seen to increase significantly in the luminal epithelium and the glandular stroma as pregnancy progressed from day 4.5 to day 5.5 (Graph 5.1A and D; Figure 5.6A and C; Figure 5.7A and C; Table 5.1). In the subepithelial stroma and the glandular epithelium, Bax protein levels did not change significantly (Graph 5.1B and C; Figure 5.6A and C; Figure 5.7A and C; Table 5.1).

Bcl-2 protein expression in the implantation sites did not change significantly in any of the regions of interest as pregnancy progressed from day 4.5 to day 5.5 (Graph 5.2A-D; Figure 5.8A and C; Figure 5.9A and C; Table 5.2).

In the implantation sites of the control pregnant animals, the Bax/Bcl-2 index did not change markedly in the luminal epithelium from day 4.5 (3.11) to day 5.5 (3.19) of pregnancy (Graph 5.3A; Table 5.3). In the subepithelial stromal compartment in the implantation sites of the control pregnant animals, the Bax/Bcl-2 index decreased slightly from a value of 2.62 to 2.18, as pregnancy progressed from day 4.5 to day 5.5 (Graph 5.3B; Table 5.3). In the glandular epithelium, the Bax/Bcl-2 index in the implantation sites was highest at day 4.5 of pregnancy (5.74) and then decreased as pregnancy progressed to day 5.5 (4.73) (Graph 5.3C; Table 5.3). In the implantation sites of the glandular stroma in the control pregnant animals, the Bax/Bcl-2 index increased as pregnancy proceeded from day 4.5 (2.53) to day 5.5 (2.64) (Graph 5.3D; Table 5.3).

By day 6.5 of pregnancy, when compared to day 5.5 of pregnancy, Bax protein levels in the implantation sites increased significantly in all endometrial compartments analysed (Graph 5.1A-D; Figure 5.6E; Figure 5.7E; Table 5.1). Bcl-2 protein levels increased significantly in the luminal epithelium and the subepithelial compartments (Graph 5.2A and B; Figure 5.8E; Table 5.2), whereas Bcl-2 levels in the glandular epithelium and glandular stroma remained the same (Graph 5.2C and D; Figure 5.9E; Table 5.2).

As pregnancy further progressed from day 5.5 to day 6.5, the Bax/Bcl-2 ratio in the luminal epithelium changed from 3.19 to 1.70, suggesting a move towards a more anti-apoptotic environment (Graph 5.3A; Table 5.3). In the subepithelial stroma of the implantation sites of the control pregnant animals, the Bax/Bcl-2 index increased again slightly to 2.35 by day 6.5 of pregnancy (Figure 5.3B; Table 5.3). The Bax/Bcl-2 index in the glandular epithelium of the implantation sites increased again to 5.00. These results suggest an intense apoptotic signal within the glandular epithelium of the

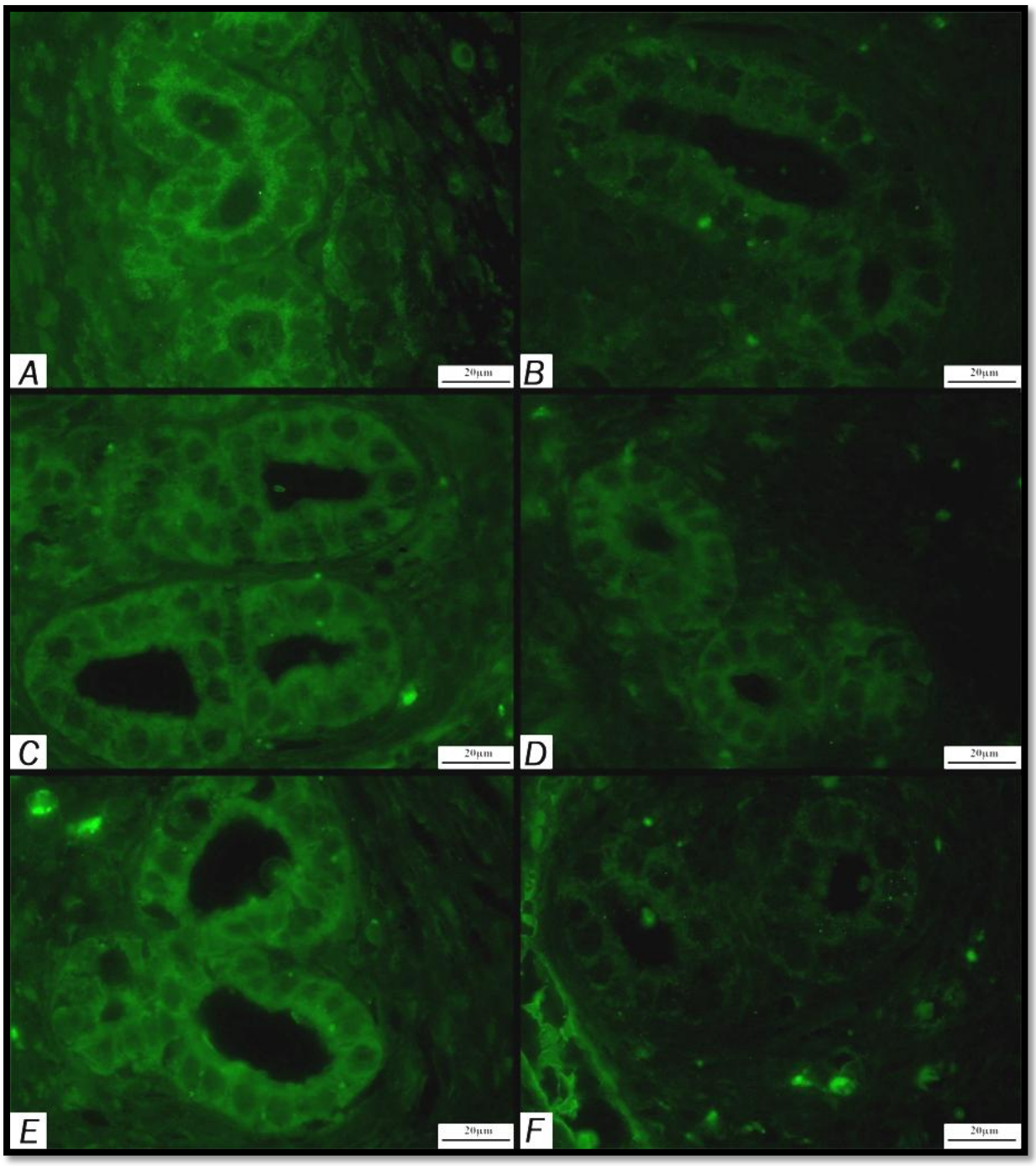


Figure 5.9 Immunofluorescent images illustrating Bcl-2 protein localisation in the glandular epithelium and the glandular stroma of the implantation and non-implantation sites in the uteri of control pregnant rats. A: Implantation site at day 4.5 of pregnancy, **B:** Non-implantation site at day 4.5 of pregnancy, **C:** Implantation site at day 5.5 of pregnancy, **D:** Non-implantation site at day 5.5 of pregnancy, **E:** Implantation site at day 6.5 of pregnancy, **F:** Non-implantation site at day 6.5 of pregnancy. Scale = 20µm.

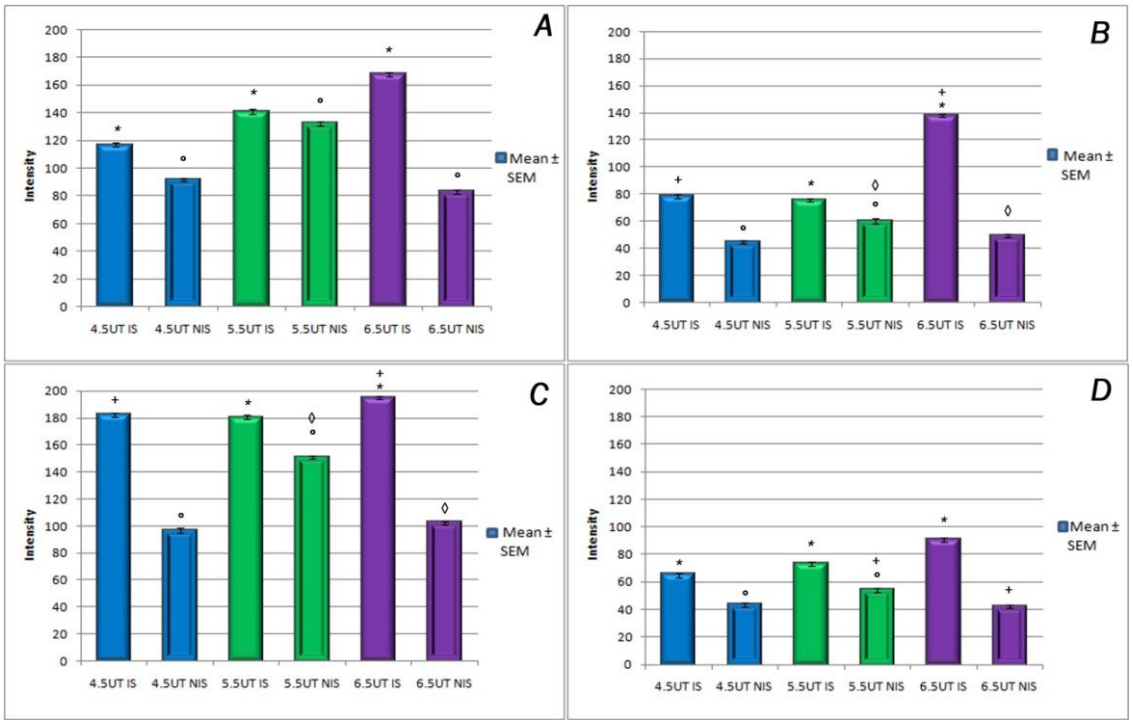
implantation sites around the time of blastocyst apposition, attachment and invasion (Graph 5.3C; Table 5.3). In the glandular stroma of the implantation sites in the control pregnant animals, the Bax/Bcl-2 index increased further with the progression of pregnancy to day 6.5 (2.81), suggesting an increase in the apoptotic signal with the progression of early pregnancy within this endometrial compartment (Graph 5.3D; Table 5.3).

In the non-implantation sites, Bax protein expression increased significantly in all endometrial compartments as pregnancy advanced from day 4.5 to day 5.5 and then decreased again significantly by similar amounts as pregnancy progressed from day 5.5 to day 6.5 (Graph 5.1A-D; Figure 5.6B, D and F; Figure 5.7B, D and F; Table 5.1).

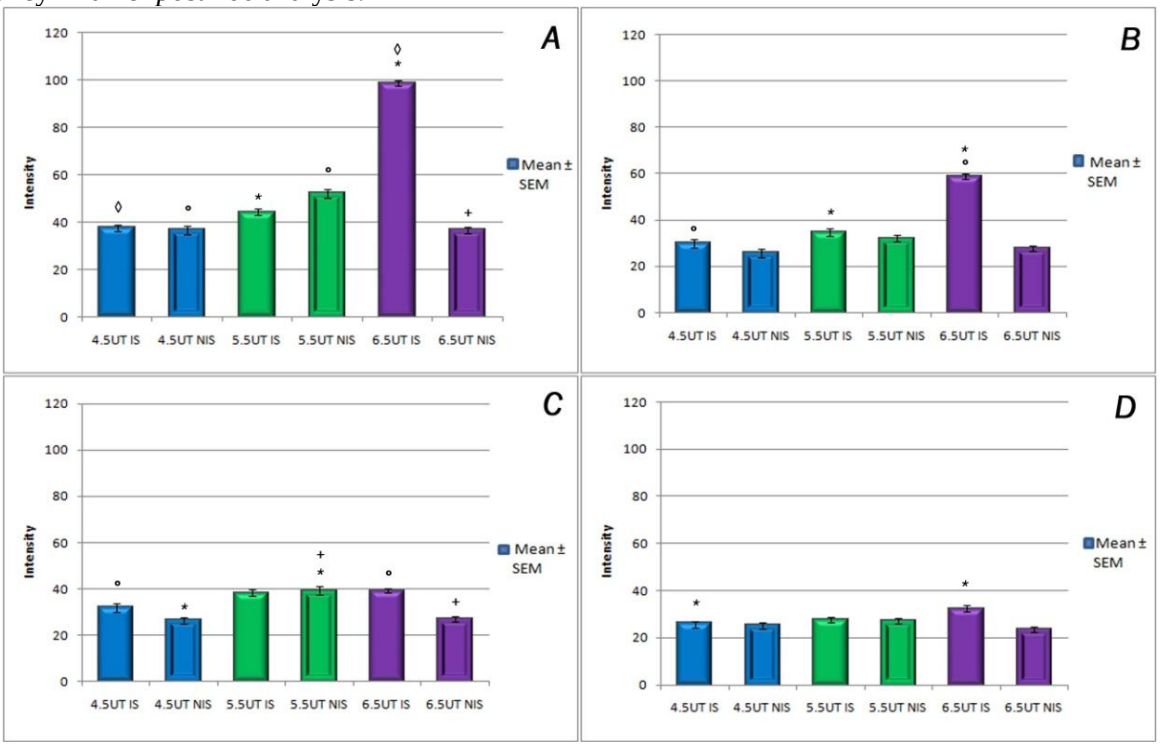
Bcl-2 protein levels in the non-implantation sites increased significantly in the luminal epithelium and glandular epithelium from day 4.5 to day 5.5 and then decreased significantly again, to a level similar to that at day 4.5 of pregnancy, with the progression from day 5.5 to day 6.5 of pregnancy (Graph 5.2A and C; Figure 5.8B, D and F; Figure 5.9B; D and F; Table 5.2). No significant differences were observed in the subepithelial or glandular stroma as pregnancy progressed from day 4.5 through to day 6.5 (Graph 5.2B and D; Figure 5.8B, D and F; Figure 5.9B; D and F; Table 5.2).

In the luminal epithelium of the non-implantation sites, the Bax/Bcl-2 index remained fairly similar from day 4.5 (2.49) to day 5.5 (2.54) with a slight decrease at day 6.5 of pregnancy (2.27), suggesting a more anti-apoptotic environment (Graph 5.3A; Table 5.3). In the non-implantation sites, the Bax/Bcl-2 index in the subepithelial stroma remained fairly constant as pregnancy proceeded from day 4.5 (1.75) to day 5.5 (1.88) and through to day 6.5 (1.78), suggesting a more anti-apoptotic environment within the non-implantation sites with regards to the subepithelial stroma (Graph 5.3B; Table 5.3). As pregnancy progressed from day 4.5 to day 5.5, the Bax/Bcl-2 index in the glandular epithelium of the non-implantation sites increased slightly from 3.67 to 3.87 and then remained fairly constant (3.89) as pregnancy further progressed to day 6.5, suggesting a small shift towards a more pro-apoptotic environment with the progression of early pregnancy (Graph 5.3C; Table 5.3). In the non-implantation sites, the Bax/Bcl-2 index in the glandular stroma increased slightly from 1.72 at day 4.5 to 2.00 at day 5.5 of pregnancy and then decreased again to 1.78 by day 6.5 of pregnancy (Graph 5.3D; Table 5.3).

In general, the Bax/Bcl-2 index was higher in the implantation sites relative to the non-implantation sites at all three days of pregnancy with regards to all the endometrial compartments analysed, suggesting a more intense pro-apoptotic signal in the implantation sites during early pregnancy. The apoptotic signal was higher in the glandular epithelium, followed by the luminal epithelium and then the glandular and subepithelial stroma (Graph 5.3A-D; Table 5.3).



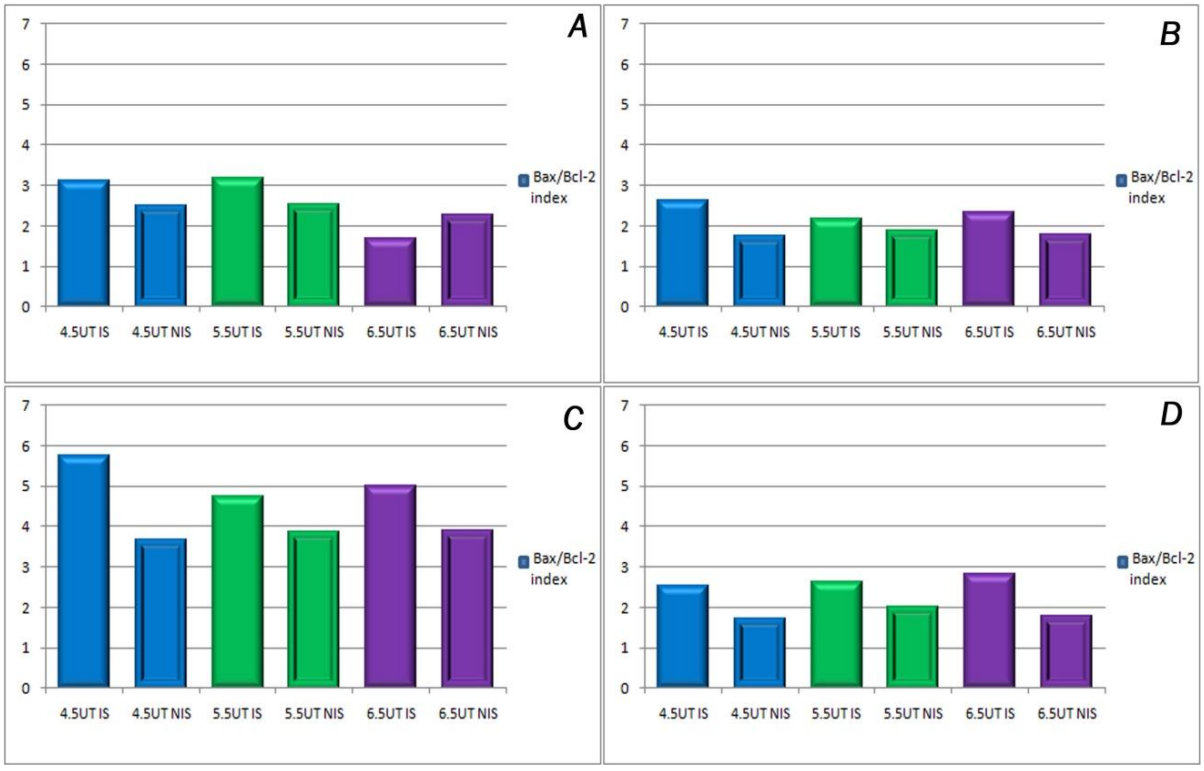
Graph 5.1 Graphical representation of the Mean ± SEM of Bax protein expression in the luminal epithelium (A), the subepithelial stroma (B), the glandular epithelium (C) and the glandular stroma (D) of the implantation (IS) and non-implantation (NIS) sites in day 4.5, day 5.5 and day 6.5 pregnant rat uteri treated with vehicle (UT) at day 3.0 of pregnancy, as obtained from image analysis of fluorescent intensities. *, °, ◊, + = significantly different ($p \leq 0.05$) using the Tukey-Kramer *post hoc* analysis.



Graph 5.2 Graphical representation of the Mean ± SEM of Bcl-2 protein expression in the luminal epithelium (A), the subepithelial stroma (B), the glandular epithelium (C) and the glandular stroma of the implantation (IS) and non-implantation (NIS) sites in day 4.5, day 5.5 and day 6.5 pregnant rat uteri treated with vehicle (UT) at day 3.0 of pregnancy, as obtained from image analysis of fluorescent intensities. *, °, ◊, + = significantly different ($p \leq 0.05$) using the Tukey-Kramer *post hoc* analysis.

Table 5.3 Bax and Bcl-2 protein levels were evaluated as mean fluorescent intensities using the image analysis software, analySIS Life Science Research program FIVE – Digital imaging Solutions (Olympus Soft Imaging Solutions). In this table, the results are expressed as an index (Bax/Bcl-2), obtained by dividing the Bax mean fluorescent intensity by the Bcl-2 mean fluorescent intensity. This was done for the endometrial compartments; the luminal epithelium, subepithelial stroma, glandular epithelium and the glandular stroma of both the implantation (IS) and non-implantation (NIS) sites of the control pregnant (UT) and RU486-treated (T) animals at days 4.5, 5.5 and 6.5 of pregnancy.

Endometrial Compartments	4.5UT IS	4.5UT NIS	5.5UT IS	5.5UT NIS	6.5UT IS	6.5UT NIS	4.5T IS	4.5T NIS	5.5T IS	5.5T NIS	6.5T IS	6.5T NIS
Luminal Epithelium	3.11	2.49	3.19	2.54	1.70	2.27	2.18	2.17	1.29	1.39	1.40	1.74
Subepithelial Stroma	2.62	1.75	2.18	1.88	2.35	1.78	1.79	1.71	0.83	1.14	1.32	1.36
Glandular Epithelium	5.74	3.67	4.73	3.87	5.00	3.83	3.55	3.88	1.48	1.83	3.10	2.53
Glandular Stroma	2.53	1.72	2.64	2.00	2.81	1.78	1.78	1.94	1.23	1.33	1.79	1.56



Graph 5.3 Graphical representation of the Bax/Bcl-2 index values in the luminal epithelium (A), the subepithelial stroma (B), the glandular epithelium (C) and the glandular stroma (D) of the implantation (IS) and non-implantation (NIS) sites in day 4.5, day 5.5 and day 6.5 pregnant rat uteri treated with vehicle (UT) at day 3.0 of pregnancy, as obtained by dividing the values of the Bax protein fluorescent intensities by the Bcl-2 protein fluorescent intensities.

5.2.1.2 The effects of RU486 on the spatiotemporal expression pattern of the Bax and Bcl-2 proteins, and the Bax/Bcl-2 index during early pregnancy

Overall, RU486 was observed to drastically decrease Bax protein levels in all the endometrial compartments analysed in both the implantation and non-implantation sites at days 4.5and 5.5 of pregnancy in comparison to the control pregnant animals (Graph 5.6A-D; Figure 5.6A-D; Figure 5.7A-D; Figure 5.10A-D; Figure 5.11A-D; Table 5.1).

With regards to Bcl-2 protein levels, RU486 had no significant effect on protein levels in any of the endometrial compartments analysed in both the implantation and non-implantation sites at day 4.5 of pregnancy relative to the control pregnant animals (Graph 5.7A-D; Figure 5.8A and B; Figure 5.9A and B; Figure 5.12A and B; Figure 5.13A and B; Table 5.2). By day 5.5 of pregnancy, Bcl-2 protein levels in both the implantation and non-implantation sites of the RU486-treated animals had increased significantly in all endometrial compartments analysed (Graph 5.5A-D; Figure 5.12C and D; Figure 5.13C and D; Table 5.2); however, no increase in Bcl-2 levels were observed in the control pregnant animals, except in the luminal epithelium of the non-implantation sites (Graph 5.2A; Figure 5.8D; Table 5.2). This resulted in significantly higher Bcl-2 protein levels in the RU486-treated animals at day 5.5 of pregnancy relative to that in the control pregnant animals at this day of pregnancy (Graph 5.7A-D; Figure 5.8C and D; Figure 5.9C and D; Figure 5.12C and D; Figure 5.13C and D; Table 5.2).

By day 6.5 of pregnancy there was an overall significant increase in Bax protein levels in all endometrial compartments analysed in the implantation sites of the RU486-treated animals (Graph 5.4A-D; Figure 5.10E; Figure 5.11E; Table 5.1); however, in the implantation sites of the control pregnant animals at day 6.5 of pregnancy, Bax protein levels increased markedly (Graph 5.1A-D; Figure 5.6E; Figure 5.7E; Table 5.1). Thus, the increase in Bax protein levels in the RU486-treated animals did not approach the levels of the control pregnant animals and Bax proteins levels remained significantly lower in the RU486-treated animals relative to the control pregnant animals (Graph 5.6A-D). Bcl-2 levels in the implantation sites at day 6.5 of pregnancy in the RU486-treated animals were significantly lower in the RU486-treated animals relative to the control pregnant (Graph 5.7A-D; Figure 5.8E; Figure 5.9E; Figure 5.12E; Figure 5.13E; Table 5.2).

In the non-implantation sites, Bax protein levels decreased in the control pregnant animals at day 6.5 of pregnancy, whereas levels increased significantly in the RU486-treated animals. The resultant Bax protein expression levels were significantly higher in the luminal epithelium and glandular stroma and significantly lower in the glandular epithelium of the RU486-treated animals relative to the control

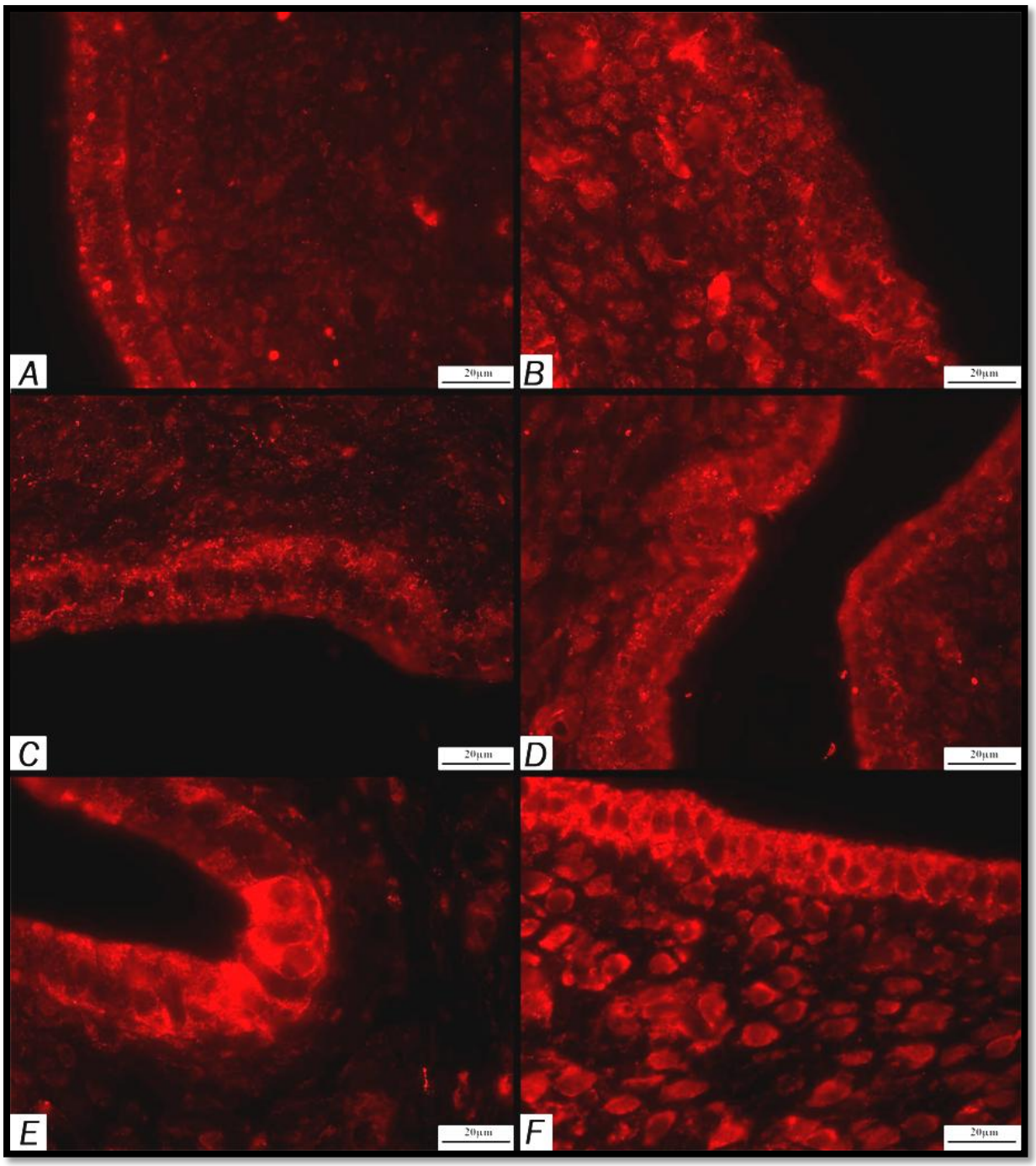


Figure 5.10 Immunofluorescent images illustrating Bax protein localisation in the luminal epithelium and the subepithelial stroma of the implantation and non-implantation sites in the uteri of RU486-treated pregnant rats. A: Implantation site at day 4.5 of pregnancy, **B:** Non-implantation site at day 4.5 of pregnancy, **C:** Implantation site at day 5.5 of pregnancy, **D:** Non-implantation site at day 5.5 of pregnancy, **E:** Implantation site at day 6.5 of pregnancy, **F:** Non-implantation site at day 6.5 of pregnancy. Scale = 20µm.

pregnant animals. No real difference was observed in the subepithelial stroma (Graph 5.6A-D; Figure 5.6F; Figure 5.7F; Figure 5.10F; Figure 5.11F; Table 5.1). Bcl-2 levels in the non-implantation sites of the RU486-treated animals were significantly higher in all endometrial compartments at day 6.5 of pregnancy, relative to the control pregnant animals (Graph 5.7A-D; Figure 5.8F; Figure 5.9F; Figure 5.12F; Figure 5.13F; Table 5.2).

After RU486 administration, the Bax/Bcl-2 index decreased in both the implantation and non-implantation sites at all three days of pregnancy with regards to all endometrial compartments analysed relative to the control pregnant animals, suggesting that RU486 induces a shift towards an overall anti-apoptotic signal in the Bax/Bcl-2 pathway (Graph 5.9A-D; Table 5.3).

In the implantation sites of the RU486-treated animals, as pregnancy progressed from day 4.5 to day 5.5, the Bax/Bcl-2 index decreased in the luminal epithelium from 2.18 to 1.29, in the subepithelial stroma from 1.79 to 0.83, in the glandular epithelium from 3.55 to 1.48 and in the glandular stroma from 1.78 to 1.23 (Graph 5.8A-D; Table 5.3). By day 6.5 of pregnancy, the Bax/Bcl-2 index in the implantation sites increased again in the luminal epithelium from 1.29 to 1.40, in the subepithelial stroma from 0.83 to 1.32, in the glandular epithelium from 1.48 to 3.10 and in the glandular stroma from 1.23 to 1.79 (Graph 5.8A-D; Table 5.3).

As pregnancy progressed from day 4.5 to day 5.5, the Bax/Bcl-2 index in the non-implantation sites decreased from 2.17 to 1.39 in the luminal epithelium, from 1.71 to 1.14 in the subepithelial stroma, from 3.88 to 1.83 in the glandular epithelium and from 1.94 to 1.33 in the glandular stroma (Graph 5.8A-D; Table 5.3), suggesting a shift towards a more anti-apoptotic environment in both the implantation and non-implantation sites with the progression of early pregnancy in the RU486-treated animals. By day 6.5 of pregnancy, the Bax/Bcl-2 index increased again to 1.74 in the luminal epithelium, to 1.36 in the subepithelial stroma, to 2.53 in the glandular epithelium and to 1.56 in the glandular stroma (Graph 5.8A-D; Table 5.3).

As in the control pregnant animals, the Bax/Bcl-2 index was highest in the glandular epithelium, followed by the luminal epithelium, the subepithelial stroma and then the glandular stroma (Graph 5.8A-D; Table 5.3).

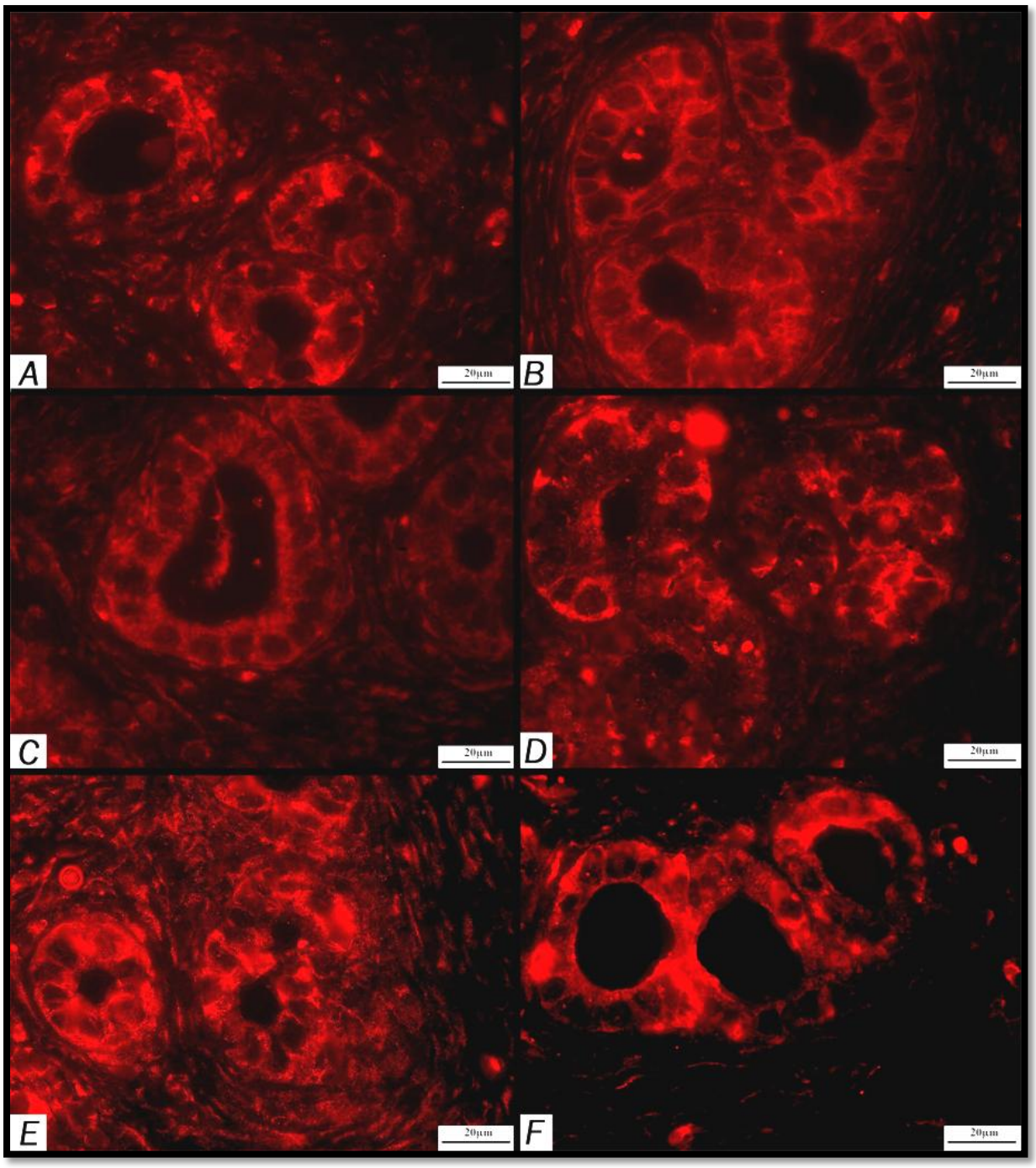
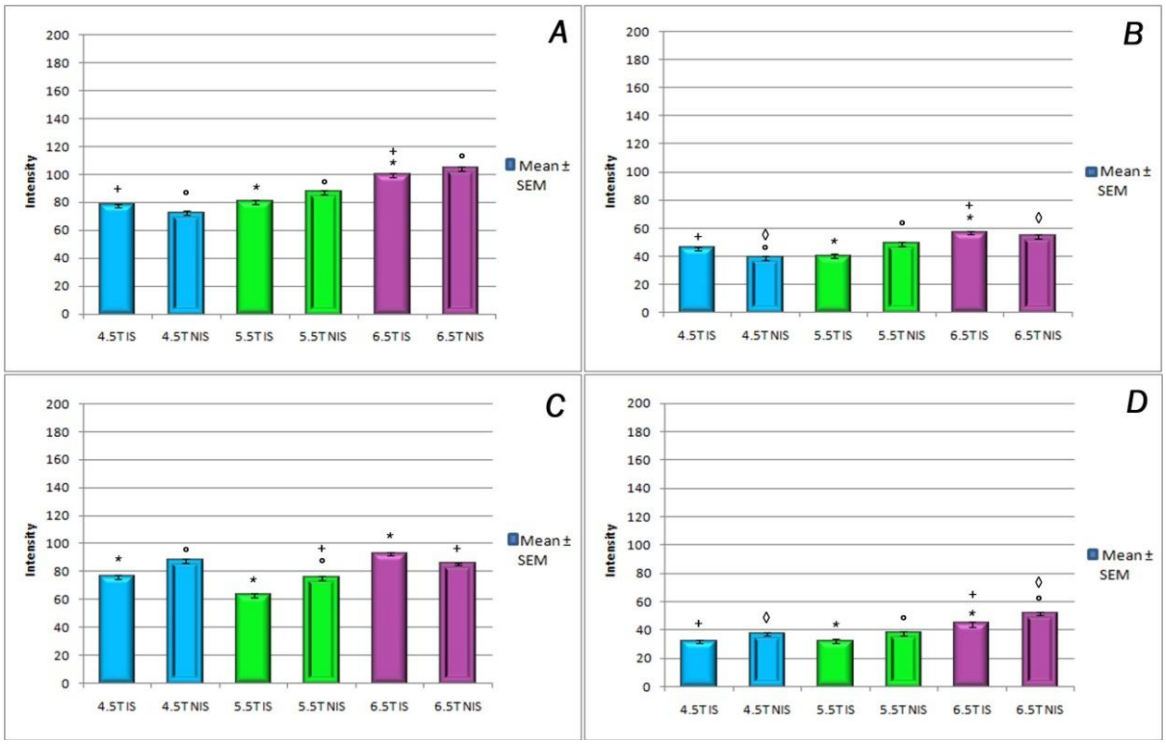
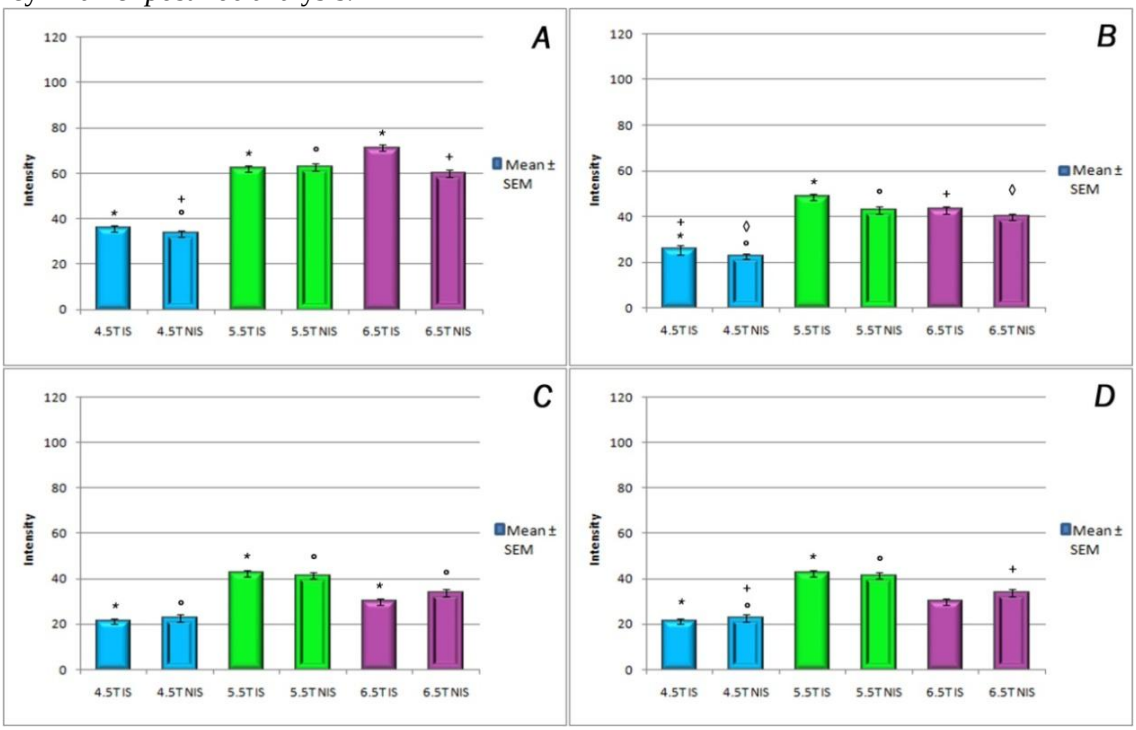


Figure 5.11 Immunofluorescent images illustrating Bax protein localisation in the glandular epithelium and the glandular stroma of the implantation and non-implantation sites in the uteri of RU486-treated pregnant rats. A: Implantation site at day 4.5 of pregnancy, **B:** Non-implantation site at day 4.5 of pregnancy, **C:** Implantation site at day 5.5 of pregnancy, **D:** Non-implantation site at day 5.5 of pregnancy, **E:** Implantation site at day 6.5 of pregnancy, **F:** Non-implantation site at day 6.5 of pregnancy. Scale = 20µm.



Graph 5.4 Graphical representation of the Mean ± SEM of Bax protein expression in the luminal epithelium (A), the subepithelial stroma (B), the glandular epithelium (C) and the glandular stroma (D) of the implantation (IS) and non-implantation (NIS) sites in day 4.5, day 5.5 and day 6.5 pregnant rat uteri treated with RU486 (T) at day 3.0 of pregnancy, as obtained from image analysis of fluorescent intensities. *, °, ◊, + = significantly different ($p \leq 0.05$) using the Tukey-Kramer *post hoc* analysis.



Graph 5.5 Graphical representation of the Mean ± SEM of Bcl-2 protein expression in the luminal epithelium (A), the subepithelial stroma (B), the glandular epithelium (C) and the glandular stroma of the implantation (IS) and non-implantation (NIS) sites in day 4.5, day 5.5 and day 6.5 pregnant rat uteri treated with RU486 (T) at day 3.0 of pregnancy, as obtained from image analysis of fluorescent intensities. *, °, ◊, + = significantly different ($p \leq 0.05$) using the Tukey-Kramer *post hoc* analysis.

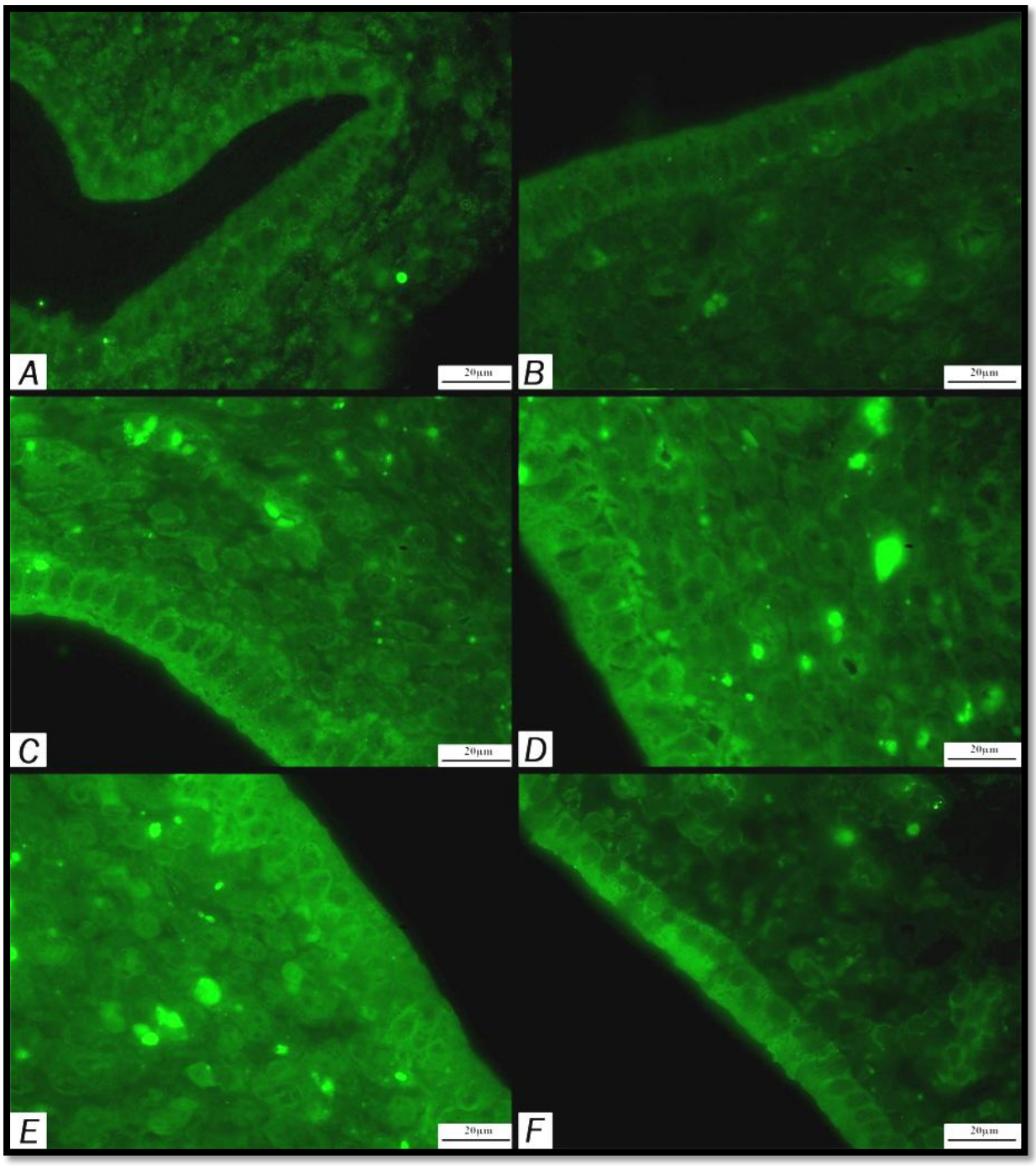
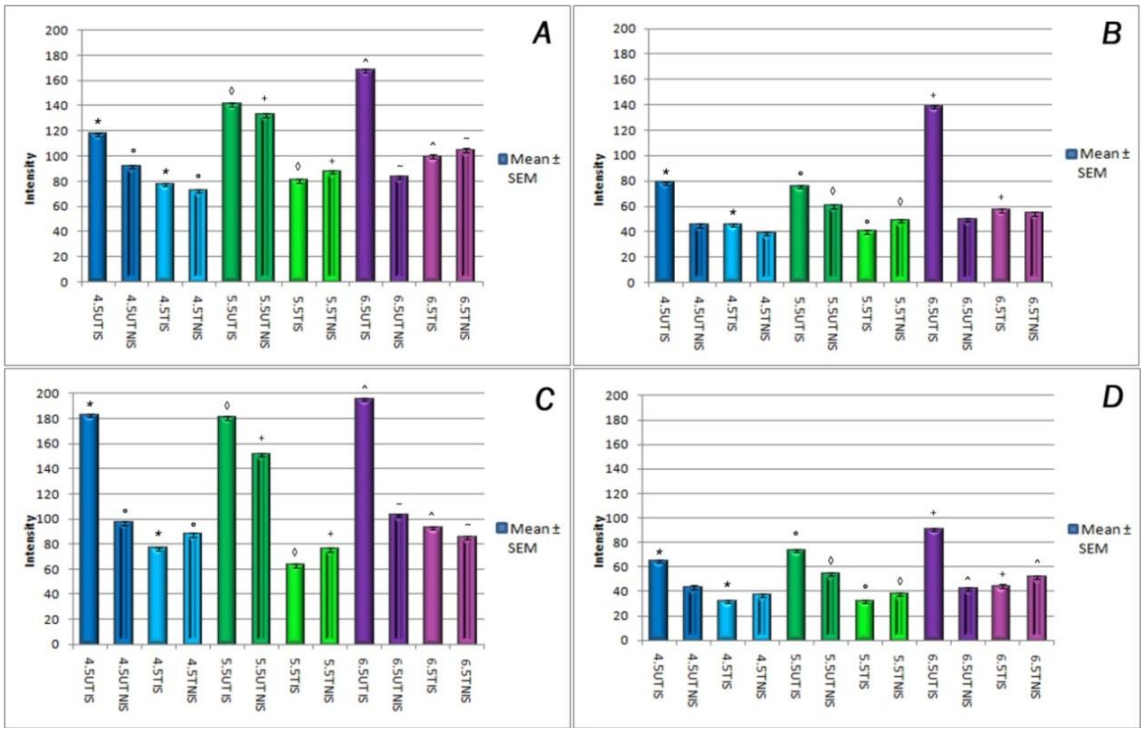
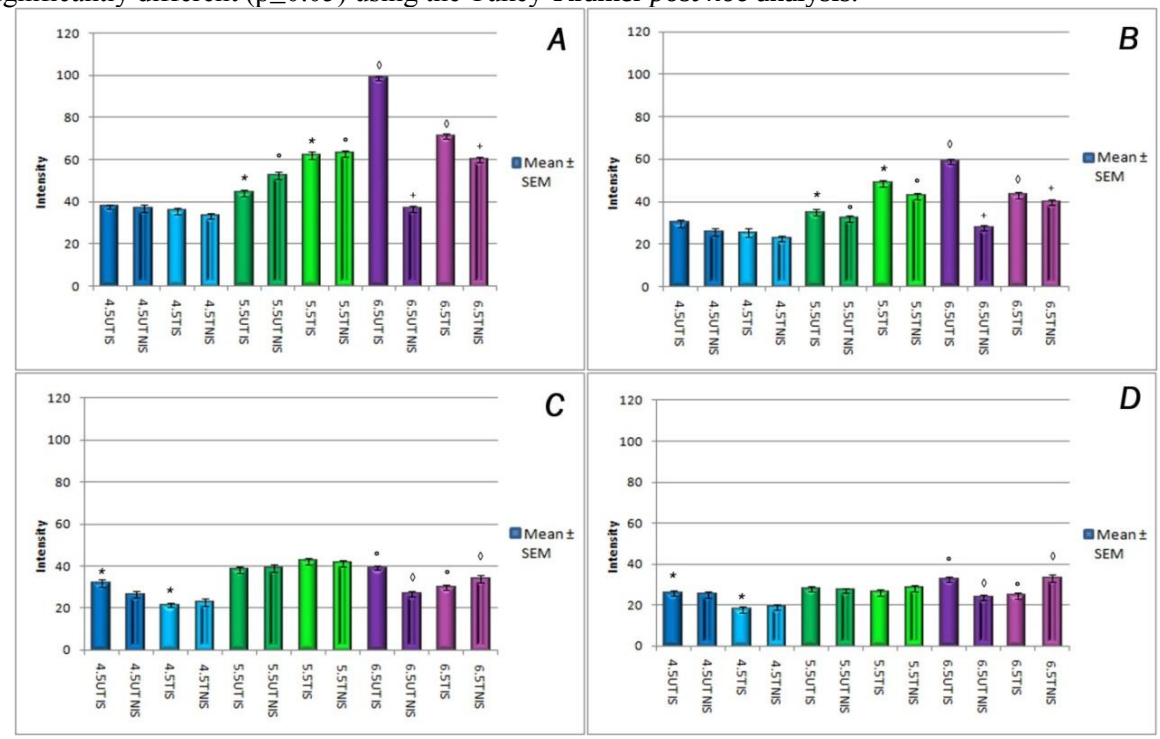


Figure 5.12 Immunofluorescent images illustrating Bcl-2 protein localisation in the luminal epithelium and the subepithelial stroma of the implantation and non-implantation sites in the uteri of RU486-treated pregnant rats. A: Implantation site at day 4.5 of pregnancy, **B:** Non-implantation site at day 4.5 of pregnancy, **C:** Implantation site at day 5.5 of pregnancy, **D:** Non-implantation site at day 5.5 of pregnancy, **E:** Implantation site at day 6.5 of pregnancy, **F:** Non-implantation site at day 6.5 of pregnancy. Scale = 20µm.



Graph 5.6 Graphical representation of the Mean ± SEM of Bax protein expression in the luminal epithelium (A), the subepithelial stroma (B), the glandular epithelium (C) and the glandular stroma (D) of the implantation (IS) and non-implantation (NIS) sites in day 4.5, day 5.5 and day 6.5 pregnant rat uteri treated with vehicle (UT) or RU486 (T) at day 3.0 of pregnancy, as obtained from image analysis of fluorescent intensities. *, °, ◊, +, ^,~ = significantly different ($p \leq 0.05$) using the Tukey-Kramer *post hoc* analysis.



Graph 5.7 Graphical representation of the Mean ± SEM of Bcl-2 protein expression in the luminal epithelium (A), the subepithelial stroma (B), the glandular epithelium (C) and the glandular stroma (D) of the implantation (IS) and non-implantation (NIS) sites in day 4.5, day 5.5 and day 6.5 pregnant rat uteri treated with vehicle (UT) or RU486 (T) at day 3.0 of pregnancy, as obtained from image analysis of fluorescent intensities. *, °, ◊, + = significantly different ($p \leq 0.05$) using the Tukey-Kramer *post hoc* analysis.

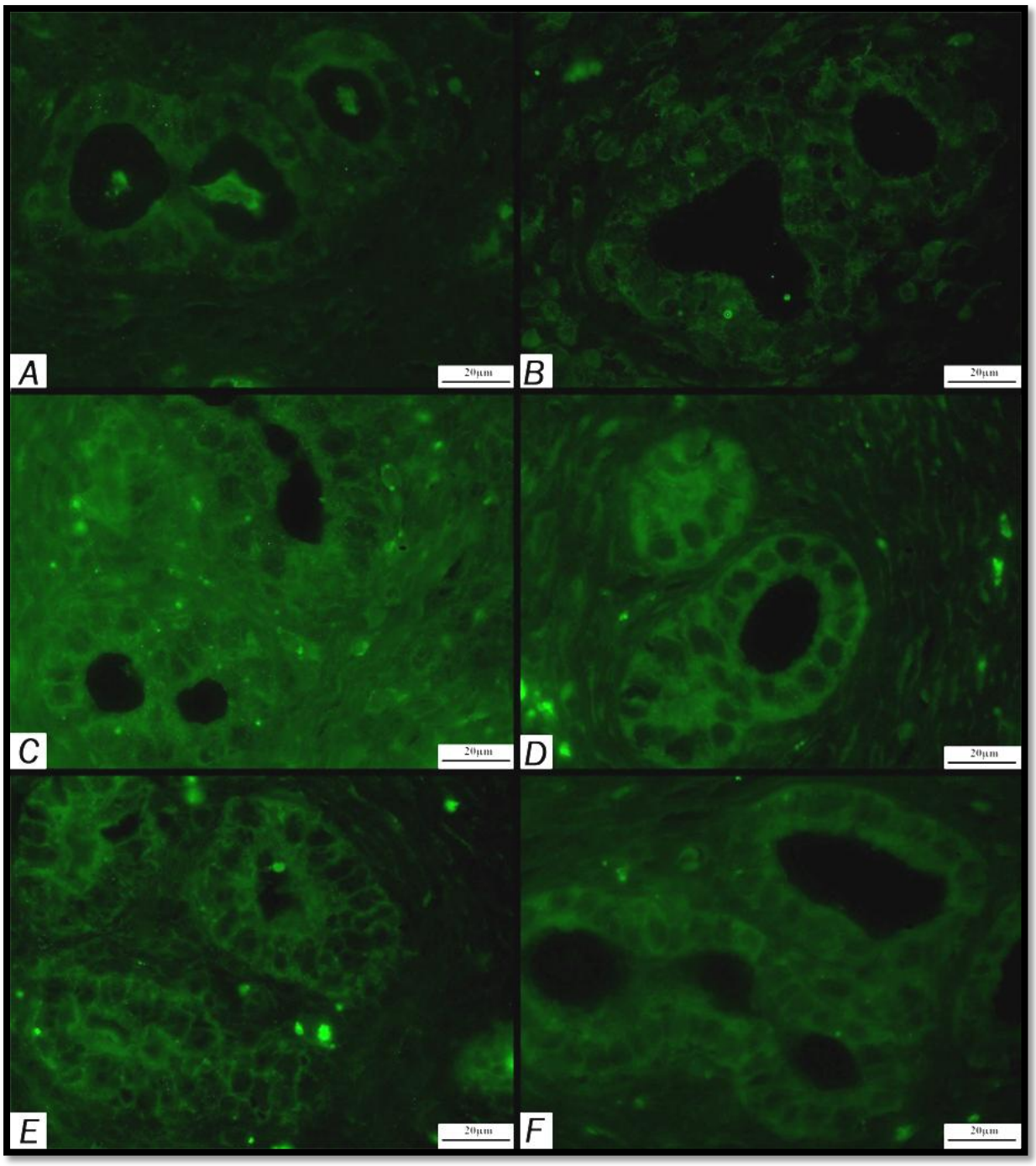
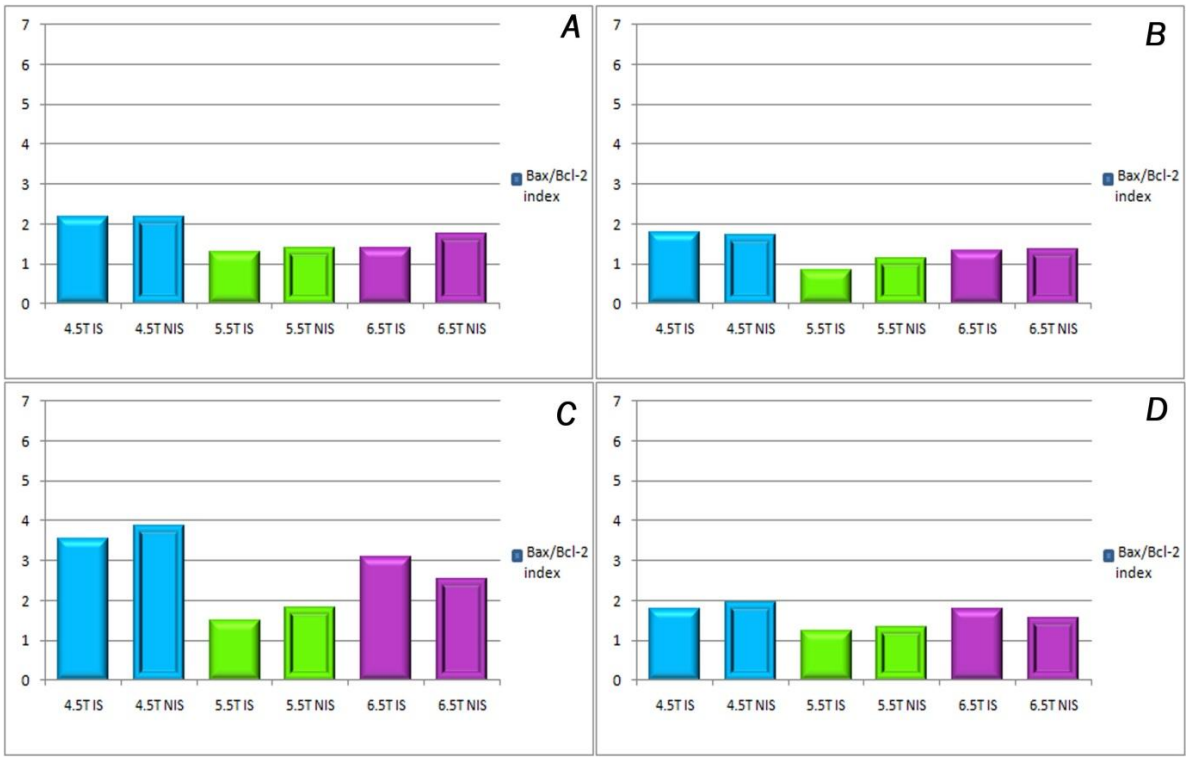
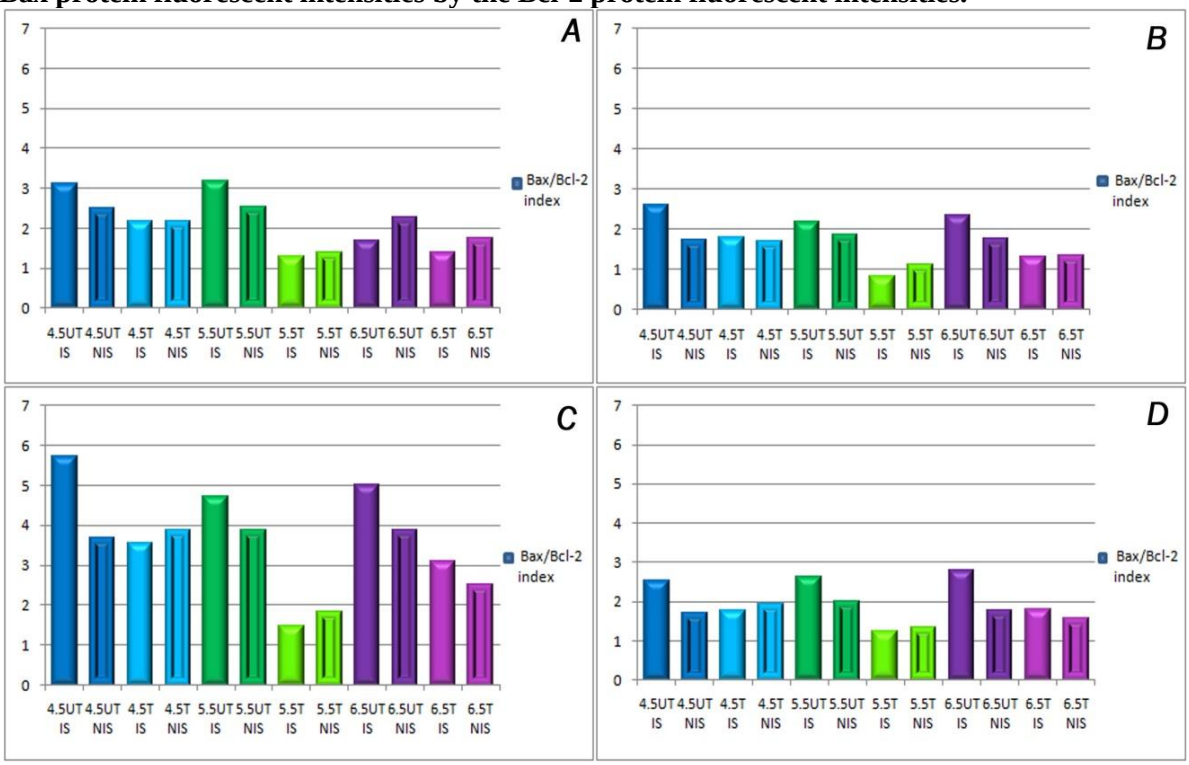


Figure 5.13 Immunofluorescent images illustrating Bcl-2 protein localisation in the glandular epithelium and the glandular stroma of the implantation and non-implantation sites in the uteri of RU486-treated pregnant rats. A: Implantation site at day 4.5 of pregnancy, **B:** Non-implantation site at day 4.5 of pregnancy, **C:** Implantation site at day 5.5 of pregnancy, **D:** Non-implantation site at day 5.5 of pregnancy, **E:** Implantation site at day 6.5 of pregnancy, **F:** Non-implantation site at day 6.5 of pregnancy. Scale = 20µm.



Graph 5.8 Graphical representation of Bax/Bcl-2 index values in the luminal epithelium (A), the subepithelial stroma (B), the glandular epithelium (C) and the glandular stroma (D) of the implantation (IS) and non-implantation (NIS) sites in day 4.5, day 5.5 and day 6.5 pregnant rat uteri treated with RU486 (T) at day 3.0 of pregnancy, as obtained by dividing the values of the Bax protein fluorescent intensities by the Bcl-2 protein fluorescent intensities.



Graph 5.9 Graphical representation of the Bax/Bcl-2 index values in the luminal epithelium (A), the subepithelial stroma (B), the glandular epithelium (C) and the glandular stroma (D) of the implantation (IS) and non-implantation (NIS) sites in day 4.5, day 5.5 and day 6.5 pregnant rat uteri treated with vehicle (UT) or RU486 (T) at day 3.0 of pregnancy, as obtained by dividing the values of the Bax protein fluorescent intensities by the Bcl-2 protein fluorescent intensities.

5.2.2 The Effects of RU486 on Apoptotic Pathway-Related Genes Expression in the Rat Uterus during Early Pregnancy

5.2.2.1 Relative quantification (RQ) analysis of Bax and Bcl-2 gene expression in the control pregnant animals

In the control pregnant animals at day 5.5 of pregnancy, Bax gene expression levels remained similar in the non-implantation sites (1.1-fold increase) relative to the implantation sites at the same day of pregnancy (Graph 5.10; Table 5.4A). Bcl-2 gene expression was seen to be up-regulated some 2.50-fold in the non-implantation sites as compared to the implantation sites at day 5.5 of pregnancy, the calibrator sample (Graph 5.11; Table 5.4B).

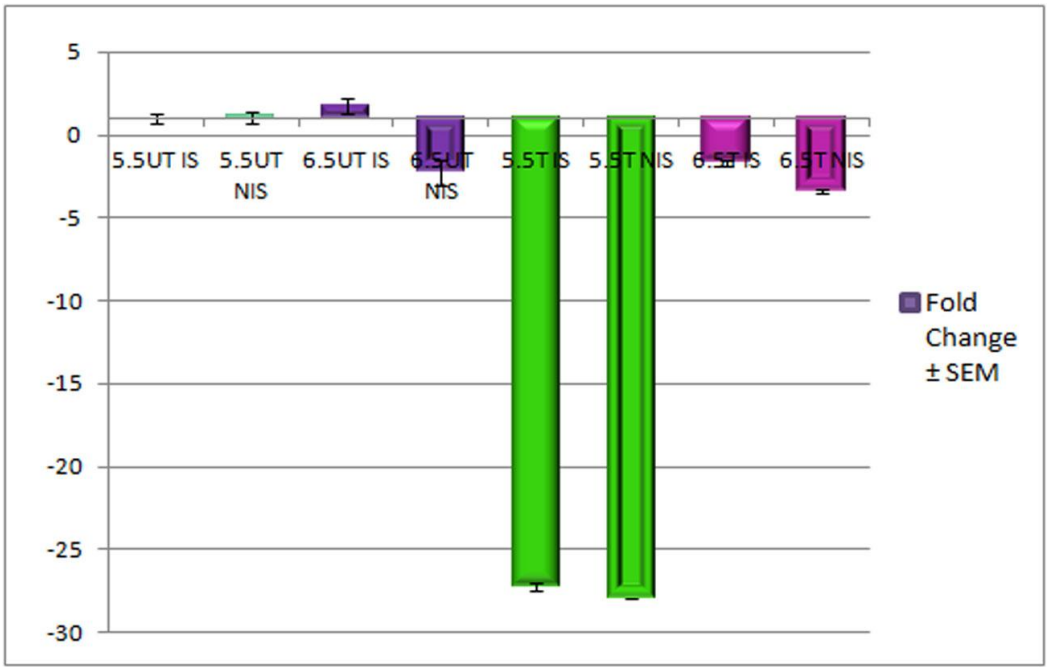
As pregnancy progressed to day 6.5, Bax gene expression was up-regulated by 1.8-fold in the implantation sites and down-regulated by 2.3-fold in the non-implantation sites as compared to gene expression in the implantation sites at day 5.5 of pregnancy (Graph 5.10; Table 5.4A). Bcl-2 gene expression was down-regulated 1.9-fold in the implantation sites and up-regulated 4.4-fold in the non-implantation sites respectively, relative to gene expression in the implantation sites at day 5.5 of pregnancy (Graph 5.11; Table 5.4B).

5.2.2.2 Relative quantification (RQ) analysis of the effects of RU486 on Bax and Bcl-2 gene expression

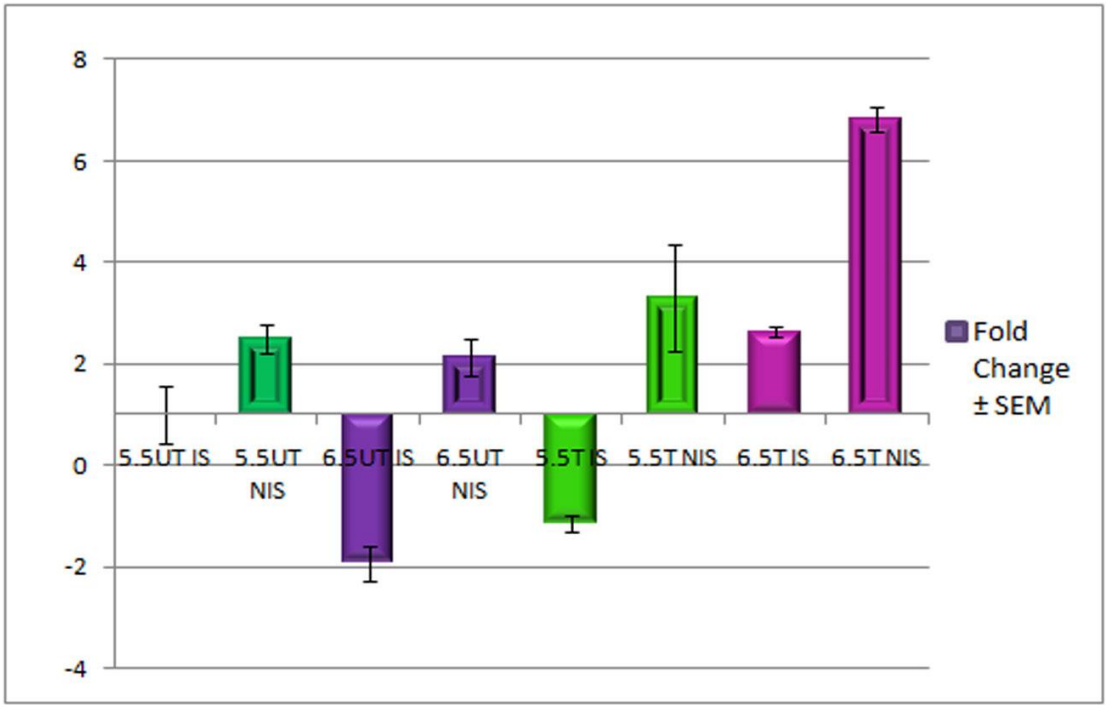
After RU486 treatment, Bax gene expression was markedly decreased by 27.3-fold in the implantation sites and 27.9-fold non-implantation sites at day 5.5 of pregnancy, in contrast to the implantation sites at day 5.5 of pregnancy in the control pregnant animals (Graph 5.10; Table 5.4A). Bcl-2 gene expression remained similar (1.1-fold decrease) in the implantation sites, but up-regulated by 3.3-fold in the non-implantation sites at day 5.5 of pregnancy as compared to the implantation sites at day 5.5 of pregnancy in the control pregnant animals (Graph 5.11; Table 5.4B).

By day 6.5 of pregnancy in the RU486-treated animals, while Bax gene expression was up-regulated by 16.2-fold in the implantation sites and 8.3-fold in the non-implantation sites in relation to day 5.5 of pregnancy in the RU486-treated animals, it was down-regulated by 1.7-fold in the implantation sites and by 3.4-fold in the non-implantation sites as compared to the calibrator sample, day 5.5 of pregnancy in the control pregnant animals (Graph 5.10; Table 5.4A). Bcl-2 gene expression was up-regulated by 2.6-fold in the implantation sites and by 6.8-fold in the non-implantation sites as compared to the calibration sample. As pregnancy progressed from day 5.5 to day 6.5, Bcl-2 gene expression in the RU486-treated animals was observed to increase by 3-fold in the implantation sites and 2-fold in the non-implantation sites (Graph 5.11; Table 5.4B).

Overall, RU486 treatment decreased Bax gene expression in both the implantation and non-implantation sites of the rat uterus at day 5.5 and 6.5 of pregnancy (Graph 5.10; Table 5.4A), whereas it was observed to increase Bcl-2 gene expression in both the implantation and non-implantation sites of the rat uterus, with the exception of the implantation sites at 5.5 days of pregnancy, where Bcl-2 gene expression remained unchanged (Graph 5.11; Table 5.4B).



Graph 5.10 Graphical representation of Bax gene expression as compared to day 5.5 in the control pregnant animals, the calibrator sample. The data is expressed as Fold Change ± SEM.
UT – untreated, **T** – treated, **IS** – implantation site, **NIS** – non-implantation site.



Graph 5.11 Graphical representation of Bcl-2 gene expression as compared to day 5.5 in the control pregnant animals, the calibrator sample. The data is expressed as Fold Change ± SEM.
UT – untreated, **T** – treated, **IS** – implantation site, **NIS** – non-implantation site.

Table 5.4 RQ analysis of Bax and Bcl-2 gene expression in the implantation (IS) and non-implantation (NIS) sites at day 5.5 and 6.5 of pregnancy in the control pregnant (UT) and RU486-treated (T) animals. A fold change of 2 or more denotes a significant difference in gene expression.

A: Bax mRNA Expression								
	Avg. C_T	**SEM**	**ΔC_T**	**SEM**	**$\Delta\Delta C_T$**	**$2^{-\Delta\Delta Ct}$**	**$Log_{10}(2^{-\Delta\Delta Ct})$**	**Fold Change ($2^{\Delta\Delta Ct}$)**
B-actin *	20.20	0.74	-	-	-	-	-	-
5.5UT IS **	22.42	1.06	2.22	0.32	0	1	0	1
5.5UT NIS	22.30	1.09	2.10	0.35	-0.12	1.09	0.04	1.09
6.5UT IS	21.60	1.20	1.40	0.45	-0.82	1.77	0.25	1.77
6.5UT NIS	23.59	1.47	3.40	0.73	1.18	0.44	-0.35	-2.27
5.5T IS	27.19	0.95	6.99	0.20	4.77	0.04	-1.44	-27.28
5.5T NIS	27.22	0.69	7.03	0.05	4.80	0.04	-1.45	-27.86
6.5T IS	23.17	0.94	2.98	0.19	0.75	0.60	-0.23	-1.68
6.5T NIS	24.17	0.85	3.97	0.11	1.75	0.30	-0.53	-3.36
B: Bcl-2 mRNA Expression								
Day of Pregnancy	**Avg. C_T**	**SEM**	**ΔC_T**	**SEM**	**$\Delta\Delta C_T$**	**$2^{-\Delta\Delta Ct}$**	**$Log_{10}(2^{-\Delta\Delta Ct})$**	**Fold Change ($2^{\Delta\Delta Ct}$)**
B-actin *	20.20	0.74	-	-	-	-	-	-
5.5UT IS **	31.65	1.31	11.45	0.57	0	1	0	1
5.5UT NIS	30.33	1.04	10.13	0.30	-1.32	2.49	0.40	2.50
6.5UT IS	32.60	1.09	12.40	0.35	0.95	0.52	-0.29	-1.93
6.5UT NIS	30.55	1.10	10.35	0.36	-1.10	2.14	0.33	2.14
5.5T IS	31.84	0.91	11.64	0.17	0.19	0.88	-0.06	-1.14
5.5T NIS	29.93	1.79	9.73	1.05	-1.72	3.30	0.52	3.29
6.5T IS	30.25	0.84	10.05	0.10	-1.40	2.64	0.42	2.64
6.5T NIS	28.88	0.97	8.68	0.23	-2.77	6.82	0.83	6.82

UT - untreated, **T** - treated, **IS** - implantation site, **NIS** - non-implantation site, **C_T** - threshold cycle, **SEM** - standard error of the mean, ***** - endogenous control, ****** - calibrator sample. **ΔC_T** = C_T (Target) - C_T (Endogenous control). **$\Delta\Delta C_T$** = ΔC_T (Target) - ΔC_T (Calibrator).

5.3 DISCUSSION

5.3.1 Alterations in the Bax/Bcl-2 Ratio is Not Responsible for the Increase in RU486-Induced Apoptosis

The appearance of the large protrusions on the surface of the luminal epithelial cells of the endometrium in the RU486-treated animals in the ultrastructure portion of the current study (Chapter 3) led to the formulation of the hypothesis that these blebs were forming due to increased apoptosis (Scholtz *et al.*, 2008). This initiated an investigation of molecular factors linked to apoptosis. Rotello *et al.* (1992) have previously noted an increase in apoptotic activity as a result of RU486 in the rabbit endometrium; however, no reports of large surface protrusions from morphological studies have been previously reported (Rotello *et al.*, 1992).

During the menstrual and oestrous cycles, remodelling of the endometrium by cellular regression, proliferation and differentiation is well known to be controlled by apoptosis (Sato *et al.*, 2003). Further, apoptosis is involved in the establishment of the stages of early pregnancy within the endometrium, which includes the proliferation of the subepithelial stromal cells into decidual cells, removal of the barrier of attachment of the blastocyst, the luminal epithelium, as well as subsequent formation of the placenta later on in early pregnancy (Welsh, 1993; Moulton, 1994; Spornitz *et al.*, 1994; Akcali *et al.*, 1996; Carson *et al.*, 2000; Tassell *et al.*, 2000; Akcali *et al.*, 2003).

During the oestrous cycle, apoptosis is highest in the luminal and glandular epithelium during oestrous and at its lowest during pro-oestrous (Mendoza-Rodríguez *et al.*, 2002; Mendoza-Rodríguez *et al.*, 2003). Throughout pro-oestrous, when follicular growth and development occurs prior to ovulation, oestrogen is the dominant hormone, whereas after ovulation, during the oestrous stage of the cycle, progesterone is the dominant hormone (Burroughs *et al.*, 2000). These results are in agreement with previous studies in the rat uterus (Spornitz *et al.*, 1994; Burroughs *et al.*, 2000) and the hamster uterus (Sandow *et al.*, 1979) and in contrast with a study in the rat uterus in which metoestrous was reported to have the highest apoptotic index within the luminal epithelial cells (Sato *et al.*, 1997). Mendoza-Rodriguez *et al.* (2002) attributed this discrepancy to the differences in the hour at which the experiments were performed. It has been suggested that a high apoptotic index is probably due to a decline in serum oestrogen levels and a rise in progesterone levels during this phase of the cycle (West *et al.*, 1978).

In 2002, Mendoza-Rodriguez and colleagues tested the levels of the transcription factor, p53, an apoptosis and cell cycle regulator (Levine, 1997), through the various stages of the oestrous cycle in the rat uterus. Their results suggest that p53 plays an important role in the proliferative phases of the

oestrous cycle and not apoptosis (Mendoza-Rodríguez *et al.*, 2002). Further, in 2003, they analysed the levels of the Bcl-2 family of proteins during the oestrous cycle within the rat uterus (Mendoza-Rodríguez *et al.*, 2003). The spatiotemporal pattern of the shift from an anti-apoptotic to a pro-apoptotic endometrium by an increase in Bax protein and mRNA levels and a decrease in Bcl-2 protein and mRNA levels during the transition from pro-oestrous to oestrous led the investigators to suggest that this induction of apoptosis is either resultant of oestrogen withdrawal, or an increase in progesterone levels (Mendoza-Rodríguez *et al.*, 2003). In both the human (Tao *et al.*, 1997) and rat (Mendoza-Rodríguez *et al.*, 2003) endometrium, the shift in the Bax/Bcl-2 ratio has been attributed to the cyclic changes in endometrial growth and regression observed in the menstrual and oestrous cycles respectively.

The apoptotic process involves over 100 genes, including the Bcl-2 gene family. The Bcl-2 family of proteins is made up of at least 16 homologues. Some homologues suppress apoptosis (Bcl-2 and Bcl-X_L), while others promote apoptosis (Bax and Bcl-X_S) when activated by phosphorylation (Oltvai *et al.*, 1993; Ruvolo *et al.*, 1998). While Bcl-2 is known to protect cells against some forms of apoptosis, it does not induce cellular proliferation, whereas Bax promotes apoptosis (Hengartner, 2000). Bax protein is able to counter the anti-apoptotic effects of Bcl-2 by forming heterodimers with Bcl-2. In view of this, it has been proposed that the ratio of Bax to Bcl-2 expression determines whether a cell undergoes apoptosis or not (Figure 5.5) (Korsmeyer *et al.*, 1993; Oltvai *et al.*, 1993; Hengartner, 2000).

Cell death within the implantation sites of the endometrium is a well-documented process necessary for the removal of the luminal epithelium, this being the barrier to implantation (Parr *et al.*, 1987; Welsh, 1993). Tassell *et al.* (2000) demonstrated a high degree of apoptotic activity within the rat endometrium prior to implantation at day 6 of pregnancy (sperm in vaginal smear was designated day 1 of pregnancy). They showed that the number of apoptotic cells, as indicated by TUNEL-positive cells, in the non-implantation sites was not significant at days 6 and 7 of pregnancy, whereas a strong TUNEL signal was recorded in both the uterine epithelium and the stroma immediately adjacent to the implantation chamber at day 6 and 7 of pregnancy (Tassell *et al.*, 2000), suggesting that apoptosis occurs in the uterine epithelium and decidual layer only within the implantation chamber of the implantation site during the tissue remodelling phase, in preparation for the implantation of a viable blastocyst (Tassell *et al.*, 2000). While Akcali *et al.* (1996) showed that decidualisation of the stromal cells and the eventual apoptosis that occurs during early pregnancy are associated with an increase in the expression of Bax and a decrease in Bcl-2 expression, no spatiotemporal expression pattern of Bax and Bcl-2 was reported in the different uterine cell compartments of the rat uterus.

In the current study, Bax protein levels increased specifically in the luminal epithelium of the implantation sites of the control pregnant animals as pregnancy progressed from day 4.5 to day 5.5, the day of blastocyst implantation, whereas Bcl-2 levels remained the same. In the non-implantation sites, while Bax levels were increased significantly, so too were Bcl-2 levels, albeit not to the same degree as Bax. The Bax/Bcl-2 index, however, did not increase substantially in either the implantation or non-implantation sites. By day 6.5 of pregnancy, the Bax/Bcl-2 index was observed to decrease significantly in the luminal epithelial compartment, suggesting a decrease in the pro-apoptotic environment at this day of pregnancy. This is in accordance with previous studies, indicating an increase in apoptosis in the implantation sites prior to blastocyst implantation is necessary for implantation to occur (Parr *et al.*, 1987; Welsh, 1993; Tassell *et al.*, 2000).

In the implantation sites of the other regions of the rat uterus, the Bax/Bcl-2 index was decreased around day 5.5 of pregnancy. In the non-implantation sites the Bax/Bcl-2 index remained fairly stable in all endometrial compartments analysed. This concurs with other studies in which apoptosis of early pregnancy, prior to blastocyst implantation, was restricted to the luminal epithelium (Tassell *et al.*, 2000).

As pregnancy further progressed from day 5.5 to day 6.5, the Bax/Bcl-2 index in the decidual layer of the implantation sites, the glandular epithelium and the glandular stroma increased, suggesting an increase in apoptotic activity within these compartments after implantation of a viable blastocyst. The Bax/Bcl-2 index in the non-implantation sites remained consistent at this stage of pregnancy. As reported previously, tissue remodelling by apoptosis at the site of blastocyst implantation is vital to ensure that the maternal blood supply is accessible to the blastocyst to sustain the developing conceptus (Welsh and Enders, 1985; Gu *et al.*, 1994).

Whole tissue homogenates showed an overall increase in Bax mRNA expression in the implantation sites and an overall decrease in the non-implantation sites as pregnancy progressed from day 5.5 to day 6.5. Bcl-2 mRNA levels decreased in both the implantation and non-implantation sites respectively, from day 5.5 to day 6.5 of pregnancy. These results suggest an overall increase in apoptosis in the implantation sites and maintenance of an anti-apoptotic stimulus in the non-implantation sites, which concur with the protein levels in the current study.

As the current study and previous studies of normal implantation (Tassell *et al.*, 2000; Mendoza-Rodríguez *et al.*, 2003) indicate that Bax and Bcl-2 play an important role in apoptosis within the endometrium, this led to the investigation of a shift in the Bax/Bcl-2 index towards cell death as a possible explanation for the increased apoptosis observed in the luminal and glandular epithelium of the RU486-treated animals. In the ultrastructure portion of the present study, the results show the

highest level of apoptotic activity was observed in the luminal epithelium as indicated by numerous apoptotic cells and apoptotic bodies (see Figures 3.11A-F in Chapter 3). The majority of apoptotic activity in the RU486-treated animals was observed at day 5.5 and 6.5 of pregnancy.

In the current study, the Bax/Bcl-2 index was lower in both the implantation and non-implantation sites in the RU486-treated animals at day 4.5 of pregnancy relative to the control pregnant animals, as a result of the significantly higher levels of Bax protein in the control pregnant animals relative to the RU486-treated animals. These results suggest that a stronger anti-apoptotic stimulus exists within the RU486-treated animals at this day of pregnancy. By day 5.5 of pregnancy, the Bax/Bcl-2 index was even lower relative to the control pregnant animals, as in all the endometrial compartments analysed Bax protein and mRNA levels were still significantly higher in the control pregnant animals relative to the RU486-treated animals. Bax mRNA levels were 28-fold lower in the implantation sites and 31-fold lower in the non-implantation sites of the RU486-treated animals relative to the control pregnant animals. Bcl-2 protein and mRNA levels were not significantly different between the control pregnant and RU486-treated animals. These data suggest maintenance of a Bax/Bcl-2 ratio in favour of cell survival within the RU486-treated animals; however, from the morphological portion of the current study it is evident that apoptotic activity is substantially increased following treatment with RU486, in agreement with a prior study in the rabbit endometrium (Rotello *et al.,* 1992). These data combined led to the suggestion that the Bax/Bcl-2 pathway is not the pathway responsible for the increased apoptosis observed in the RU486-treated animals within this study.

Mendoza-Rodriguez *et al.* (2003) suggested that the increase in apoptosis observed during the oestrous cycle as a result of a shift in the Bax/Bcl-2 ratio towards a pro-apoptotic environment, was a consequence of oestrogen withdrawal or increased progesterone levels. RU486 has previously been reported to block oestrogen effects on the endometrium as this anti-progestin is also able to bind to ERs (McDonnell and Goldman, 1994; Chwalisz *et al.*, 1995; Chwalisz *et al.*, 1998). If a shift in the Bax/Bcl-2 ratio to a pro-apoptotic environment was under the influence of oestrogen withdrawal, then a change in the Bax/Bcl-2 ratio as a result of RU486 administration would be expected. This, however, is not the case in the present study. Thus, it is more likely that an increase in progesterone levels regulates an increase in the Bax/Bcl-2 ratio towards a more pro-apoptotic environment. As RU486 partially blocks progesterone binding and subsequent progesterone action on the endometrium, it is possible that the decrease in the Bax/Bcl-2 ratio and subsequent anti-apoptotic environment is directly related to the decrease in progesterone signalling in the RU486-treated endometrium. These results further suggest that Bax and Bcl-2 are not responsible for the RU486-induced increase in apoptosis observed during early pregnancy.

In a recent study in ovariectomised mice, an increase in the apoptotic index within both the luminal and glandular epithelium was observed one day postovariectomy and in the stromal cells two days after ovariectomy without hormonal replacement (Sato *et al.*, 2003). By day 5 postovariectomy, levels of apoptosis had decreased significantly in the epithelial compartments as well as in the uterine stromal cells. These results suggest that ovariectomy induces apoptosis within the uterus, resulting in rapid involution (Sato *et al.*, 2003). In the current study, by day 5.5 of pregnancy, apoptotic activity in the RU486-treated animals was observed to be high (see Chapter 3) in both the glandular and epithelial compartments with levels highest within the luminal epithelium, in agreement with the Sato study (Sato *et al.*, 2003). This supports the hypothesis that RU486 results in a more hormonally under-stimulated uterus rather than one displaying unopposed oestrogen action (Scholtz *et al.*, 2008). Burroughs *et al.* (2000) reported maximal apoptosis in all cell types when progesterone and oestrogen levels were both low (Burroughs *et al.*, 2000). However, the results in the current study suggest that this increase in apoptosis is not driven by a shift in the Bax/Bcl-2 ratio towards cell death, when the PRs and ERs are partially inactivated by RU486, but is possibly regulated by another apoptotic pathway.

Gao *et al.* (2001) suggested that Bax and Bcl-2 are not regulated by the ovarian hormones as woman treated with ovarian hormones to maintain the luteal phase of the menstrual cycle did not show significantly increased levels of Bcl-2 mRNA, suggesting that it is unlikely that Bcl-2 is involved in cell survival within the endometrium during the secretory phase of the menstrual cycle (Koh *et al.*, 1995; Gao *et al.*, 2001).

It is possible that Bax and Bcl-2 levels within the normal pregnant animals are under the control of factors other than the ovarian hormones, as in the present study the expression of these proteins differs within the various endometrial cell compartments during early pregnancy. The fact that inhibition of the effects of both the ovarian hormones oestrogen and progesterone by RU486 did not result in significant changes in Bax and Bcl-2 levels, lends credibility to their suggestion that these apoptotic factors are not regulated solely by progesterone and oestrogen (Gao *et al.*, 2001).

Analysis of Bcl-2 levels in the mouse endometrium show that ovariectomy and the subsequent loss of ovarian hormone regulation has very little effect on the expression of this apoptotic factor (Sato *et al.*, 2003). In the present study, neither Bcl-2 protein nor Bcl-2 mRNA levels were markedly changed following administration of RU486. The similarity of the results between the ovariectomised animals in Sato *et al.* (2003) and the RU486-treated animals of the current study, makes the concept of a hormonally under-stimulated uterus due to RU486 administration as a postcoital contraceptive more credible (Scholtz *et al.*, 2008).

Sato *et al.* (2003) demonstrated increased levels of TNF-α, and Fas and Fas-ligand (FasL) 24h after ovariectomy within the endometrium. Both TNF-α and Fas and FasL have been reported to be involved in the up-regulation of apoptosis (Hunt *et al.*, 1992; Yamashita *et al.*, 1999). This led the investigators to suggest that the increase in apoptotic cell death observed in the ovariectomised mouse uterus is mediated by the Fas and TNF-α pathways (Sato *et al.*, 2003). A study on the effects of RU486 on the expression of the Fas and FasL genes within the rat uterus demonstrated, however, that both Fas and FasL expression levels were decreased as a result of RU486 administration within the mouse endometrium (Gao *et al.*, 2001), suggesting that this is not the pathway responsible for the RU486-induced increase in apoptosis either.

In an endometrial cell line progesterone was shown to decrease apoptosis by increasing the ratio of Bcl-X_L to Bcl-X_S, which favours cell survival, whereas RU486 was shown to inhibit this effect by increasing the ratio of the Bcl-X splice variants, Bcl-X_S to Bcl-X_L towards cell death. Bcl-X_L inhibits cell death, whereas Bcl-X_S promotes apoptosis (Chao *et al.*, 1995; Sumantran *et al.*, 1995).

Future studies investigating the expression of the Bcl-X splice variants Bcl-X_L and Bcl-X_S are needed to ascertain whether this pathway is indeed responsible for the drastic increase in apoptotic activity observed in the RU486-treated rat uterus. The use of RT-qPCR and *in situ* hybridisation to evaluate the expression pattern of the Bcl-X splice variants would help to better elucidate the mechanisms controlling the RU486-induced increase in apoptotic activity observed during early pregnancy.

CHAPTER 6

THE EFFECT OF RU486 ON ANGIOGENESIS DURING EARLY PREGNANCY IN THE RAT UTERUS

6.1 INTRODUCTION

Another early pregnancy event that this study addresses is the increase in angiogenesis around the time of blastocyst implantation in the vicinity of the implantation sites. This increase in angiogenesis occurs in two separate angiogenic events; the first involves an increase in vascular permeability that occurs in the implantation sites of the endometrium prior to implantation (Psychoyos, 1961; Rogers *et al.*, 1982); and the second being an increase in endothelial cell proliferation, which is essential for the expansion of the capillary network within the stromal portion of the endometrium to accommodate and sustain the implanting and developing embryo (Goodger and Rogers, 1993). As this increase in endometrial angiogenesis is regulated by angiogenic growth factors; including, Vascular Endothelial Growth Factor (VEGF), basic Fibroblast Growth Factor (bFGF) and Platelet-derived Growth Factor (PDGF), the effects of RU486 on the expression patterns of these key factors were analysed in this study.

6.1.1 Angiogenesis and the Endometrium

Angiogenesis is a physiological process, involving the proliferation and migration of endothelial cells and their subsequent assembly to form new blood vessels, arising from pre-existing vessels (Folkman and Shing, 1992). Developmental angiogenesis is an essential, highly regulated process in early growth (Risau, 1997), whereas pathological angiogenesis plays an important role in the growth and maintenance of many solid tumours, chronic inflammatory disorders, endometriosis and diabetic retinopathy (Hanahan and Folkman, 1996). Physiological angiogenesis does not occur often in adult tissue except in wound healing (Folkman and Shing, 1992; Risau, 1997) and in the adult female reproductive tract. It can be said that the growth, development and later regression of vasculature are central features of reproduction, during folliculogenesis and formation of the corpus luteum, as well as in the endometrium of primates during the menstrual cycle (for a review see Gargett and Rogers, 2001) and during blastocyst implantation and subsequent placentation (Torry and Torry, 1997).

During the different stages of the menstrual cycle, the requirement for vessel growth and regression differs both spatially and temporally. Here, there are three distinct stages during which angiogenesis occurs (Rogers and Gargett, 1998); Firstly, following menstruation to repair the ruptured blood vessels of the vascular bed; secondly, during the proliferative phase where the rapid regrowth of the endometrium is accompanied by endothelial growth; and thirdly during the secretory phase where the spiral arterioles exhibit significant growth and coiling. Immediately below the luminal epithelium, a

subepithelial capillary plexus also develops during the menstrual cycle (Fanger and Barker, 1961; Peek *et al.*, 1992). During the early to mid-secretory phases, blood flow to this plexus reaches a maximum in preparation for the implantation of a viable blastocyst (Gannon *et al.*, 1997).

In the adult tissue, angiogenesis occurs by at least three different mechanisms; including, sprouting, intussusception and vessel elongation. Sprouting angiogenesis (Figure 6.1), the best known form of angiogenesis, occurs during neovascularisation of avascular tissue, for example, during the rapid growth of the corpus luteum following ovulation. Sprouting or classical angiogenesis begins with activation of the endothelial cells by angiogenic growth factors acting to release specific proteases, which subsequently degrade the basement membrane. Loss of the integrity of the basement membrane allows endothelial cells to escape from the original vessel walls, to migrate into their surrounding matrix, where they and coalesce to form tubules. As the tubules extend toward the source of the angiogenic stimulus, endothelial cells migrate in tandem using adhesion molecules, usually integrins. A new basement membrane is then deposited and the vessel undergoes vascular maturation involving the recruitment of mural or support cells, including, pericytes or smooth muscle cells in the large vessels (Klagsbrun and D'Amore, 1991; Risau, 1997).

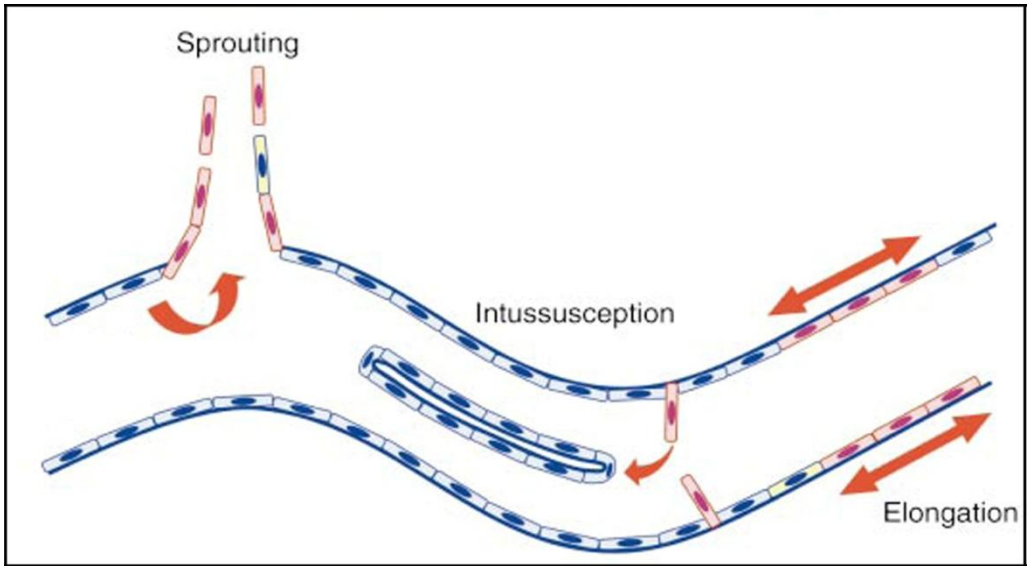


Figure 6.1 Schematic representation of the three different mechanisms of angiogenesis; sprouting, intussusception and elongation (Gargett and Rogers, 2001).

Intussusception (Figure 6.1), also known as splitting angiogenesis, produces a network or arcade of parallel vessels and was first observed in neonatal rats (Burri and Tarek, 1990). In this type of vessel formation, the capillary wall extends into the lumen to split a single vessel in two. There are four main phases to this kind of blood vessel formation. Initially the two opposing capillary walls establish an area of contact. The endothelial cell junctions are then reorganized and the vessel bilayer perforated to allow for penetration by growth factors and cells. An interstitial core, filled with pericytes and myofibroblasts, is formed between the two new vessels at the area of contact. These cells begin laying

down collagen fibers into the core to provide an extracellular matrix for growth of the vessel luminae. Finally, the newly divided vessel is remodelled into two discrete capillaries (Burri and Tarek, 1990; Risau, 1997). It is hypothesised that the endometrial subepithelial capillary plexus is formed by intussusceptive angiogenesis (Gargett *et al.*, 2002).

The third type of physiological angiogenesis is elongation and vessel widening (Figure 6.1). This type of new vessel formation is thought to occur as existing vessels restructure in response to the metabolic demands of the surrounding cells. This process has also been described as remodelling or pruning (Risau, 1997) and is most likely to occur during endometrial growth (Rogers and Gargett, 1998).

Several endothelial cell proliferation studies show that classical or sprouting angiogenesis does not occur in the human endometrium, as proliferating endothelial cells are always observed within vessel profiles. No sprouts have been identified in these endothelial cell proliferation studies (reviewed in Rogers and Gargett, 1998). It is also important to note that immunohistochemical identification of the marker for sprouting endothelium, $\alpha_\gamma\beta_3$ integrin, has only been observed in existing vessel profiles (Hii and Rogers, 1998), suggesting that angiogenesis occurring within the endometrium occurs by non-sprouting mechanisms. Gambino *et al.* (2002) showed that the endometrial angiogenesis occurring in the early to mid/late proliferative phase of the menstrual cycle is by vessel elongation. It is hypothesised that the spiral arterioles grow by elongation throughout the menstrual cycle and that formation of the endometrial subepithelial capillary plexus during the proliferative and mid-secretory stages is by intussusceptive angiogenesis (Gargett and Rogers, 2001).

During early pregnancy, within the endometrium, two vascular events symbolize the early stages of implantation of a viable blastocyst. The first event is the localised increase in vascular permeability observed within the implantation sites, which is one of the first indicators of the forthcoming implantation site. In the endometrium, this increase in vascular permeability can be identified by the appearance of blue uterine bands as a result of Pontamine sky blue, Evans blue or Trypan blue given intravenously. These dyes, which bind to plasma proteins, especially albumin, within the blood vessels, leak into the surrounding tissues only in the areas where increased vascular permeability has occurred (Psychoyos, 1970; Rogers *et al.*, 1982). This increased vascular permeability has been reported in many species; including, rats (Psychoyos, 1970; Rogers *et al.*, 1982), guinea-pigs (Deanesly, 1967) and sheep (Boshier, 1970) and is considered to be essential for the formation of the decidua during early pregnancy (Psychoyos, 1961). Ma *et al.* (2001) showed that this increase in vascular permeability prior to blastocyst implantation is under the control of the ovarian hormone oestrogen as evident by an increase in vascular permeability and oedema in ovariectomised mice treated with oestrogen (Ma *et al.*, 2001). In addition, it was established that progesterone has little effect on this increase in vascular permeability (Ma *et al.*, 2001).

In an endothelial cell migration assay utilising cultured endometrial cell explants, a significant migratory response of the endothelial cells towards the explants occurred only with explants from day 5 pregnant rats, with minimal levels returning by day 6 of pregnancy (Abberton and Rogers, 1995). This migration was initiated in explants from day 5 of pregnancy, at around 5h, before the earliest detectable signs of embryo implantation (Abberton and Rogers, 1995), suggesting that angiogenesis may be occurring in the rat endometrium around the time of blastocyst implantation (Goodger and Rogers, 1993). Goodger and Rogers (1993) showed an increase in endothelial cell proliferation around this stage of pregnancy, suggesting that the second vascular event of early pregnancy is an increase in proliferation of the endothelial cells. This extensive neovascularisation of the endometrium takes place upon decidual transformation in response to implantation of a blastocyst. The increase in decidual mass is accompanied by induction of neovascularisation and formation of an anastomising network traversing the maternal decidua and converging on the embryo (Shweiki *et al.*, 1993). This vascular network supplies the maternal contribution of the future placenta (Shweiki *et al.*, 1993). In the rat endometrium, this increase in endothelial cell proliferation begins at around day 3 of pregnancy (spermatozoa in vaginal smear designated day 1 of pregnancy) and continues to increase as pregnancy progresses through to days 6 and 7, where it is restricted to the implantation sites (Goodger and Rogers, 1993). These investigators suggested two separate mechanisms involved in the regulation of uterine endothelial cell proliferation during early pregnancy; an initial maternally controlled mechanism regulated by progesterone that occurs throughout the entire endometrium from day 3 of pregnancy and a second embryonic stimulus that occurs around the time of implantation, only in the vicinity of the blastocyst (Goodger and Rogers, 1993). Thus, the restriction of the increase in endothelial cell proliferation at days 6 and 7 of pregnancy may be as a result of embryonic regulation rather than regulation by a maternal factor/s.

Angiogenesis that occurs in the endometrium is under the overall control of the ovarian hormones oestrogen and progesterone, mediated via their receptors. Their receptors function as hormone-activated transcription factors and modulators of gene expression in target cells (Barkhem *et al.*, 1998; Hewitt and Korach, 2000b). There are many conflicting reports as to which ovarian hormone promotes angiogenesis and which one inhibits it. Ma *et al.* (2001) indicated an increase in vascular permeability, but a decrease in vascular density during the late oestrogenic response, suggesting an inhibitory role for oestrogen. In a separate study, Hastings *et al.* (2003) showed that while oestrogen had a stimulatory effect on vascular permeability, cellular mitosis and DNA and RNA synthesis, it did not stimulate endothelial cell proliferation. In contrast, Heryanto and Rogers (2002) reported a rapid increase in endothelial cell proliferation within 24h of oestrogen treatment in ovariectomised mice, suggesting an angiogenic response. In addition, the rapid vessel growth observed in the proliferative stage of the menstrual cycle is associated with increasing concentrations of oestrogen (Gambino *et al.*, 2002).

Previous studies have hypothesised a two phase response of oestrogen on angiogenesis within the endometrium. The first response of oestrogen induces angiogenesis in the form of increased vascular permeability. This increase in vascular permeability is followed by increased angiogenesis within the decidual bed to ensure an adequate blood supply to the implanting blastocyst for nourishment and development (Ma *et al.*, 2001; Heryanto and Rogers, 2002). Oestrogen has been shown to have an inhibitory effect on this vascular event (Ma *et al.*, 2001; Walter *et al.*, 2005). This is further confirmed by the fact that ER-α (-/-) mice display an increase in vascular density, as well as the expression of VEGF and Flk-1 mRNA in the absence of oestrogen effects via ER-α (Ma *et al.*, 2001). In contrast, progesterone has been implicated in the induction and regulation of this angiogenic response (Walter *et al.*, 2005). In ovariectomised mice, administration of progesterone alone resulted in the highest incident of endometrial cell proliferation, whereas priming of the endometrium by oestrogen, which occurs during early pregnancy, resulted in a decrease in this progesterone-regulated induction in cell proliferation (Walter *et al.*, 2005). The mediation of this anti-oestrogenic effect on endothelial angiogenesis and the pathways involved remain unclear. Regulation of endothelial angiogenesis during early pregnancy by progesterone is further confirmed by a significant increase in endothelial cell proliferation occurring in the rat uterus prior to implantation when plasma progesterone concentrations are increasing (Goodger and Rogers, 1993). Due to the evidence that this increase in endothelial cell proliferation is under the control of the ovarian hormone, it follows that the antiprogestin RU486 would have an adverse effect on this angiogenic response of early pregnancy.

In a study by Gambino *et al.* (2002) it was reported that the angiogenic mechanism responsible for the increase in vasculature during the early/mid secretory phase, under the regulation of progesterone, was most likely to be by intussusceptions. It is also at this stage of the menstrual cycle that the growth and coiling of the spiral arterioles occurs and is thus also regulated by progesterone. In the rat endometrium, endothelial cell proliferation was shown to increase significantly during early pregnancy, when the plasma levels of progesterone are increasing in preparation for blastocyst implantation (Goodger and Rogers, 1993). Ma *et al.* (2001) showed that progesterone increased vascular density in ovariectomised rats while having little effect on vascular permeability.

Walter *et al.* (2005) demonstrated that during early pregnancy, progesterone stimulates endothelial cell proliferation within the endometrium and priming the uterus with oestrogen is not required for progesterone to exact its effect on endothelial proliferation. In effect, priming of the uterus with oestrogen was reported to have an inhibitory effect on progesterone-induced endometrial angiogenesis (Walter *et al.*, 2005).

In an attempt to explain the differences reported, it is suggested that the ovarian hormones acting at different stages of the menstrual cycle and during pregnancy may control different types of

angiogenesis, as metabolic needs change. It is also highly probable that events of endometrial angiogenesis are regulated at a local level by factors other than progesterone and oestrogen. It has been hypothesised that numerous different angiogenic factors may be involved during endometrial angiogenesis. These include vascular endothelial growth factor (VEGF) (Torry and Torry, 1997; Smith, 1998), fibroblast growth factor (FGF) (Ferriani *et al.*, 1993) and platelet-derived growth factor (PDGF) (Smith, 1995; Weston and Rogers, 2000).

6.1.1.1 Vascular endothelial growth factor (VEGF)

The VEGF family consists of VEGF-A, VEGF-B, VEGF-C, VEGF-D and placenta growth factor, each with variable interactions with the VEGF receptors. VEGF-A is the best known of the VEGF family of glycoproteins. VEGF-A is a heparin-binding, secreted homodimeric glycoprotein of 30-46 kDa (Ferrara and Davis-Smyth, 1997). It was originally identified as a protein produced by tumour cells, able to increase vascular permeability of capillaries to proteins. It was because of this property that it was initially known as vascular permeability factor (VPF) (Dvorak *et al.*, 1995). It was subsequently reported to be an endothelial cell-specific angiogenic protein that appeared to play an important role in both physiological and pathological neovascularisation (Ferrara and Davis-Smyth, 1997).

VEGF-A genes in both the human and murine models are organised into eight exons and seven introns. Alternative exon splicing of the last four exons of the VEGF gene (the first four are conserved) generates different molecular species which have 121, 145, 165, 189 or 206 amino acids ($VEGF_{121}$, $VEGF_{145}$, $VEGF_{165}$, $VEGF_{189}$, $VEGF_{206}$) (Ferrara and Davis-Smyth, 1997). In the mouse, three isoforms of the VEGF gene have been identified, which are shorter by one amino acid ($VEGF_{120}$, $VEGF_{164}$, $VEGF_{188}$) (Ferrara and Davis-Smyth, 1997). Each VEGF isoform has variable interactions with heparin, the extracellular matrix and the VEGF receptors (Girling and Rogers, 2009). In most human systems, the predominant molecular species are $VEGF_{165}$ and $VEGF_{121}$, whereas $VEGF_{189}$ is only minimally present and $VEGF_{206}$ has only been reported in the cDNA library of the human foetal liver (Ferrara and Davis-Smyth, 1997).

VEGFs act through at least three members of the type III tyrosine kinase family receptors; the c-fms-like tyrosine kinase (Flt-1) or VEGF receptor 1 (VEGFR-1), Flt-4 or VEGF receptor 3 (VEGFR-3) or the kinase domain insert-containing receptor (Flk-1/KDR) or VEGF receptor 2 (VEGFR-2) (Shibuya *et al.*, 1990; Matthews *et al.*, 1991). VEGF-A binds to Flt-1 and Flk-1/KDR, whereas VEGF-C and D interact with Flt-4 (Shibuya *et al.*, 1990; Quinn *et al.*, 1993). Both receptors bind VEGF with high affinity; however, Flt-1 binds with a higher affinity than Flk-1/KDR (de Vries *et al.*, 1992; Millauer *et al.*, 1993). The VEGF-A receptors are primarily expressed on vascular endothelial cells (Millauer *et al.*, 1993). Recently, another multifunctional VEGF receptor has been identified, neuropilin-1 (NRP-

1). NRP-1 acts as a receptor for at least five different ligands, one of which is $VEGF_{165}$. In the human endometrium NRP-1 is expressed as a $VEGF_{165}$-specific receptor (Neufeld *et al.*, 1994; Soker *et al.*, 1998). NRP-1 is reported to increase $VEGF_{165}$ binding to Flk-1, when they are co-expressed in the endothelial cell (Soker *et al.*, 1998).

Studies have attempted to correlate VEGF-A mRNA and protein expression with the different stages of the menstrual cycle; however, the expression patterns reported are inconsistent (Shifren *et al.*, 1996; Torry *et al.*, 1996; Sharkey *et al.*, 1999; Graubert *et al.*, 2001; Chabbert-Buffet *et al.*, 2005; Lee *et al.*, 2008). Torry *et al.* (1996) described a 3- to 6-fold increase in endometrial VEGF mRNA during the oestrogen regulated secretory phase. In contrast, Shifren *et al.* (1996) found an increase of 1.26, 2.0- and 3.6-fold in VEGF mRNA during the mid and late proliferative and secretory phases of the menstrual cycle respectively. The cyclic changes of VEGF expression reported in the literature are consistent with regulation by the ovarian hormones, progesterone and oestrogen. In ovariectomised rats, both oestrogen and progesterone were observed to increase VEGF mRNA levels within the uterus (Cullinan-Bove and Koos, 1993).

With regards to the first vascular event of early pregnancy, Ma *et al.* (2001) demonstrated that the increase in vascular permeability coincides with an increase in VEGF mRNA expression and its receptor, Flk-1, suggesting that VEGF is important for uterine vascular permeability changes induced by oestrogen during this first vascular event of early pregnancy (Ma *et al.*, 2001). In agreement with this hypothesis, a study using an antibody to VEGF to systemically block VEGF action within the rat endometrium was able to demonstrate that anti-VEGF reduced the endometrial vascular permeability response in a dose-dependent manner (Rabbani and Rogers, 2001). At high levels of anti-VEGF, although almost no blue bands indicative of increased vascular permeability within the endometrium were observed, as the dose of anti-VEGF was decreased, the levels of vascular permeability increased, as indicated by an increase in the number of stained bands of the implantation sites (Rabbani and Rogers, 2001).

With regards to the second vascular event of early pregnancy, Walter *et al.* (2005) noted an increase in endothelial cell proliferation, mediated in part by VEGF, following progesterone administration; as VEGF anti-serum was observed to significantly inhibit endothelial cell proliferation in mice treated with progesterone only. VEGF anti-serum did not, however, inhibit the progesterone-induced endothelial cell proliferation when the endometrium was primed with oestrogen (Walter *et al.*, 2005), suggesting that in the presence of oestrogen, VEGF is not the only factor driving the increase in endothelial cell proliferation during early pregnancy. This study also reported the most intense VEGF tissue immunostaining in the glandular and luminal epithelium of the mouse uterus (Walter *et al.*, 2005). In a study on a human breast cancer cell line, progesterone increased VEGF protein

expression, which could be blocked by the antiprogestin RU486, indicating that the induction is mediated by the PR (Hyder *et al.*, 1998).

6.1.1.2 Basic fibroblast growth factor (bFGF)

The fibroblast growth factor (FGF) family, expressed in a variety of adult and foetal tissue, is a family of structurally related, biologically active, peptides with a strong affinity for heparin, consisting of at least twenty two members (Itoh and Ornitz, 2004). Basic fibroblast growth factor (bFGF) is a single-chain, nonglycosylated, cationic polypeptide which exists as an 18kDa form within the extracellular matrix and cytoplasm and a 20-24kDa form within the nucleus (Renko *et al.*, 1990). Basic FGF is mitogenic for a number of cells derived from the mesoderm, including, fibroblasts and endothelial cells, as well as a potent promoter of angiogenesis (Gospodarowicz, 1974).

The FGF family of growth factors bind to four distinct transmembrane tyrosine kinase receptors (FGF-R1, -R2, -R3 and -R4) with different affinities (Hyder and Stancel, 1999). FGF-R1 is the most common cellular receptor. These FGF receptors are membrane bound receptors that dimerise upon binding to FGF. This results in the activation of tyrosine kinase activity and autophosphorylation of the receptor. Receptor activation gives rise to a signal transduction cascade that leads to gene activation and diverse biological responses; including, cell differentiation, proliferation, and matrix dissolution, thus initiating a process of mitogenic activity critical for the growth of endothelial cells, fibroblasts, and smooth muscle cells (Hyder and Stancel, 1999). Basic FGF binds most commonly to the FGF-R1 and FGF-R2 receptors (Wollenhaupt *et al.*, 2004).

Basic FGF has both potent pro-proliferative and angiogenic activities and may thus be important for tissue remodelling and neovascularisation within the endometrium (Reynolds *et al.*, 1998). A process involved in the precise priming of the uterus in anticipation of blastocyst implantation is the proliferation and differentiation of the uterine stromal cells into decidual cells around the time of blastocyst implantation (Tachi *et al.*, 1972). It has long been accepted that this decidual cell response is under the control of the ovarian hormone, progesterone, as stromal cells do not divide in the absence of progesterone and further, stromal cell proliferation can be blocked by progesterone antibodies (Rider *et al.*, 1986). In addition, the ability of RU486 to inhibit the decidual cell response, suggests that progesterone action is mediated through its receptor protein (Cullingford and Pollard, 1988). Studies using rat and human stromal cell lines indicate that while progesterone is necessary for cell proliferation to occur, it is not sufficient, as cultured stromal cells required additional factors for this (Irwin *et al.*, 1991; Cohen *et al.*, 1993). Both bFGF and FGF receptors (FGF-R1) are present spatially and temporally in proliferating stromal cells in the rat uterus around days 3.5 - 5.5 of pregnancy (Rider and Psychoyos, 1994; Rider *et al.*, 1995). Coupled with the finding that FGF-R1 immunolocalises to the perinuclear region of the uterine stromal cells, these data suggest a function

for bFGF in these cells (Prudovsky *et al.*, 1994; Rider *et al.*, 1995). This hypothesis is further supported by reports that the addition of Suramin, an inhibitor of tyrosine kinase receptor activation, to uterine stromal cell cultures has an inhibitory effect on the growth-stimulatory activity of progesterone and bFGF (Piva *et al.*, 1996).

While bFGF localisation patterns observed by immunohistochemical analysis vary among studies, FGF staining has been reported in the basal lamina of the uterine blood vessels in both the endometrium and myometrium; in uterine stromal fibroblasts and the extracellular matrix, in myometrial cells as well as in both the glandular and luminal epithelial compartments and in the endothelial cells (Sangha *et al.*, 1997). Epithelial, stromal and myometrial bFGF expression has been reported during the menstrual (Sangha *et al.*, 1997) and oestrous cycles and early pregnancy (Carlone and Rider, 1993; Srivastava *et al.*, 1998), and it has been suggested that bFGF may act to control the cellular changes involved in the remodelling of the endometrium in preparation for the implantation of a viable blastocyst (Carlone and Rider, 1993). This hypothesis is, in part, supported by reports that bFGF is localised within the uterine epithelial and stromal compartments, as well as in the extracellular matrix in pseudopregnant rat uteri and in the epithelial compartment in the proliferative phase of the menstrual cycle (Carlone and Rider, 1993; Wei *et al.*, 2004). Specifically, localisation of bFGF is induced in luminal epithelial and decidual cells at the site of embryo implantation (Carlone and Rider, 1993). Wordinger *et al.* (1994) reported similar bFGF localisation patterns in pregnant rat uteri, suggesting a possible role for bFGF in formation of the decidual layer as well as angiogenesis. The importance of bFGF in blastocyst implantation is emphasised as rodents immunised against bFGF were unable to establish pregnancy (Buscaglia *et al.*, 1991).

Basic FGF was the first growth factor shown to have angiogenic properties (Smith, 1998). Not only does bFGF have an effect on the proliferation and differentiation of the epithelial and stromal compartments, but also plays a role in the angiogenesis and remodelling of the endometrial blood supply around the time of pregnancy, necessary for increased nutrient and oxygen demand. Both VEGF and bFGF gene expression has been reported within the decidual layer of the rat uterus. VEGF mRNA levels are maintained at a constant level throughout the development of the decidua, whereas bFGF mRNA expression fluctuates throughout the developmental period (Srivastava *et al.*, 1998). In the decidua of the rat uterus, bFGF mRNA and protein expression increased significantly at day 9.5 to 11.5 of pseudopregnancy. In normal pregnant animals, this is the time where extensive angiogenesis occurs within the decidual layer to become continuous with the blood spaces with the invading trophoblast cells (Welsh and Enders, 1991). The investigators thus suggested that bFGF plays an important role in the regulation of the proliferation of the blood vessels during the decidual response (Srivastava *et al.*, 1998).

No secretory signal sequence exists for bFGF, suggesting that endometrial neovascularisation may be partially regulated by bFGF from the surrounding cells, such as in the stromal or smooth muscle cells (Reynolds *et al.*, 1998). In the rhesus monkey, the high expression of both bFGF and its receptors in the decidual layer implies a role in the control of both the proliferation and differentiation of the stromal cells as well as in angiogenesis (Sangha *et al.*, 1997). Grimwood *et al.* (1995) established that bFGF is unable to exact an angiogenic response on its own within the endometrium, as it was unable to induce proliferation in endothelial cells obtained from the human decidua.

Although steroid hormonal control of bFGF has been established, reports nevertheless differ as to whether oestrogen or progesterone is the principle player. In the mouse uterus, Wordinger *et al.* (1992) reported no alterations in bFGF localisation during the oestrous cycle, or following ovariectomy and steroid hormone supplementation in animals. Further studies reported bFGF induction in the primate uterus by oestrogen (Samathanam *et al.*, 1998) and that progesterone is a potent stimulator of bFGF expression in the rat endometrium (Rider and Psychoyos, 1994; Rider *et al.*, 1997).

6.1.1.3 Platelet-derived growth factor (PDGF)

The heparin-binding growth factor, platelet-derived growth factor (PDGF) is a 30kDa, cationic disulfide-linked dimer made up of two related polypeptide chains, designated A and B, and are assembled to form three biologically active isoforms, the heterodimer (PDGF-AB) and the homodimers (PDGF-AA and PDGF-BB) (Heldin *et al.*, 1985; Fretto *et al.*, 1993; Munson *et al.*, 1995). The A- and B- chains of PDGF are encoded by two distinct genes and are inactive when undimerised (Kelly *et al.*, 1991).

PDGF acts by binding to two specific, high affinity protein tyrosine kinase receptors, PDGF receptor-α and -β (PDGFR-α and PDGFR-β). These PDGF receptors differ in ligand binding specificity, in that the α-receptor is able to bind all three isoforms of PDGF with high and fairly equal affinities. In contrast, the β-receptor is only able to bind PDGF-BB with a similar high affinity. This receptor binds PDGF-AB with a 10-fold lower affinity than it does PDGF-BB and does not appear to recognise PDGF-AA (Westermark *et al.*, 1990). In 1991, Ueno *et al.* suggested that PDGF receptor dimerisation, mediated by ligand binding, is necessary for signal transduction, thus it is now widely accepted that the αα-receptor binds to all three isoforms of PDGF, whereas the ββ-receptor binds only to PDGF-BB with high affinity. The PDGF-AB and PDGF-AA isoforms bind with a lower affinity and a very low affinity respectively (Fretto *et al.*, 1993; Osterlund *et al.*, 1996). Binding of PDGF to its receptors leads to activation of the receptor tyrosine kinase and to subsequent initiation of cytoplasmic signal transduction pathways, which in turn lead to the migration, proliferation and differentiation of PDGF-responsive cell types (Kelly *et al.*, 1991; Fretto *et al.*, 1993).

The predominant role of PDGF is to stimulate the proliferation of cells of mesenchymal origin and has been linked to the aetiology of a number of human diseases such as atherosclerosis, glomerulonephritis and cancer (Ross *et al.*, 1985). In normal physiology, PDGF plays an important role in the control of growth, differentiation and activation of a variety of cell types via interactions with their receptors in target tissues (Carpenter and Cohen, 1979; Ross *et al.*, 1985; Westermark *et al.*, 1990). Within the endometrium, PDGF is considered to be essential for implantation as neutralisation of PDGF by antibodies administered to pregnant mice significantly decreased the rate of implantation and the size of the implantation sites (Holmes *et al.*, 1997). In a study on the rat endometrium, PDGF was shown to localise just prior to implantation. On day 2.5 of pregnancy, PDGF was observed in the apical surfaces and lateral membranes of the uterine epithelial cells, as well as within the underlying basement membrane (Slater and Murphy, 1999). By day 5.5, the day of blastocyst implantation, the intensity of PDGF labelling in these areas had increased to a maximum. In this study, a correlation between PDGF and fibronectin localisation was reported, suggesting a role in the preparation of the uterine epithelial cells for blastocyst attachment and invasion (Slater and Murphy, 1999).

A study by Jaber and Kan (1998) on the mouse endometrium reported a localisation of PDGF in both the luminal and glandular epithelium as well as within the stromal cells throughout the first 7 days of pregnancy, with a maximum intensity around days 4 and 5 of pregnancy, the time of blastocyst implantation. During the oestrous cycle, however, no PDGF localisation was observed (Jaber and Kan, 1998). The occurrence of cell proliferation and differentiation in the endometrium during early pregnancy in preparation for blastocyst implantation, coupled with their findings and the important regulatory role of PDGF in controlling of growth, differentiation and activation of a variety of cells (Carpenter and Cohen, 1979; Ross *et al.*, 1985; Westermark *et al.*, 1990), lead the investigators of this study to suggest that PDGF may participate in the preparation of the endometrium for blastocyst implantation by controlling the proliferation and differentiation of the endometrial cells during early pregnancy (Jaber and Kan, 1998).

PDGF has also been implicated in the decidual response of early pregnancy within the human endometrium. PDGF, PDGFR and a stimulatory effect of PDGF on DNA was observed in the decidual cells of the human endometrium (Saji *et al.*, 1997). All three isoforms of PDGF were localised in the decidual layer with PDGF-AB and PDGF-BB having a significantly greater effect on DNA synthesis than PDGF-AA. This study also reported the presence of both PDGF receptor types and that PDGF-BB had an 8-fold higher binding affinity than PDGF-AA (Saji *et al.*, 1997). Giudice (1994) suggested that endometrial stromal cells are a source of PDGF that may act in an autocrine manner on the stromal cells to stimulate proliferation and in a paracrine manner on the neighbouring epithelium.

In addition, PDGF has been established as one of the growth factors directly involved in angiogenesis. Specifically, PDGF has been implicated in the maturation and remodelling of vessels during angiogenesis through the recruitment of vascular smooth muscle cells and pericytes (Armulik *et al.*, 2005). Rolny *et al.* (2006) reported that PDGFR-β promotes early endothelial cell differentiation, probably guided by PDGF-BB. In pig uterus, reported localisation of the PDGF receptors (α and β) in the endometrium and myometrium of the cycling and pregnant porcine uterus was up-regulated by oestrogen (Rodriguez-Martinez *et al.*, 1992). An additional study in the pig endometrium reported strong expression of the PDGF receptors in the endothelial/perivascular areas of the subepithelial layer, suggesting a role for this growth factor in the angiogenic response in the porcine endometrium during early pregnancy (Persson and Rodriguez-Martinez, 1997).

Since remodelling of the endometrium during early pregnancy, in response to an implanting blastocyst, is under the control of the ovarian hormones oestrogen and progesterone, it was hypothesised in the present study, that the partial antiprogestin RU486 would have an effect on this critical response of early pregnancy. The studies indicating that VEGF, bFGF and PDGF are important in both vascular permeability and endometrial cell proliferation during early pregnancy, led to this investigation of the spatiotemporal expression pattern of these angiogenic pathway-related growth factors during early pregnancy, with a particular focus on the possible effects of RU486, as a partial progesterone and oestrogen antagonist, on their localisation and expression.

6.2 RESULTS

6.2.1 Immunofluorescence Analysis of VEGF, bFGF and PDGF Protein Spatiotemporal Expression Patterns in the RU486-Treated Rat Endometrium.

Immunofluorescence was performed on each tissue section with primary antibodies raised against VEGF, bFGF and PDGF, in order to determine the spatiotemporal expression pattern of these angiogenic pathway-related growth factors during early. Following treatment with RU486 at day 3.0 of pregnancy, the spatiotemporal pattern of VEGF, bFGF and PDGF expression was analysed to observe what effect, if any, RU486 may have on angiogenic pathway-related growth factor localisation and expression.

6.2.1.1 The spatiotemporal expression pattern of the VEGF and bFGF proteins within the control pregnant animals

In the implantation sites of the control pregnant animals, VEGF protein expression was increased significantly in all endometrial compartments analysed as pregnancy progressed from day 4.5 to day 5.5, with the exception of in the glandular stroma where the increase in protein levels was not significant (Graph 6.1A-F; Figure 6.2A and C; Figure 6.3A and C; Figure 6.4A and C; Table 6.1). This increase was mimicked in bFGF protein expression in the implantation sites of the control pregnant animals with regards to all endometrial compartments analysed (Graph 6.2A-F; Figure 6.5A and C; Figure 6.6A and C; Figure 6.7A and C; Table 6.2). The increase was similar in the bFGF protein levels relative to the VEGF protein levels, except in the glandular stroma where the increase in bFGF protein expression was significantly higher as a result of the lack of increase in VEGF protein expression in this compartment. At day 5.5 of pregnancy, both VEGF and bFGF protein levels were highest in the glandular epithelium, followed by the luminal epithelium and then the blood vessels. In the stromal compartments, both VEGF and bFGF protein levels were similar (Graph 6.1A-F; Graph 6.2A-F; Figure 6.2A and C; Figure 6.3A and C; Figure 6.4A and C; Figure 6.5A and C; Figure 6.6A and C; Figure 6.7A and C; Table 6.1; Table 6.2).

By day 6.5 of pregnancy, VEGF and bFGF protein expression in the implantation sites remained stable in all endometrial compartments analysed, except in the blood vessels where expression decreased significantly (Graph 6.1A-F; Graph 6.2A-F; Figure 6.2E; Figure 6.3E; Figure 6.4E; Figure 6.5E; Figure 6.6E; Figure 6.7E; Table 6.1; Table 6.2). This decrease was more pronounced in bFGF expression. By this day of pregnancy, VEGF protein levels were significantly higher in the luminal epithelium and subepithelial stroma relative to bFGF protein levels.

Table 6.1 One-way ANOVA and Tukey Kramer *post hoc* analysis of VEGF protein expression in the luminal epithelium, the subepithelial stroma, the glandular epithelium, the glandular stroma, the blood vessels and the stroma surrounding the blood vessels of the implantation (IS) and non-implantation (NIS) sites between days 4.5, 5.5 and 6.5 of pregnancy in the control pregnant (UT) and RU486-treated (T) animals showing groups that are significantly different ($p \leq 0.05$). Groups not connected by the same letter are significantly different.

Group									Mean
Luminal Epithelium									
6.5UT NIS	A								137.686
6.5UT IS	A	B							130.804
5.5UT IS		B							124.883
5.5UT NIS			C						113.565
6.5T NIS				D					84.618
6.5T IS				D					81.148
4.5UT NIS					E				69.307
5.5T IS					E				68.675
4.5UT IS					E	F			67.338
4.5T IS						F	G		59.688
5.5T NIS							G		58.263
4.5T NIS								H	48.65
Subepithelial Stroma									
6.5UT NIS	A								87.2457
6.5UT IS		B							78.8357
5.5UT IS		B							75.5967
5.5UT NIS			C						59.045
6.5T NIS			C	D					55.7167
5.5T NIS			C	D	E				51.33
4.5UT NIS				D	E	F			49.56
6.5T IS				D	E	F			48.5117
4.5UT IS					E	F			45.635
5.5T IS						F	G		42.445
4.5T IS							G		36.4267
4.5T NIS							G		34.27
Glandular Epithelium									
6.5UT NIS	A								142.371
5.5UT IS	A								141.684
6.5UT IS	A								139.31
5.5UT NIS	A								137.76
4.5UT IS		B							85.541
4.5UT NIS		B							84.746
4.5T NIS				C					61.303
6.5T IS				C	D				55.456
6.5T NIS					D				52.434
5.5T IS					D		E		48.754
4.5T IS					D		E		48.047
5.5T NIS							E		41.732
Glandular Stroma									
6.5UT NIS	A								72.1543
5.5UT IS	A	B							67.8333
5.5UT NIS		B							62.8417
6.5UT IS		B	C						61.2914
4.5UT IS		B	C						60.1202
4.5UT NIS			C	D					54.4304
4.5T NIS				D	E				46.5867
5.5T NIS					E		F		43.985
6.5T NIS					E		F		43.235
4.5T IS					E		F		42.7933
6.5T IS					E		F		40.2283
5.5T IS							F		36.77

Blood Vessels								
6.5UT NIS	A							107.114
5.5UT IS		B						95.807
6.5UT IS			C					86.215
5.5UT NIS			C					79.225
4.5UT IS				D				66.532
4.5UT NIS				D	E			64.472
4.5T NIS					E	F		57.47
5.5T IS						F	G	54.34
6.5T IS						F	G	53.374
4.5T IS						F	G	50.129
5.5T NIS							G	47.427
6.5T NIS							G	46.923
Stroma Surrounding the Blood Vessels								
6.5UT IS	A							77.13
5.5UT IS	A	B						74.745
6.5UT NIS		B						67.8314
4.5UT IS			C					57.3465
5.5UT NIS			C					55.265
4.5T NIS			C	D				53.6517
4.5UT NIS			C	D				53.5383
6.5T IS				D	E			46.58
5.5T IS					E			45.174
4.5T IS					E			45.1617
6.5T NIS					E		F	39.5567
5.5T NIS							F	35.4033

In the non-implantation sites of the control pregnant animals, VEGF protein levels increased significantly in all endometrial compartments analysed as pregnancy progressed from day 4.5 to day 5.5, with the exception of in the stroma surrounding the blood vessels were expression remained constant (Graph 6.1A-F; Figure 6.2B and D; Figure 6.3B and D; Figure 6.4B and D; Table 6.1).

This significant increase was comparable in bFGF expression levels in all endometrial compartments analysed, with the exception of the subepithelial stroma where levels remained stable (Graph 6.2A-F; Figure 6.5B and D; Figure 6.6B and D; Figure 6.7B and D; Table 6.2). VEGF and bFGF protein levels were highest in the glandular epithelium, followed by the luminal epithelium and then in the blood vessels. In the stromal compartments, VEGF and bFGF protein expression levels were similar with the exception of bFGF expression in the subepithelial stroma which was significantly lower (Graph 6.1A-F; Graph 6.2A-F; Figure 6.2B and D; Figure 6.3B and D; Figure 6.4B and D; Figure 6.5B and D; Figure 6.6B and D; Figure 6.7B and D; Table 6.1; Table 6.2).

By day 6.5 of pregnancy, VEGF protein expression in the non-implantation sites continued to increase in all endometrial compartments analysed, with the exception of in the glandular epithelium where levels remained constant (Graph 6.1A-F; Figure 6.2F; Figure 6.3F; Figure 6.4F; Table 6.1). Alternatively, bFGF protein levels only increased significantly in the subepithelial stroma at this day of pregnancy and decreased significantly in the glandular stroma (Graph 6.2A-F; Figure 6.5F; Figure 6.6F; Figure 6.7F; Table 6.2).

Table 6.2 One-way ANOVA and Tukey Kramer *post hoc* analysis of bFGF protein expression in the luminal epithelium, the subepithelial stroma, the glandular epithelium, the glandular stroma, the blood vessels and the stroma surrounding the blood vessels of the implantation (IS) and non-implantation (NIS) sites between days 4.5, 5.5 and 6.5 of pregnancy in the control pregnant (UT) and RU486-treated (T) animals showing groups that are significantly different ($p \leq 0.05$). Groups not connected by the same letter are significantly different.

Group								Mean
Luminal Epithelium								
5.5UT IS	A							124.745
6.5UT IS	A	B						119.191
6.5UT NIS		B						114.416
5.5UT NIS		B						114.388
4.5UT NIS			C					71.188
6.5T IS			C	D				66.558
4.5UT IS			C	D				66.025
5.5T IS				D	E			63.062
6.5T NIS					E			57.391
4.5T IS						F		48.16
5.5T NIS						F	G	46.537
4.5T NIS							G	39.378
Subepithelial Stroma								
5.5UT IS	A							73.675
6.5UT IS	A	B						67.8043
6.5UT NIS		B						62.3814
5.5UT NIS			C					49.7483
4.5UT NIS			C	D				46.4317
6.5T IS				D	E			42.085
6.5T NIS				D	E			41.4533
5.5T NIS					E	F		39.2367
4.5UT IS					E	F		38.145
5.5T IS						F	G	32.9233
4.5T IS							G	28.27
4.5T NIS							G	27.1083
Glandular Epithelium								
5.5UT NIS	A							144.596
6.5UT NIS		B						136.37
5.5UT IS		B						134.955
6.5UT IS		B						134.94
4.5UT NIS			C					81.58
4.5UT IS				D				69.66
6.5T IS				D	E			65.791
4.5T NIS					E			61.608
6.5T NIS						F		51.169
4.5T IS						F		47.664
5.5T IS							G	38.929
5.5T NIS							G	32.329
Glandular Stroma								
5.5UT IS	A							70.5017
6.5UT NIS	A							69.44
5.5UT NIS	A							65.4483
6.5UT IS		B						56.4571
4.5T NIS		B	C					50.595
4.5UT IS			C	D				48.4417
4.5UT NIS			C	D	E			46.3467
4.5T IS				D	E			43.135
6.5T IS					E			40.225
6.5T NIS					E			39.1733
5.5T IS							F	30.7617
5.5T NIS							F	27.7233

Blood Vessels									
5.5UT IS	A								106.748
6.5UT NIS	A								104.344
5.5UT NIS	A								102.012
6.5UT IS		B							81.617
4.5UT IS			C						67.952
4.5UT NIS			C	D					66.61
6.5T IS				D	E				59.788
4.5T NIS					E	F			56.392
5.5T IS					E	F	G		51.959
4.5T IS						F	G		50.1
6.5T NIS							G	H	45.989
5.5T NIS								H	39.86
Stroma Surrounding the Blood Vessels									
6.5UT IS	A								78.3086
5.5UT IS	A								78.1633
5.5UT NIS		B							66.235
6.5UT NIS		B							64.3114
4.5UT IS			C						54.5733
4.5T NIS			C						53.9
4.5UT NIS			C						52.625
5.5T IS					D				44.1167
6.5T IS					D				43.6467
4.5T IS					D				43.0683
6.5T NIS							E		36.4067
5.5T NIS								F	28.4867

By this day of pregnancy, VEGF protein expression levels in the non-implantation sites were also significantly higher in the luminal and subepithelial stroma relative to bFGF protein levels.

In general, the increase in VEGF protein levels and that of bFGF protein levels with the progression of pregnancy from day 4.5 through to day 6.5 in the control pregnant animals was comparable in most of the endometrial compartments.

It is important to note that VEGF and bFGF protein expression was similar between the implantation and non-implantation sites at day 4.5 of pregnancy (Graph 6.1A-F; Graph 6.2A-F; Figure 6.2A and B; Figure 6.3A and B; Figure 6.4A and B; Figure 6.5A and B; Figure 6.6A and B; Figure 6.7A and B; Table 6.1; Table 6.2). By day 5.5 of pregnancy, VEGF protein levels were significantly higher only in the subepithelial stroma, the blood vessels, and the stroma surrounding the blood vessels of the implantation sites, whereas bFGF levels were significantly higher only in the subepithelial stroma of the implantation sites (Graph 6.1A-F; Graph 6.2A-F; Figure 6.2C and D; Figure 6.3C and D; Figure 6.4C and D; Figure 6.5C and D; Figure 6.6C and D; Figure 6.7C and D; Table 6.1; Table 6.2).

By day 6.5 of pregnancy, only VEGF protein expression in the blood vessels was markedly higher in the implantation sites, whereas bFGF levels were similar between the implantation and non-implantation sites (Graph 6.1A-F; Graph 6.2A-F; Figure 6.2E and F; Figure 6.3E and F; Figure 6.4E and F; Figure 6.5E and F; Figure 6.6E and F; Figure 6.7E and F; Table 6.1; Table 6.2)

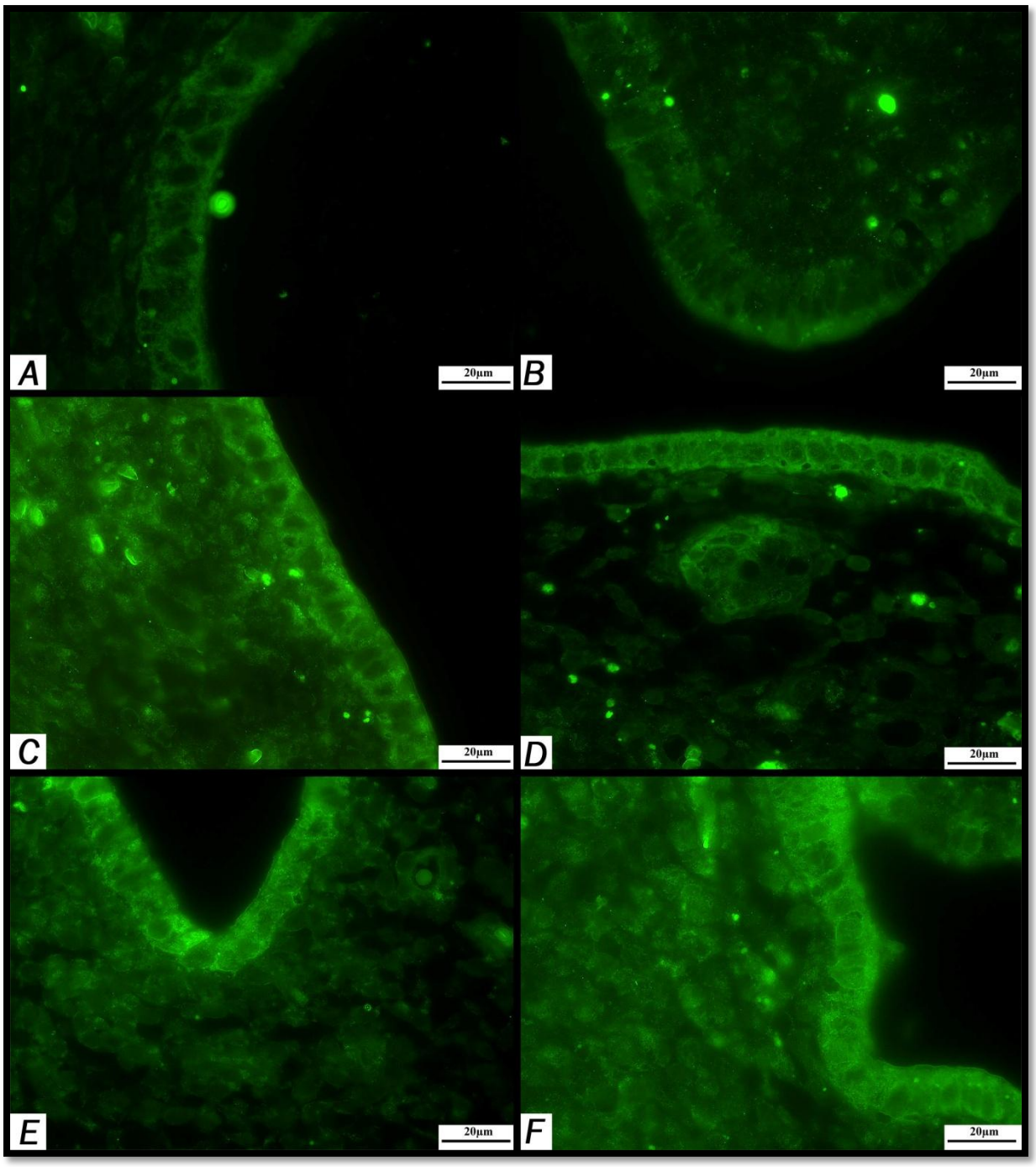
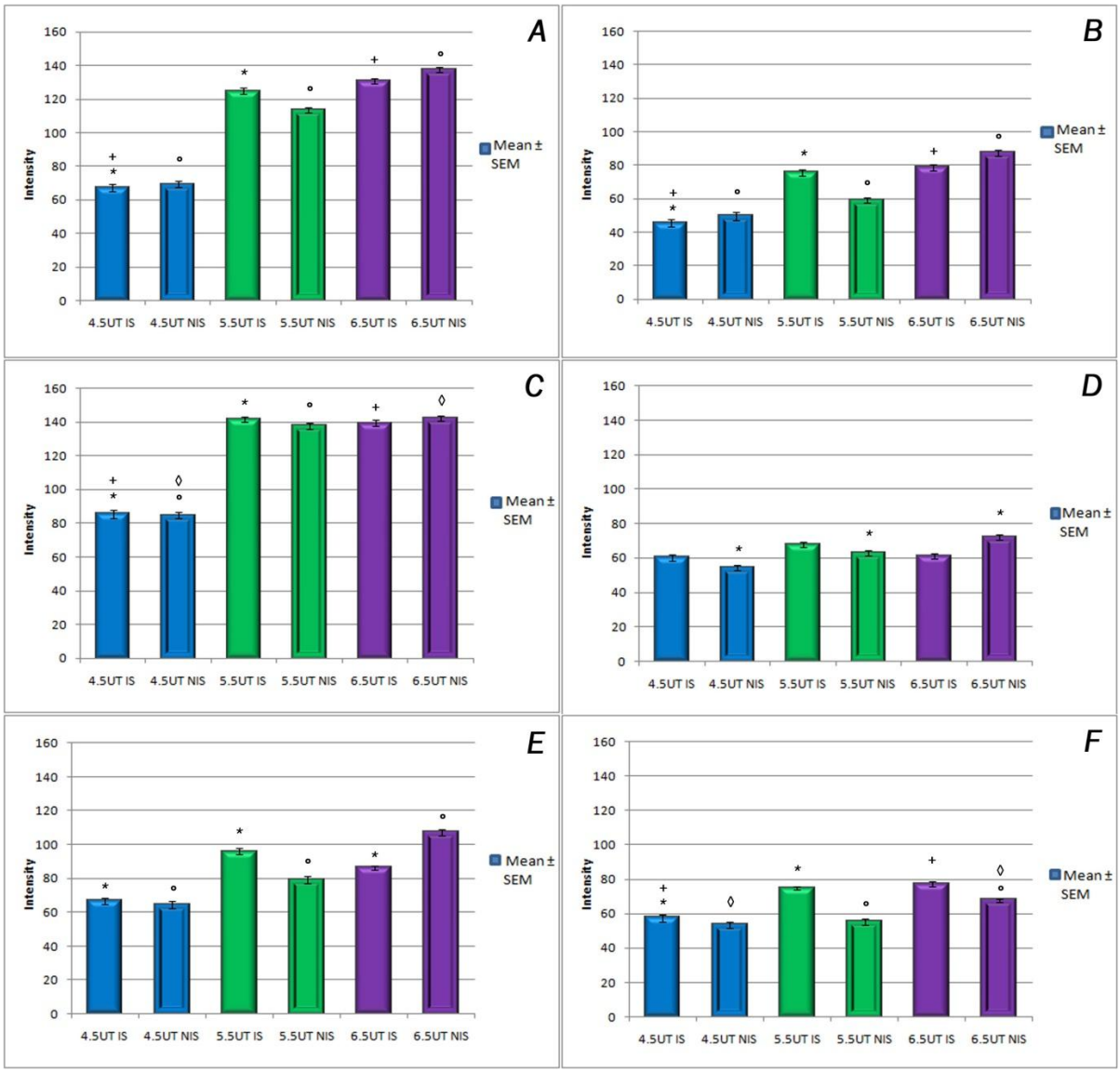


Figure 6.2 Immunofluorescent images illustrating VEGF protein localisation in the luminal epithelium and the subepithelial stroma of the implantation and non-implantation sites in the uteri of control pregnant rats. A: Implantation site at day 4.5 of pregnancy, **B:** Non-implantation site at day 4.5 of pregnancy, **C:** Implantation site at day 5.5 of pregnancy, **D:** Non-implantation site at day 5.5 of pregnancy, **E:** Implantation site at day 6.5 of pregnancy, **F:** Non-implantation site at day 6.5 of pregnancy. Scale = 20µm.



Graph 6.1 Graphical representation of the Mean ± SEM of VEGF protein expression in the luminal epithelium (A), the subepithelial stroma (B), the glandular epithelium (C), the glandular stroma (D), the blood vessels (E) and the stroma surrounding the blood vessels (F) of the implantation (IS) and non-implantation (NIS) sites in day 4.5, day 5.5 and day 6.5 pregnant rat uteri treated with vehicle (UT) at day 3.0 of pregnancy, as obtained from image analysis of fluorescent intensities. *, °, +, ◊ = significantly different ($p \leq 0.05$) using the Tukey-Kramer *post hoc* analysis.

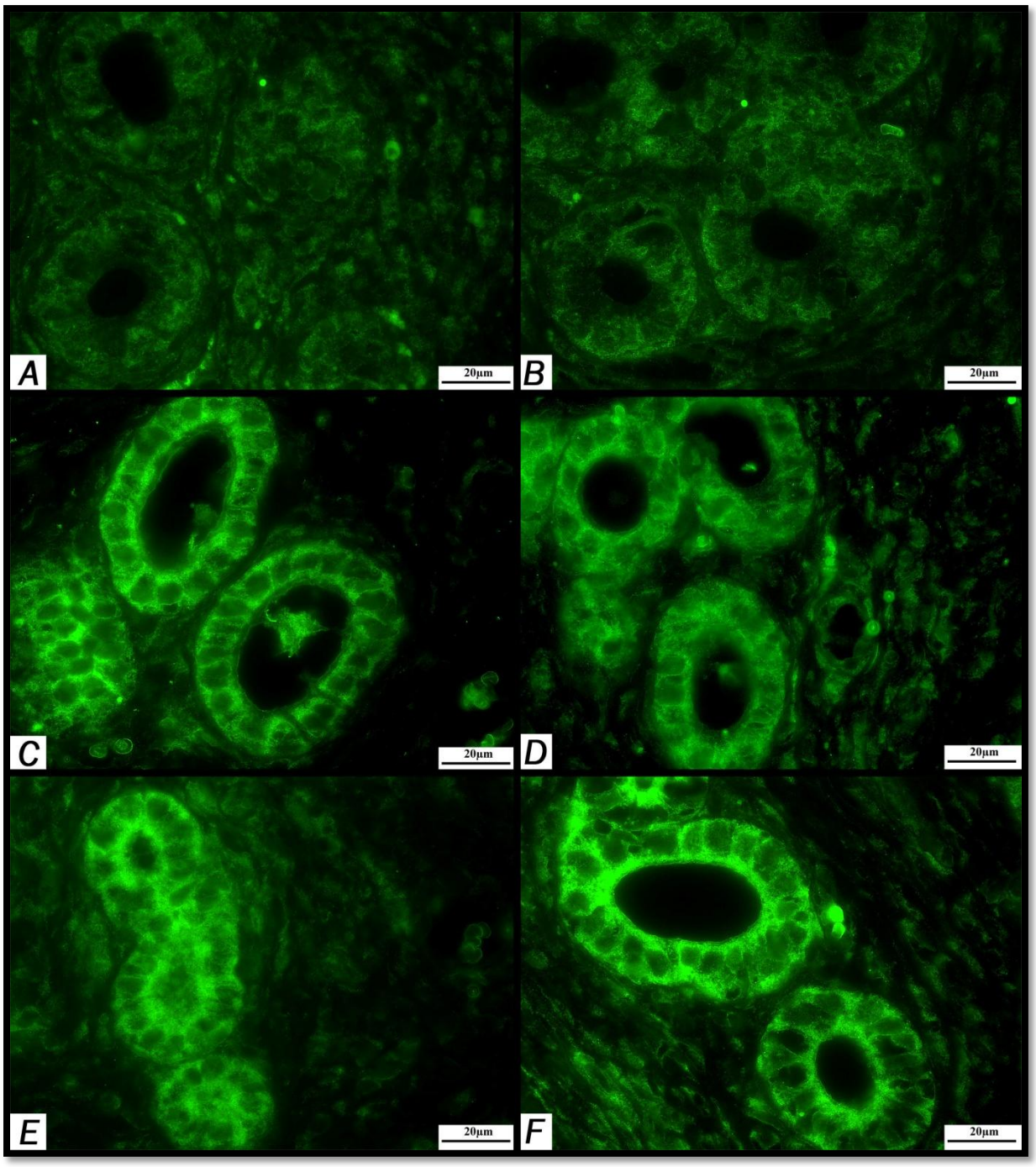
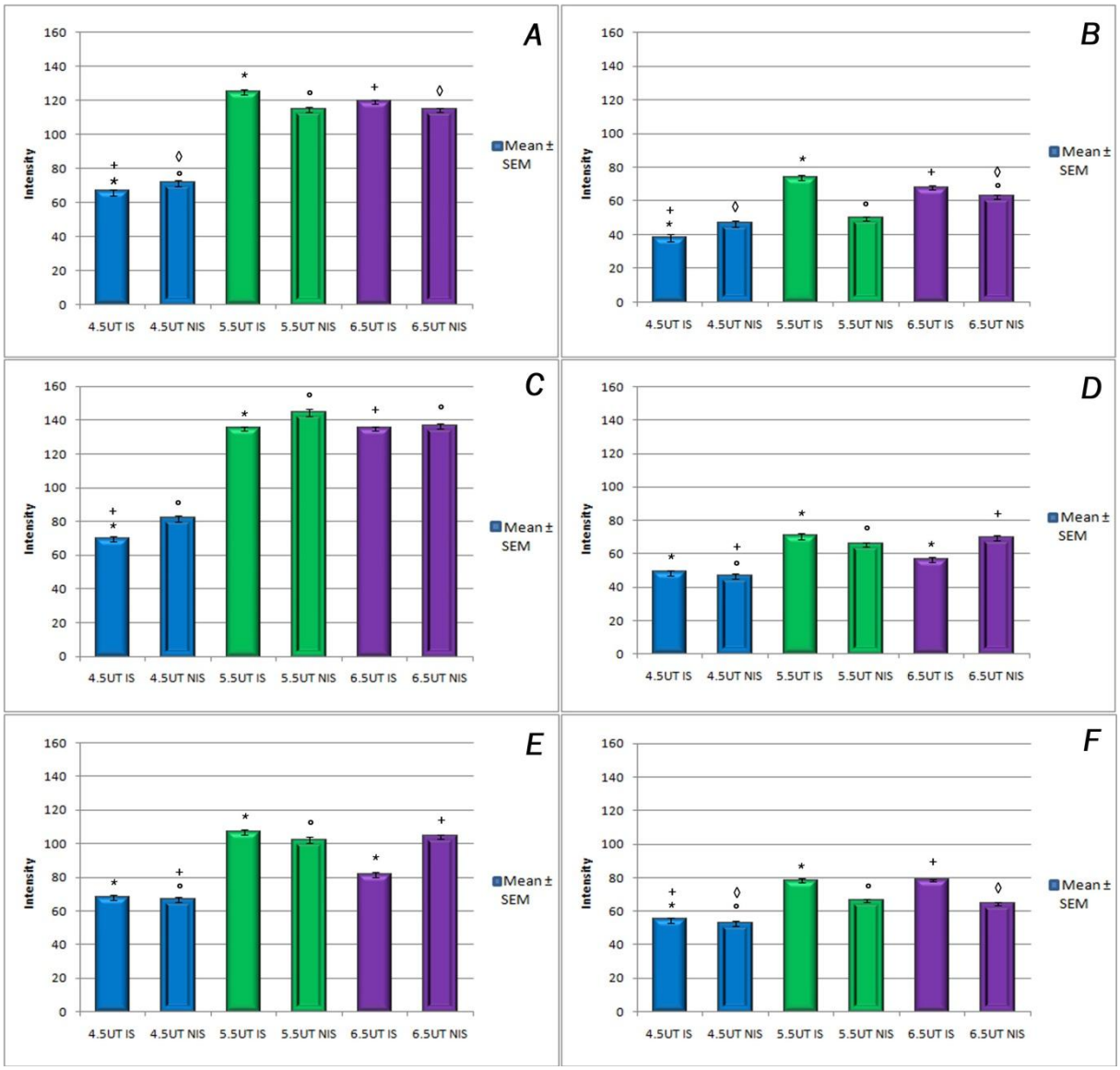


Figure 6.3 Immunofluorescent images illustrating VEGF protein localisation in the glandular epithelium and the glandular stroma of the implantation and non-implantation sites in the uteri of control pregnant rats. A: Implantation site at day 4.5 of pregnancy, **B:** Non-implantation site at day 4.5 of pregnancy, **C:** Implantation site at day 5.5 of pregnancy, **D:** Non-implantation site at day 5.5 of pregnancy, **E:** Implantation site at day 6.5 of pregnancy, **F:** Non-implantation site at day 6.5 of pregnancy. Scale = 20µm.



Graph 6.2 Graphical representation of the Mean ± SEM of bFGF protein expression in the luminal epithelium (A), the subepithelial stroma (B), the glandular epithelium (C), the glandular stroma (D), the blood vessels (E) and the stroma surrounding the blood vessels (F) of the implantation (IS) and non-implantation (NIS) sites in day 4.5, day 5.5 and day 6.5 pregnant rat uteri treated with vehicle (UT) at day 3.0 of pregnancy, as obtained from image analysis of fluorescent intensities. *, °, +, ◊ = significantly different ($p \leq 0.05$) using the Tukey-Kramer *post hoc* analysis.

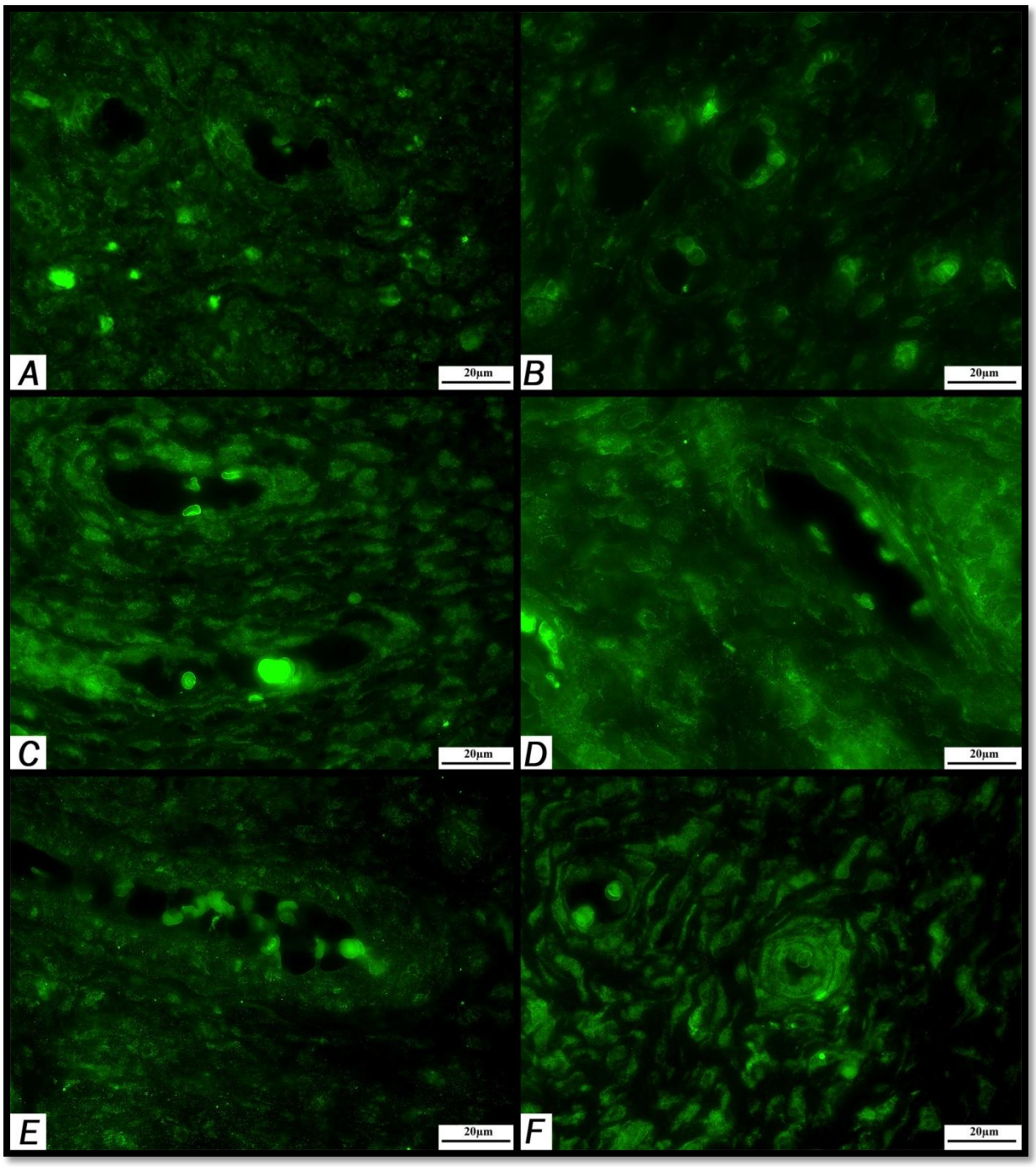


Figure 6.4 Immunofluorescent images illustrating VEGF protein localisation in the blood vessels and the stroma surrounding the blood vessels of the implantation and non-implantation sites in the uteri of control pregnant rats. A: Implantation site at day 4.5 of pregnancy, **B:** Non-implantation site at day 4.5 of pregnancy, **C:** Implantation site at day 5.5 of pregnancy, **D:** Non-implantation site at day 5.5 of pregnancy, **E:** Implantation site at day 6.5 of pregnancy, **F:** Non-implantation site at day 6.5 of pregnancy. Scale = 20µm.

6.2.1.2 The effects of RU486 on VEGF and bFGF protein spatiotemporal expression patterns

Treatment with RU486 significantly decreased VEGF protein levels in all the endometrial compartments of the implantation sites, except in the luminal epithelium at day 4.5 of pregnancy (Graph 6.5A-F; Figure 6.2A; Figure 6.3A; Figure 6.4A; Figure 6.8A; Figure 6.9A; Figure 6.10A; Table 6.1). In the non-implantation sites, VEGF protein levels were only significantly decreased in the luminal epithelium, the subepithelial stroma and the glandular epithelium at day 4.5 of pregnancy (Graph 6.5A-F; Figure 6.2B; Figure 6.3B; Figure 6.4B; Figure 6.8B; Figure 6.9B; Figure 6.10; Table 6.1). By day 5.5 of pregnancy, VEGF protein levels in both the implantation and non-implantation sites had increased significantly in the control pregnant animals; however, RU486 inhibited this increase in all endometrial compartments analysed (Graph 6.5A-F; Figure 6.2C and D; Figure 6.3C and D; Figure 6.4C and D; Figure 6.8C and D; Figure 6.9C and D; Figure 6.10C and D; Table 6.1). At day 6.5 of pregnancy, VEGF protein expression remained constant in the RU486-treated animals, so VEGF protein levels were significantly lower in all endometrial compartments of both the implantation and non-implantation sites, relative to the control pregnant animals, as a result of treatment with RU486 (Graph 6.3A-F; Graph 6.5A-F; Figure 6.2E and F; Figure 6.3E and F; Figure 6.4E and F; Figure 6.8E and F; Figure 6.9E and F; Figure 6.10E and F; Table 6.1).

This was also true for bFGF protein levels, where the increase in bFGF expression at day 5.5 of pregnancy in both the implantation and non-implantation sites of the control pregnant animals was inhibited by RU486 (Graph 6.6A-F; Figure 6.5C and D; Figure 6.6C and D; Figure 6.7C and D; Figure 6.11C and D; Figure 6.12C and D; Figure 6.13C and D; Table 6.2). Basic FGF protein levels in all endometrial compartments of both the implantation and non-implantation sites were significantly reduced by RU486 at all three days of pregnancy (Graph 6.4A-F; Graph 6.6A-F; Figure 6.5A-F; Figure 6.6A-F; Figure 6.7A-F; Figure 6.11A-F; Figure 6.12A-F; Figure 6.13A-F; Table 6.2). The overall increase in bFGF protein levels in the RU486-treated animals as pregnancy progressed from day 4.5 through to day 6.5 was not sufficient to close the gap between the bFGF protein levels in the drug-treated and control pregnant animals (Graph 6.4A-F; Graph 6.6A-F; Figure 6.5A-F; Figure 6.6A-F; Figure 6.7A-F; Figure 6.11A-F; Figure 6.12A-F; Figure 6.13A-F; Table 6.2)..

In summary, RU486 inhibited the increase in VEGF and bFGF protein expression observed in the implantation and non-implantation sites of the control pregnant animals at days 5.5 and 6.5 of pregnancy.

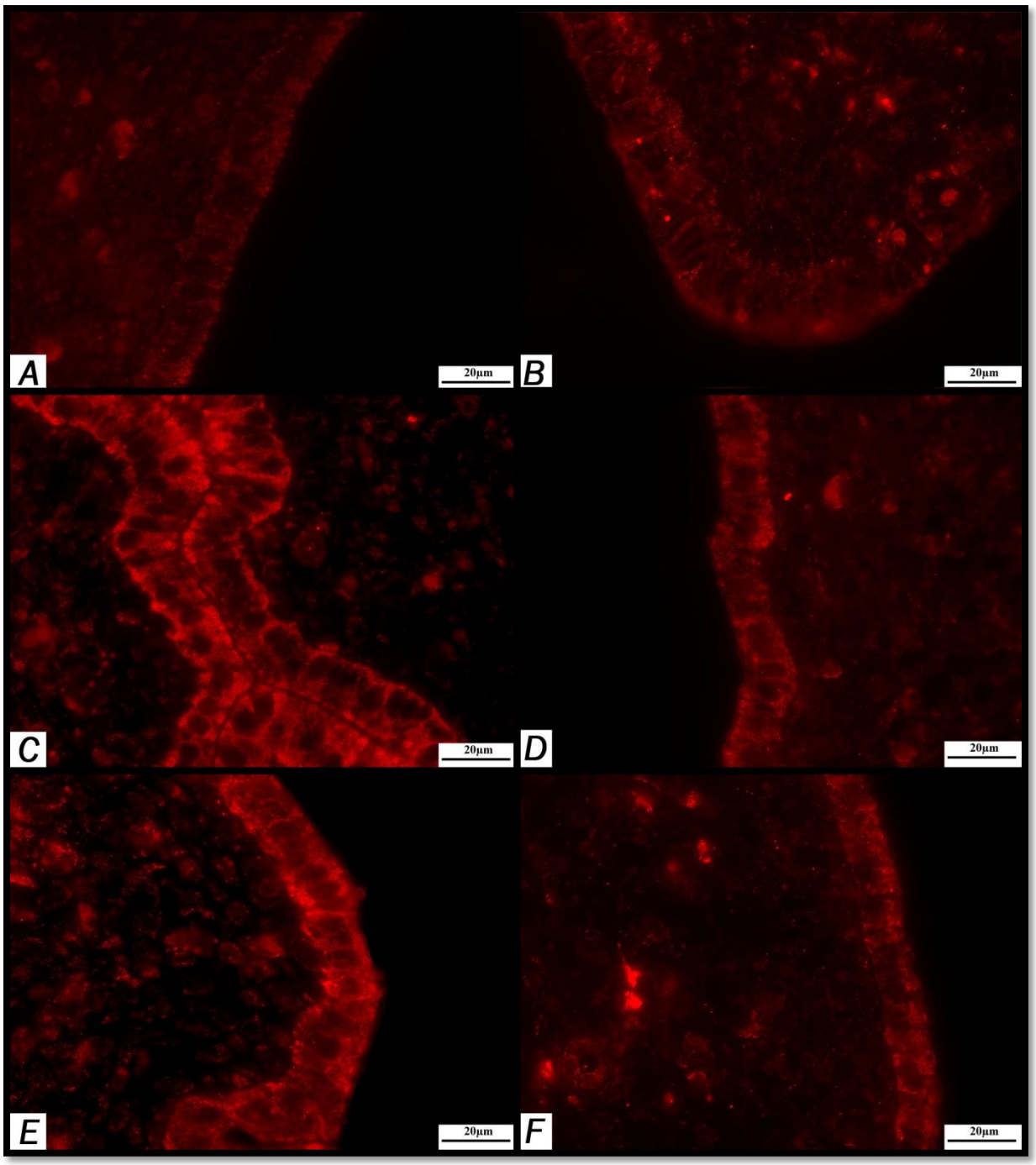
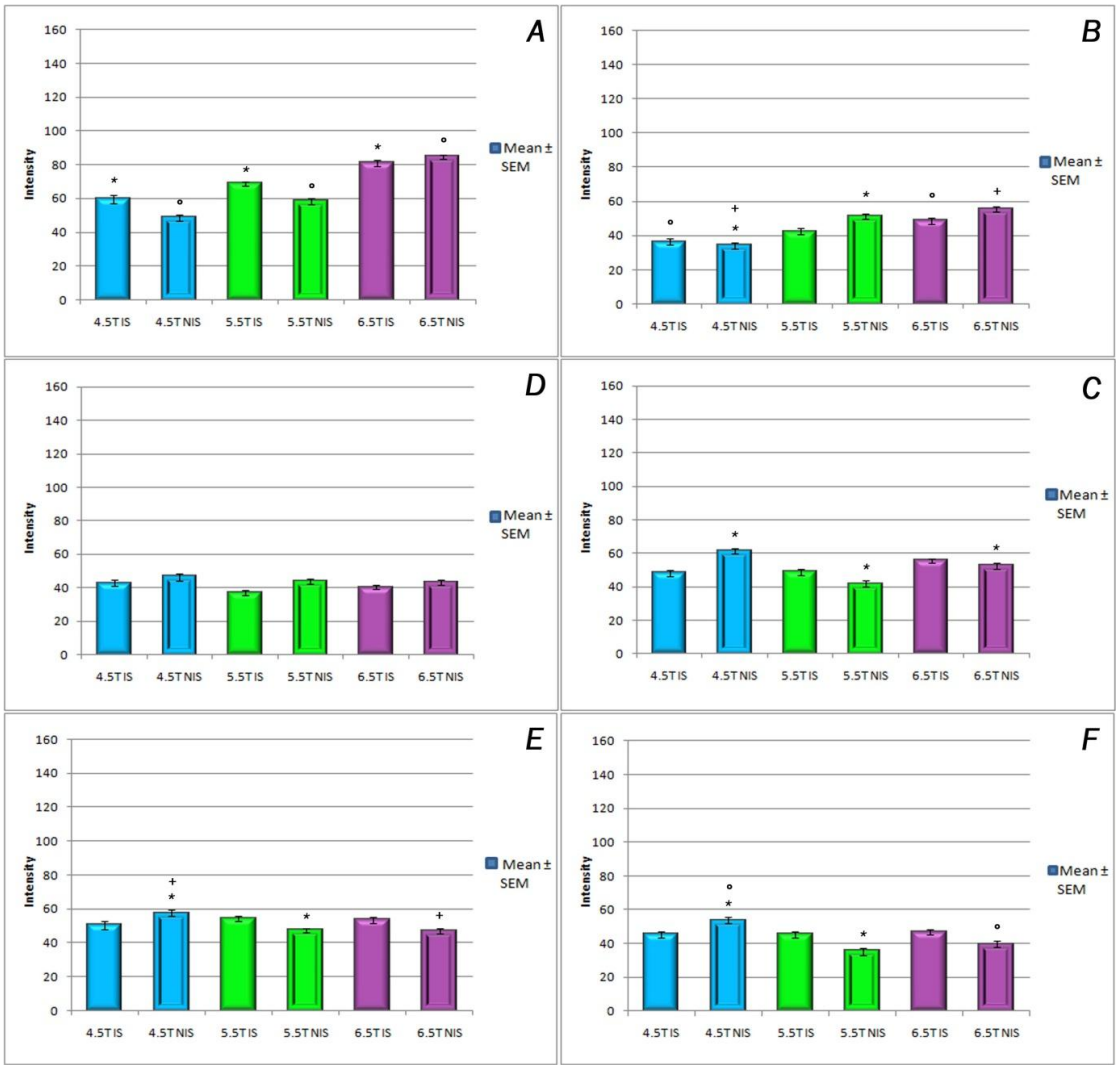


Figure 6.5 Immunofluorescent images illustrating bFGF protein localisation in the luminal epithelium and the subepithelial stroma of the implantation and non-implantation sites in the uteri of control pregnant rats. A: Implantation site at day 4.5 of pregnancy, **B:** Non-implantation site at day 4.5 of pregnancy, **C:** Implantation site at day 5.5 of pregnancy, **D:** Non-implantation site at day 5.5 of pregnancy, **E:** Implantation site at day 6.5 of pregnancy, **F:** Non-implantation site at day 6.5 of pregnancy. Scale = 20µm.



Graph 6.3 Graphical representation of the Mean ± SEM of VEGF protein expression in the luminal epithelium (A), the subepithelial stroma (B), the glandular epithelium (C), the glandular stroma (D), the blood vessels (E) and the stroma surrounding the blood vessels (F) of the implantation (IS) and non-implantation (NIS) sites in day 4.5, day 5.5 and day 6.5 pregnant rat uteri treated with RU486 (T) at day 3.0 of pregnancy, as obtained from image analysis of fluorescent intensities. *, °, + = significantly different ($p \leq 0.05$) using the Tukey-Kramer *post hoc* analysis.

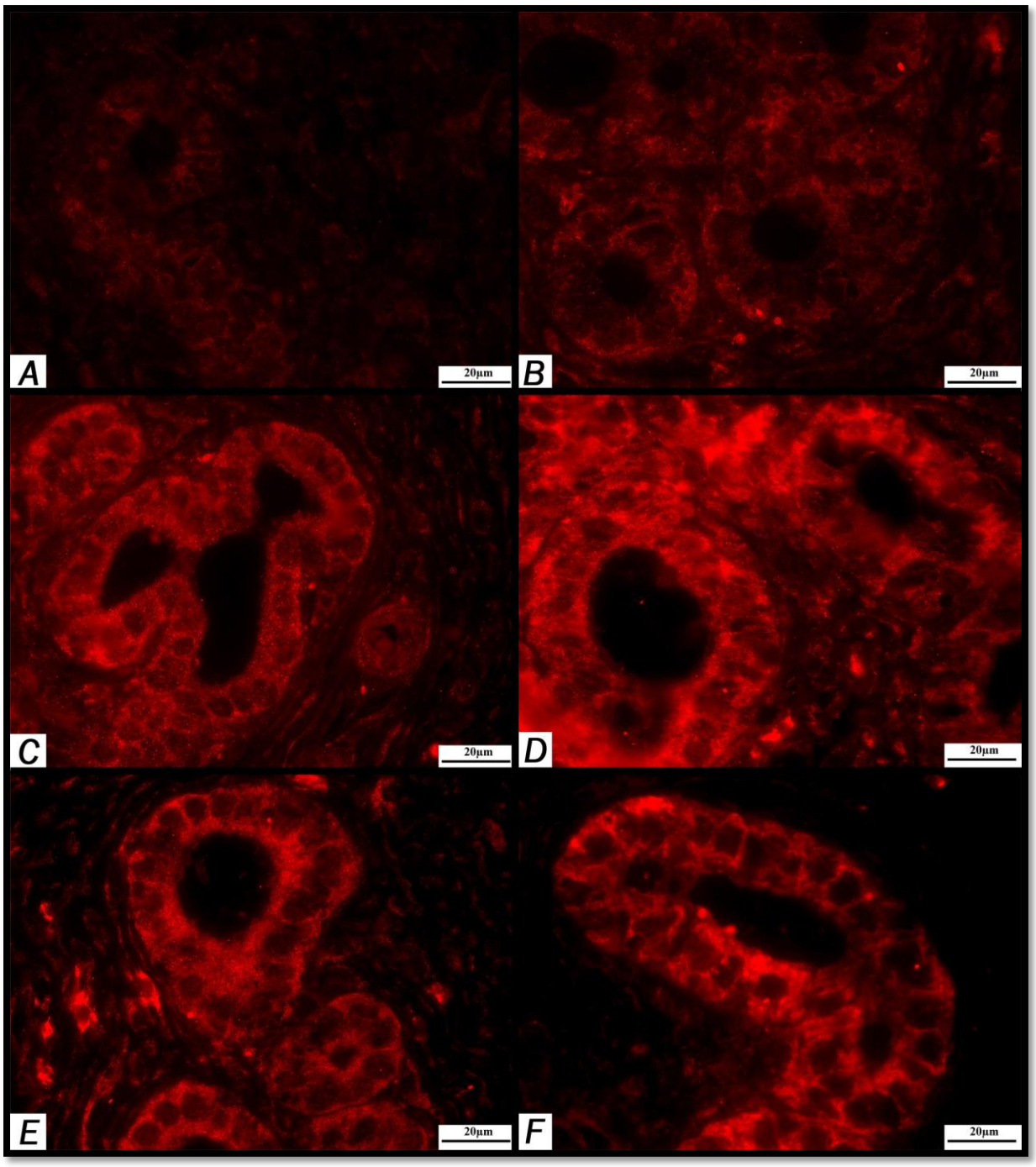
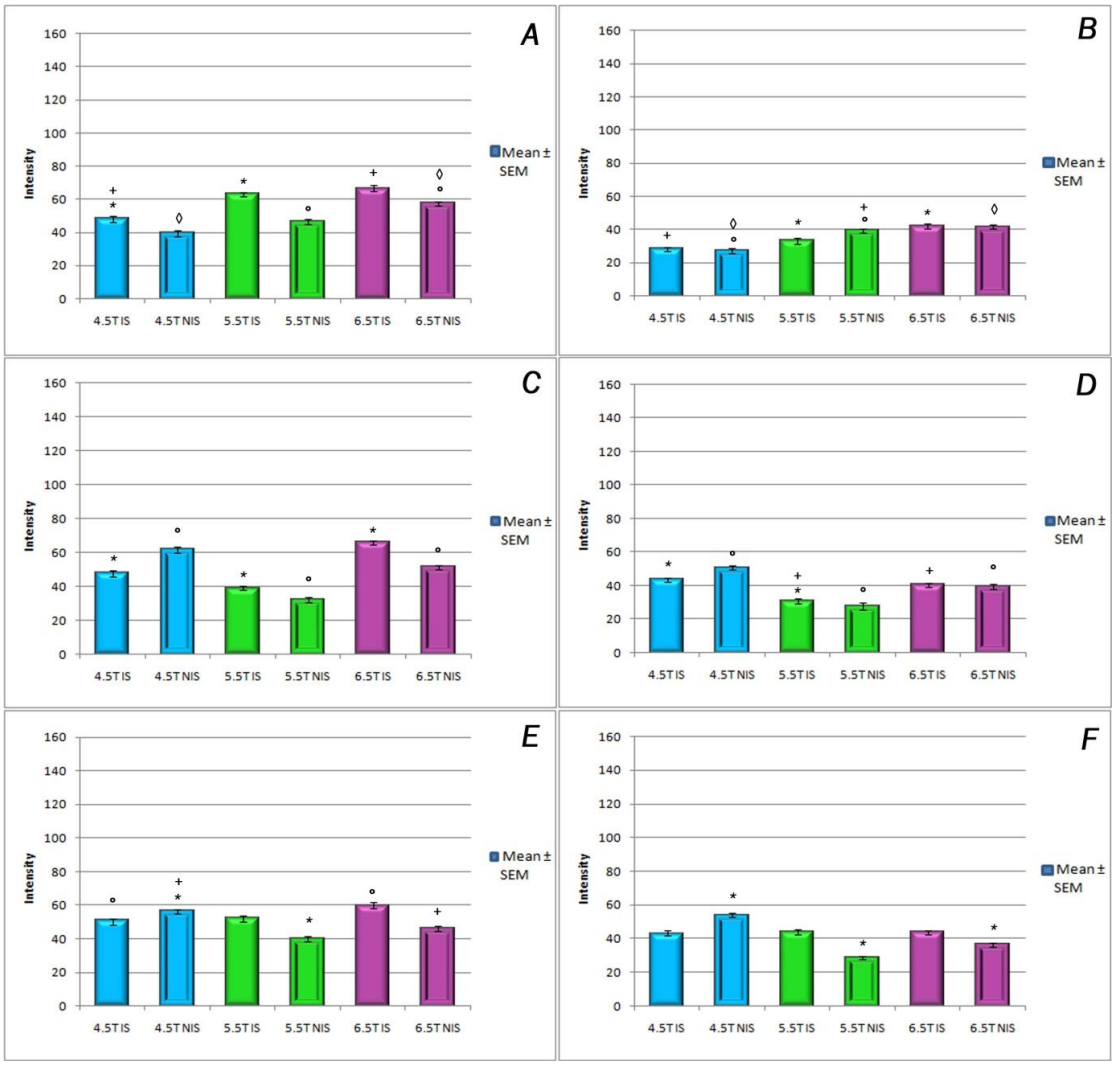


Figure 6.6 Immunofluorescent images illustrating bFGF protein localisation in the glandular epithelium and the glandular stroma of the implantation and non-implantation sites in the uteri of control pregnant rats. A: Implantation site at day 4.5 of pregnancy, **B:** Non-implantation site at day 4.5 of pregnancy, **C:** Implantation site at day 5.5 of pregnancy, **D:** Non-implantation site at day 5.5 of pregnancy, **E:** Implantation site at day 6.5 of pregnancy, **F:** Non-implantation site at day 6.5 of pregnancy. Scale = 20µm.



Graph 6.4 Graphical representation of the Mean ± SEM of bFGF protein expression in the luminal epithelium (A), the subepithelial stroma (B), the glandular epithelium (C), the glandular stroma (D), the blood vessels (E) and the stroma surrounding the blood vessels (F) of the implantation (IS) and non-implantation (NIS) sites in day 4.5, day 5.5 and day 6.5 pregnant rat uteri treated with RU486 (T) at day 3.0 of pregnancy, as obtained from image analysis of fluorescent intensities. *, °, +, ◊ = significantly different ($p \leq 0.05$) using the Tukey-Kramer *post hoc* analysis.

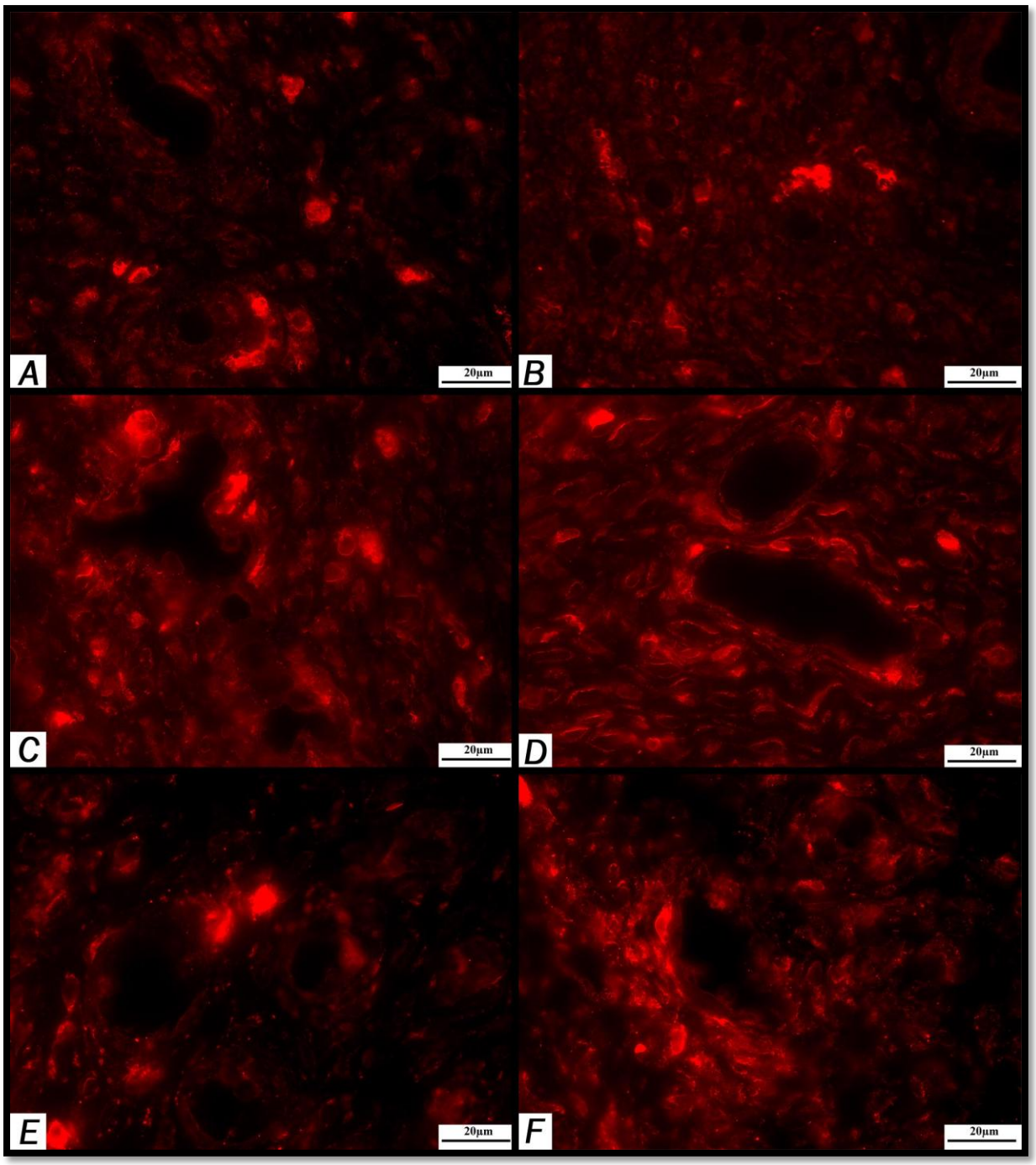
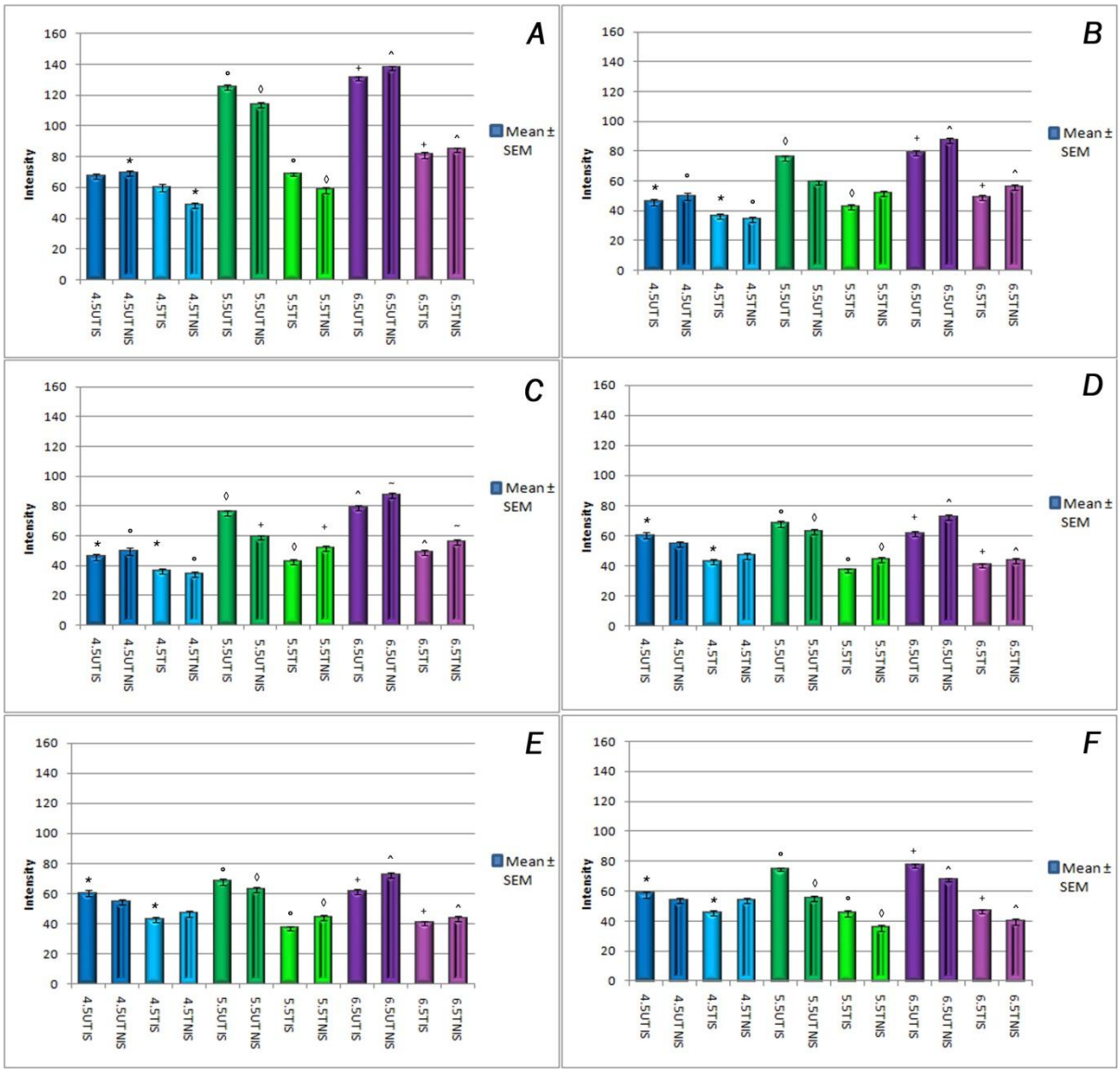


Figure 6.7 Immunofluorescent images illustrating bFGF protein localisation in the blood vessels and the stroma surrounding the blood vessels of the implantation and non-implantation sites in the uteri of control pregnant rats. A: Implantation site at day 4.5 of pregnancy, **B:** Non-implantation site at day 4.5 of pregnancy, **C:** Implantation site at day 5.5 of pregnancy, **D:** Non-implantation site at day 5.5 of pregnancy, **E:** Implantation site at day 6.5 of pregnancy, **F:** Non-implantation site at day 6.5 of pregnancy. Scale = 20µm.



Graph 6.5 Graphical representation of the Mean ± SEM of VEGF protein expression in the luminal epithelium (A), the subepithelial stroma (B), the glandular epithelium (C), the glandular stroma (D), the blood vessels (E) and the stroma surrounding the blood vessels (F) of the implantation (IS) and non-implantation (NIS) sites in day 4.5, day 5.5 and day 6.5 pregnant rat uteri treated with vehicle (UT) or RU486 (T) at day 3.0 of pregnancy, as obtained from image analysis of fluorescent intensities. *, °, +, ◊, ^,~ = significantly different ($p \leq 0.05$) using the Tukey-Kramer *post hoc* analysis.

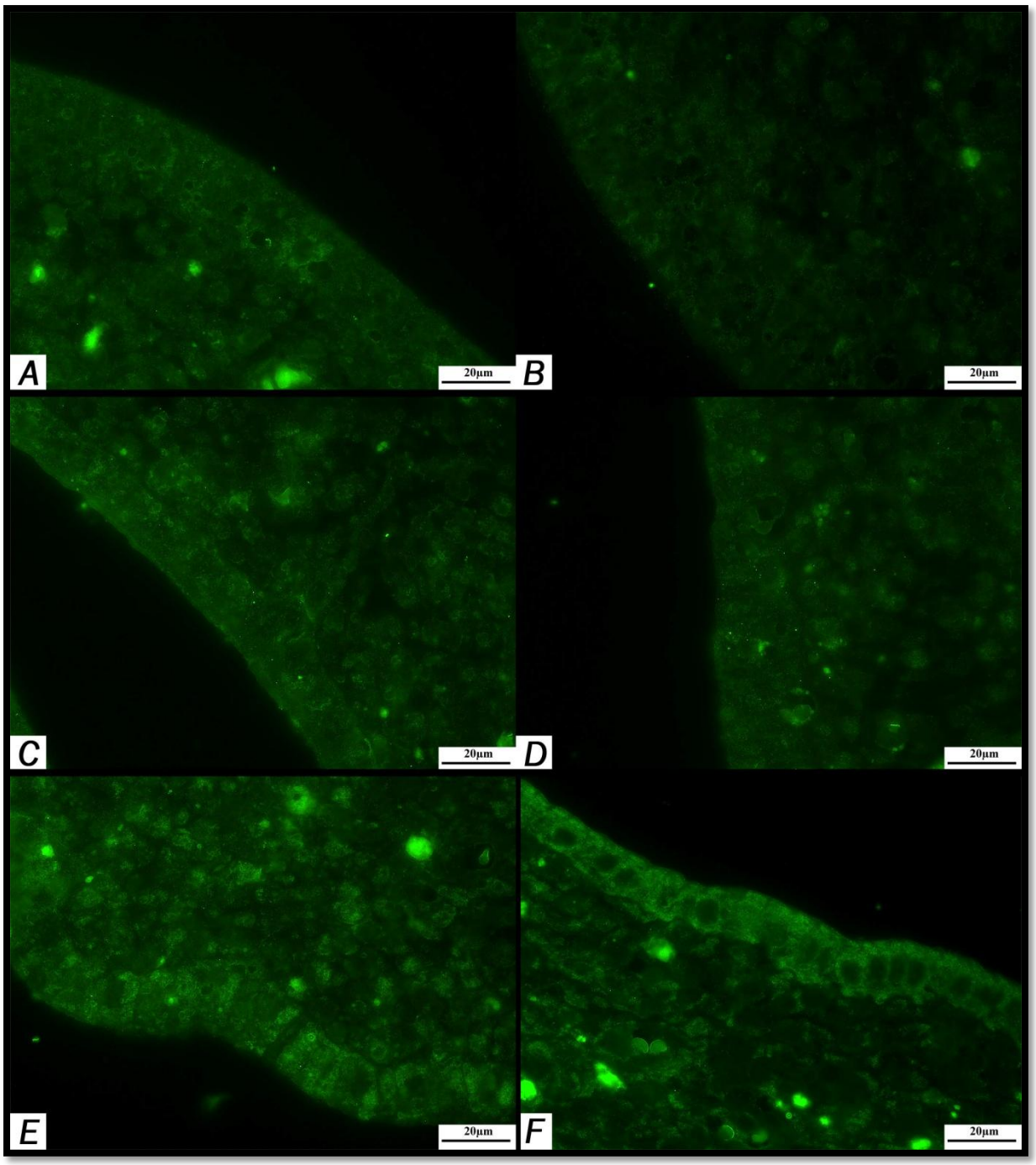
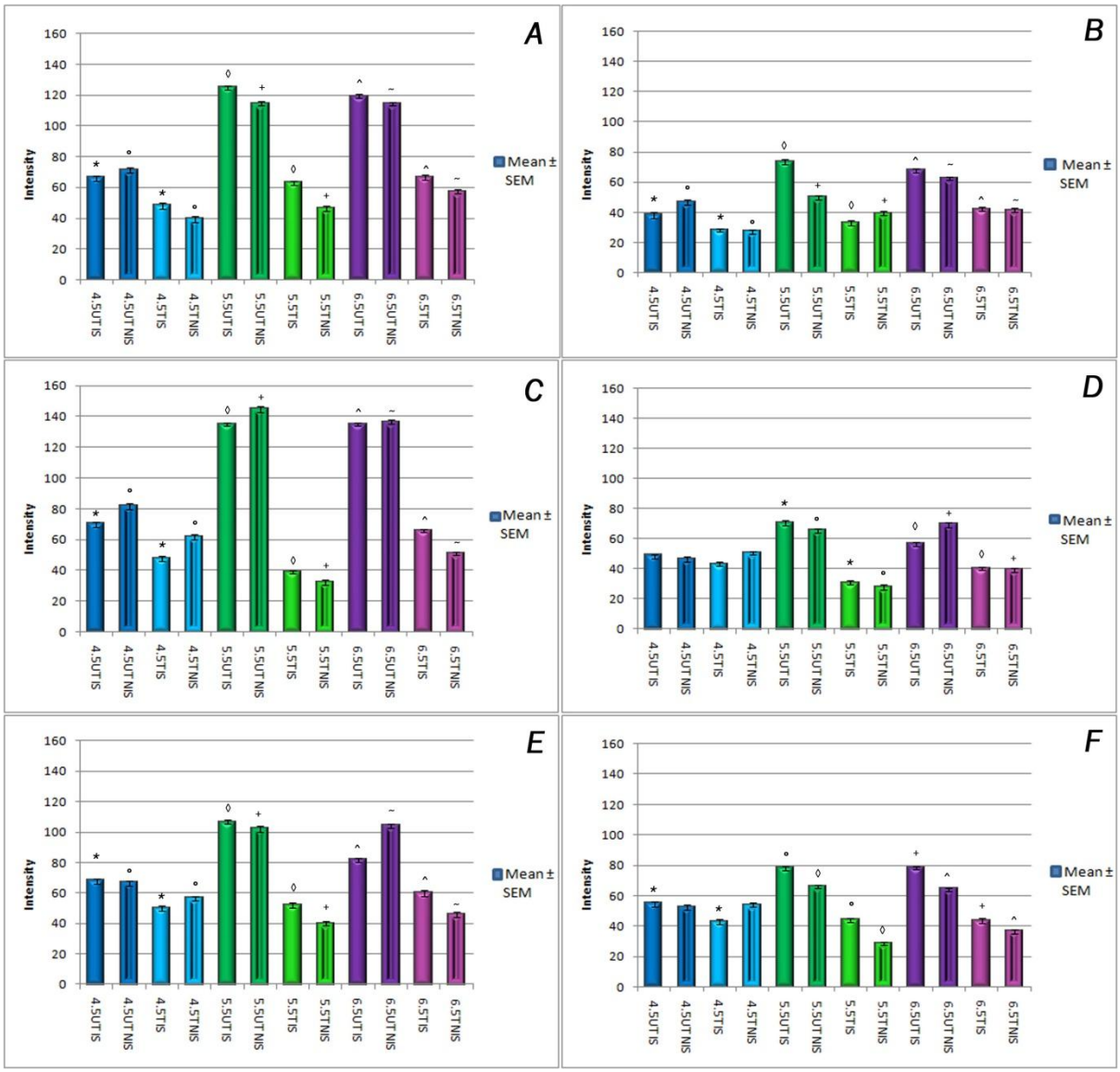


Figure 6.8 Immunofluorescent images illustrating VEGF protein localisation in the luminal epithelium and the subepithelial stroma of the implantation and non-implantation sites in the uteri of RU486-treated pregnant rats. A: Implantation site at day 4.5 of pregnancy, **B:** Non-implantation site at day 4.5 of pregnancy, **C:** Implantation site at day 5.5 of pregnancy, **D:** Non-implantation site at day 5.5 of pregnancy, **E:** Implantation site at day 6.5 of pregnancy, **F:** Non-implantation site at day 6.5 of pregnancy. Scale = 20µm.



Graph 6.6 Graphical representation of the Mean ± SEM of bFGF protein expression in the luminal epithelium (A), the subepithelial stroma (B), the glandular epithelium (C), the glandular stroma (D), the blood vessels (E) and the stroma surrounding the blood vessels (F) of the implantation (IS) and non-implantation (NIS) sites in day 4.5, day 5.5 and day 6.5 pregnant rat uteri treated with vehicle (UT) or RU486 (T) at day 3.0 of pregnancy, as obtained from image analysis of fluorescent intensities. *, °, +, ◊, ^,~ = significantly different ($p \leq 0.05$) using the Tukey-Kramer *post hoc* analysis.

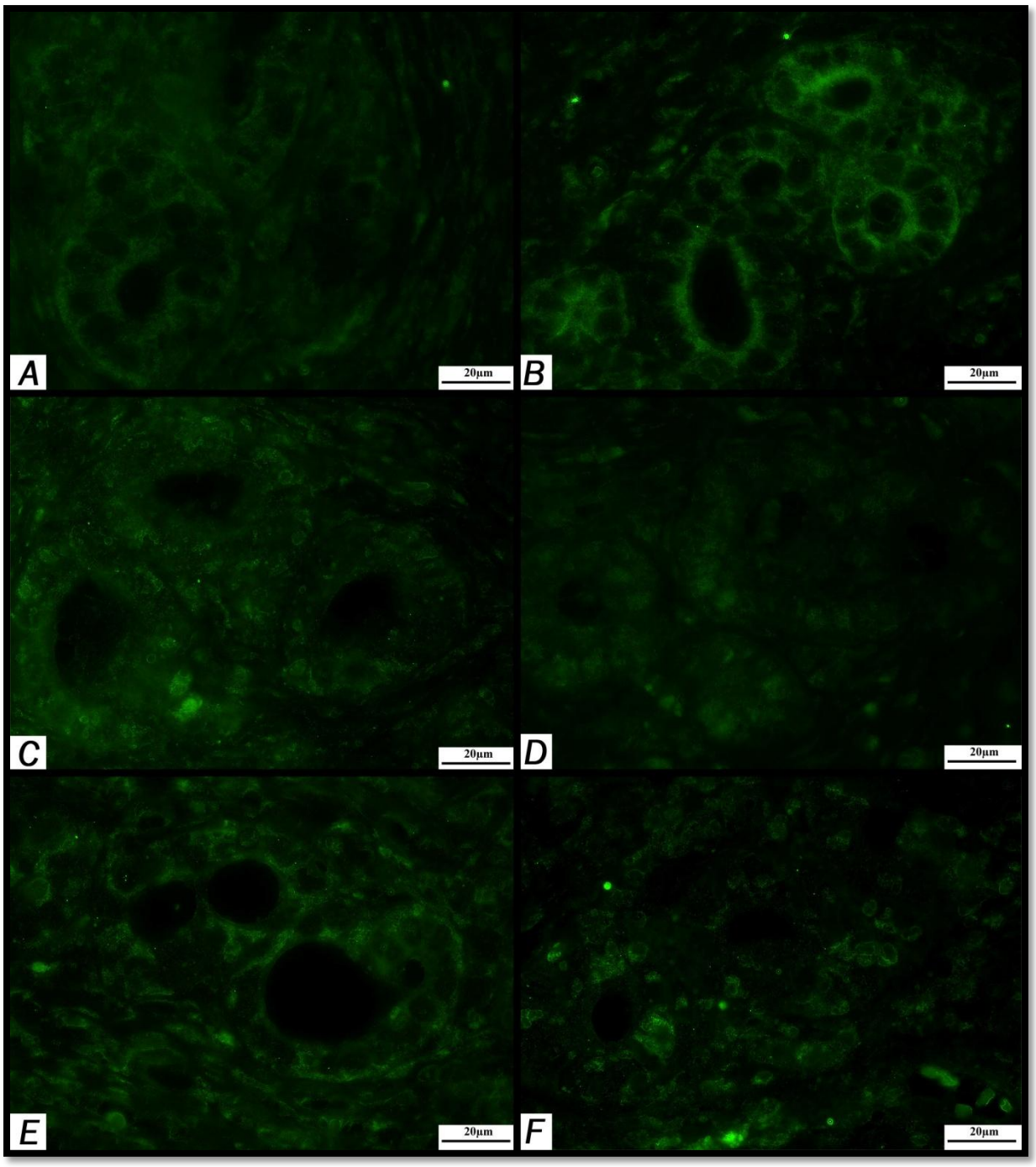


Figure 6.9 Immunofluorescent images illustrating VEGF protein localisation in the glandular epithelium and the glandular stroma of the implantation and non-implantation sites in the uteri of RU486-treated pregnant rats. A: Implantation site at day 4.5 of pregnancy, **B:** Non-implantation site at day 4.5 of pregnancy, **C:** Implantation site at day 5.5 of pregnancy, **D:** Non-implantation site at day 5.5 of pregnancy, **E:** Implantation site at day 6.5 of pregnancy, **F:** Non-implantation site at day 6.5 of pregnancy. Scale = 20µm.

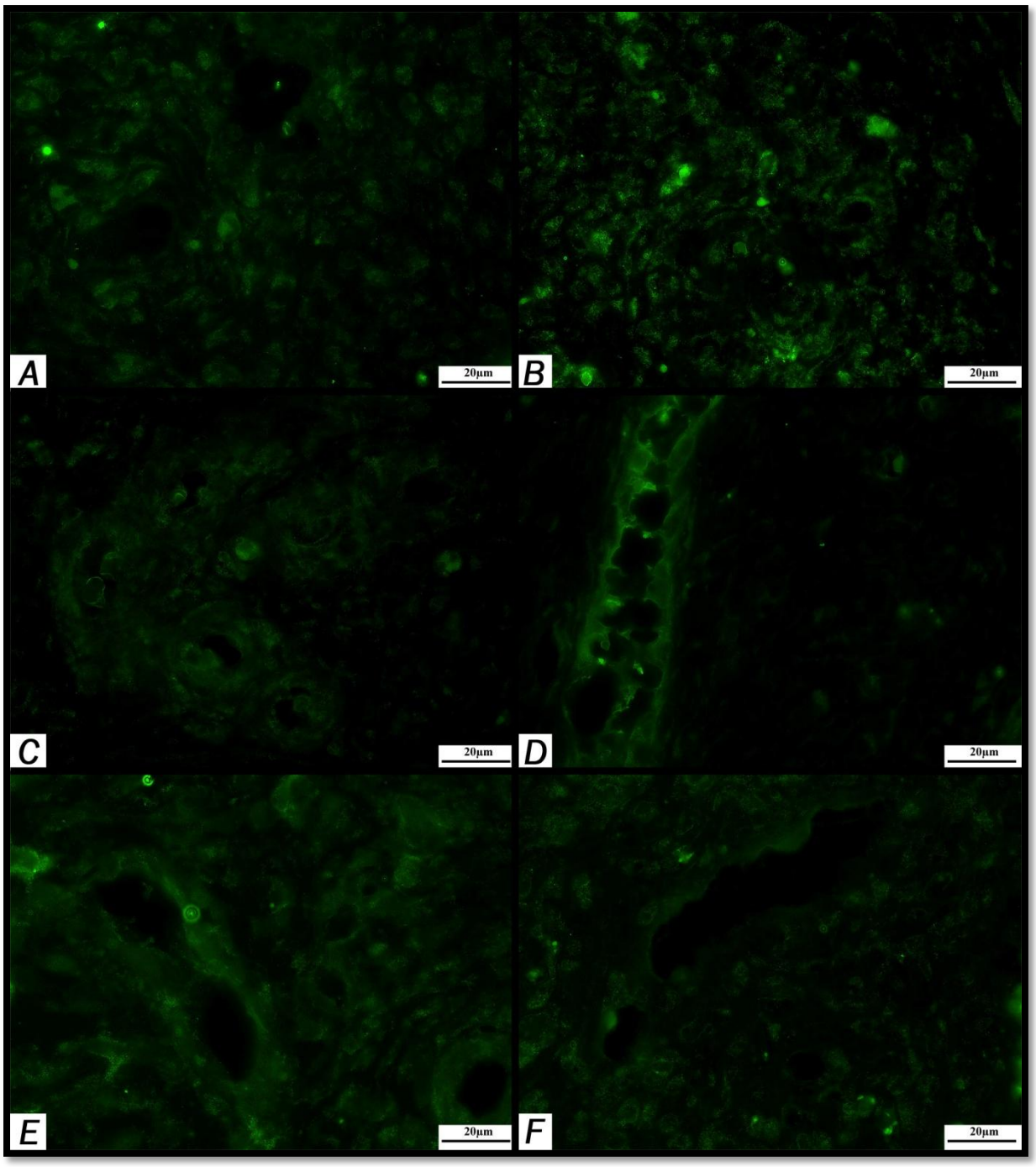


Figure 6.10 Immunofluorescent images illustrating VEGF protein localisation in the blood vessels and the stroma surrounding the blood vessels of the implantation and non-implantation sites in the uteri of RU486-treated pregnant rats. A: Implantation site at day 4.5 of pregnancy, **B:** Non-implantation site at day 4.5 of pregnancy, **C:** Implantation site at day 5.5 of pregnancy, **D:** Non-implantation site at day 5.5 of pregnancy, **E:** Implantation site at day 6.5 of pregnancy, **F:** Non-implantation site at day 6.5 of pregnancy. Scale = 20µm.

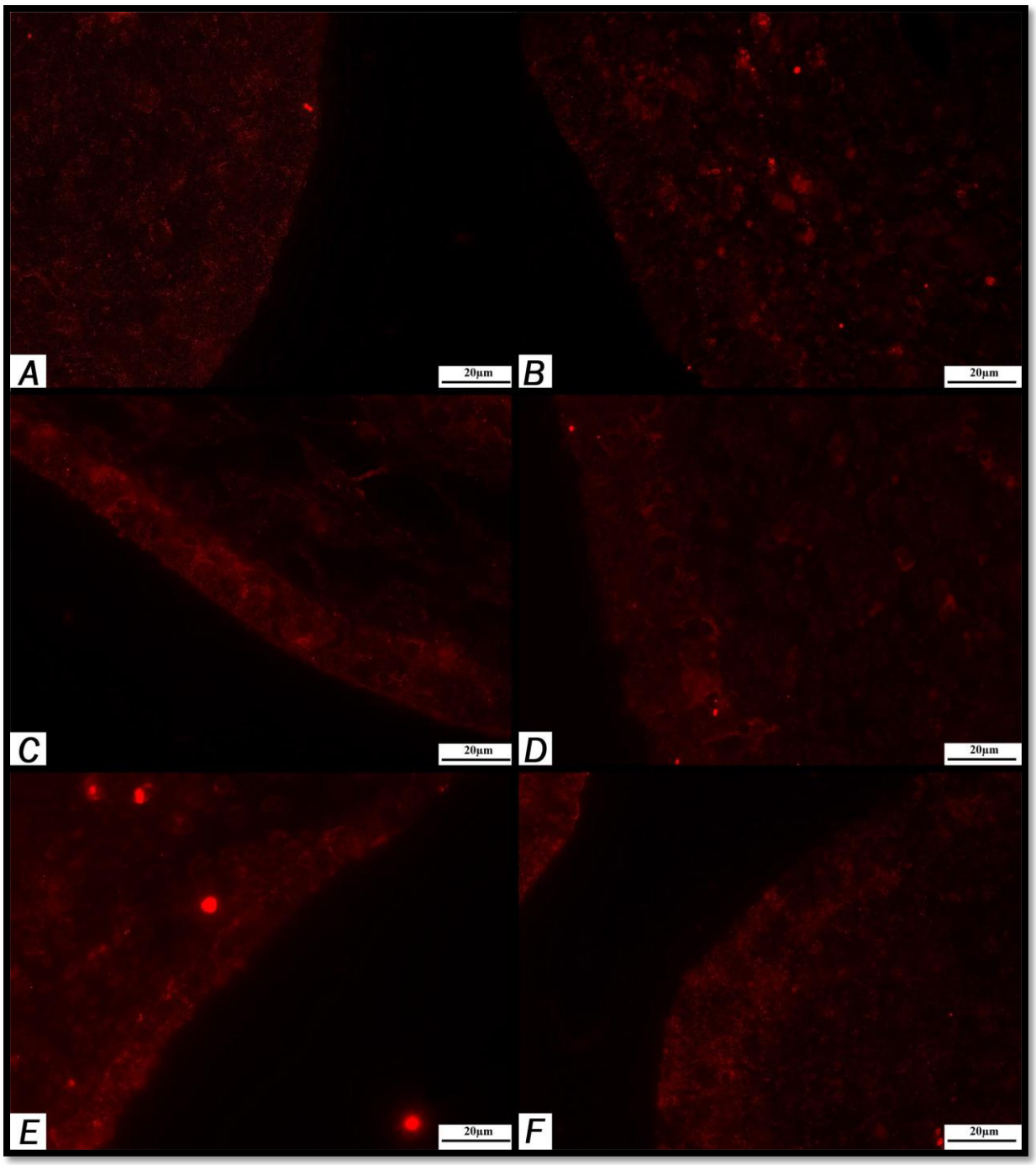


Figure 6.11 Immunofluorescent images illustrating bFGF protein localisation in the luminal epithelium and the subepithelial stroma of the implantation and non-implantation sites in the uteri of RU486-treated pregnant rats. A: Implantation site at day 4.5 of pregnancy, **B:** Non-implantation site at day 4.5 of pregnancy, **C:** Implantation site at day 5.5 of pregnancy, **D:** Non-implantation site at day 5.5 of pregnancy, **E:** Implantation site at day 6.5 of pregnancy, **F:** Non-implantation site at day 6.5 of pregnancy. Scale = 20µm.

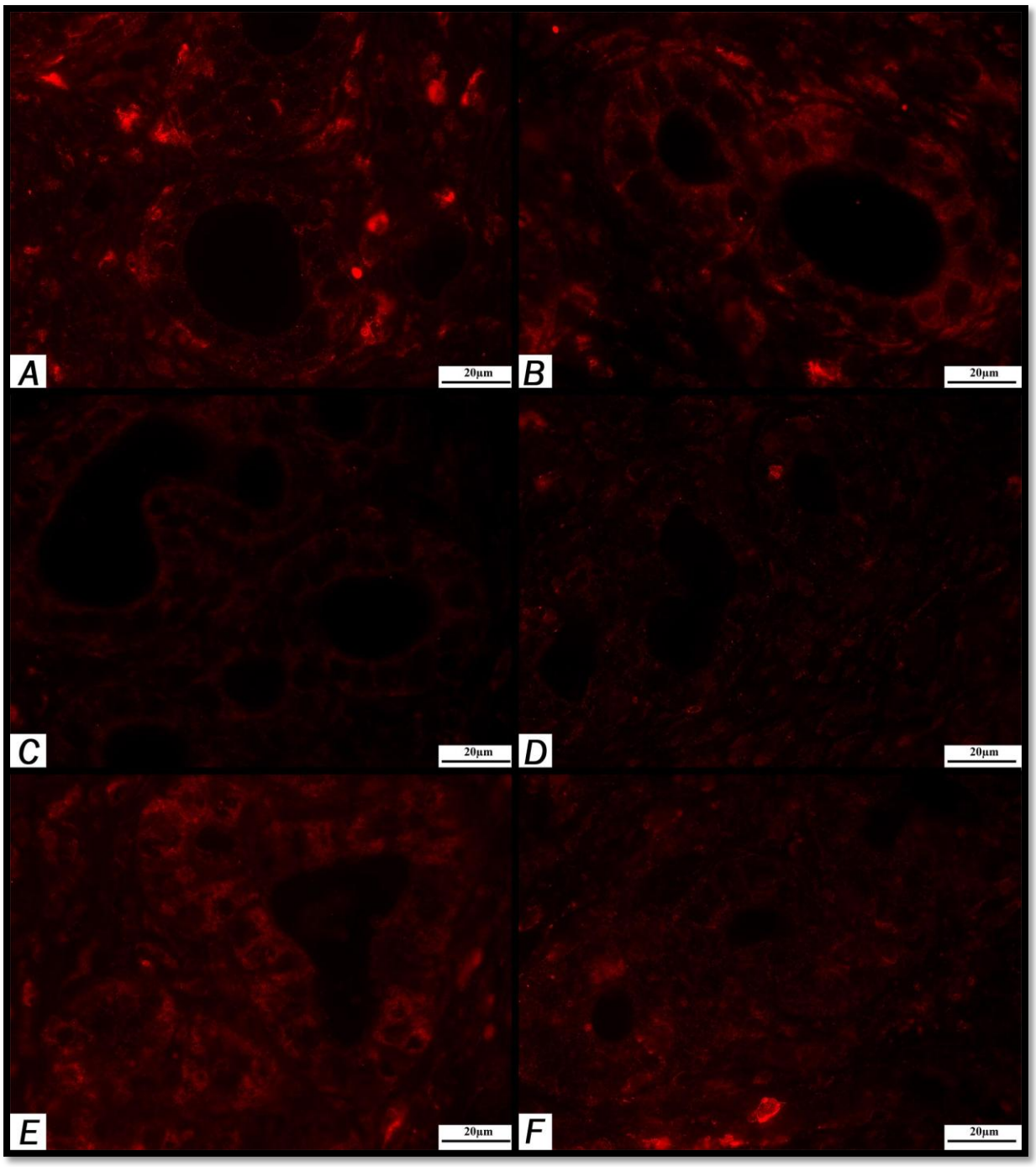


Figure 6.12 Immunofluorescent images illustrating bFGF protein localisation in the glandular epithelium and the glandular stroma of the implantation and non-implantation sites in the uteri of RU486-treated pregnant rats. A: Implantation site at day 4.5 of pregnancy, **B:** Non-implantation site at day 4.5 of pregnancy, **C:** Implantation site at day 5.5 of pregnancy, **D:** Non-implantation site at day 5.5 of pregnancy, **E:** Implantation site at day 6.5 of pregnancy, **F:** Non-implantation site at day 6.5 of pregnancy. Scale = 20µm.

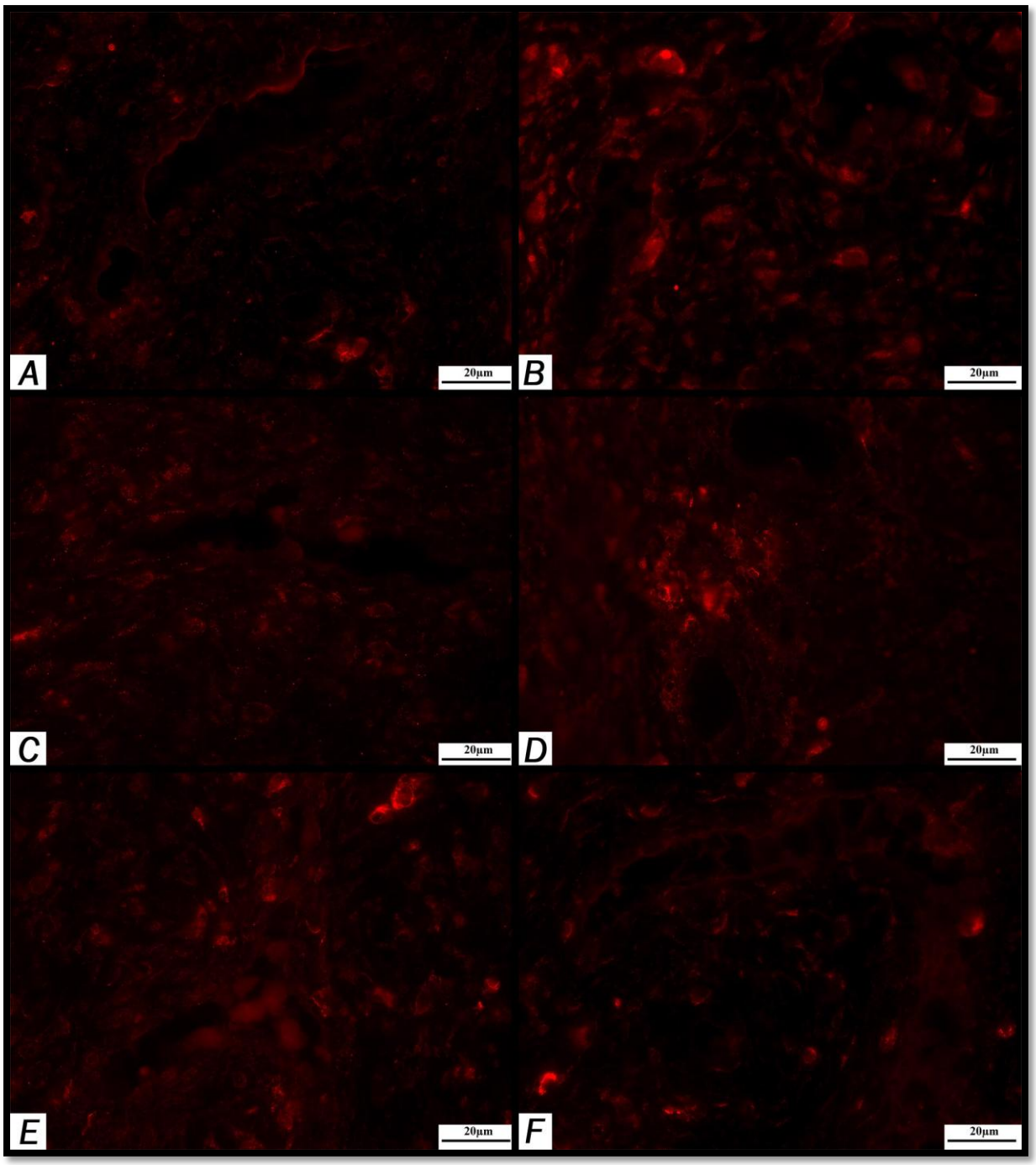


Figure 6.13 Immunofluorescent images illustrating bFGF protein localisation in the blood vessels and the stroma surrounding the blood vessels of the implantation and non-implantation sites in the uteri of RU486-treated pregnant rats. A: Implantation site at day 4.5 of pregnancy, **B:** Non-implantation site at day 4.5 of pregnancy, **C:** Implantation site at day 5.5 of pregnancy, **D:** Non-implantation site at day 5.5 of pregnancy, **E:** Implantation site at day 6.5 of pregnancy, **F:** Non-implantation site at day 6.5 of pregnancy. Scale = 20µm.

6.2.1.3 The spatiotemporal expression pattern of the PDGF protein within the control pregnant animals

The only similarities in PDGF expression relative to VEGF and bFGF expression was the increase in protein expression, observed in the implantation and non-implantation sites in the control pregnant animals at day 5.5 of pregnancy, of all three growth factors.

With the progression of pregnancy from day 4.5 to day 5.5, PDGF protein levels in the implantation sites were significantly increased within all the endometrial compartments analysed (Graph 6.7A-F; Figure 6.14A and C; Figure 6.15A and C; Figure 6.16A and C; Table 6.3). The increase in PDGF was highest in the glandular epithelium, followed by the blood vessels, the luminal epithelium, the subepithelial stroma and then the glandular stroma and that surrounding the blood vessels. In general, the increase in PDGF protein expression was more pronounced than that of VEGF and bFGF, with the exception of in the luminal epithelium where the increases in growth factor levels were similar. By day 6.5 of pregnancy, PDGF protein levels decreased significantly in all endometrial compartments analysed (Graph 6.7A-F; Figure 6.14E; Figure 6.15E; Figure 6.16E; Table 6.3).

In the non-implantation sites of the control pregnant animals, PDGF protein levels were significantly increased in all endometrial compartments inclusive of days 4.5 to 5.5 of pregnancy (Graph 6.7A-F; Figure 6.14B and D; Figure 6.15B and D; Figure 6.16B and D; Table 6.3). PDGF protein levels were highest in the luminal epithelium, followed by the glandular epithelium and the blood vessels. PDGF protein levels in the stromal compartments were fairly similar, but lower than that in the other compartments. As in the implantation sites, PDGF protein levels in the non-implantation sites decreased significantly in each endometrial compartment by day 6.5 of pregnancy (Graph 6.7A-F; Figure 6.14F; Figure 6.15F; Figure 6.16F; Table 6.3). PDGF protein levels were highest in the luminal epithelium, followed by the blood vessels, the glandular epithelium and lastly the stromal compartments, at this day of pregnancy.

At day 4.5 of pregnancy, PDGF levels while similar in the implantation and non-implantation sites, at day 5.5 of pregnancy, PDGF levels were markedly higher in all the endometrial compartments of the implantation sites relative to the non-implantation sites (Graph 6.7A-F; Figure 6.14A-D; Figure 6.15A-D; Figure 6.16A-D; Table 6.3). By day 6.5 of pregnancy, this drastic difference between the two areas was absent (Graph 6.7A-F; Figure 6.14E and F; Figure 6.15E and F; Figure 6.16E and F; Table 6.3).

Table 6.3 One-way ANOVA and Tukey Kramer *post hoc* analysis of PDGF protein expression in the luminal epithelium, the subepithelial stroma, the glandular epithelium, the glandular stroma, the blood vessels and the stroma surrounding the blood vessels of the implantation (IS) and non-implantation (NIS) sites between days 4.5, 5.5 and 6.5 of pregnancy in the control pregnant (UT) and RU486-treated (T) animals showing groups that are significantly different ($p \leq 0.05$). Groups not connected by the same letter are significantly different.

Group								Mean
Luminal Epithelium								
6.5T NIS	A							129.752
5.5UT IS	A							123.899
6.5T IS		B						105.213
5.5T IS		B						103.363
5.5T NIS		B						102.815
5.5UT NIS		B	C					99.555
4.5T NIS			C					93.346
4.5T IS				D				84.666
6.5UT NIS					E			72.879
6.5UT IS					E	F		65.465
4.5UT IS						F	G	63.408
4.5UT NIS							G	57.293
Subepithelial Stroma								
5.5UT IS	A							102.283
6.5T NIS		B						85.859
6.5T IS		B	C					80.874
5.5T IS		B	C					79.649
5.5T NIS			C					77.008
5.5UT NIS				D				66.543
4.5T NIS				D				66.221
6.5UT IS				D	E			60.71
4.5T IS					E	F		56.473
6.5UT NIS					E	F		55.849
4.5UT NIS						F	G	51.321
4.5UT IS							G	47.008
Glandular Epithelium								
5.5UT IS	A							156.248
6.5T IS		B						98.533
5.5UT NIS			C					90.34
5.5T NIS			C					87.146
5.5T IS			C					86.1
6.5T NIS			C					83.406
6.5UT IS				D				70.087
4.5T NIS					E			59.45
6.5UT NIS					E			58.704
4.5T IS					E	F		53.643
4.5UT NIS					E	F		52.398
4.5UT IS						F		48.516
Glandular Stroma								
5.5UT IS	A							97.5862
6.5T NIS			B					62.6283
5.5T NIS			B	C				59.4754
5.5T IS			B	C				56.6085
6.5T IS			B	C				56.0712
6.5UT IS				C				55.8448
5.5UT NIS				C				55.3819
4.5UT NIS						D		43.7333
6.5UT NIS						D		43.6979
4.5T NIS						D		43.0754
4.5UT IS						D		42.7083
4.5T IS						D		40.6083

Blood Vessels							
5.5UT IS	A						125.058
5.5T NIS		B					99.059
5.5T IS			C				90.618
5.5UT NIS				D			82.516
6.5T IS				D			82.486
6.5T NIS				D			82.086
6.5UT IS					E		69.555
4.5T NIS					E		69.418
6.5UT NIS					E		67.214
4.5T IS						F	57.647
4.5UT NIS						F	51.837
4.5UT IS						F	51.54
Stroma Surrounding the Blood Vessels							
5.5UT IS	A						103.545
6.5UT IS		B					70.372
5.5T NIS		B					68.649
6.5T IS		B	C				66.577
5.5UT NIS		B	C	D			65.834
6.5T NIS			C	D			60.102
5.5T IS				D			58.923
4.5T NIS						E	46.721
4.5UT IS						E	45.748
4.5T IS						E	43.781
6.5UT NIS						E	42.787
4.5UT NIS						E	41.477

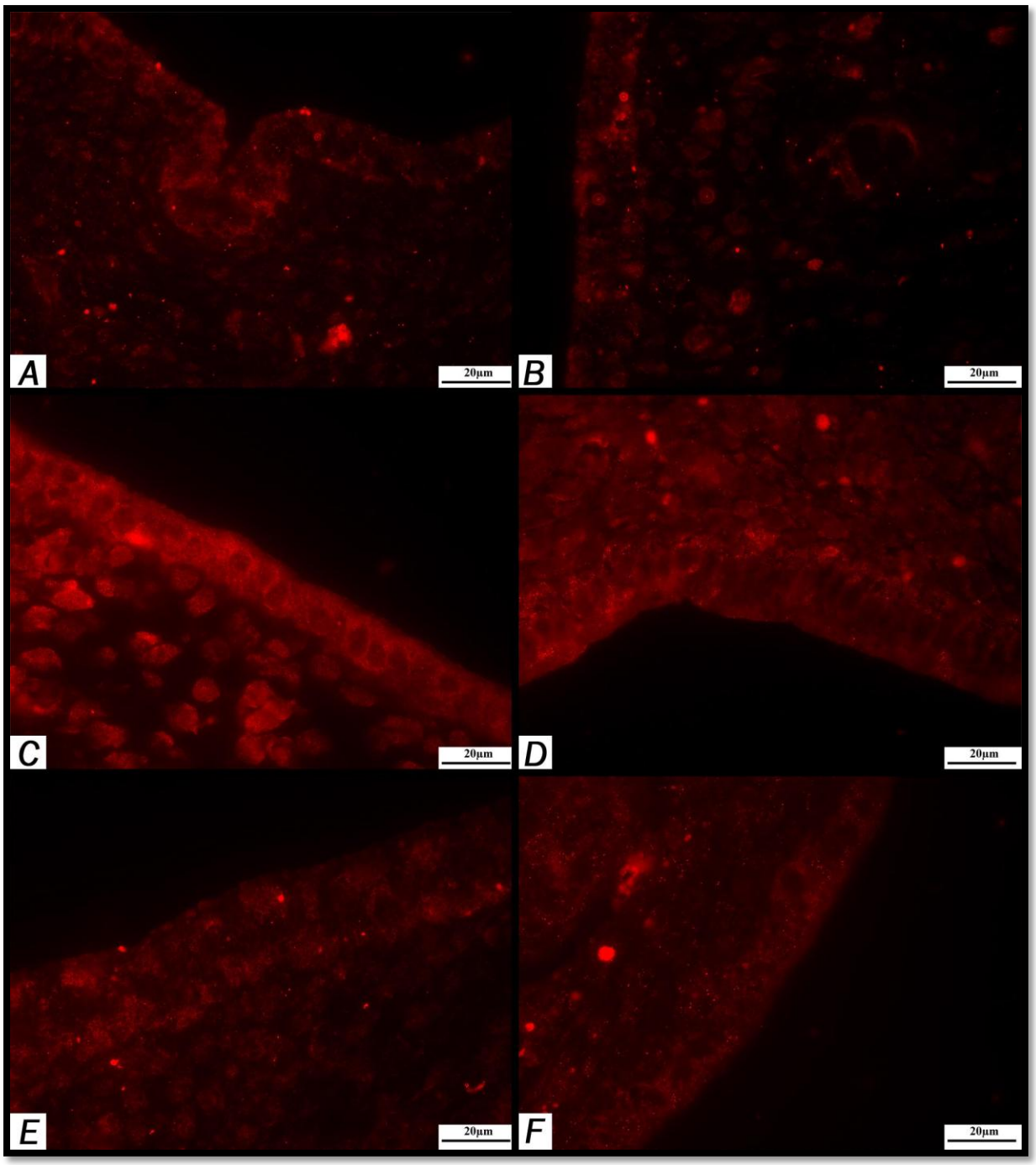
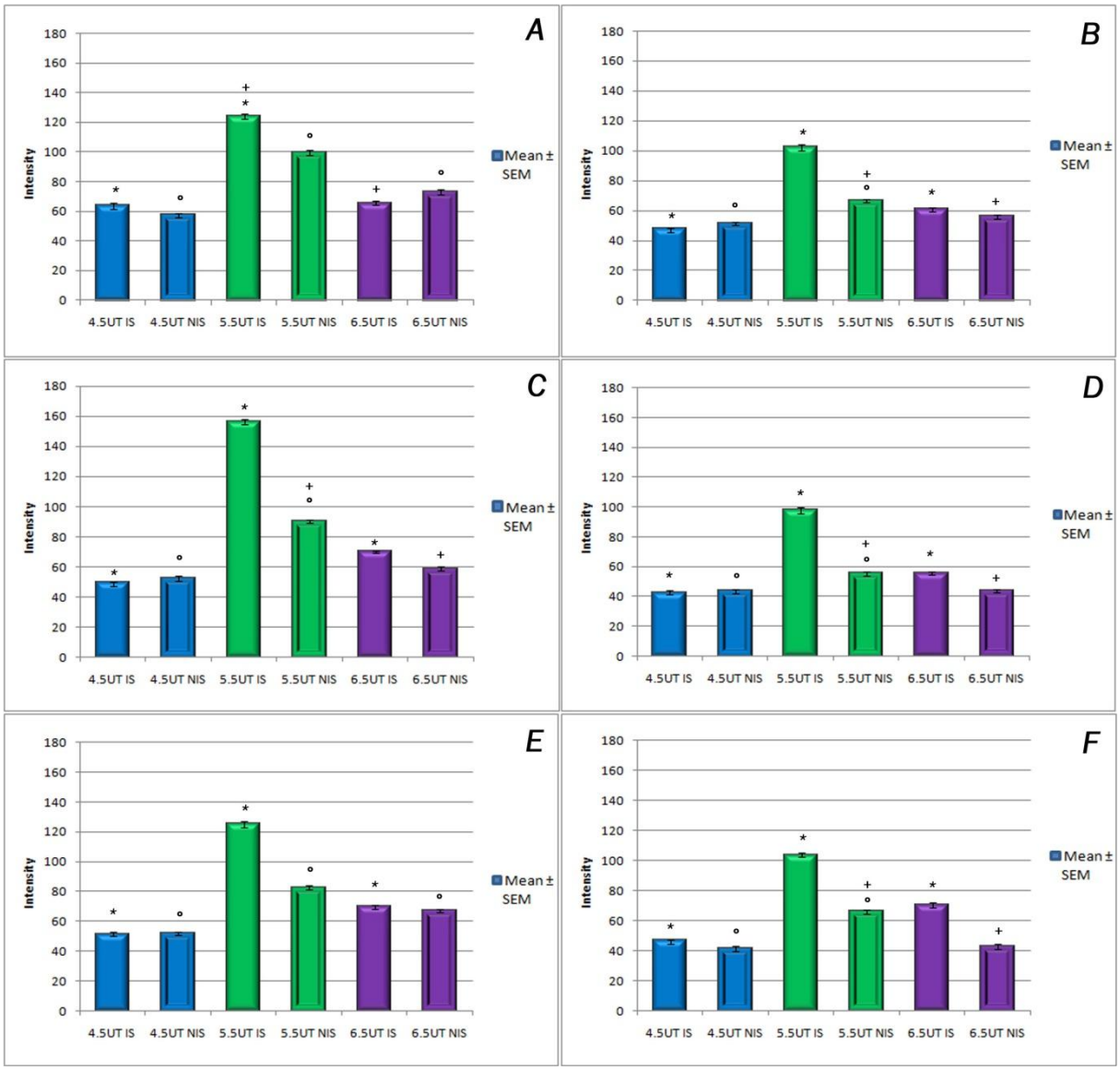


Figure 6.14 Immunofluorescent images illustrating PDGF protein localisation in the luminal epithelium and the subepithelial stroma of the implantation and non-implantation sites in the uteri of control pregnant rats. A: Implantation site at day 4.5 of pregnancy, **B:** Non-implantation site at day 4.5 of pregnancy, **C:** Implantation site at day 5.5 of pregnancy, **D:** Non-implantation site at day 5.5 of pregnancy, **E:** Implantation site at day 6.5 of pregnancy, **F:** Non-implantation site at day 6.5 of pregnancy. Scale = 20µm.



Graph 6.7 Graphical representation of the Mean ± SEM of PDGF protein expression in the luminal epithelium (A), the subepithelial stroma (B), the glandular epithelium (C), the glandular stroma (D), the blood vessels (E) and the stroma surrounding the blood vessels (F) of the implantation (IS) and non-implantation (NIS) sites in day 4.5, day 5.5 and day 6.5 pregnant rat uteri treated with vehicle (UT) at day 3.0 of pregnancy, as obtained from image analysis of fluorescent intensities. *, °, + = significantly different ($p \leq 0.05$) using the Tukey-Kramer *post hoc* analysis.

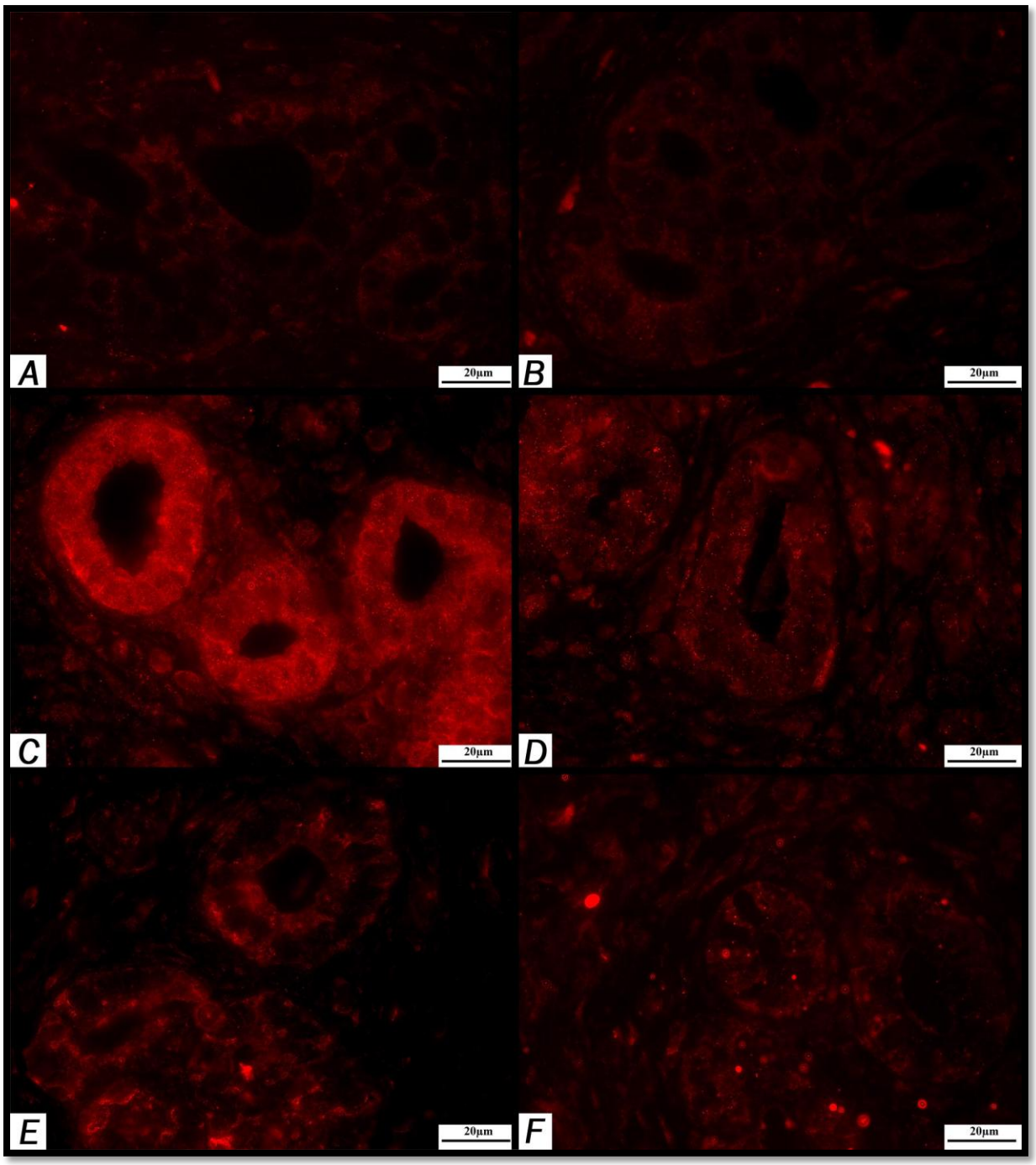


Figure 6.15 Immunofluorescent images illustrating PDGF protein localisation in the glandular epithelium and glandular stroma of the implantation and non-implantation sites in the uteri of control pregnant rats. A: Implantation site at day 4.5 of pregnancy, **B:** Non-implantation site at day 4.5 of pregnancy, **C:** Implantation site at day 5.5 of pregnancy, **D:** Non-implantation site at day 5.5 of pregnancy, **E:** Implantation site at day 6.5 of pregnancy, **F:** Non-implantation site at day 6.5 of pregnancy. Scale = 20µm.

6.2.1.4 The effects of RU486 on the spatiotemporal expression pattern of the PDGF protein

PDGF protein levels were significantly higher in both the implantation and non-implantation sites at day 4.5 of pregnancy in the luminal epithelium and subepithelial stroma as a result of RU486 treatment relative to the control pregnant animals. In the glandular epithelium, glandular stroma, blood vessels and stroma surrounding the blood vessels, PDGF protein levels were similar in both the RU486-treated and control pregnant animals (Graph 6.9A-F; Figure 6.14A and B; Figure 6.15A and B; Figure 6.16A and B; Figure 6.17A and B; Figure 6.18A and B; Figure 6.19A and B; Table 6.3). By day 5.5 of pregnancy, while PDGF protein levels in the RU486-treated animals increased (Graph 6.8A-F), the marked increase in PDGF levels in the implantation sites of the control pregnant animals resulted in significantly higher levels of PDGF protein levels in all endometrial compartments analysed of the implantation sites within this group (Graph 6.9A-F; Figure 6.14C; Figure 6.15C; Figure 6.16C; Figure 6.17C; Figure 6.18C; Figure 6.19C; Table 6.3). Thus, RU486 was not able to inhibit this marked increase in PDGF protein levels observed in the implantation sites of the control pregnant animals. In the non-implantation sites at day 5.5 of pregnancy, PDGF protein levels did not increase as markedly in the control pregnant animals, so levels were similar in the RU486-treated and control pregnant animals (Graph 6.9A-F; Figure 6.14D; Figure 6.15D; Figure 6.16D; Figure 6.17D; Figure 6.18D; Figure 6.19D; Table 6.3). By day 6.5 of pregnancy, a significant decrease in PDGF protein levels was demonstrated in the implantation and non-implantation sites of the control pregnant animals (Graph 6.7A-F). No decrease was demonstrated in the RU486-treated animals (Graph 6.8A-F), resulting in significantly higher PDGF protein levels in the implantation and non-implantation sites of the RU486-treated animals at this day of pregnancy (Graph 6.9A-F; Figure 6.14E and F; Figure 6.15E and F; Figure 6.16E and F; Figure 6.17E and F; Figure 6.18E and F; Figure 6.19E and F; Table 6.3).

In summary, inhibition of PDGF protein levels by RU486 was only demonstrated in the implantation sites at day 5.5 of pregnancy.

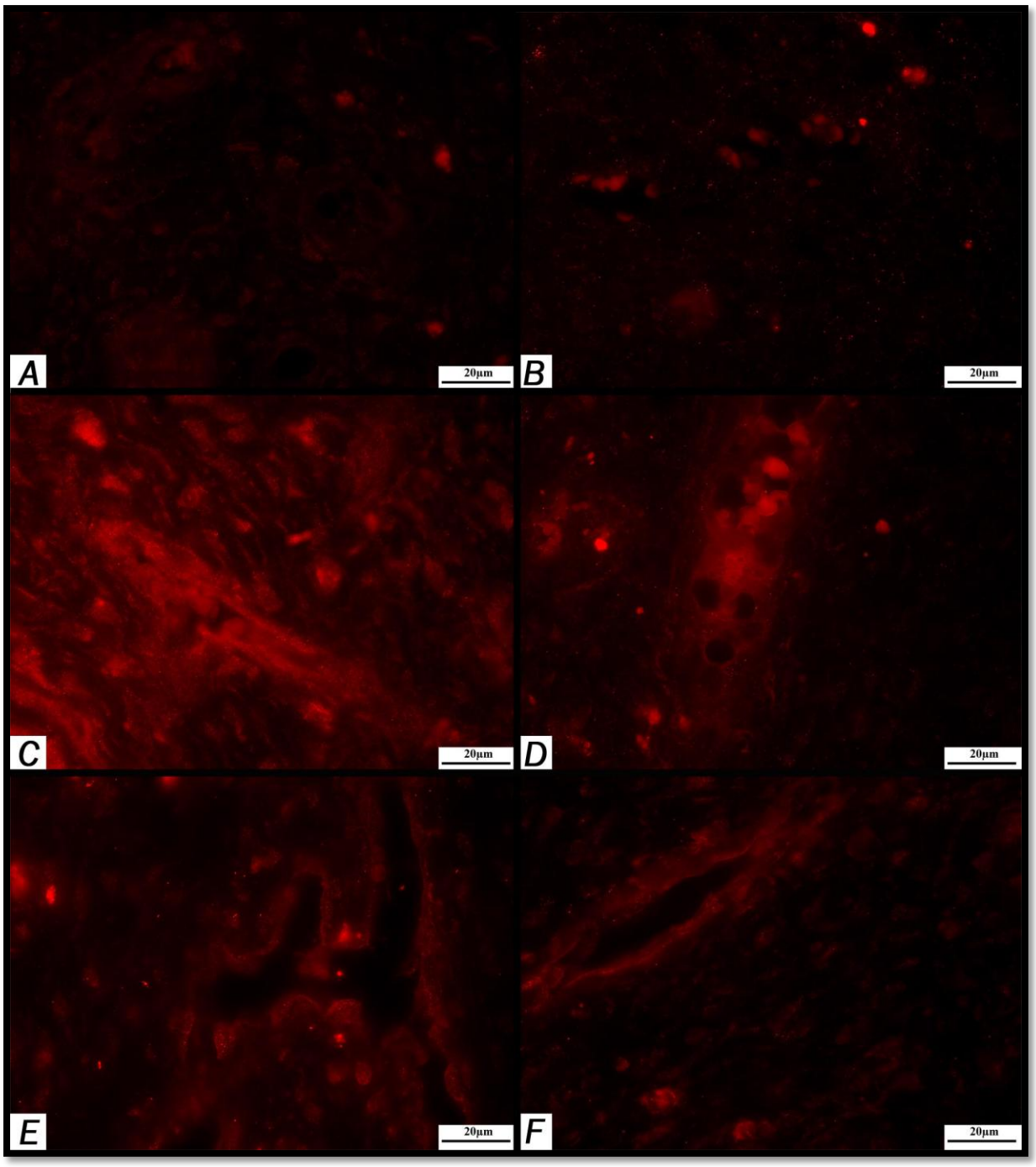
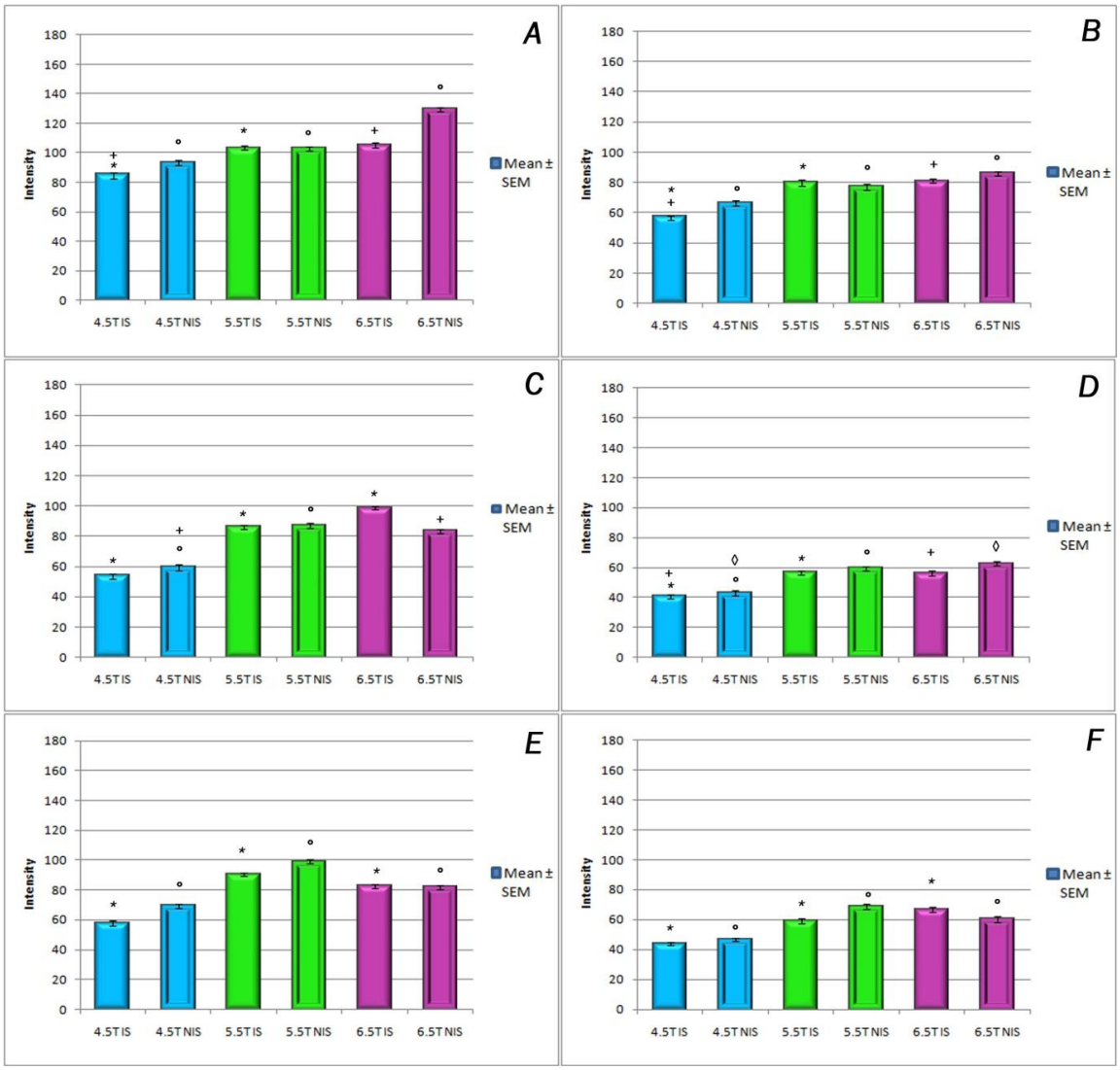


Figure 6.16 Immunofluorescent images illustrating PDGF protein localisation in the blood vessels and the stroma surrounding the blood vessels of the implantation and non-implantation sites in the uteri of control pregnant rats. A: Implantation site at day 4.5 of pregnancy, **B:** Non-implantation site at day 4.5 of pregnancy, **C:** Implantation site at day 5.5 of pregnancy, **D:** Non-implantation site at day 5.5 of pregnancy, **E:** Implantation site at day 6.5 of pregnancy, **F:** Non-implantation site at day 6.5 of pregnancy. Scale = 20µm.



Graph 6.8 Graphical representation of the Mean ± SEM of PDGF protein expression in the luminal epithelium (A), the subepithelial stroma (B), the glandular epithelium (C), the glandular stroma (D), the blood vessels (E) and the stroma surrounding the blood vessels (F) of the implantation (IS) and non-implantation (NIS) sites in day 4.5, day 5.5 and day 6.5 pregnant rat uteri treated with RU486 (T) at day 3.0 of pregnancy, as obtained from image analysis of fluorescent intensities. *, °, +, ◊ = significantly different ($p \leq 0.05$) using the Tukey-Kramer *post hoc* analysis.

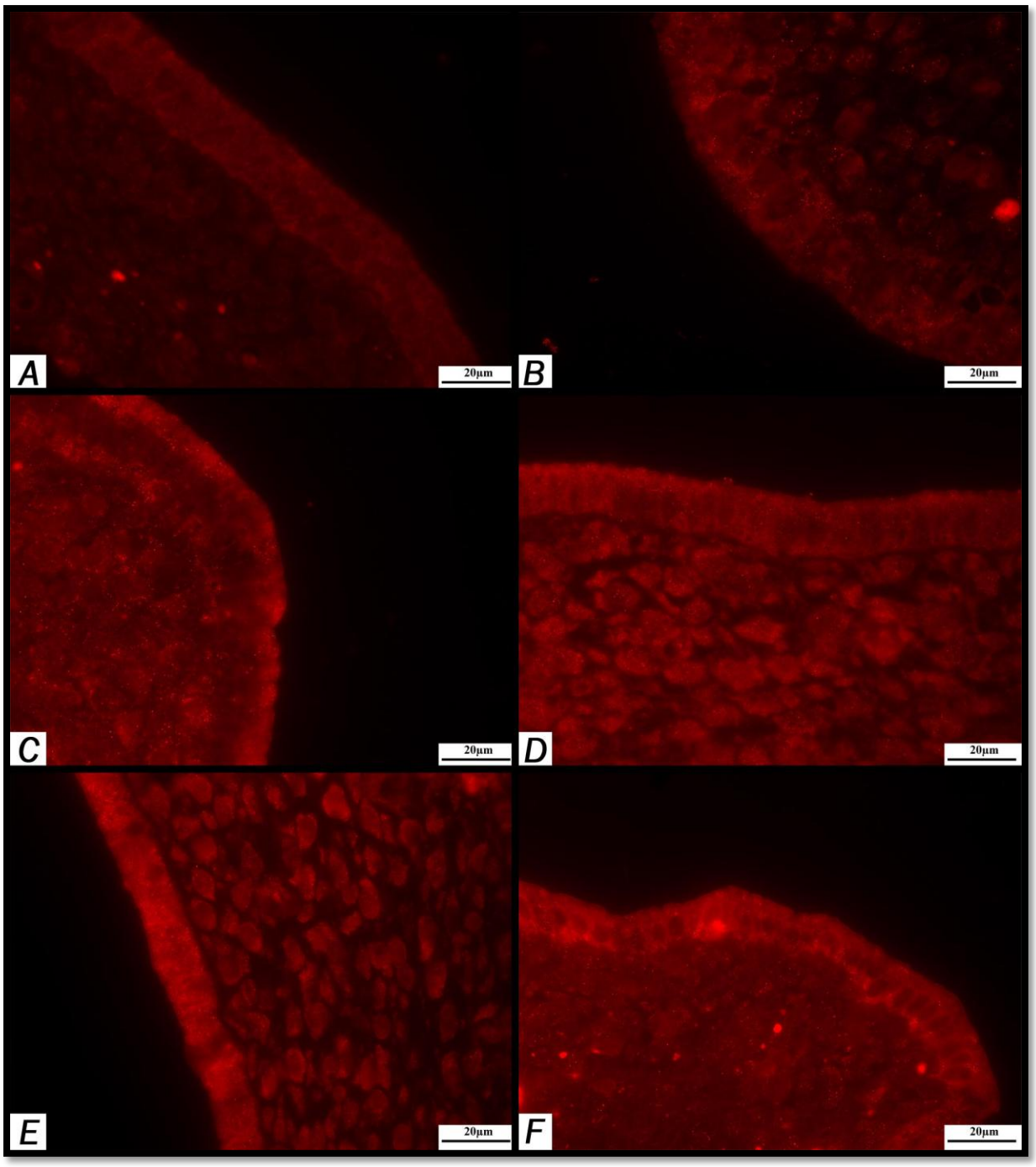
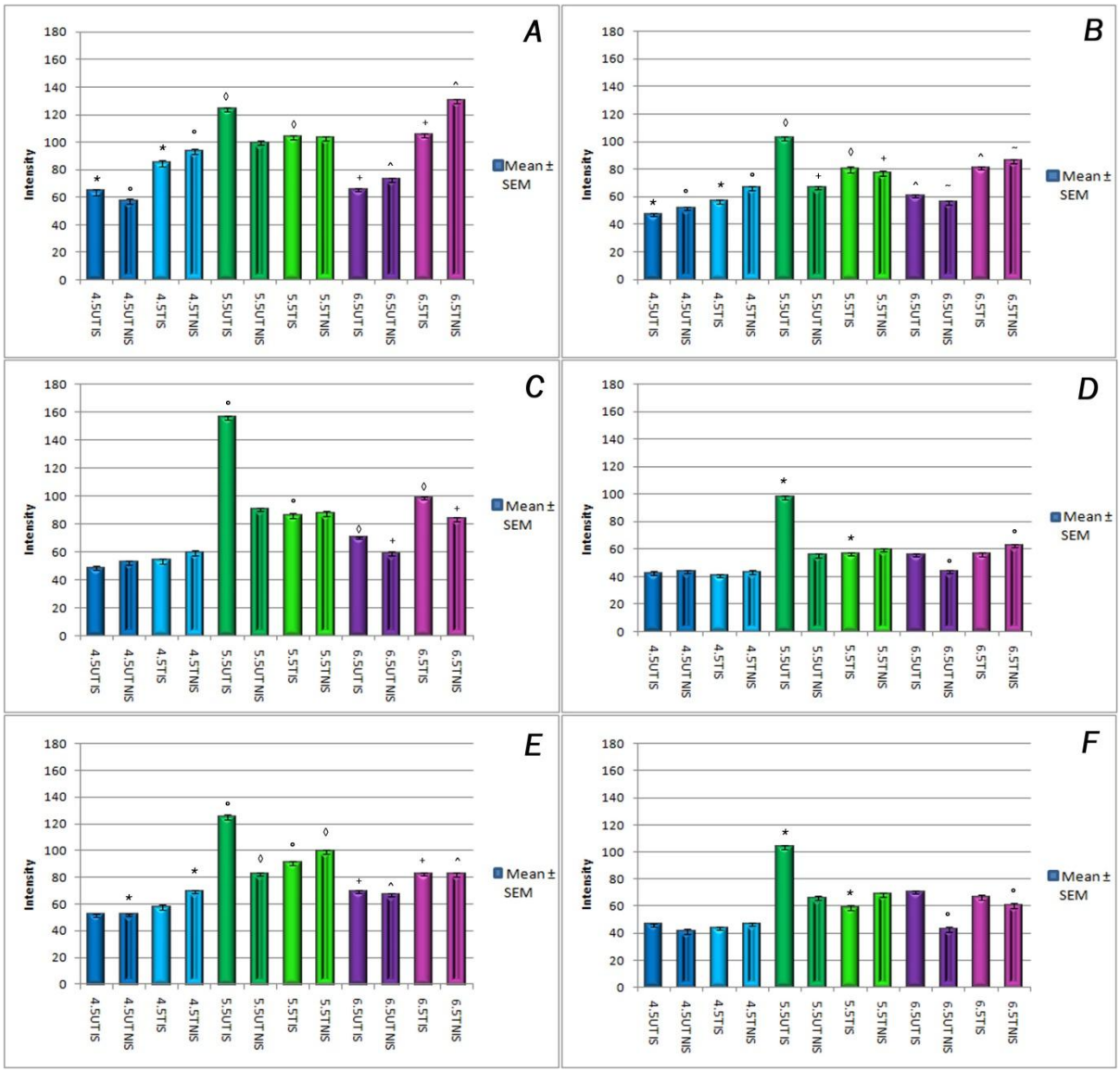


Figure 6.17 Immunofluorescent images illustrating PDGF protein localisation in the luminal epithelium and the subepithelial stroma of the implantation and non-implantation sites in the uteri of RU486-treated pregnant rats. A: Implantation site at day 4.5 of pregnancy, **B:** Non-implantation site at day 4.5 of pregnancy, **C:** Implantation site at day 5.5 of pregnancy, **D:** Non-implantation site at day 5.5 of pregnancy, **E:** Implantation site at day 6.5 of pregnancy, **F:** Non-implantation site at day 6.5 of pregnancy. Scale = 20µm.



Graph 6.9 Graphical representation of the Mean ± SEM of PDGF protein expression in the luminal epithelium (A), the subepithelial stroma (B), the glandular epithelium (C), the glandular stroma (D), the blood vessels (E) and the stroma surrounding the blood vessels (F) of the implantation (IS) and non-implantation (NIS) sites in day 4.5, day 5.5 and day 6.5 pregnant rat uteri treated with vehicle (UT) or RU486 (T) at day 3.0 of pregnancy, as obtained from image analysis of fluorescent intensities. *, °, +, ◊, ^,~ = significantly different ($p \leq 0.05$) using the Tukey-Kramer *post hoc* analysis.

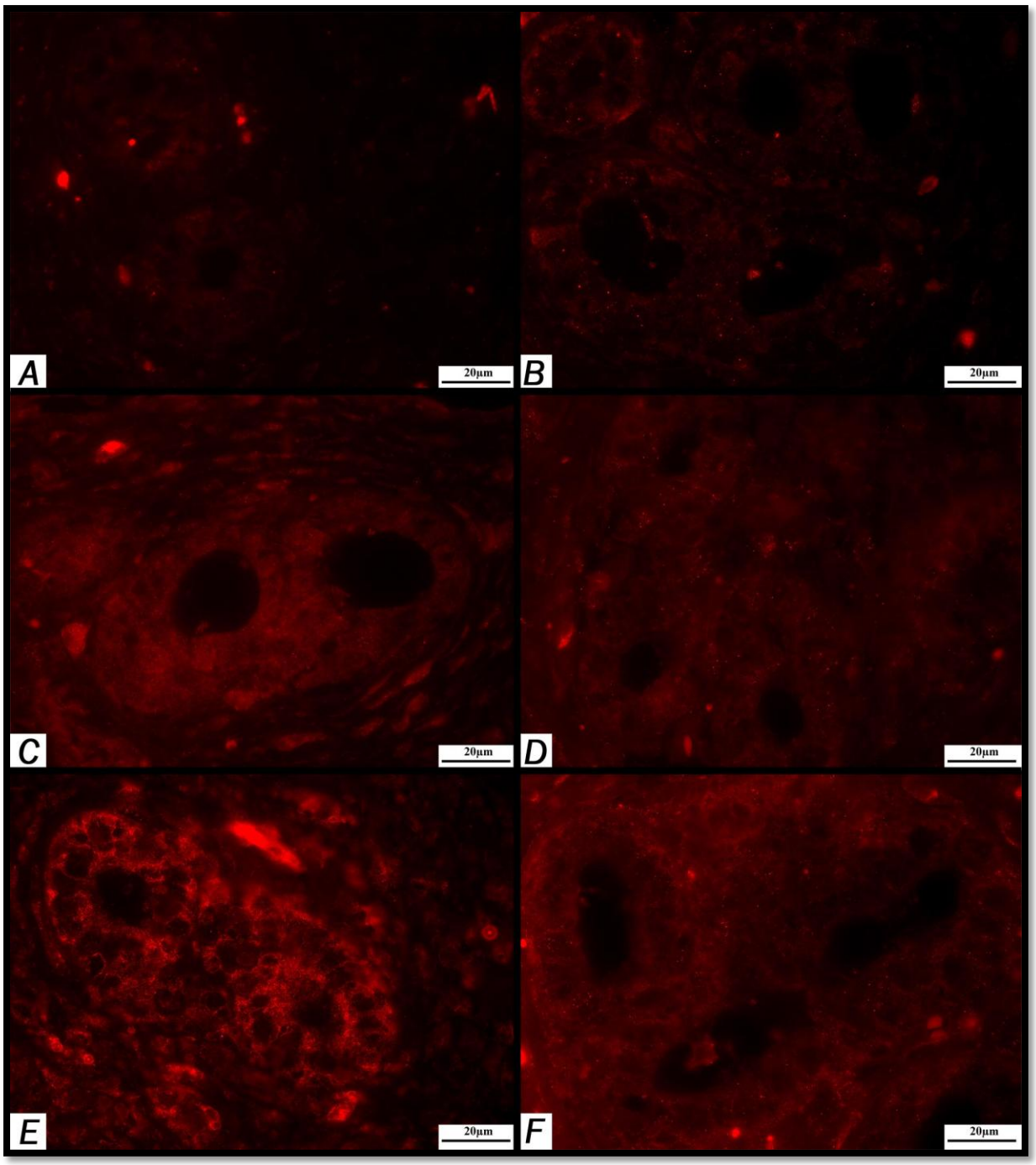


Figure 6.18 Immunofluorescent images illustrating PDGF protein localisation in the glandular epithelium and the glandular stroma of the implantation and non-implantation sites in the uteri of RU486-treated pregnant rats. A: Implantation site at day 4.5 of pregnancy, **B:** Non-implantation site at day 4.5 of pregnancy, **C:** Implantation site at day 5.5 of pregnancy, **D:** Non-implantation site at day 5.5 of pregnancy, **E:** Implantation site at day 6.5 of pregnancy, **F:** Non-implantation site at day 6.5 of pregnancy. Scale = 20µm.

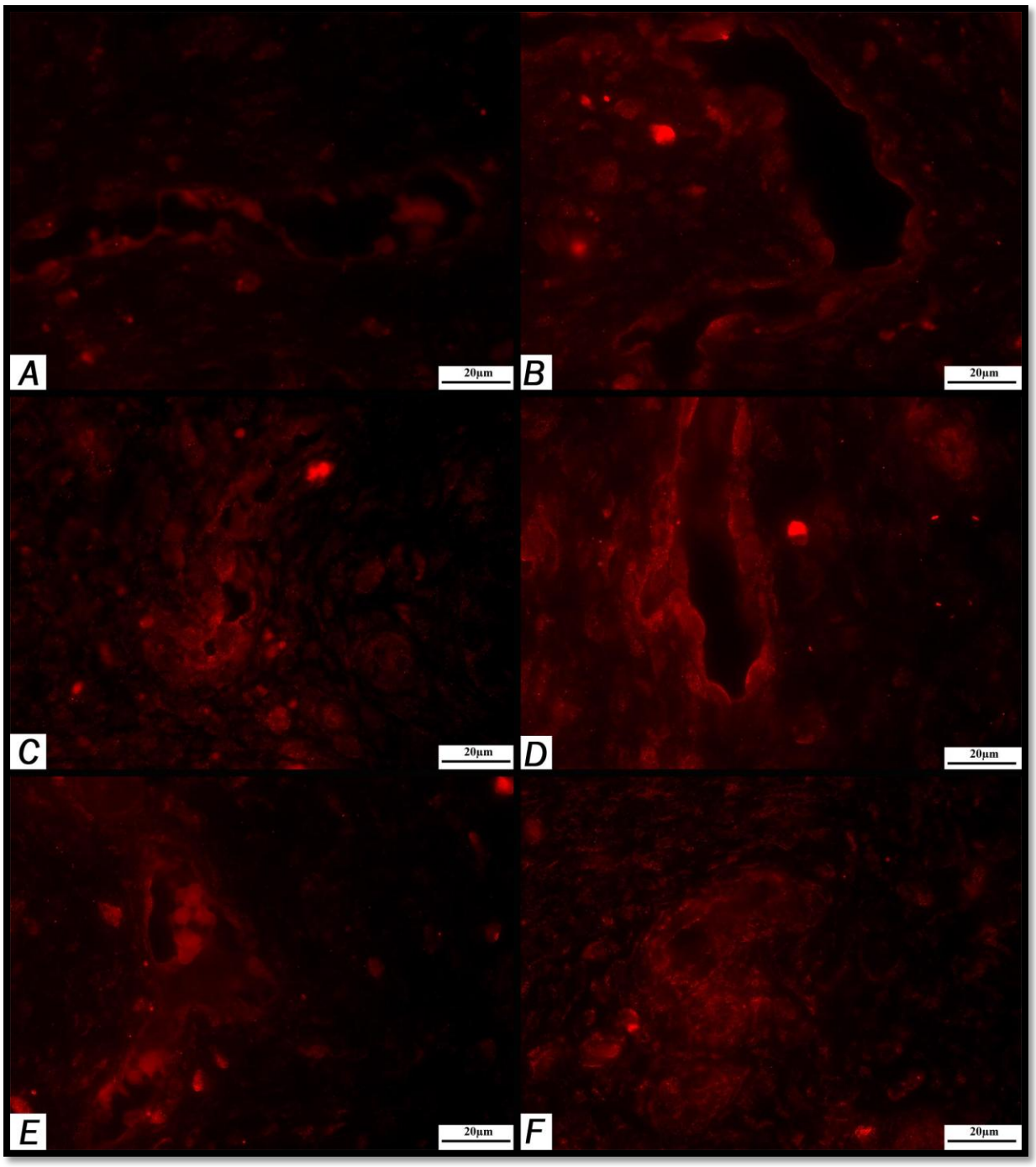


Figure 6.19 Immunofluorescent images illustrating PDGF protein localisation in the blood vessels and the stroma surrounding the blood vessels of the implantation and non-implantation sites in the uteri of RU486-treated pregnant rats. A: Implantation site at day 4.5 of pregnancy, **B:** Non-implantation site at day 4.5 of pregnancy, **C:** Implantation site at day 5.5 of pregnancy, **D:** Non-implantation site at day 5.5 of pregnancy, **E:** Implantation site at day 6.5 of pregnancy, **F:** Non-implantation site at day 6.5 of pregnancy. Scale = 20µm.

6.2.2 The Effects of RU486 on Angiogenic Pathway-Related Gene Expression in the Rat Uterus during Early Pregnancy

The effect of RU486 on the expression of the angiogenic pathway-related genes, VEGF, bFGF and PDGF, in the implantation and non-implantation sites of the rat uterus at days 5.5 and 6.5 of pregnancy was analysed by relative quantification reverse transcriptase real-time PCR. Only days 5.5 and 6.5 of pregnancy were analysed in the current study as it was considered that these two days are the most important with regards to the implantation process, as implantation and invasion occur on these days, respectively. The increase in endometrial angiogenesis of early pregnancy occurs simultaneously with the implantation process, as an increase in the capillary network is vital to sustain the developing embryo. As implantation occurs at day 5.5 of pregnancy in the implantation sites, this group was chosen as the calibrator sample. As relative quantification analysis was conducted, all results are relative to this group.

6.2.2.1 Relative quantification (RQ) analysis of VEGF and bFGF gene expression

6.2.2.1.1 Analysis of VEGF and bFGF Gene Expression in the Control Pregnant Animals

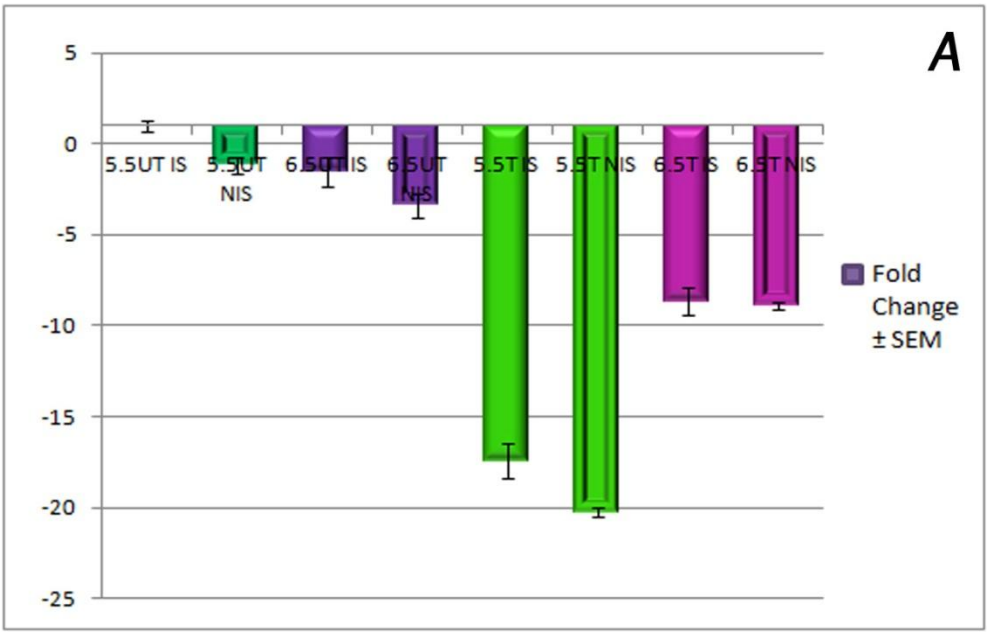
At day 5.5 of pregnancy, VEGF gene expression remained fairly similar (1.1-fold decrease) in the non-implantation sites relative to the implantations sites, the calibrator sample (Graph 6.10; Table 6.4A). This was also true for bFGF protein expression (1.1-fold increase) (Graph 6.11; Table 6.4B). By day 6.5 of pregnancy, VEGF protein expression was slightly down-regulated by 1.6-fold in the implantation sites and by 3.4-fold in the non-implantation sites, relative to the calibrator sample (Graph 6.10; Table 6.4A). Alternatively, bFGF gene expression was significantly down-regulated by 4-fold in the implantation sites and remained similar (1.04-fold increase) in the non-implantation sites, relative to the calibrator sample (Graph 6.11; Table 6.4B).

In general, there was a decrease in VEGF and bFGF gene expression from day 5.5 to 6.5 of pregnancy in the control pregnant animals, as reflected in the immunofluorescence experiments.

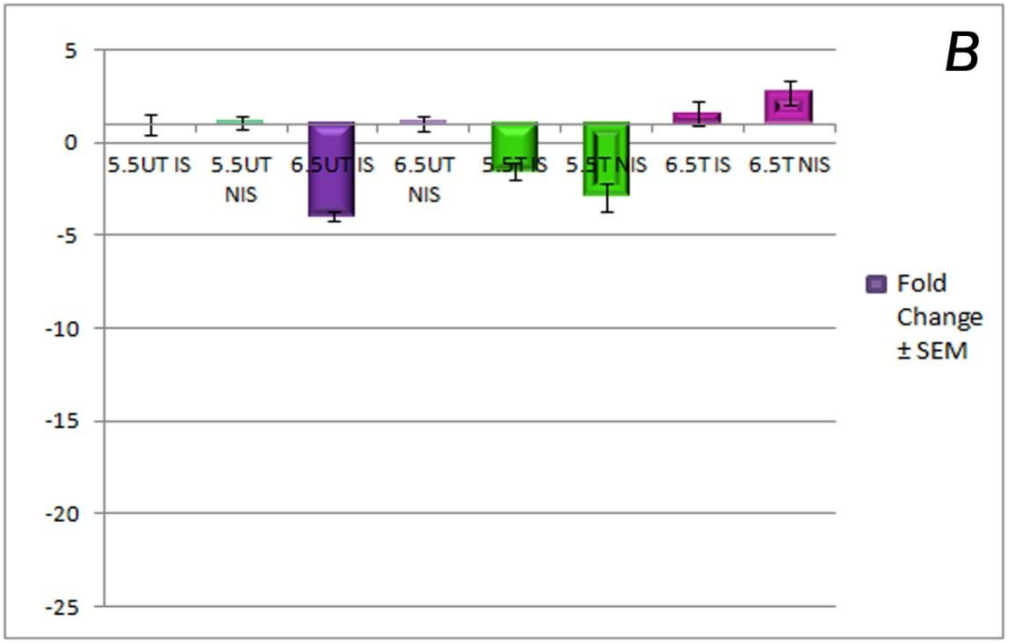
Table 6.4 RQ analysis of VEGF and bFGF gene expression in the implantation (IS) and non-implantation (NIS) sites at day 5.5 and 6.5 of pregnancy in the control pregnant (UT) and RU486-treated (T) animals. A fold change of 2 or more represents a significant difference in gene expression.

A: VEGF mRNA Expression								
Day of Pregnancy	**Avg. C_T**	**SEM**	**ΔC_T**	**SEM**	**$\Delta\Delta C_T$**	**$2^{-\Delta\Delta Ct}$**	**$Log_{10}(2^{-\Delta\Delta Ct})$**	**Fold Change**
B-actin *	20.20	0.74	-	-	-	-	-	-
5.5UT IS **	29.11	1.03	8.91	0.29	0	1	0	1
5.5UT NIS	29.30	1.20	9.10	0.46	0.19	0.88	-0.06	-1.14
6.5UT IS	29.77	1.54	9.57	0.80	0.66	0.63	-0.20	-1.58
6.5UT NIS	30.88	1.38	10.68	0.64	1.77	0.29	-0.53	-3.40
5.5T IS	33.24	0.96	13.03	0.96	4.12	0.06	-1.24	-17.45
5.5T NIS	33.45	0.45	13.25	0.29	4.34	0.05	-1.31	-20.26
6.5T IS	32.23	1.5	12.03	0.76	3.12	0.12	-0.94	-8.67
6.5T NIS	32.26	0.93	12.06	0.19	3.15	0.11	-0.95	-8.87
B: bFGF mRNA Expression								
Day of Pregnancy	**Avg. C_T**	**SEM**	**ΔC_T**	**SEM**	**$\Delta\Delta C_T$**	**$2^{-\Delta\Delta Ct}$**	**$Log_{10}(2^{-\Delta\Delta Ct})$**	**Fold Change**
B-actin *	20.20	0.74	-	-	-	-	-	-
5.5UT IS **	25.14	0.20	4.94	0.54	0	1	0	1
5.5UT NIS	25.02	0.37	4.82	0.37	-0.12	1.08	0.03	1.08
6.5UT IS	27.13	0.99	6.93	0.25	2.00	0.25	-0.60	-3.99
6.5UT NIS	25.07	0.29	4.87	0.45	-0.06	1.04	0.02	1.04
5.5T IS	25.79	1.19	5.59	0.45	0.65	0.64	-0.20	-1.57
5.5T NIS	26.68	1.48	6.48	0.74	1.54	0.34	-0.46	-2.91
6.5T IS	24.48	0.13	4.27	0.62	-0.66	1.58	0.20	1.58
6.5T NIS	23.70	0.09	3.50	0.65	-1.43	2.70	0.43	2.70

UT - untreated, **T** - treated, **IS** - implantation site, **NIS** - non-implantation site, **C_T** - threshold cycle, **SEM** - standard error of the mean, ***** - endogenous control, ****** - calibrator sample. **ΔC_T** = C_T (Target) - C_T (Endogenous control). **$\Delta\Delta C_T$** = ΔC_T (Target) - ΔC_T (Calibrator).



Graph 6.10 Graphical representation of VEGF gene expression as compared to day 5.5 in the control pregnant animals, the calibrator sample. The data is expressed as the Fold Change ± SEM.
UT – untreated, **T** – treated, **IS** – implantation site, **NIS** – non-implantation site.



Graph 6.11 Graphical representation of bFGF gene expression as compared to day 5.5 in the control pregnant animals, the calibrator sample. The data is expressed as the Fold Change ± SEM.
UT – untreated, **T** – treated, **IS** – implantation site, **NIS** – non-implantation site.

6.2.2.1.2 Analysis of the Effects of RU486 on VEGF and bFGF Gene Expression

After RU486 administration, VEGF gene expression was significantly down-regulated by 17.4-fold in the implantation sites and 20.3-fold in the non-implantation sites at day 5.5 of pregnant, relative to the calibrator sample (Graph 6.10; Table 6.4A). By day 6.5 of pregnancy, VEGF gene expression was 8.7-fold and 8.9-fold lower in the implantation and non-implantation sites respectively, in the RU486-treated animals (Graph 6.10; Table 6.4A). This is as a result of a 2-fold and 2.30-fold increase in VEGF gene expression in the implantation and non-implantation sites respectively, in the RU486-treated animals with the progression of pregnancy from day 5.5 to day 6.5 (Graph 6.10).

RU486 administration did not have a major effect on bFGF gene expression. At day 5.5 of pregnancy, RU486 administration resulted in a 1.6-fold and 2.9-fold decrease in bFGF expression in the implantation and non-implantation sites respectively, relative to the calibrator (Graph 6.11; Table 6.4B). By day 6.5 of pregnancy, bFGF gene expression levels in the RU486-treated animals were higher in the implantation and non-implantation sites relative to the control pregnant animals (Graph 6.11). Relative to the calibrator sample, bFGF expression was 1.6-fold and 2.7-fold higher in the implantation and non-implantation sites of the RU486-treated animals respectively (Graph 6.11; Table 6.4B).

In summary, RU486 had a marked effect on VEGF gene expression in both the implantation and non-implantation sites at day 5.5 of pregnancy, the day of blastocyst implantation. This dramatic inhibition of gene expression was not demonstrated in bFGF gene expression as a result of treatment with RU486.

6.2.2.2 Relative quantification (RQ) analysis of PDGF gene expression

6.2.2.2.1 Analysis of PDGF Gene Expression in the Control Pregnant Animals

At day 5.5 of pregnancy, PDGF gene expression was slightly up-regulated by 1.8-fold in the non-implantation sites relative to the implantation sites, the calibrator sample (Graph 6.12; Table 6.5). PDGF gene expression was increased by 2-fold in the implantation sites and decreased by 1.5-fold in the non-implantation sites respectively, at day 6.5 of pregnancy, relative to the calibrator sample (Graph 6.12; Table 6.5). However, PDGF gene expression in the implantation sites was increased as pregnancy progressed from day 5.5 to day 6.5 of pregnancy, which is also reflected in the present immunofluorescence study.

6.2.2.2.2 Analysis of the Effects of RU486 on PDGF Gene Expression

RU486 had a marked effect on PDGF gene expression. At day 5.5 of pregnancy, RU486 down-regulated gene expression by 27-fold and 38.6-fold in the implantation and non-implantation sites

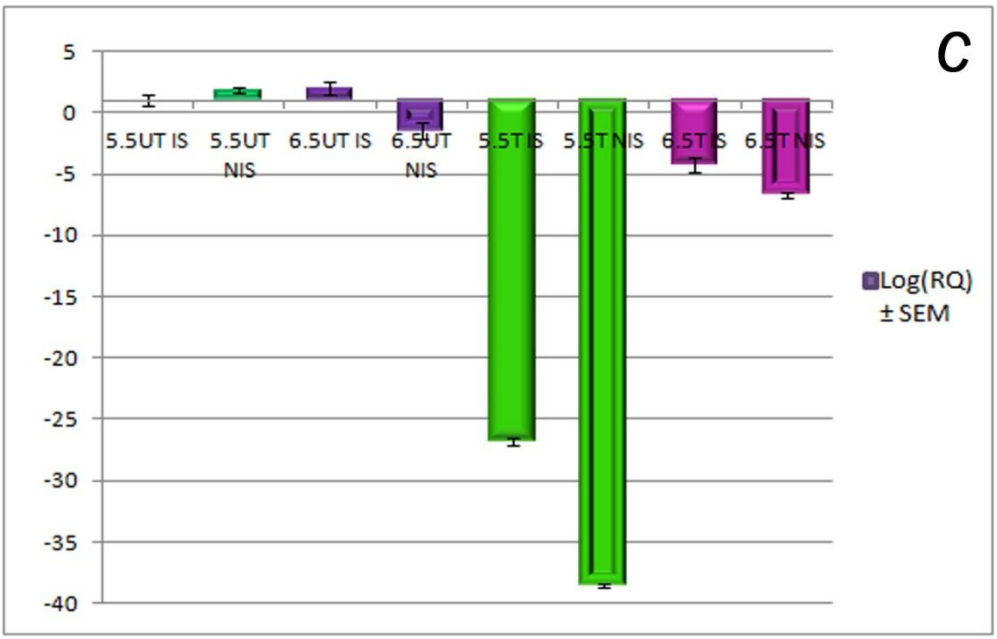
respectively, relative to the calibrator sample (Graph 6.12; Table 6.5). By day 6.5 of pregnancy, PDGF gene expression was 4.3-fold and 6.7-fold lower in the implantation and non-implantation sites of the RU486-treated animals, relative to the calibrator (Graph 6.12; Table 6.5), as a result of a 6.3-fold and 5.9-fold increase in PDGF gene expression in the implantation and non-implantation sites, respectively, of the RU486-treated animals as pregnancy progressed from day 5.5 to day 6.5 (Graph 6.12).

In summary, RU486 had a drastic effect on VEGF and PDGF gene expression in both the implantation and non-implantation sites at day 5.5 of pregnancy, the day of blastocyst implantation.

Table 6.5 RQ analysis of PDGF gene expression in the implantation (IS) and non-implantation (NIS) sites at day 5.5 and 6.5 of pregnancy in the control pregnant (UT) and RU486-treated animals. A fold change of 2 or more represents a significant difference in gene expression.

PDGF mRNA Expression								
Day of Pregnancy	**Avg. C_T**	**SEM**	**ΔC_T**	**SEM**	**$\Delta\Delta C_T$**	**$2^{-\Delta\Delta Ct}$**	**$Log_{10}(2^{-\Delta\Delta Ct})$**	**Fold Change**
B-actin *	20.20	0.74	-	-	-	-	-	-
5.5UT IS **	29.27	1.20	9.08	0.46	0	1	0	1
5.5UT NIS	28.41	0.96	8.22	0.22	-0.86	1.81	0.26	1.81
6.5UT IS	28.29	1.31	8.09	0.57	-0.98	1.98	0.30	1.98
6.5UT NIS	29.86	1.41	9.66	0.67	0.59	0.67	-0.18	-1.50
5.5T IS	34.02	1.07	13.82	0.33	4.75	0.04	-1.43	-26.82
5.5T NIS	34.54	0.54	14.35	0.20	5.27	0.03	-1.59	-38.57
6.5T IS	31.38	1.35	11.18	0.61	2.11	0.23	-0.63	-4.31
6.5T NIS	32.01	0.98	11.81	0.24	2.74	0.15	-0.82	-6.67

UT - untreated, **T** - treated, **IS** - implantation site, **NIS** - non-implantation site, **C_T** - threshold cycle, **SEM** - standard error of the mean, ***** - endogenous control, ****** - calibrator sample. **ΔC_T** = C_T (Target) - C_T (Endogenous control). **$\Delta\Delta C_T$** = ΔC_T (Target) - ΔC_T (Calibrator).



Graph 6.12 Graphical representation of PDGF gene expression as compared to day 5.5 in the control pregnant animals, the calibrator sample. The data is expressed as the Fold Change ± SEM.
UT – untreated, **T** – treated, **IS** – implantation site, **NIS** – non-implantation site.

6.3 DISCUSSION

6.3.1 The Effects of RU486 on the Angiogenic Pathway-Related Growth Factors

6.3.1.1 Vascular permeability

During early pregnancy, one of the first vascular events to occur is the localised increase in vascular permeability in the implantation sites. This occurrence is visualised with the aid of the high molecular weight dye, Pontamine Sky blue, which selectively accumulates within the uterine implantation sites (Finn and McLaren, 1967). This increase in vascular permeability has been noted to coincide with an increased expression of VEGF mRNA, as well as its receptor, Flk1; so linking VEGF to this early oestrogen-induced event (Ma *et al.*, 2001).

In the present study, increased vascular permeability, as indicated by the presence of blue bands by Pontamine Sky blue, was either not visible or was drastically reduced within the RU486-treated animals, suggesting that this vascular event is impaired in the RU486-treated endometrium. In support of this, at a molecular level, both VEGF mRNA and protein levels decrease after RU486 administration here. Not only is RU486 able to effectively block progesterone signalling within the endometrium by binding to the PR, it has also been reported to bind to the ER and subsequently restrict oestrogen action, with more than 80% efficiency as compared to the pure oestrogen antagonist ICI 164382 (McDonnell and Goldman, 1994; Chwalisz *et al.*, 1995; Chwalisz *et al.*, 1998).

This ability of RU486 to block oestrogen signalling within the endometrium may account for the decreased VEGF expression and subsequent decrease in vascular permeability associated with this antagonist, confirming the overall hypothesis of the current study, that RU486 results in a hormonally under-stimulated uterus (Scholtz *et al.*, 2008).

6.3.1.2 Endometrial cell proliferation and differentiation

6.3.1.2.1 The Spatiotemporal Expression Pattern of VEGF and bFGF in the Pregnant Rat Endometrium

Since the uterus is composed of heterogeneous cell types that undergo rapid and dynamic changes during early pregnancy, each endometrial compartment, excluding the myometrium, was examined for cell specific expression of the angiogenic pathway-related growth factors VEGF, bFGF and PDGF, by immunofluorescence. In this study, VEGF protein levels were significantly increased in all regions of the implantation and non-implantation sites from days 4.5 to day 5.5 of pregnancy. In agreement with a previous study in the mouse endometrium (Walter *et al.*, 2005), the most intense VEGF immunofluorescence was observed within the glandular epithelium with slightly less intense

staining in the luminal epithelium and then in the blood vessels, with the lowest levels of intensity observed within the stroma. In the decidual layer of the implantation sites, the increase in VEGF expression was also substantial. By day 6.5 of pregnancy VEGF expression was not significantly different in the implantation sites, whereas in the non-implantation sites, expression levels continued to increase significantly to a level similar to that in the implantation sites. These results were mimicked in VEGF expression within the implantation sites, which remained similar as pregnancy progressed from day 5.5 to day 6.5. In contrast, VEGF levels in the non-implantation sites decreased significantly by 3-fold. Paradoxically, however, VEGF when detected by *in situ* hybridisation in the mouse uterus, an increase in mRNA levels within the luminal epithelial and subepithelial stromal cells in the implantation sites immediately surrounding the blastocyst was demonstrated (Chakraborty *et al.*, 1995; Halder *et al.*, 2000). In an attempt to explain this discrepancy here, it is suggested that as whole tissue homogenates were used in this RT-qPCR study of the rat uterus, neither up- nor down-regulation of VEGF within the various endometrial compartments can be detected. Thus, due to this overall analysis of VEGF, more subtle changes in VEGF expression may be attenuated and may not be adequately discerned. Certainly, these reported levels may be influenced by the stroma, this being one of the biggest endometrial compartments within the uterus. It is possible that the low levels of VEGF expression reported in the stroma may lessen the reported increases in VEGF expression within the luminal epithelial and subepithelial stroma compartments as demonstrated by *in situ* hybridisation (Chakraborty *et al.*, 1995; Halder *et al.*, 2000). It would seem that further studies on VEGF levels in each endometrial compartment within the rat uterus are necessary to better explain this discrepancy.

In the human endometrium, VEGF has been localised within the glandular epithelium, leading investigators to propose that VEGF is secreted into the endometrial lumen where it might serve as a trophic signal to the apposing blastocyst (Hornung *et al.*, 1998). The fact that human trophoblast cells express VEGF receptors supports their hypothesis (Cooper *et al.*, 1995). Interestingly, both Flt-1 and Flk-1 type VEGF receptors have been observed on invasive human cytotrophoblasts (Torry and Torry, 1997) and further, Flk-1 receptor has been shown to mediate the mitogenic response of VEGF (Keyt *et al.*, 1996). This led the researchers to postulate that the endometrial luminal associated VEGF may provide trophic, permeability, or differentiation signals to the apposing blastocyst and developing trophectoderm (Hornung *et al.*, 1998). Shweiki *et al.* (1993) also reported high levels of VEGF mRNA in the extra-embryonic giant trophoblast cells. They suggest that VEGF produced and presumably secreted by these giant trophoblast cells could produce a gradient of angiogenic activity which would help direct the growth and/or migration of the maternal endothelial cells towards the implanting blastocyst (Shweiki *et al.*, 1993). Thus, it is possible that VEGF expression reported in the glandular and luminal epithelium in the current study and in previous studies in mice (Goodger and Rogers, 1993; Shweiki *et al.*, 1993; Chakraborty *et al.*, 1995; Walter *et al.*, 2005) and rabbits (Das *et*

al., 1997), plays a role in the controlling of the invasion of the blastocyst. The decrease in VEGF immunofluorescence staining within the glandular and luminal epithelial compartments observed as a result of RU486 administration may further elucidate how RU486 exacts its effects on the endometrium in preventing implantation of a blastocyst; this decrease in VEGF expression may inhibit communication with the blastocyst preparing for invasion and implantation.

Analyses of bFGF immunofluorescence staining demonstrated a significant increase in bFGF protein levels in both the implantation and non-implantation sites as pregnancy progressed from day 4.5 to day 5.5. This finding is in accordance with a previous study in the rat endometrium by Carlone and Rider (1993). In the present study, bFGF protein levels within the luminal and glandular epithelium and the blood vessels of the implantation and non-implantation sites were all fairly similar at day 4.5 of pregnancy, whereas by day 5.5 of pregnancy, bFGF protein levels were highest in the glandular epithelium, followed by the luminal epithelium and finally the blood vessels. Protein levels within the subepithelial stromal layer were the lowest. In the study by Carlone and Rider (1993), they demonstrated a decrease in bFGF expression in the myometrium and endometrium at days 3.5 and 4.5 of pregnancy, whereas bFGF expression at the apical surface of the luminal and glandular epithelium was maintained at a constant level. This is in accordance with the current results at day 4.5 of pregnancy, where bFGF expression levels were low in the stromal compartments, but maintained in both the luminal and glandular epithelium as well as in the blood vessels. By day 5.5 of pregnancy, bFGF protein levels increased significantly in the both the implantation and non-implantation sites with regards to the luminal epithelium, the glandular epithelium and the glandular stroma. Protein expression in the subepithelial stroma was, however, only increased in the implantation sites at this day of pregnancy, and not in the non-implantation sites. The study by Carlone and Rider (1993) also demonstrated a difference in bFGF protein expression in subepithelial stroma of the implantation and non-implantation sites, which they attributed to the increase in decidualisation in the implantation sites at this day of pregnancy and the lack of a decidual response in the non-implantation sites.

By day 6.5 of pregnancy, bFGF protein levels in the implantation and non-implantation sites had not changed significantly within any of the endometrial compartments analysed. RT-qPCR studies indicated that bFGF mRNA levels decreased by 4-fold in the implantation sites, but did not change in the non-implantation sites. This decrease in bFGF mRNA levels in the implantation sites can be attributed to a reduction in myometrial bFGF protein expression. It must be mentioned that while bFGF protein levels within the myometrium were not analysed within this study, previous research has indicated a decrease in myometrial bFGF levels around this day of pregnancy (Carlone and Rider, 1993). This could account for the overall decrease in bFGF mRNA levels in whole tissue homogenates, as used in the present study. Alternatively, there is a growing body of evidence indicating that growth factors such as VEGF (Cooper *et al.*, 1995), FGF (Vlodavsky *et al.*, 1987;

Saksela and Rifkin, 1990) and PDGF (Raines and Ross, 1992) are stored within the extracellular matrix (ECM) and released with its degradation as bioactive forms. In such an instance, bFGF mRNA levels may thus be decreased by day 6.5 of pregnancy due to the availability of sufficient bFGF protein stored within the ECM at this stage of pregnancy. Further studies on bFGF mRNA levels subsequent to day 6.5 of pregnancy would better elucidate this hypothesis. As bFGF proteins are not secretory products and tethered within the ECM, they need to be mobilised in a biologically active form by the actions of heparin or heparin sulphate (Vlodavsky *et al.*, 1987; Folkman *et al.*, 1988). This binding of FGF to heparin sulphate is an essential step for the binding of this growth factor to its high affinity receptors (Rapraeger *et al.*, 1991; Yayon *et al.*, 1991). Moscatelli *et al.* (1991) reported that these cell associated heparin sulphate proteoglycans provide a sustained release reservoir that can mediate long-term responses to short exposures of bFGF. Thus it follows that a short pulse of bFGF mRNA expression may be adequate to synthesise sufficient quantities of bFGF protein to exact its effects during early pregnancy.

In contrast to results of the present study, Carlone and Rider (1993) reported high levels of bFGF protein expression in the luminal epithelium of the implantation sites and negligible levels in the non-implantation sites. In the current study, bFGF levels were only slightly lower in the luminal epithelium of the non-implantation sites relative to the implantation sites. A possible reason for this discrepancy is as of yet, unknown. It is possible that the differences may arise due to the analysis techniques used as in the current study image analysis software was used to determine the mean fluorescent intensities of each region of interest.

Carlone and Rider (1993) attributed the difference in bFGF localisation patterns in the luminal epithelium to the presence of the blastocyst in the implantation sites and suggested that the increase in bFGF expression in both the luminal epithelium and subepithelial stroma of the implantation sites could be controlled either by the implanting embryo or by uptake from extracellular stores. To confirm their hypothesis that the presence of an embryo is important to increase uterine bFGF expression, decidualisation was induced in hormonally sensitised rats, in the absence of an embryo. Their study indicated that luminal epithelial and subepithelial (decidual) cells from both the artificially stimulated uterine horn and the control horn (in which no decidual response was artificially stimulated) failed to express intracellular bFGF, clearly demonstrating a role of the embryo in initiating the increase in uterine cellular bFGF (Carlone and Rider, 1993).

In the mouse endometrium, bFGF protein expression was reported to be consistently undetectable in the glandular epithelium of the non-implantation sites in the peri-implantation stage of early pregnancy. In the luminal epithelium, the extracellular matrix and the stroma of the non-implantation sites immunolocalisation of bFGF was reported. In the implantation sites of the mouse endometrium,

the luminal epithelial cells were reactive for bFGF as well as the in the stroma surrounding the primary decidual zone (Wordinger *et al.*, 1994). It is suggested that species related differences may account for the disparities in the spatiotemporal pattern of bFGF protein expression within the endometrium of each of the Sprague-Dawley rat (Carlone and Rider, 1993), the mouse (Wordinger *et al.*, 1994) and the Wistar rat, the subject of the present study. Moreover, another contributory effect to these differing results may relate to the time at which the animals were sacrificed; the mice were sacrificed at midday on the designated day of pregnancy (Wordinger *et al.*, 1994); Wistar rats (the present study) were sacrificed two hours later, at 2pm. With regards to the Sprague-Dawley rats, no time was provided (Carlone and Rider, 1993). Other important differences concern the age of the uterine tissue studied; Carlone and Rider (1993) analysed uterine horns from day 2-6 of pregnancy (day of sperm in vaginal smear designated day 1), whereas in the present study, analysis was restricted to days 4.5-6.5 (day of sperm in vaginal smear designated day 0.5) of pregnancy; and in the mouse (Wordinger *et al.*, 1994) endometria spanning days 6-9 (day of sperm in vaginal smear designated day 1) of pregnancy were investigated. Note that day 6 of pregnancy in the mouse endometrium correlates to day 6.5 in the rat uterus within the current study.

6.3.1.2.1.1 Regulation of VEGF and bFGF

The spatiotemporal analysis of VEGF and bFGF expression patterns within the endometrium of the control pregnant animals followed a very similar pattern as pregnancy progressed from day 4.5 through to day 6.5 of pregnancy; both growth factors increased significantly in the endometrial compartments analysed of the implantation and non-implantation sites as pregnancy progressed from day 4.5 to day 5.5 and then remained similar as pregnancy further progressed to day 6.5. The increase in VEGF expression was more marked relative to that of bFGF, thus by day 6.5 of pregnancy, VEGF protein levels were significantly higher.

The similarities in the spatiotemporal expression patterns of these growth factors, strongly suggests that they act together within the endometrium during early pregnancy. In support of this hypothesis, it has previously been suggested that the angiogenic activity of VEGF is dependent on interactions with other factor/s present within the endothelial environment (Hanahan and Folkman, 1996; Pepper *et al.*, 1996a). Basic FGF has, for example, been reported to act synergistically with VEGF to induce angiogenesis both *in vitro* and *in vivo* (Pepper *et al.*, 1992; Asahara *et al.*, 1995; Hu and Fan, 1995) and additionally has been shown to stimulate the synthesis of VEGF in a number of tumour cell lines (Tsai *et al.*, 1995). Further, the expression of the receptor, VEGFR-2 (Flk-1), in cultured endothelial cells was increased by bFGF (Mandriota and Pepper, 1997). These observations suggest that bFGF may play an important regulatory role, triggering angiogenesis when VEGF is already present and/or in up-regulating VEGF-induced angiogenesis when this process has already started (Mandriota and Pepper, 1997).

In a study on VEGF- induced *in vitro* angiogenesis, anti-bFGF antibodies were able to inhibit this process in a dose-dependent manner (Mandriota and Pepper, 1997). The converse is also true (Smith, 1998). Although bFGF has previously been reported to increase VEGFR-2 expression, this was not the mechanism through which anti-bFGF inhibits VEGF-induced angiogenesis, as VEGFR-2 expression was not down-regulated (Mandriota and Pepper, 1997). In addition, the researchers were able to demonstrate that this inhibition of VEGF-induced angiogenesis is not mediated either by inhibition of endogenous bFGF-induced endothelial cell proliferation or apoptosis of the endothelial cells by anti-bFGF, this as bFGF has been demonstrated to be a survival factor for cultured endothelial cells (Araki *et al.*, 1990; Mandriota and Pepper, 1997). Angiogenesis is dependent on a precise equilibrium between proteinases, essential for ECM degradation, and proteinase inhibitors, which protect the ECM from excessive proteinase-mediated destruction (Pepper *et al.*, 1996b). VEGF addition to cultured endothelial cells promotes pericellular proteolysis, whereas anti-bFGF antibodies blocked this VEGF-induction of proteolysis, resulting in a net anti-proteolysis effect (Mandriota and Pepper, 1997).

6.3.1.2.1.2 The effects of RU486 on VEGF and bFGF expression patterns

Following treatment with RU486, VEGF levels were significantly lower at all three days of pregnancy analysed. At day 5.5 of pregnancy, this decrease was the most dramatic, inclusive of both VEGF protein and mRNA levels. RU486 caused an almost 18-fold decrease in VEGF expression in both the implantation and non-implantation sites at day 5.5 of pregnancy. By day 6.5 of pregnancy VEGF levels had increased in the RU486-treated animals as a result of the limited half-life of RU486, serving to reduce the difference between the control pregnant animals and the RU486-treated animals. These results concur with a previous study in the rat uterus in which VEGF expression was blocked by the antiprogestin RU486 (Hyder *et al.*, 2000). In addition, increased VEGF expression by progesterone was blocked by RU486 in a breast cell line, suggesting that VEGF is mediated by PR (Hyder *et al.*, 2000).

Ma *et al.* (2001) demonstrated that in ovariectomised mice, the modest VEGF and Flk-1 mRNA levels seen without hormonal replacement were decreased significantly by treatment with oestrogen, whereas treatment with progesterone resulted in an increase in VEGF and Flk-1 mRNA levels. This led the investigators to formulate the hypothesis that oestrogen-induced early endometrial vascular permeability and stromal oedema are mediated by an early induction of VEGF and Flk-1 protein in the stromal bed, whereas, in contrast, the attenuated uterine angiogenesis during the late oestrogenic growth phase is the result of suppressed VEGF and Flk-1 mRNA expression in the stromal bed (Ma *et al.*, 2001). The findings of the current study partially support this hypothesis, as VEGF protein and mRNA levels in the current study were seen to decrease at around day 6.5 of pregnancy, after

blastocyst implantation, a time at which a peak in endometrial angiogenesis is required to sustain a pregnancy. This may relate to the second oestrogen response in the ovariectomised animals characterised by a decrease in VEGF mRNA levels (Ma *et al.*, 2001). In addition, despite a decrease in VEGF protein and mRNA levels observed within the present study as a result of RU486, these levels were still fairly high, suggesting that the combined decrease of both ovarian hormones as a result of RU486, results in a base level of VEGF as seen in the ovariectomised animals without hormone replacement (Ma *et al.*, 2001). It is also feasible that an additional regulatory factor/s influences this basal level of VEGF. Hypoxia and PDGF-BB have been shown to increase VEGF mRNA expression in a rabbit vascular smooth muscle cell line (Stavri *et al.*, 1995). Further studies on the effect of PDGF-BB on VEGF in the endometrium are needed to determine whether this is the cause of the base level of VEGF observed within the endometrium.

Using an antiserum to VEGF, Walter *et al.* (2005) showed that the stimulation of endothelial cell proliferation by progesterone is mediated, in part, by VEGF. In addition, this increase in VEGF expression by progesterone is mediated by its receptor (PR) as expression of VEGF mRNA and its receptor, Flk-1, in PR (-/-) mice was minimal, which could not be altered in ovariectomised PR (-/-) mice treated with oestrogen or progesterone (Ma *et al.*, 2001). In ovariectomised mice lacking hormonal replacement, VEGF mRNA levels were modest throughout the endometrium; however, treatment with progesterone caused an increase in VEGF expression, specifically within the stromal compartment (Ma *et al.*, 2001). Together, these results provide an explanation for the decrease seen in VEGF protein and mRNA levels by the antiprogestin RU486, suggesting that a decrease in endothelial angiogenesis in early pregnancy occurs as a result of inhibition of progesterone action via pharmacological treatment with RU486. In summary, the lack of, or impaired vascular permeability, together with subsequent inhibition of the decidual response, coupled with decreased VEGF levels leading to diminished endothelial angiogenesis, could certainly result in an unreceptive endometrium, unable to sustain a viable blastocyst.

Studies have found that progesterone-induced endothelial cell proliferation is not completely blocked by VEGF anti-serum. They attributed this lack of inhibition to parallel mechanisms that drive angiogenesis and that anti-VEGF may not be sufficient to prevent endometrial angiogenesis (Rabbani and Rogers, 2001; Heryanto and Rogers, 2002). This suggests that VEGF this is not the only factor involved in mediating progesterone induced endometrial angiogenesis and that other mechanisms may compensate for the reduction in VEGF activity. In the present study, bFGF levels were also examined within normal pregnancy as well as in RU486-treated animals. Basic FGF is another growth factor that has been reported to be important in angiogenesis. In bovine microvascular endothelial cells, a synergy between bFGF and VEGF has been demonstrated, wherein anti-FGF antibodies block VEGF-induced angiogenesis and *vice-versa*. This decrease in VEGF expression is not mediated by its

receptor as a decrease in VEGFR-2 (Flk-1) was not observed (Mandriota and Pepper, 1997; Smith, 1998). In addition, it has been suggested that bFGF is unlikely to be angiogenic in isolation within the endometrium since it lacks the ability to induce proliferation in endothelial cells derived from human decidua (Grimwood *et al.*, 1995).

As a result of the paralleled increase in bFGF in all the endometrial compartments of both the implantation and non-implantation sites at day 5.5 of pregnancy in the current study, a possible regulatory role of progesterone and/or oestrogen in regulating the increase in bFGF protein expression rather than mediation from the implanting embryo is suggested here. In support of this, previous studies have suggested that progesterone is a potent stimulator of bFGF expression within the endometrium (Rider *et al.*, 1997), whereas Fujimoto *et al.* (1996) and Rider *et al.* (1997) demonstrated an increase in bFGF expression by oestrogen. In a study by Rider and Psychoyos (1994) administration of the progesterone antagonist RU486 during early pregnancy resulted in a loss of bFGF expression in the stromal cells, inhibition of their proliferation and implantation failure. This loss of bFGF expression in the stromal cells was surprisingly not paralleled in the epithelial cells (Rider and Psychoyos, 1994). These results suggest that expression of bFGF in the luminal epithelium is not controlled by the implanting embryo, as implantation of a viable blastocyst does not occur in the RU486-treated animals. The expression of bFGF within the stromal cells may be regulated by the implanting blastocyst as the administration of RU486 and subsequent loss of a receptive endometrial state results in a reduction in stromal bFGF expression. In the present study, the Carlone and Rider (1993) study and the Wordinger *et al.* (1994) study, bFGF expression was higher in the subepithelial stroma in the implantation sites relative to the non-implantation sites around the time of blastocyst attachment and implantation.

In contrast to the investigation by Rider and Psychoyos (1994), RU486 administration at day 3.0 of pregnancy in the present study resulted in a significant reduction of bFGF expression in the luminal epithelium, the subepithelial stroma, the glandular epithelium and the glandular stroma of both the implantation and non-implantation sites at all three days of pregnancy. A possible explanation for this discrepancy is that in the Rider and Psychoyos (1994) study, RU486 was administered at days 1 and 2 postcoitum and the decrease in stromal bFGF expression was reported at day 4 of pregnancy (day of copulatory plug designated day 1), whereas in the current study, RU486 was administered at day 3 postcoitum and days 4.5, 5.5 and 6.5 of pregnancy were included in the study (day of sperm in vaginal smear designated day 0.5) As pregnancy progressed from day 4.5 to day 5.5, bFGF expression in both the implantation and non-implantation sites of the RU486-treated animals increased in the luminal epithelium and the subepithelial stroma, whereas bFGF expression decreased in the glandular epithelium and the glandular stroma. In the blood vessels and stroma surrounding the blood vessels, bFGF expression remained constant with the progression of pregnancy to day 5.5 in the implantation

sites and decreased in the non-implantation sites. By day 6.5 of pregnancy, bFGF protein levels increased in all endometrial compartments in both the implantation and non-implantation sites. Analysis of bFGF mRNA expression following treatment with RU486, mimicked the protein expression pattern as bFGF mRNA levels increased by 2.5-fold in the implantation sites and by 7.7-fold in the non-implantation sites. This increase in bFGF expression in the RU486-treated animals with the progression of pregnancy can be attributed to the half-life of RU486; once RU486 is metabolised and vacates the PR for binding by progesterone, any progesterone effects previously inhibited by RU486 are re-established. This increase in bFGF expression with an increase in progesterone signalling confirms the hypothesis of the current study; that bFGF is regulated by one of the ovarian hormones, oestrogen or progesterone, rather than by the implanting blastocyst.

In contrast to findings of the present study, Wordinger *et al.* (1992) showed that bFGF localisation was neither influenced by the stage of the oestrous cycle nor ovariectomy alone, neither was it influenced by steroid hormone supplementation, suggesting that bFGF expression is not regulated by the ovarian hormones. However, in accordance with the hypothesis of the current study, Rider, Carlone and Foster (1997) reported an increase in bFGF mRNA as a result of steroid treatments relative to the vehicle control animals; bFGF expression increased following oestrogen administration, as well as with a combination of progesterone and oestrogen. The combination, however, repressed bFGF mRNA accumulation, relative to oestrogen treatment alone (Rider *et al.*, 1997). In addition, other reports suggest regulation of bFGF by oestrogen, as Carlone and Rider (1993) reported an increase in stromal cell bFGF expression in the ovariectomised rat endometrium following treatment with oestrogen. Further, bFGF increased in a human endometrial adenocarcinoma cell line after oestrogen supplementation (Presta, 1988). It has previously been suggested that RU486 has both an antiprogestin and anti-oestrogen affect on the rat endometrium as RU486 results in a more hormonally under-stimulated endometrium (Scholtz *et al.*, 2008). In addition, it has previously been reported that RU486 is able to block oestrogenic responses with over 80% efficiency (McDonnell and Goldman, 1994). It is thus possible that the decrease in bFGF expression reported in the present study, following RU486 administration may be a consequence of such an inhibition of oestrogen action, rather than inhibition of progesterone. Likewise, the increase in bFGF expression in the RU486-treated animals with the progression of pregnancy and metabolism of RU486 may be due to an increased ability of oestrogen to bind to its receptors with the activation of its signalling pathways.

If the hypothesis of the present study is correct, then the increase in bFGF expression observed in both the implantation and non-implantation sites in the control pregnant animals at day 5.5 of pregnancy in the current study may be as a result of the increase in oestrogen expression indicative of early pregnancy and necessary in rodents for initiation of implantation of a viable blastocyst. If bFGF expression is regulated by the ovarian hormone oestrogen within the rat endometrium then this would

account for the overall increase in bFGF expression observed in the endometrial compartments in both the implantation and non-implantation sites in the current study. This in contrast to the spatiotemporal difference in bFGF expression reported within the various endometrial compartments by Carlone and Rider (1993).

6.3.1.2.2 The Spatiotemporal Expression Pattern of PDGF in the Pregnant Rat Endometrium

The predominant role of platelet-derived growth factor (PDGF) is to stimulate the proliferation of mesenchymal cells, which includes vascular tissue and connective tissue (Ross *et al.*, 1985). As this growth factor has been identified in various tissue and cell types, including the endometrium (for a review see Habenicht *et al.*, 1990), immunofluorescent methods were used in this study to localise the cellular distributions of PDGF in the rat endometrium, specifically at days 4.5, 5.5 and 6.5 of early pregnancy. In addition, any possible changes in the localisation of PDGF were assessed, following treatment with the partial antiprogestin RU486.

In the control pregnant animals at day 4.5 of pregnancy, PDGF protein was localised to cells of the luminal and glandular epithelium as well as in the stromal compartments of both the implantation and non-implantation sites, this being in agreement with previous studies on PDGF localisation in the mouse (Jaber and Kan, 1998) and rat (Slater and Murphy, 1999) endometrium. This study additionally demonstrates PDGF localisation in the blood vessels of the endometrium, consistent with a previous study of early pregnancy in the porcine endometrium (Persson and Rodriguez-Martinez, 1997). The present study found that PDGF localisation was similar in all endometrial compartments analysed, inclusive of the implantation and non-implantation sites at day 4.5 of pregnancy.

As pregnancy progressed from day 4.5 to day 5.5, PDGF protein levels increased considerably in all endometrial compartments analysed in both the implantation and non-implantation sites. This increase was more marked in the implantation sites, resulting in considerably higher levels of PDGF protein in the endometrial compartments of the implantation sites. This marked increase in PDGF localisation was also reported in the mouse endometrium around the time of blastocyst implantation (Jaber and Kan, 1998); however, the differences between the implantation and non-implantation sites was not analysed. They did, however, report an increase in PDGF expression in the decidual boundary zone surrounding an implanted embryo, at day 7 of pregnancy (the equivalence of day 7.5 of pregnancy in the rat endometrium). It is important to note that no PDGF localisation was observed in the implanting embryo (Jaber and Kan, 1998). Slater and Murphy (1999) reported an increase in PDGF localisation to the apical surface and the lateral plasma membrane of the luminal epithelial cells with the progression of early pregnancy, maximal levels being detected on day 6 (presence of sperm in vaginal smear designated day 1) of pregnancy. They attributed this increase in PDGF to a role in preparing the

luminal epithelium for attachment and invasion by the implanting blastocyst, since PDGF localised to all the surfaces along the path of the invading trophoblastic invadapodia; including, the apical surface, the lateral plasma membranes and basement membrane (Slater and Murphy, 1999). This observation could account for the considerably higher levels of PDGF reported specifically in the implantation sites at day 5.5 of pregnancy in the current study, as the pathway for the invasion of the trophoblastic invadapodia would exist primarily in the implantation sites.

By day 6.5 of pregnancy, PDGF protein levels decreased significantly in all endometrial compartments of both the implantation and non-implantation sites. Slater and Murphy similarly reported a decrease in PDGF in the luminal epithelium at this day of pregnancy; however, they attributed this apparent loss in PDGF localisation to an increase in stromal labelling, resulting in masking of the PDGF localisation in the luminal epithelial cells. In the present study, as PDGF protein levels were considerably reduced in all of the endometrial areas, the reported decrease is clearly not as a result of masking by an increase stromal expression of PDGF expression.

In addition to studying the expression pattern of PDGF during early pregnancy, Slater and Murphy (1999) investigated the spatiotemporal localisation of the extracellular matrix adhesive protein, fibronectin (FN); an important mediator of cell migration and attachment. Their findings suggest that FN is up-regulated by PDGF during early pregnancy within the basement membrane and the underlying stroma. In addition, they suggested that this synergy between PDGF and FN is necessary for preparation of the uterine epithelial cells for attachment and invasion by providing a pathway for the trophoblastic invadapodia and the breaching of the basement membrane by the decidual cells (Slater and Murphy, 1999). If one of the roles of PDGF during early pregnancy is to stimulate the expression of other factors such as FN, then the increase in PDGF expression at day 5.5 of pregnancy, as reported in this study, may be sufficient to drive the subsequent invasion and implantation of the blastocyst. Moreover, the reported decrease in PDGF expression at day 6.5 may well be as a result of a down-regulatory stimulus by one of the increased factors, functioning through a negative-feedback loop. More research is needed to better elucidate this decrease in PDGF expression at this day of pregnancy.

In contrast to this decrease in the implantation sites with regards to PDGF protein levels, PDGF mRNA levels increased by 2-fold as pregnancy progressed from day 5.5 to day 6.5. In the non-implantation sites, however, the significant decrease in protein levels was reflected in the PDGF mRNA levels, as here there was a reduction by 2.75-fold with the progression of pregnancy. This increase in PDGF mRNA levels in the implantation sites can possibly be explained by dilution of effects due to the use of whole tissue homogenates as PDGF expression was not analysed in one of the largest endometrial compartment, the myometrium. The possibility that PDGF protein expression

increases in the myometrium as pregnancy proceeds, and that this increase is responsible for the overall increase in PDGF expression in the implantation sites reported here, is supported by an increase in proliferative activity in the myometrium and mesometrial triangle around days 5.5 and 6.5 of pregnancy with the degree of proliferative activity in the non-implantation sites remaining low (see Goodger and Rogers, 1993). It is suggested here that, were PDGF to be responsible for driving this increase in cell proliferation, then it is feasible that it is this increase that is specifically responsible for the overall increase in PDGF expression in the implantation sites reported in this study, spanning days 5.5 to 6.5 of pregnancy in the rat uterus.

In the study by Jaber and Kan (1998), they suggested that the localisation of PDGF to the luminal and glandular epithelium around the time of blastocyst implantation may be due to secretion of this growth factor by the associated endometrial cells. It has previously been postulated that uterine secretions are vital to ensure the luminal environment contains factors necessary to support the initial development of the embryo (Gray *et al.*, 2002). In this regard, Thibodeaux *et al.* (1993) found that PDGF provides a similar developmental stimulus for bovine embryos during the beginning stages of development to that of the oviductal epithelial cells. Jaber and Kan (1998) reported PDGF localisation in the embryo at the blastocyst stage, prior to implantation. Once the embryo had implanted into the uterine wall, no PDGF localisation was observed (Jaber and Kan, 1998). A study on the mouse embryo demonstrated expression of the protein and mRNA for the receptor for PDGF, PDGF-R, in pre-implantation embryos at the blastocyst stage with low levels of PDGF expression in the post-implantation embryo prior to day 7 of pregnancy (Palmieri *et al.*, 1992). When combined, these results suggest that PDGF may play an important role in supporting the development of the blastocyst in an autocrine/paracrine manner. It thus follows that the increase in PDGF expression in the luminal epithelium reported in this study may be as a result of this crucial role for PDGF, and moreover, may be the mechanism through which the blastocyst implants specifically in the implantation sites where increased vascular permeability occurs, this being regulated maternally (Ma *et al.*, 2001). Support for this hypothesis wherein the embryo and endometrium communicate through PDGF and PDGF-R during early pregnancy is supported by neutralisation of PDGF by anti-PDGF antibodies, which results in a significant reduction in both the implantation rate and size of the implantation sites, so confirming an important role for PDGF in the endometrium during early pregnancy (Holmes *et al.*, 1997).

6.3.1.2.2.1 The effects of RU486 on PDGF expression patterns

Jaber and Kan (1998) reported low levels of PDGF during the oestrous cycle in the mouse endometrium, followed by increased PDGF protein localisation in the luminal and glandular epithelium as well as the stroma during the first 7 days of early pregnancy. This led them to conclude that PDGF plays an important role in early gestation (Jaber and Kan, 1998). It is known that in

preparation for blastocyst implantation, the different cellular compartments of the endometrium undergo changes in cell proliferation and differentiation (Ljungkvist, 1972a). Taking into account the roles of PDGF in controlling growth, differentiation and activation of various cell types (Ross *et al.*, 1985; Westermark *et al.*, 1990; Raines and Ross, 1992) and its markedly increased endometrial concentrations corresponding to blastocyst implantation, as documented in this study, it is highly likely that PDGF plays an important role in remodelling and preparing the endometrium for implantation. In confirming an important role for PDGF in the endometrium during early pregnancy, neutralisation of PDGF in the mouse endometrium, prior to implantation, results in a significant reduction in both the implantation rate and size of the implantation sites (Holmes *et al.*, 1997). In view of this finding, an inhibition of the considerable decrease in PDGF expression by PDGF during early pregnancy may be one of the mechanisms through which RU486 exacts its anti-pregnancy effect.

In the current study, RU486 administration at day 3.0 of pregnancy resulted in higher levels of PDGF protein expression in the luminal epithelium and subepithelial stroma at day 4.5 of pregnancy in the implantation and non-implantation sites of the RU486-treated animals, relative to the control pregnant animals. In the other endometrial compartments analysed, PDGF levels were similar in both the control pregnant and RU486-treated animals. This lack of decrease in the RU486-treated animals cannot be attributed to unopposed oestrogen action, thereby suggesting a regulatory role of oestrogen in PDGF expression, as it has been demonstrated in previous portions of this research that RU486 results in a more hormonally under-stimulated endometrium, rather than one over-stimulated by oestrogen. These results thus suggest that PDGF is not regulated by either of the ovarian hormones, oestrogen or progesterone, and must, therefore, be regulated by another factor/s not influenced by blocking progesterone signalling by RU486.

At day 5.5 of pregnancy in the control pregnant animals, this study demonstrated a considerable increase in PDGF protein levels in all endometrial compartments analysed, particularly in the implantation sites. Though administration of RU486 inhibited the significantly higher expression of PDGF in the implantation sites at this day of pregnancy, PDGF levels still remained high at this day of pregnancy. This confirms the hypothesis suggested earlier that PDGF expression in the implantation sites is controlled, in part, by the implanting blastocyst as the considerable increase in PDGF expression in the implantation sites is lost in the RU486-treated animals as a consequence of a lack of a signalling blastocyst in the lumen. The high levels of PDGF protein expression in the RU486-treated animals at all three days of pregnancy, together with the expression of PDGF protein at similar levels in the non-implantation sites of the control pregnant animals, suggests that the overall control of PDGF in the endometrium is by a factor/s independent of both the implanting blastocyst and the ovarian hormones. In support of this hypothesis, previous studies report that PDGF is

regulated by growth factors such as TNFα and interferon γ (IFNγ) in carcinoma cell lines, as well as in the human endometrium (see Smith, 1998). Studies on the effect of RU486 on the expression of these growth factors during early pregnancy would be crucial to better understanding the regulation of PDGF in the endometrium.

In contrast to the immunolocalisation pattern of PDGF, expression of PDGF mRNA was considerably decreased by 27-fold in the implantation sites and 39-fold in the non-implantation sites at day 5.5 of pregnancy, relative to the calibrator sample, this as a result of RU486 administration. By day 6.5 of pregnancy, PDGF mRNA levels had increased in the RU486-treated animals and thus the difference was 4.3-fold in the implantation sites and 6.7-fold in the non-implantation sites relative to the calibrator sample at day 6.5 of pregnancy. This discrepancy can be explained by a previous report that PDGF is one of the growth factors that, like bFGF, can be stored in the extracellular matrix (Raines and Ross, 1992). Thus, it can be postulated that RU486 possibly does not have an effect of PDGF protein levels as sufficient PDGF is stored within the extracellular matrix to be released as necessary within the endometrium of the RU486-treated animals. There was a gradual increase in PDGF protein levels in the RU486-treated animals with the progression of pregnancy within this study, suggesting that PDGF is released from the extracellular stores. By day 6.5 of pregnancy, PDGF protein levels began to decrease in the non-implantation sites of the RU486-treated animals, which could be explained by a decline in PDGF proteins stored in the extracellular matrix for release. The considerable decrease in PDGF mRNA levels as a result of RU486 administration suggests that at the level of gene expression (mRNA), PDGF is regulated by one of or both the ovarian hormones, oestrogen and progesterone. The increase in PDGF mRNA expression in the RU486-treated animals from day 5.5 to day 6.5 of pregnancy can be attributed to the half-life of RU486. As RU486 metabolises, progesterone, and to a smaller degree oestrogen, are able to bind to their receptor and exact their effects on the endometrium. It would follow that were PDGF regulated by oestrogen or progesterone, expression should increase with an increase in ovarian hormone receptor binding and signalling; and this characteristic has been demonstrated in the present study. Studies in animals at day 7.5 of pregnancy and onward would be beneficial to ascertain whether this hypothesis is correct and whether this decrease in PDGF mRNA levels is reflected in PDGF protein levels once the extracellular stores are depleted.

6.3.1.3 Endothelial cell proliferation

PDGF has also been reported to play an important role in the increased angiogenesis of early pregnancy to sustain the implanting and developing embryo (Rodriguez-Martinez *et al.*, 1992). In this study, PDGF protein levels in the blood vessels and in the stroma (i.e. stromal cells and endothelial cells) were increased significantly around the time of implantation, with the most marked increase occurring in the implantation sites. By day 6.5 of pregnancy, PDGF levels had decreased again

considerably in these endometrial compartments. In a study using cultured rat endometrial explants to measure angiogenic activity, as demonstrated by the migration of vascular endothelial cells towards the explants, indicated an increase in endothelial cell migration in response to explants taken from day 4.5 pregnant rats. This increase in endothelial cell migration returned to minimal levels by day 5.5 of pregnancy (Abberton and Rogers, 1995). In addition, in a study on endothelial cell proliferation before and after embryo implantation, the endothelial cell proliferative index increased around the entire endometrium on days 3.5 and 4.5 of pregnancy and continued to increase in the implantation sites at days 5.5 and 6.5 of pregnancy. In the non-implantation sites, however, the endothelial cell proliferative index fell sharply at this stage of pregnancy (Goodger and Rogers, 1993).

PDGF has been implicated in the maturation and remodelling of vessels during angiogenesis through the recruitment of vascular smooth muscle cells and pericytes (Armulik *et al.*, 2005). In addition, PDGF-B and PDGF-BR mRNA knockout experiments have indicated an important role for PDGF signalling in the establishment of functional blood vessels through the recruitment of stabilising mural cells to the developing blood vessels (reviewed in von Tell *et al.*, 2006). The recorded increase in PDGF levels within implantation sites in this study would seem to correlate not only with increased endothelial cell migration just prior to implantation, but also to an increase in endothelial cell proliferation around the time of blastocyst implantation; hence, a possible role for PDGF in angiogenesis during early pregnancy in the rat uterus is suggested here. More specifically, it is suggested here that the increased endothelial cell migration that occurs at day 4.5 of pregnancy triggers the increase in PDGF expression observed at day 5.5 of pregnancy in both the implantation and non-implantation sites, either directly or indirectly via another factor/s.

It is further suggested here that this increase in PDGF expression partially controls the increase in endothelial cell proliferation reported at day 5.5 of pregnancy in the implantation sites, directly or indirectly, as PDGF levels are higher in the implantation sites at this day of pregnancy. In support of this hypothesis, the endothelial cell proliferative index has been reported to be similar in both the implantation and non-implantation sites at day 4.5 of pregnancy (Goodger and Rogers, 1993). This is reflective of the PDGF expression levels recorded in the present study. In addition, by day 5.5 of pregnancy, PDGF protein levels were highest in the implantation sites relative to the non-implantation sites, as mirrored by the highest rate of endothelial cell proliferation at this particular stage of pregnancy (Goodger and Rogers, 1993).

However, the increase in endothelial cell proliferation was demonstrated from as early as day 2.5 of pregnancy, albeit at low levels initially until day 5.5 of pregnancy (Goodger and Rogers, 1993). In contrast, the increase in endothelial cell migration was only observed at day 4.5 of pregnancy (Abberton and Rogers, 1995), thus it may be that the increase in PDGF expression drives the change

in endothelial cell proliferative patterns observed at day 5.5 of pregnancy, between the implantation and non-implantation sites and not necessarily the increase in endothelial cell proliferation itself. Goodger and Rogers (1993) suggested two separate mechanisms controlling endothelial cell division in the endometrium around the time of blastocyst implantation. They hypothesised that the first mechanism is maternally controlled throughout the endometrium prior to implantation, while the second mechanism is an embryo mediated signal acting locally, subsequent to embryo implantation (Goodger and Rogers, 1993). If this hypothesis is correct then it may be that the considerable increase in PDGF expression is controlled by the implanting blastocyst at day 5.5 of pregnancy, which may in turn control the increase in endothelial cell proliferation at day 5.5 of pregnancy. In actuality, PDGF expression decreases, but is not lost at day 6.5 of pregnancy, as is the case with PDGF localisation on the embryo itself (Palmieri *et al.*, 1992). This supports the hypothesis that PDGF expression is, at least partially, controlled by the blastocyst. The factor/s involved in the loss of PDGF expression in the implanting embryo and the decrease in PDGF expression in the endometrium at the same stage of pregnancy remain to be established.

The continued increase in endothelial cell proliferation (Goodger and Rogers, 1993), despite the decrease in PDGF expression, suggests that while PDGF is necessary to drive the increase in proliferation, it does not control the down-regulation of this process. As discussed previously, both VEGF and bFGF levels remain high at day 6.5 of pregnancy in both the implantation and non-implantation sites. It has been reported previously that PDGF is one of the growth factors, like bFGF, able to regulate VEGF-induced angiogenesis (Stavri *et al.*, 1995). Thus, it is possible that the higher levels of PDGF expression in the implantation sites at day 5.5 of pregnancy specifically, may result in an increase in VEGF-induced endothelial cell proliferation, so providing an explanation for the continued high levels of proliferation observed at this stage of pregnancy. The lack of PDGF regulation in the non-implantation sites may account for the reduction of proliferation observed in the non-implantation sites.

6.3.1.4 The angiogenic pathway-related growth factors and the decidual response

In addition to increased VEGF expression within the blood vessels and the stroma in the current study, VEGF protein levels were seen to be significantly higher in the decidual layer of the implantation sites at day 5.5 of pregnancy. Despite similar levels of bFGF protein in the luminal epithelium, glandular epithelium and glandular stroma in both the implantation and non-implantation sites, analysis of bFGF protein expression also revealed an increase in protein expression in the implantation sites relative to the non-implantation sites. Similar increases in VEGF and bFGF expression in the decidua of early pregnancy have previously been reported in the human endometrium (Sugino *et al.*, 2002), the mouse endometrium (Shweiki *et al.*, 1993; Wordinger *et al.*,

1994) and the rat endometrium (Carlone and Rider, 1993). Shweiki *et al.* (1993) suggested that the transformation of the stromal cells into decidual cells leads to an up-regulation of VEGF expression within the decidual cells. This increase in VEGF production by the decidua may potentially support the proliferation of interspersed endothelial cells, essential for the expansion of the decidual vasculature (Shweiki *et al.*, 1993). Shweiki *et al.* (1993) also demonstrated that only cells having undergone decidual transformation expressed VEGF, which would account for the increase in VEGF expression described in the present study within the decidual layer, as pregnancy proceeded from day 4.5 to day 5.5.

In the mouse endometrium, Wordinger *et al.* (1994) reported the expression of bFGF in the subepithelial stroma at the embryo-stroma interface during the peri-implantation stage and suggested a role for bFGF in the initial invasion of the blastocyst into the surrounding decidua, since it is known that this growth actor is able to stimulate collagenases and plasminogen activator. In the rat uterus, Carlone and Rider (1993) reported low levels of matrix-associated bFGF in the periluminal (subepithelial) region of the non-implantation sites. This was also true for the implantation sites; however, at day 5.5 of pregnancy peri-nuclear expression of bFGF was restricted to the decidual cells in the implantation sites (Carlone and Rider, 1993). The current study did not distinguish between matrix-associated or nuclear-associated bFGF expression and thus it is likely that the increase in bFGF expression in the implantation sites in the present study is as a result of the nuclear-associated bFGF reported by Carlone and Rider (1993). Since growth factors, including bFGF, have been known to be stored in the extracellular matrix (Bashkin *et al.*, 1989; Logan and Hill, 1992), the differences in matrix-associated bFGF expression led the investigators to suggest that extracellular bFGF may be utilised during decidualisation and implantation (Carlone and Rider, 1993). In artificially induced deciduoma, the loss of matrix-associated bFGF was also observed in the periluminal region of the stroma (Carlone and Rider, 1993), suggesting that this loss in matrix-associated bFGF is not controlled by the implanting blastocyst.

Not only is PDGF a potent mitogen for angiogenic precursor cells, but also for fibroblasts (Ross *et al.*, 1985). Coupled with the observed localisation of PDGF to the subepithelial stroma in this study, specifically in the implantation sites, these data suggest that a particular role for PDGF in the decidual response of early pregnancy. A study on stromal cell proliferation demonstrated a dose-dependent increase by PDGF, suggesting that PDGF is a potent mitogen for human endometrial stromal cells (Surrey and Halme, 1991). A study on human decidual cells reported the production of PDGF, the presence of PDGF-R and a stimulatory effect of PDGF on DNA synthesis, suggesting a role for PDGF in this cellular compartment during early pregnancy (Saji *et al.*, 1997).

As the decidual response was reduced in the RU486-treated animals, it follows that VEGF and bFGF levels within the subepithelial layer would decrease as a result of RU486 treatment, as demonstrated in this study. PDGF levels, however, did not decrease as a result of RU486 treatment, suggesting that the decrease in the decidual response in the RU486-treated is not regulated by this growth factor. It would, therefore, seem that of the three growth factors investigated here, VEGF and bFGF are the most likely candidates responsible for the decidual response of early pregnancy.

As decidualisation is accompanied by extensive angiogenesis to ensure foetal survival, it is postulated that this increase in VEGF expression within the deicidal layer reported in previous studies (Shweiki *et al.*, 1993), and including the current study, may potentially support the proliferation of interspersed endothelial cells, these being essential for the expansion of the decidual vasculature.

In accordance with the current study, Rider and Psychoyos (1994) reported a decrease in bFGF expression within the stromal cells following RU486 administration. FGFs are potent mitogens that bind to heparin sulphate proteoglycans (Vlodavsky *et al.*, 1987) and stimulate the migration of endothelial cells (Montesano *et al.*, 1986). This suggests that the increase in bFGF expression in the subepithelial stroma of the implantation sites in the control pregnant animals may also play a role in the expansion of decidual vasculature and that administration with RU486 may act to inhibit this increase in angiogenesis vital to the survival of an implanted blastocyst. It is thus postulated here that this decrease in angiogenesis within the decidual bed may be an additional mechanism through which RU486 is able to inhibit progression of pregnancy and thus function as a reliable postcoital contraceptive.

CHAPTER 7

THE EFFECTS OF RU486 ON SELECTED ENDOMETRIAL BIOMARKERS DURING EARLY PREGNANCY IN THE RAT UTERUS

7.1 INTRODUCTION

The last endometrial event of implantation analysed was the control of the endometrial biomarkers; Leukaemia Inhibitory Factor (LIF), Mucin-1 (Muc-1) and Calcitonin, which have been reported previously to be crucial to the establishment of the window of receptivity (Giudice, 1999; Carson *et al.*, 2000; Cavagna and Mantese, 2003). The up- or down-regulation of these biomarkers around the time of blastocyst implantation in the implantation sites of the endometrium identify them as biological markers of uterine receptivity. All three biomarkers analysed play a crucial role in blastocyst implantation and subsequent pregnancy; in LIF null mice, implantation is unable to occur (Stewart *et al.*, 1992); the anti-adhesive nature of Muc-1 requires that this biomarker must be down-regulated at the time of implantation in order to remove this barrier to blastocyst implantation (Aplin, 1997); and *in utero* Calcitonin antisense oligodeoxynucleotide administration severely impairs implantation in rats (Zhu *et al.*, 1998b). These data combined led to the formulation of the hypothesis that if RU486 had an inverse effect on the expression patterns of these endometrial biomarkers during early pregnancy, then this may inhibit blastocyst implantation.

7.1.1 Endometrial Biomarkers

There are multiple factors involved in the process of embryonic implantation. Some signals arise from the blastocyst, while others are associated with the endometrium. As the endometrium is the particular focus of the present study, one needs to consider the molecular milieu of the endometrial compartments, particularly of those cells most closely associated with implantation. The understanding of the regulation of the genes involved here requires a correlative analysis between gene expression and the period of implantation. Also, valuable information is gained from investigating the effects of the up- or down-regulation of factors on the modulation of gene expression and implantation.

The window of receptivity or implantation is thought to occur around cycle days 20-24 in humans and correspondingly around days 4.5 to 5.5 of pregnancy in the rat. This period of maximum uterine receptivity to implantation is defined by documented changes in morphology, gene expression and potential molecular markers; inclusive of the localised expression of certain known peptides and proteins (Murphy, 2000a; Cavagna and Mantese, 2003; Achache and Revel, 2006; Wang and Dey, 2006). In order for successful implantation of the blastocyst to occur during this window of receptivity the embryo must be of good quality and the endometrium must be receptive to ensure the

embryo-maternal interactions necessary for the attachment and invasion of the blastocyst into the endometrium (Cavagna and Mantese, 2003).

Early implantation abnormalities are the major cause of pregnancy failure in both assisted reproduction and natural pregnancy (Cavagna and Mantese, 2003). Identification of biological markers of uterine receptivity may help to improve implantation rates in natural and assisted reproductive cycles, or may help to establish efficient contraceptions (Dey *et al.*, 2004; Achache and Revel, 2006; Wang and Dey, 2006). These peptide and protein biomarkers need to meet certain criteria so as to be classed as a biomarker of uterine receptivity, as described by Zhu *et al.* (1998a): "it should be present in the endometrium, preferably at or near the site of implantation. It should appear within the window of implantation, or precede it by a certain amount of time, and disappear with the termination of the receptive phase". In addition, Kumar *et al.* (1998) state that "by definition, a true marker of uterine receptivity should have a relevant functional role during the implantation process".

While a number of biomarkers of implantation have already been established; including, LIF, Muc-1 and Calcitonin (Giudice, 1999; Carson *et al.*, 2000; Cavagna and Mantese, 2003; Achache and Revel, 2006), not all of these biomarkers disappear completely following the window of receptivity. It is therefore suggested here that these biomarkers should change significantly and consistently around the time of blastocyst implantation in order to be classified as a biomarker of endometrial receptivity. The endometrial biomarkers described by Giudice (1999) have been shown to be important in the implantation process. It is thus likely that the administration of RU486 during early pregnancy could have a detrimental effect on the expression of these biomarkers, possibly resulting in or being part of the disruption in pregnancy associated with RU486 administration.

7.1.1.1 Leukaemia inhibitory factor (LIF)

LIF is a pleiotropic glycoprotein of the interleukin-6 family, which is not only expressed in the endometrium and associated with normal implantation, but is expressed at low levels in many different tissues. Although LIF exhibits a number of biological functions; including, modulation of proliferation and differentiation, and cell survival, all of which are associated with blastocyst development and implantation (Hilton and Gough, 1991; Carson *et al.*, 2000), its exact function in implantation is yet to be determined. LIF exerts its effects by binding to two dimerising receptor subunits, the LIF receptor (LIF-R) and glycoprotein 130 (gp130). The binding of LIF to its low affinity receptor (LIF-R) causes an association with gp130, subsequently resulting in signal transduction (Figure 7.1) (Davis *et al.*, 1993).

Significant levels of LIF have been reported in uterine flushings from the endometrium of fertile woman (Laird *et al.*, 1997), which coincides with LIF levels observed in the mid-late secretory phases

of the menstrual cycle (Arici *et al.*, 1995; Vogiagis *et al.*, 1996). In the uterine flushings of woman with proven, yet unexplained, infertility, LIF concentrations were significantly lower than those obtained from fertile woman at the same stage of the menstrual cycle (Laird *et al.*, 1997). This decrease in LIF expression around the expected time of blastocyst implantation may contribute to the early pregnancy failure rate being so high.

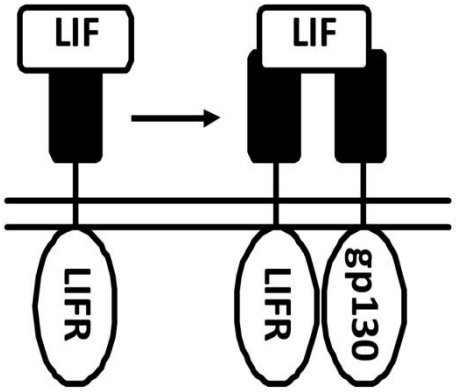


Figure 7.1 Schematic representation of the LIF receptor complex. LIF binds to its receptor, LIFR. Gp130 is then bound to form a heterodimer, which results in signal transduction (Vogiagis and Salamonsen, 1999).

Gene inactivation experiments in mice show an absolute requirement for LIF in order for successful implantation to take place (Stewart *et al.*, 1992). LIF-deficient mice, though found to have normal blastocysts, were unable to initiate implantation. When these blastocysts were transplanted to wild-type recipient females, normal implantation and development occurred. In addition, the treatment of the LIF (-/-) females with recombinant LIF resulted in successful implantation of the blastocyst as well as a decidual response. Collectively, these data suggest that LIF plays a crucial role in the regulation of implantation and moreover, in the absence of LIF, the mouse embryo is only able to develop normally up to the blastocyst stage (Stewart *et al.*, 1992).

Stewart (1994) reported that LIF is also essential for decidualisation during early pregnancy, as attempts to induce decidualisation in LIF-deficient female mice was unsuccessful. In a study by Laird *et al.* (1997) it was reported that LIF concentrations were significantly lower in women with unexplained infertility, supported by findings of mutations in the coding region of the LIF gene in some infertile woman (Giess *et al.*, 1999). These findings suggest that LIF plays a crucial role in blastocyst implantation during early pregnancy.

In the endometrium of mice, LIF mRNA and protein is expressed in high quantities in the glandular epithelium at day 0.5 of pregnancy (day 0.5 being the day of the vaginal plug) and declines by day 2.5 (Shen and Leder, 1992). A second burst of LIF expression occurs at day 3.5 of pregnancy (the day of blastocyst implantation in mice). By day 5 of pregnancy, after blastocyst implantation, LIF expression

declines and remains at this low level throughout the remainder of the gestation period (Bhatt *et al.*, 1991). This increase in LIF expression around the time of blastocyst implantation and subsequent decline in LIF levels is also observed in pseudopregnant mice, indicating that LIF is maternally controlled rather than induced by a signal originating from the blastocyst (Bhatt *et al.*, 1991; Shen and Leder, 1992).

LIF exacts its effect by binding to the low affinity LIF receptor (LIFR). This leads to binding of a second low affinity receptor component, gp130, to this complex to form a heterodimer, resulting in a receptor combination that generates a high affinity binding site (Figure 7.1) (Gearing *et al.*, 1991; Gearing *et al.*, 1992; Ip *et al.*, 1992). In the mouse endometrium, it has been suggested that uterine epithelial-derived LIF acts in a paracrine manner on the blastocyst and/or as an autocrine regulator of endometrial epithelium to allow the implantation of a blastocyst (Stewart *et al.*, 1992).

In the ovariectomised mouse endometrium, LIF protein expression is up-regulated by 17β-estradiol alone or a combination of 17β-estradiol and progesterone. Progesterone alone has no apparent effect on LIF protein expression in the endometrium of mice (Yang *et al.*, 1996). Conversely, in the same study by Yang *et al.* (1996), in the rabbit endometrium, LIF protein expression was upregulated by administration of progesterone alone or a combination of 17β-estradiol and progesterone. 17β-oestradiol alone had no apparent effect on LIF protein expression in the rabbit endometrium (Yang *et al.*, 1996). A study by Ding *et al.* (2008) showed that LIF is also important for uterine receptivity and implantation in the progesterone-primed uterus, specifically in the hamster endometrium.

LIF expression appears to be regulated by oestradiol in the mouse since the two peaks of LIF expression coincide with physiologically elevated levels of oestrogen (Bhatt *et al.*, 1991; Yang *et al.*, 1996). It is also possible that the priming of the uterus by progesterone prior to the oestrogen peak is important for LIF expression during early pregnancy, as the administration of a combination of 17β-oestradiol and progesterone up-regulated LIF expression. However, in the rabbit and the hamster endometria, LIF expression seems to be under progesterone control (Yang *et al.*, 1996; Ding *et al.*, 2008). Likewise, in the human endometrium, LIF expression is highest during the post-ovulatory phase when the endometrium is under the influence of progesterone (Sharkey *et al.*, 1999). Further, in human studies, treatment with RU486 immediately post-ovulation was shown to reduce endometrial immunolocalisation of LIF within the glands at the expected time of implantation (Danielsson *et al.*, 1997).

7.1.1.2 Mucin-1 (Muc-1)

Prior to the window of receptivity, both the trophectoderm of the blastocyst and the apical surface of the uterine epithelium are nonadhesive in nature. In order to facilitate apposition and attachment of the blastocyst to the uterine apical epithelial surface during the window of receptivity, both tissues must be converted to an adhesive-competent state (Carson *et al.*, 2000). Mucins are large, high-molecular-weight (250 – 500 kDa), highly glycosylated molecules found on many cell surfaces (Dominguez *et al.*, 2002). One of the most well-known mucins, Muc-1, also known as episialin, makes up part of the glycocalyx covering the apical membrane of the uterine epithelial cells (Jones and Murphy, 1994) and extends further than the other components of the glycocalyx; around 200 – 500nm from the epithelial cell surface (Hilkens *et al.*, 1992).

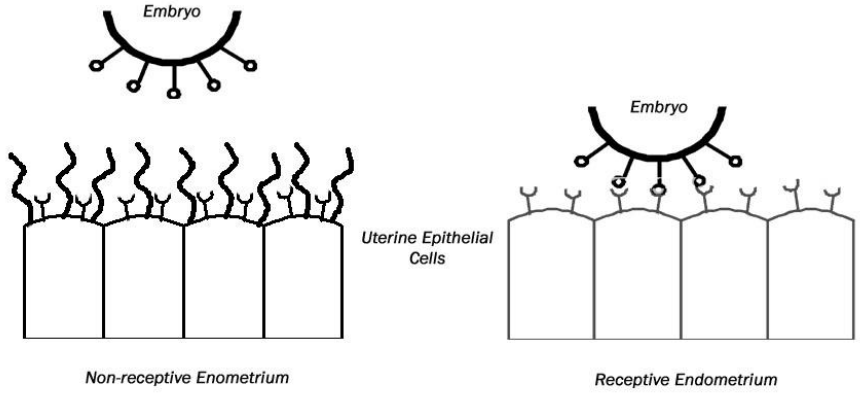


Figure 7.2 Schematic representation of the function of Muc-1 as an anti-adhesive molecule and a barrier to blastocyst implantation. The extended structure of Muc-1 prevents the blastocyst from interacting with the apical surface of the maternal tissue when the endometrium is unreceptive. The removal of this barrier to implantation allows the blastocyst to attach during the receptive phase (adapted from Surveyor *et al.*, 1995).

.

One of the most important properties of Muc-1 is its role as an anti-adhesive mucin. In the endometrium it is expressed predominantly on the apical surface of the uterine epithelium and is believed to play a role in embryo attachment (Figure 7.2) (Hey *et al.*, 1994), as well as to provide a physical barrier to enzymatic attack and infection (McAuley *et al.*, 2007). This anti-adhesiveness of Muc-1 appears to be related to its structure. It has a short cytoplasmic domain and a large extracellular domain containing a variable number of tandem repeat (VNTR) units. These VNTR units are made up of a conserved 20 amino acid sequence each of which contains five potential O-glycosylation sites (Lancaster *et al.*, 1990). At the cell surface, it is thought that Muc-1 takes on an extended conformation due to its long hydrophilic VNTR domain and extensive glycosylation. Because of this, it probably extends outward from the apical surface further than receptors that mediate cell-cell adhesion, thus masking them. In this way, Muc-1 may act to inhibit the interaction of the blastocyst with the adhesion molecules, such as integrins and cadherins, on the surface of the endometrial epithelium generating the hypothesis that Muc-1 acts as a uterine barrier to implantation (Aplin *et al.*,

2001). This barrier must be removed in order to allow the close contact between the blastocyst and the maternal endometrium necessary to insure successful implantation.

In order for Muc-1 to be a barrier to blastocyst implantation, it must be localised on the external surface of the uterine epithelium (Isaacs and Murphy, 2003). Using an ultrastructural cytochemical method, Isaacs and Murphy (2003) demonstrated that Muc-1 is localised to the apical region of the uterine epithelial cells, with the strongest expression along the outer surfaces of the microvilli. When the endometrium is receptive to blastocyst implantation, Muc-1 was not detected ultrastructurally, lending more credibility to the hypothesis that Muc-1 acts as a barrier to blastocyst implantation (Isaacs and Murphy, 2003).

Muc-1 expression in the uterus is cycle dependent and is strongly influenced by the steroid hormones in many species; including, mice (Surveyor *et al.*, 1995), pigs (Bowen *et al.*, 1997), rabbits (Hoffman *et al.*, 1998), sheep (Johnson *et al.*, 2001) and baboons (Hild-Petito *et al.*, 1996). Not only does the expression of Muc-1 differ during the menstrual or oestrous cycles, but also from species to species. In the mouse, Muc-1 protein expression in the luminal and glandular epithelium is high during pro-oestrous, oestrous and meta-oestrous as well as during early pregnancy. These levels decline in the luminal epithelium during di-oestrous and in both epithelia from around day 3 to day 4 of pregnancy until at least day 6.

Muc-1 mRNA expression is high at oestrous and during the first few days of pregnancy. By day 4 of pregnancy, Muc-1 mRNA expression declines drastically (Surveyor *et al.*, 1995). The highest levels of both Muc-1 protein and mRNA expression coincide with the highest levels of oestrogen. In ovariectomised mice lacking hormonal replacement, Muc-1 is still expressed in the endometrium at very low levels. Surveyor *et al.* (1995) have shown that oestrogen stimulates the expression of Muc-1 mRNA, whereas progesterone alone has no effect. Progesterone does, however, antagonise the stimulatory effect of oestrogen, and so indirectly effects Muc-1 expression (Surveyor *et al.*, 1995).

In the rat endometrium, DeSouza *et al.* (1998) reported that Muc-1 protein expression is high during oestrous and early pregnancy in both the glandular and luminal epithelium and that a decrease in luminal epithelial Muc-1 protein expression is apparent around the time of blastocyst implantation (day 4.5 of pregnancy), with the loss of the glycocalyx (Jones and Murphy, 1994). This loss of Muc-1 protein expression is not observed in the glandular epithelium (DeSouza *et al.*, 1998). Muc-1 is still, however, expressed in a few punctuate foci during the receptive phase which could represent possible non-implantation sites. From day 7.5 of pregnancy, Muc-1 protein expression increases again in the luminal epithelial compartment. Muc-1 mRNA also exhibits a drastic decrease from oestrous to day 4.5 of pregnancy (DeSouza *et al.*, 1998). This loss of Muc-1 is most probably due to the action of

steroid hormones and not the presence of the preimplantation blastocysts, as unilateral ligation of a uterine horn does not prevent Muc-1 loss at day 4.5 of pregnancy (DeSouza *et al.*, 1998).

In the pig endometrium, the Muc-1 expression pattern is similar to that observed in the mouse endometrium (Bowen *et al.*, 1997). In both mice and pigs, Muc-1 protein expression decreases in both the glandular and luminal epithelium, with a greater loss in the luminal uterine epithelium (Bowen *et al.*, 1997). In rabbits, the marked reduction in Muc-1 protein expression is restricted to the implantation sites around the time of uterine receptivity. A high level of Muc-1 protein is maintained in the non-implantation sites. These findings have led to the formation of the hypothesis that Muc-1 down-regulation in the rabbit is accomplished via signals produced by the blastocyst (Hoffman *et al.*, 1998). In contrast to other species, in the human, Muc-1 protein and mRNA levels increase during the time of endometrial receptivity in a manner similar to that observed in rabbits; here there is an overall increase in Muc-1 expression during the receptive phase under the influence of progesterone, except at the implantation sites, where Muc-1 is locally reduced by the blastocyst (Meseguer *et al.*, 2001; Brayman *et al.*, 2004).

7.1.1.3 Calcitonin

Calcitonin is a 32-amino-acid peptide hormone that has long been known to be synthesised and secreted primarily by the parafollicular C cells of the thyroid gland in response to hypercalcaemia (Austin and Heath, 1981). The best described physiological role of Calcitonin is to regulate the calcium levels in bone and kidney cells. Interestingly, studies have shown that Calcitonin is briefly expressed in the uterine epithelium of the rat uterus around the time of optimal endometrial receptivity (Ding *et al.*, 1994). Calcitonin mRNA expression in the rat uterus increases at day 2.5 of pregnancy and reaches a peak on day 4.5, the day before blastocyst implantation and then begins to decline by day 5.5 of pregnancy, the day of blastocyst implantation. By day 6.5 of pregnancy, no Calcitonin mRNA is detected within the rat uterus (Ding *et al.*, 1994). Calcitonin protein expression is restricted to the glandular epithelium of the rat endometrium in the stage-specific expression pattern seen with Calcitonin mRNA, further supporting the fact that Calcitonin expression temporally coincides with blastocyst implantation (Ding *et al.*, 1994).

Expression of Calcitonin within the uterus is stimulated by the ovarian hormone, progesterone. Ovariectomised rats that were treated with progesterone alone showed a 20-fold increase in Calcitonin synthesis. When an initial treatment with oestrogen was administered to the ovariectomised rats prior to progesterone, Calcitonin gene expression was significantly increased (Ding *et al.*, 1994). However, when such rats were treated with oestrogen and progesterone together, oestrogen was shown to antagonise the progesterone-mediated increase in Calcitonin expression (Ding *et al.*, 1994). The increase in Calcitonin expression observed in the day 2.5 pregnant rat uterus coincides with the surge

in circulating progesterone seen after fertilisation. Progesterone levels rise again on day 4.5 of pregnancy and remain high until term (Wiest, 1970).

Although progesterone levels remain unchanged at days 4.5 to 6.5 of pregnancy (Psychoyos, 1970), Calcitonin expression is progressively down-regulated. The mechanism of this stage-specific decline and termination of Calcitonin synthesis is presently unknown. It is important to note that during the postimplantation phase of pregnancy, when oestrogen levels remain low, the high levels of progesterone do not induce Calcitonin expression. This indicates that while progesterone is essential for Calcitonin gene expression, it is not sufficient to switch on gene expression (Ding *et al.*, 1994). It is thus hypothesised that in addition to progesterone and oestrogen, certain stage-specific factors must be involved in the regulation of Calcitonin expression (Ding *et al.*, 1994).

Further studies have shown that the administration of a Calcitonin antisense oligodeoxynucleotide resulted in the reduction of Calcitonin synthesis in the uterus during the preimplantation phase and consequently severely impairs implantation of rat embryos (Zhu *et al.*, 1998b). This study supports the hypothesis that Calcitonin plays an important role in uterine receptivity and blastocyst implantation.

Studies on the spatiotemporal expression of Calcitonin in the human endometrium on various days of the menstrual cycle reveals that Calcitonin mRNA is expressed during the postovulatory midsecretory phase, days 17-25, of the menstrual cycle, with maximal expression occurring between days 19-21, the time of blastocyst implantation. Very little Calcitonin mRNA was detected in the preovulatory proliferative phase, days 5-14, or the late secretory phase, days 26-28 (Kumar *et al.*, 1998). It was also shown in this study that Calcitonin protein expression is localised predominantly in the glandular epithelial cells of the human endometrium (Kumar *et al.*, 1998).

Previous studies have indicated that Calcitonin gene expression is regulated by progesterone in the rat uterus. The presence of Calcitonin in the progesterone-dominant secretory phase of the menstrual cycle supports the hypothesis that Calcitonin is similarly regulated in the human endometrium (Kumar *et al.*, 1998). In addition, treatment of woman with the antiprogestin, RU486, drastically reduced Calcitonin expression in the human endometrium, showing that the synthesis of Calcitonin is indeed regulated by the steroid hormone, progesterone (Kumar *et al.*, 1998).

If the action of RU486 is to bind to the PRs, thus blocking progesterone binding and thus the transcription of these progesterone-dependent genes, then it is likely that one or more of the above mentioned biomarkers of the window of receptivity will be up- or down-regulated. Such modulation of one or more of these genes may be the mechanism through which RU486 blocks implantation of the blastocyst and thus pregnancy.

7.2 RESULTS

7.2.1 Immunofluorescence Analysis of the Spatiotemporal Expression Patterns of the LIF, Muc-1 and Calcitonin Proteins in the RU486-Treated Rat Endometrium.

Immunofluorescence was performed on each tissue section with primary antibodies raised against LIF, Muc-1 and Calcitonin, in order to determine the spatiotemporal expression pattern of these implantation biomarkers to endometrial receptivity during early pregnancy. Following treatment with RU486 at day 3.0 of pregnancy, the spatiotemporal pattern of LIF, Muc-1 and Calcitonin protein expression was analysed to observe what effect, if any, RU486 may have on the localisation and expression of these endometrial biomarkers.

7.2.1.1 The spatiotemporal expression pattern of the LIF, Muc-1 and Calcitonin proteins within the control pregnant animals

In both the implantation and non-implantation sites at day 4.5 of pregnancy in the control pregnant animals, LIF protein levels were relatively high in the luminal and glandular epithelium. Levels were lower in the subepithelial and glandular stroma; however, levels in these endometrial compartments were also fairly high (Graph 7.1A-D; Figure 7.3A and B; Figure 7.4A and B; Table 7.1). At this day of pregnancy, LIF protein levels in the implantation sites were similar in the luminal and glandular epithelium, whereas protein levels in the subepithelial stroma were higher than that of the glandular stroma (Graph 7.1A-D; Figure 7.3A; Figure 7.4A; Table 7.1). In the non-implantation sites at day 4.5 of pregnancy, LIF protein levels were higher in the luminal epithelium, the subepithelial stroma and the glandular stroma relative to that in the implantation sites. LIF protein levels in the glandular epithelium were similar in the implantation and non-implantation sites (Graph 7.1A-D; Figure 7.3A and B; Figure 7.4A and B; Table 7.1).

Although Muc-1 protein levels at day 4.5 of pregnancy were much lower than LIF levels (Graph 7.1A-D; Graph 7.2A-D), levels were still fairly high in the luminal epithelium of the implantation and non-implantation sites. Levels in the glandular epithelium were lower relative to the luminal epithelium with Muc-1 protein levels the lowest in the subepithelial stroma and glandular stroma (Graph 7.2A-D; Figure 7.5A and B; Figure 7.6A and B; Table 7.2). Muc-1 protein levels between the implantation and non-implantation sites were similar in all the endometrial compartments analysed at day 4.5 of pregnancy (Graph 7.2A-D; Figure 7.5A and B; Figure 7.6A and B; Table 7.2).

Table 7.1 One-way ANOVA and Tukey Kramer *post hoc* analysis of LIF protein expression in the luminal epithelium, the subepithelial stroma, the glandular epithelium and the glandular stroma of the implantation (IS) and non-implantation (NIS) sites between days 4.5, 5.5 and 6.5 in the control pregnant (UT) and RU486-treated (T) animals showing groups that are significantly different ($p \leq 0.05$). Groups not connected by the same letter are significantly different.

Group							Mean
Luminal Epithelium							
5.5UT IS	A						192.88
5.5UT NIS	A						183.42
4.5UT NIS	A	B					177.57
6.5T IS		B	C				157.70
4.5UT IS		B	C				156.41
5.5T IS			C				150.53
5.5T NIS			C	D			144.05
4.5T NIS				D	E		127.28
6.5T NIS				D	E		124.58
6.5UT NIS				D	E		123.25
4.5T IS					E		109.79
6.5UT IS					E		105.21
Subepithelial Stroma							
4.5UT NIS	A						127.21
5.5UT IS	A						120.10
5.5UT NIS	A						112.25
4.5UT IS		B					92.24
5.5T NIS		B	C				91.31
6.5UT NIS			C	D			76.26
5.5T IS				D			73.20
4.5T NIS				D			70.40
6.5T IS				D	E		69.93
6.5UT IS				D	E		68.87
6.5T NIS					E	F	55.11
4.5T IS						F	53.12
Glandular Epithelium							
4.5UT IS	A						159.09
5.5UT NIS	A						156.45
5.5UT IS	A						152.04
4.5UT NIS	A						151.44
5.5T IS	A						150.66
5.5T NIS	A	B					136.95
6.5T IS		B	C				117.20
4.5T NIS			C	D			110.56
6.5UT NIS			C	D	E		98.71
6.5T NIS				D	E		89.51
6.5UT IS					E		84.82
4.5T IS					E		79.57
Glandular Stroma							
5.5UT NIS	A						82.42
4.5UT NIS	A	B					79.96
5.5UT IS	A	B	C				74.74
4.5UT IS		B	C	D			65.86
4.5T NIS			C	D	E		60.64
5.5T IS				D	E	F	56.62
6.5T IS					E	F	49.85
6.5T NIS						F	41.94
4.5T IS						G	40.94
6.5UT IS						G	40.63
6.5UT NIS						G	39.27
5.5T NIS						G	38.99

Calcitonin protein levels were the lowest at day 4.5 of pregnancy relative to the other two endometrial biomarkers (Graph 7.1A-D; Graph 7.2A-D; Graph 7.3A-D). Calcitonin protein levels in the endometrial compartments were similar in both the implantation and non-implantation sites at day 4.5 of pregnancy. The highest level of Calcitonin protein expression in both the implantation and non-implantation sites was demonstrated in the luminal epithelium followed by the glandular epithelium, then the subepithelial stroma and finally the glandular stroma (Graph 7.3A-D; Figure 7.7A and B; Figure 7.8A and B; Table 7.3).

As pregnancy progressed from day 4.5 to day 5.5, LIF protein expression in the implantation sites increased significantly in the luminal epithelium and the subepithelial stroma (Graph 7.1A and B; Figure 7.3A and C; Table 7.1). LIF levels in the glandular epithelium and glandular stroma remained constant (Graph 7.1C and D; Figure 7.4A and C; Table 7.1). In contrast, Muc-1 protein levels in the implantation sites were decreased significantly in the luminal and glandular epithelium as well as the subepithelial and glandular stroma as pregnancy progressed from day 4.5 to day 5.5 (Graph 7.2A-D; Figure 7.5A and C; Figure 7.6A and C; Table 7.2). Calcitonin protein levels in the implantation sites were decreased significantly in the luminal and glandular epithelium as well as the subepithelial stroma as pregnancy progressed to day 5.5. No significant difference was demonstrated in the decrease in Calcitonin protein levels in the glandular stroma (Graph 7.3A-D; Figure 7.7A and C; Figure 7.8A and C; Table 7.3).

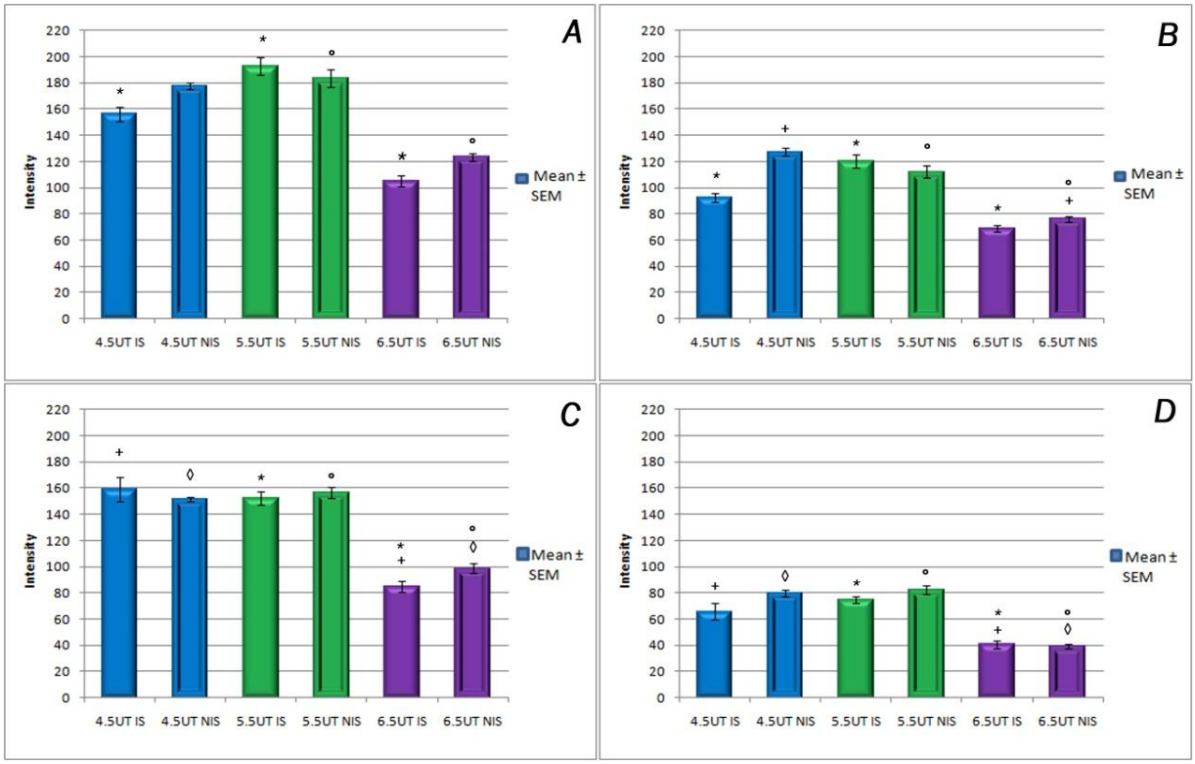
In the non-implantation sites, LIF protein levels remained fairly constant in all endometrial compartments analysed, as pregnancy progressed from day 4.5 to day 5.5 (Graph 7.1A-D; Figure 7.3B and D; Figure 7.4B and D; Table 7.1). In contrast, Muc-1 protein levels decreased significantly, to similar levels seen in the implantation sites, in the luminal and glandular epithelium as well as the glandular stroma of the non-implantation sites (Graph 7.2A, C and D; Figure 7.5B and D; Figure 7.6B and D; Table 7.2). This was also true for Calcitonin levels in the non-implantation sites where levels were demonstrated to decrease significantly in the luminal and glandular epithelium as well as the subepithelial stroma (Graph 7.3A, B and C; Figure 7.7B and D; Figure 7.8B and D; Table 7.3), to levels similar to that in the implantation sites.

By day 6.5 of pregnancy, LIF protein levels decreased significantly in all endometrial compartments of the implantation sites (Graph 7.1A-D; Figure 7.3E; Figure 7.4E; Table 7.1). In contrast, Muc-1 protein levels increased significantly in all endometrial compartments with the exception of the subepithelial stroma (Graph 7.2A-D; Figure 7.5E; Figure 7.6E; Table 7.2). This increase in Muc-1 expression was accompanied by an increase in Calcitonin protein levels in all endometrial compartments of the implantation sites at day 6.5 of pregnancy (Graph 7.3A-D; Figure 7.7E; Figure 7.8E; Table 7.3).

Table 7.2 One-way ANOVA and Tukey Kramer *post hoc* analysis of Muc-1 protein expression in the luminal epithelium, the subepithelial stroma, the glandular epithelium and the glandular stroma of the implantation (IS) and non-implantation (NIS) sites between days 4.5, 5.5 and 6.5 in the control pregnant (UT) and RU486-treated (T) animals showing groups that are significantly different ($p \leq 0.05$). Groups not connected by the same letter are significantly different.

Group							Mean
Luminal Epithelium							
6.5T NIS	A						84.395
6.5T IS	A						81.125
4.5UT NIS	A	B					78.22333
4.5UT IS	A	B	C				75.61833
5.5T NIS	A	B	C				74.265
4.5T NIS	A	B	C				69.20167
4.5T IS		B	C				62.85
5.5T IS		B	C				62.48333
6.5UT IS			C				60.42
6.5UT NIS					D		42.06833
5.5UT NIS					D		35.68833
5.5UT IS					D		34.41333
Subepithelial Stroma							
4.5T IS	A						40.89333
5.5T NIS	A	B					40.08167
6.5T NIS	A	B	C				36.02167
6.5T IS	A	B	C				34.51833
4.5T NIS		B	C	D			30.37
5.5T IS			C	D	E		29.87833
4.5UT IS			C	D	E		28.07167
6.5UT IS				D	E	F	22.47
4.5UT NIS					E	F	20.14833
6.5UT NIS						F	17.855
5.5UT IS						F	17.13667
5.5UT NIS						F	15.41667
Glandular Epithelium							
4.5UT IS	A						58.19167
4.5UT NIS	A	B					51.86167
6.5T IS	A	B	C				50.03333
4.5T NIS	A	B	C				46.20667
5.5T IS		B	C	D			43.27
6.5T NIS		B	C	D			42.12167
4.5T IS		B	C	D			42.09333
6.5UT IS		B	C	D			39.33333
5.5T NIS			C	D			37.00833
6.5UT NIS				D			32.34333
5.5UT NIS						E	10.69167
5.5UT IS						E	8.715
Glandular Stroma							
6.5T IS	A						30.05
4.5T IS	A	B					28.415
4.5UT IS	A	B					26.39
4.5UT NIS	A	B	C				24.695
5.5T IS	A	B	C				24.30667
6.5T NIS		B	C	D			19.97667
4.5T NIS		B	C	D			19.96667
6.5UT IS			C	D			16.41667
5.5T NIS			C	D			16.10833
6.5UT NIS				D	E		11.67
5.5UT IS					E	F	3.2
5.5UT NIS						F	2.518333

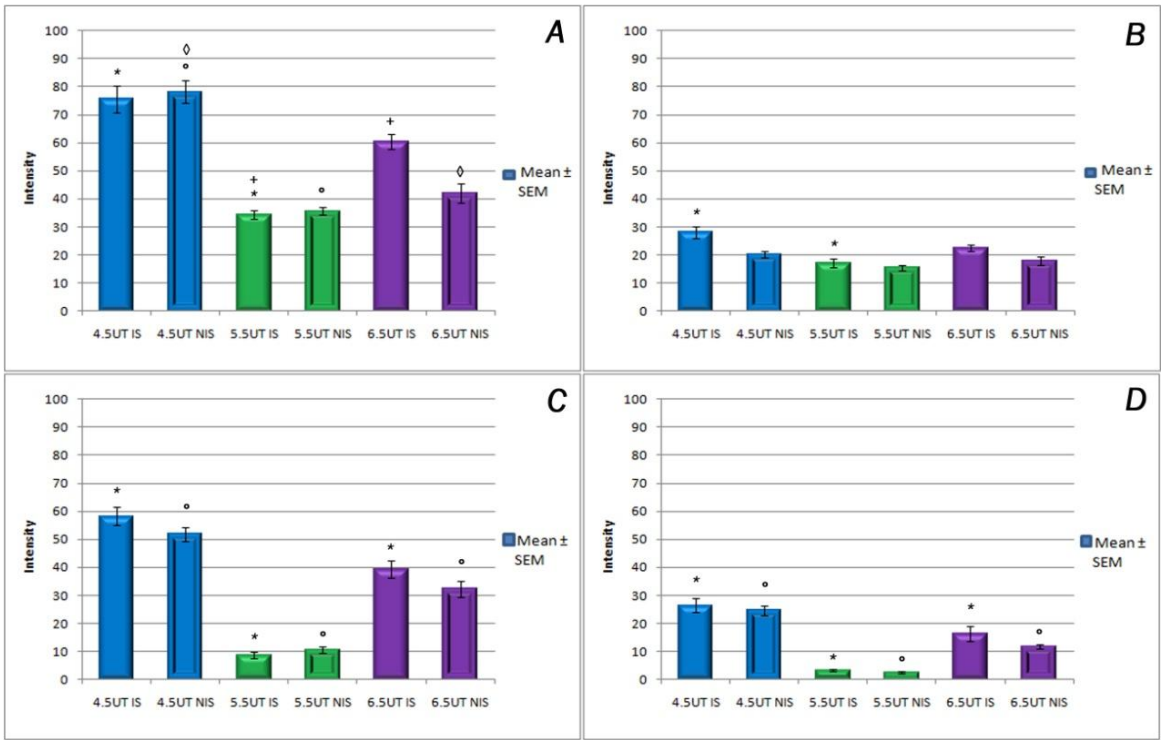
By day 6.5 of pregnancy, the significant decrease in LIF protein levels demonstrated in all endometrial compartments analysed in the implantation sites was reflected in the non-implantation sites (Graph 7.1A-F; Figure 7.3F; Figure 7.4F; Table 7.1). Muc-1 protein levels were increased in the glandular epithelium and glandular stroma of the non-implantation sites at this day of pregnancy (Graph 7.2C and D; Figure 7.5F; Figure 7.6F; Table 7.2). Calcitonin protein levels increased significantly in the subepithelial stroma as well as in the glandular epithelium and glandular stroma in the non-implantation sites at day 6.5 of pregnancy (Graph 7.3B-D; Figure 7.7F; Figure 7.8F; Table 7.3).



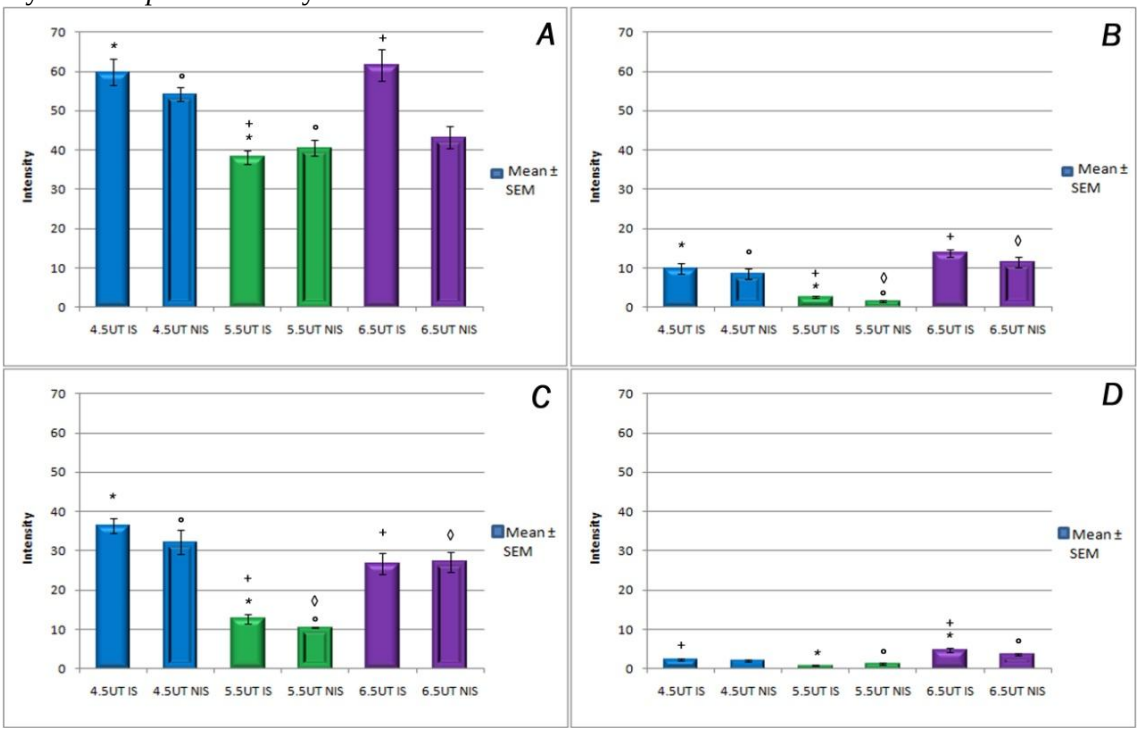
Graph 7.1 Graphical representation of the Mean ± SEM of LIF protein expression in the luminal epithelium (A), the subepithelial stroma (B), the glandular epithelium (C) and the glandular stroma (D) of the implantation (IS) and non-implantation (NIS) sites in day 4.5, day 5.5 and day 6.5 pregnant rat uteri treated with vehicle (UT) at day 3.0 of pregnancy, as obtained from image analysis of fluorescent intensities. *, °, +, ◊ = significantly different ($p \leq 0.05$) using the Tukey-Kramer *post hoc* analysis.

Table 7.3 One-way ANOVA and Tukey Kramer *post hoc* analysis of Calcitonin protein expression in the luminal epithelium, the subepithelial stroma, the glandular epithelium and the glandular stroma of the implantation (IS) and non-implantation (NIS) sites between days 4.5, 5.5 and 6.5 in the control pregnant (UT) and RU486-treated (T) animals showing groups that are significantly different ($p \leq 0.05$). Groups not connected by the same letter are significantly different.

Group					Mean
Luminal Epithelium					
6.5UT IS	A				61.58
4.5UT IS	A				59.77167
4.5UT NIS	A	B			54.19667
6.5T IS	A	B	C		48.38167
6.5T NIS		B	C		45.445
6.5UT NIS		B	C		43.18167
5.5T IS		B	C	D	41.23667
5.5UT NIS			C	D	40.54
4.5T NIS			C	D	38.66
5.5UT IS			C	D	38.2
5.5T NIS			C	D	37.865
4.5T IS				D	28.31167
Subepithelial Stroma					
6.5UT IS	A				13.76833
6.5UT NIS	A	B			11.45833
5.5T IS	A	B			10.42333
4.5UT IS	A	B	C		9.91
6.5T IS		B	C		9.043333
4.5UT NIS		B	C		8.48
6.5T NIS		B	C		8.436667
4.5T NIS			C	D	5.473333
5.5T NIS				D	3.415
4.5T IS				D	3.388333
5.5UT IS				D	2.606667
5.5UT NIS				D	1.491667
Glandular Epithelium					
4.5UT IS	A				36.44833
4.5UT NIS	A	B			32.2
6.5T IS	A	B			30.39
4.5T NIS	A	B			29.61167
5.5T NIS	A	B			29.22167
6.5UT NIS	A	B	C		27.21
5.5T IS	A	B	C		27.13167
6.5UT IS	A	B	C		26.75917
6.5T NIS		B	C		25.51333
4.5T IS			C	D	18.145
5.5UT IS				D	12.75333
5.5UT NIS				D	10.455
Glandular Stroma					
5.5T IS	A				7.446667
6.5UT IS		B			4.786667
6.5UT NIS		B	C		3.593333
6.5T IS		B	C		3.38
6.5T NIS		B	C	D	3.128333
5.5T NIS			C	D	E 2.533333
4.5UT IS			C	D	E 2.371667
4.5UT NIS			C	D	E 2.063333
4.5T NIS			C	D	E 1.901667
5.5UT NIS				D	E 1.291667
4.5T IS				D	E 1.231667
5.5UT IS					E 0.835



Graph 7.2 Graphical representation of the Mean ± SEM of Muc-1 protein expression in the luminal epithelium (A), the subepithelial stroma (B), the glandular epithelium (C) and the glandular stroma (D) of the implantation (IS) and non-implantation (NIS) sites in day 4.5, day 5.5 and day 6.5 pregnant rat uteri treated with vehicle (UT) at day 3.0 of pregnancy, as obtained from image analysis of fluorescent intensities. *, °, +, ◊ = significantly different ($p \leq 0.05$) using the Tukey-Kramer *post hoc* analysis.



Graph 7.3 Graphical representation of the Mean ± SEM of Calcitonin protein expression in the luminal epithelium (A), the subepithelial stroma (B), the glandular epithelium (C) and the glandular stroma (D) of the implantation (IS) and non-implantation (NIS) sites in day 4.5, day 5.5 and day 6.5 pregnant rat uteri treated with vehicle (UT) at day 3.0 of pregnancy, as obtained from image analysis of fluorescent intensities. *, °, +, ◊ = significantly different ($p \leq 0.05$) using the Tukey-Kramer *post hoc* analysis.

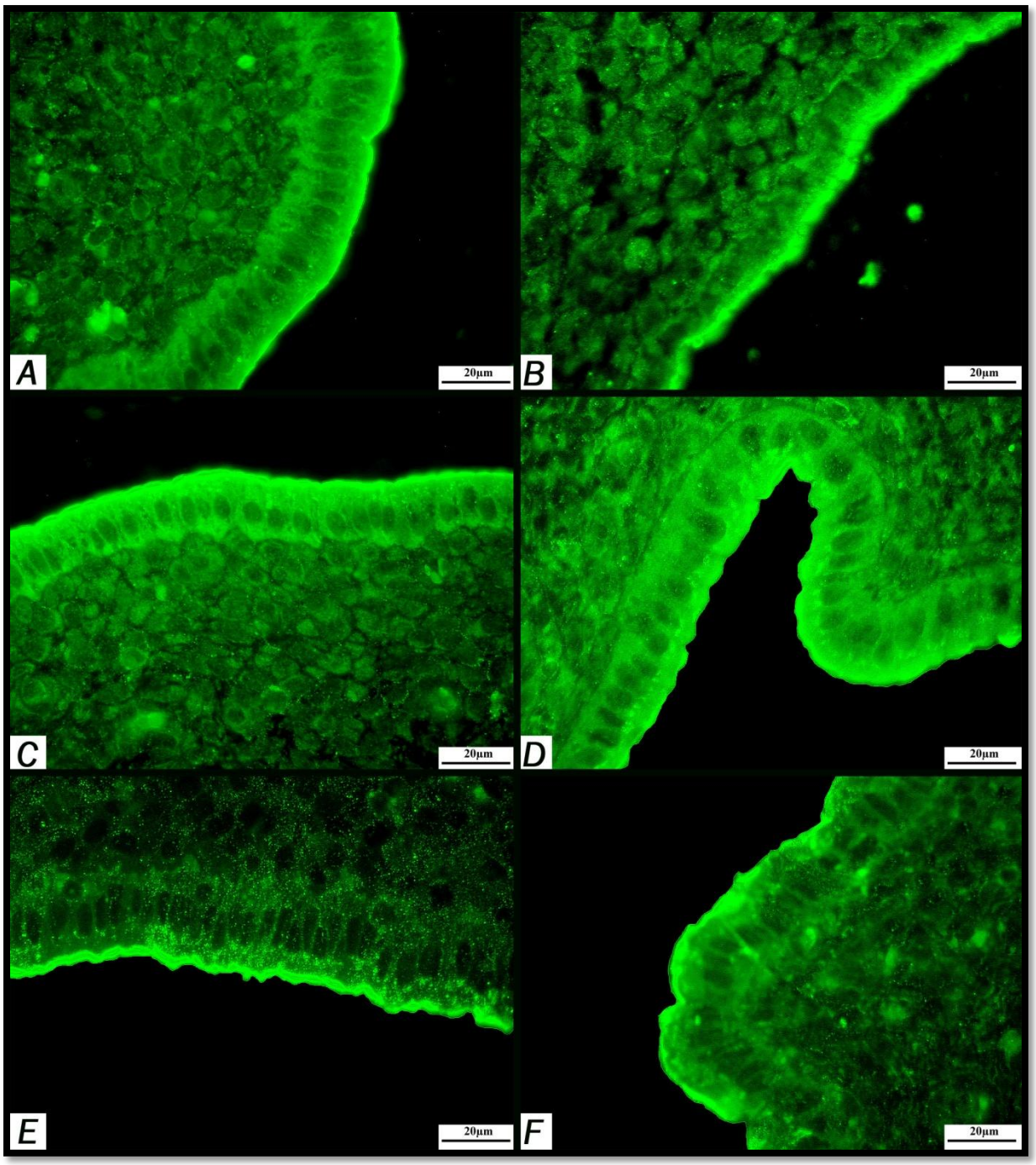


Figure 7.3 Immunofluorescent images illustrating LIF protein localisation in the luminal epithelium and the subepithelial stroma of the implantation and non-implantation sites in the uteri of control pregnant rats. A: Implantation site at day 4.5 of pregnancy, **B:** Non-implantation site at day 4.5 of pregnancy, **C:** Implantation site at day 5.5 of pregnancy, **D:** Non-implantation site at day 5.5 of pregnancy, **E:** Implantation site at day 6.5 of pregnancy, **F:** Non-implantation site at day 6.5 of pregnancy. Scale = 20µm.

7.2.1.2 The effects of RU486 on the spatiotemporal protein expression patterns of LIF, Muc-1 and Calcitonin

After treatment with RU486 at day 3.0 of pregnancy, LIF protein levels were significantly lower in all the endometrial compartments analysed of both the implantation and non-implantation sites at day 4.5 of pregnancy, relative to the control pregnant animals (Graph 7.7A-D; Figure 7.3A and B; Figure 7.4A and B; Figure 7.9A and B; Figure 7.10A and B; Table 7.1).

By day 5.5 of pregnancy, LIF protein levels in the implantation sites of the RU486-treated animals increased significantly in all the endometrial compartments (Graph 7.4A-D; Figure 7.9C; Figure 7.10C; Table 7.1). This increase in LIF protein levels was only reflected in the subepithelial stroma and the glandular epithelium of the non-implantation sites. In the glandular stroma of the non-implantation sites, LIF protein levels decreased significantly as pregnancy progressed to day 5.5 in the RU486-treated animals (Graph 7.4A-D; Figure 7.9D; Figure 7.10D; Table 7.1). The increase in LIF protein expression was not sufficient to close the gap between LIF levels in the luminal epithelium, the subepithelial stroma or the glandular stroma of the implantation and non-implantation sites, so levels remained significantly lower in the RU486-treated animals with regards to these endometrial compartments. LIF protein levels in the glandular epithelium were similar in both the control pregnant and RU486-treated animals at this day of pregnancy (Graph 7.7A-D; Figure 7.3C and D; Figure 7.4C and D; Figure 7.9C and D; Figure 7.10C and D; Table 7.1).

By day 6.5 of pregnancy, when LIF protein levels decreased significantly in the implantation and non-implantation sites of the control pregnant animals, levels in the implantation sites of the RU486-treated animals remained constant, with the exception of in the glandular epithelium were LIF levels decreased significantly (Graph 7.7A-D). This resulted in significantly higher levels of LIF protein in the luminal and glandular epithelium of the implantation sites in the RU486-treated animals relative to the control pregnant animals (Graph 7.7A and C; Figure 7.3E; Figure 7.4E; Figure 7.9E; Figure 7.10E; Table 7.1).

In the non-implantation sites of the RU486-treated animals at day 6.5 of pregnancy, LIF protein levels decreased significantly in the subepithelial stroma and glandular epithelium at this day of pregnancy (Graph 7.4B and C). This resulted in significantly lower levels in the subepithelial stroma of the non-implantation sites of the RU486-treated animals relative to the control pregnant animals. LIF protein levels in the other endometrial compartments were not significantly different between the control pregnant and RU486-treated animals (Graph 7.7A-D; Figure 7.3F; Figure 7.4F; Figure 7.9F; Figure 7.10F; Table 7.1).

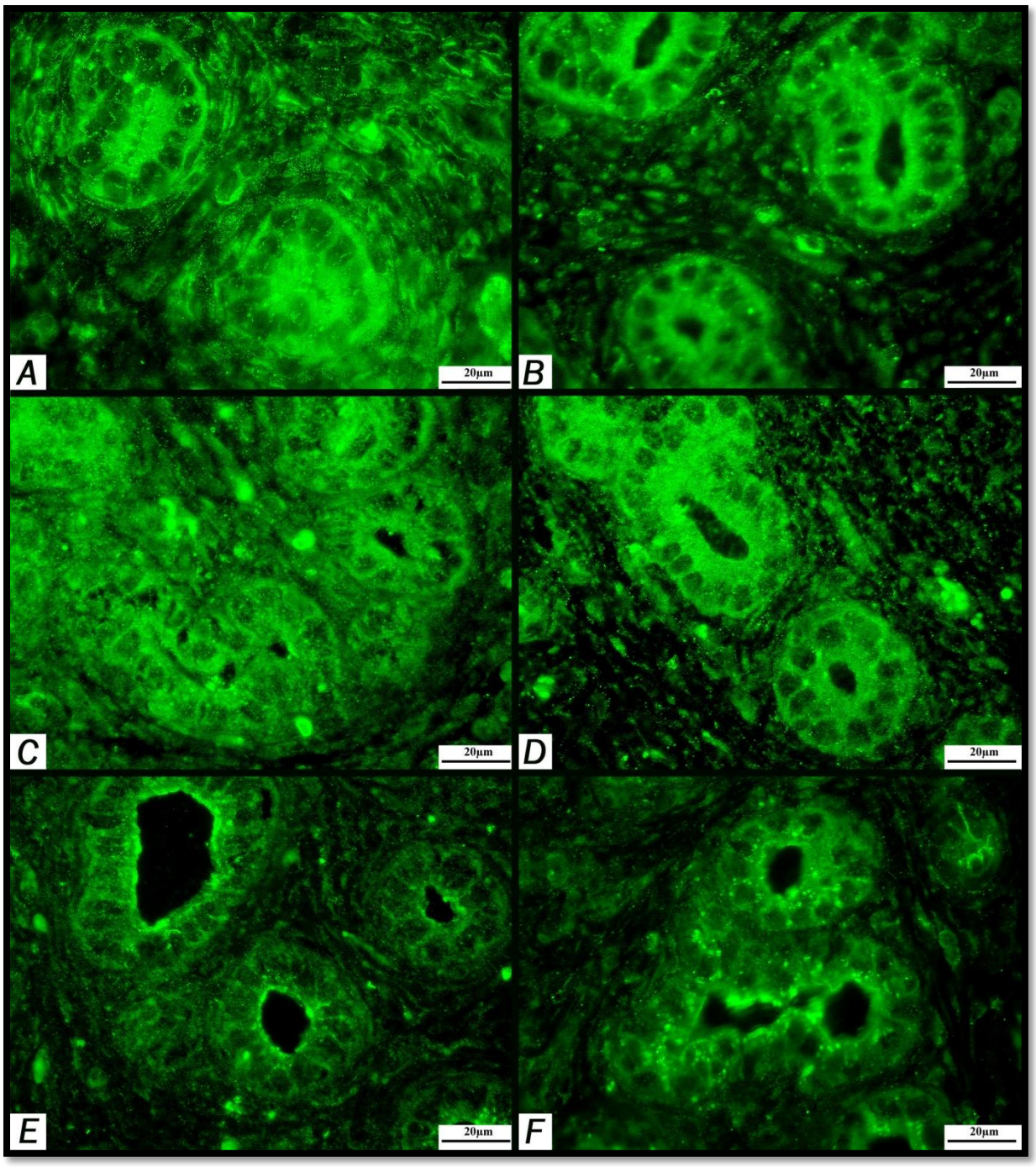


Figure 7.4 Immunofluorescent images illustrating LIF protein localisation in the glandular epithelium and the glandular stroma of the implantation and non-implantation sites in the uteri of control pregnant rats. A: Implantation site at day 4.5 of pregnancy, **B:** Non-implantation site at day 4.5 of pregnancy, **C:** Implantation site at day 5.5 of pregnancy, **D:** Non-implantation site at day 5.5 of pregnancy, **E:** Implantation site at day 6.5 of pregnancy, **F:** Non-implantation site at day 6.5 of pregnancy. Scale = 20µm.

With regards to Muc-1 protein levels, RU486 did not have a significant effect on levels in the luminal epithelium or glandular stroma of both the implantation and non-implantation sites at day 4.5 of pregnancy. In the subepithelial stroma, Muc-1 protein levels were significantly higher in the implantation and non-implantation sites at day 4.5 of pregnancy, as a result of RU486 treatment. In the glandular epithelium, RU486 caused a significant decrease in Muc-1 levels in the implantation sites, but not in the non-implantation sites at this day of pregnancy (Graph 7.8A-D; Figure 7.5A and B; Figure 7.6A and B; Figure 7.11A and B; Figure 7.12A and B; Table 7.2).

By day 5.5 of pregnancy, Muc-1 protein levels in all the endometrial compartments of both the implantation and non-implantation sites were significantly decreased in the control pregnant animals (Graph 7.2A-D; Figure 7.5C and D; Figure 7.6C and D; Table 7.2). RU486 blocked this decrease in Muc-1 protein expression, thus levels were significantly higher in the RU486-treated animals in all endometrial compartments at day 5.5 of pregnancy (Graph 7.8A-D; Figure 7.5C and D; Figure 7.6C and D; Figure 7.11C and D; Figure 7.12C and D; Table 7.2).

By day 6.5 of pregnancy, Muc-1 levels in the control pregnant animals had begun to reappear, whereas levels in the RU486-treated animals did not change significantly (Graph 7.2A-D; Graph 7.5A-D). Muc-1 levels remained significantly higher in the luminal epithelium and subepithelial stroma in the implantation and non-implantation sites of the RU486-treated animals; however, the difference was not as marked as that at day 5.5 of pregnancy (Graph 7.4A and B; Figure 7.5E and F; Figure 7.11E and F; Table 7.2).

In the glandular epithelium, Muc-1 levels in the implantation and non-implantation sites were similar in the RU486-treated animals relative to the control pregnant animals (Graph 7.8C; Figure 7.6E and F; Figure 7.12E and F; Table 7.2). With regards to the glandular stroma, Muc-1 levels remained significantly higher in the implantation sites of the RU486-treated animals relative to the control pregnant animals; however, in the non-implantation sites, Muc-1 levels were not significantly higher in the RU486-treated animals (Graph 7.8D; Figure 7.6E and F; Figure 7.12E and F; Table 7.2).

Calcitonin protein levels decreased significantly in the luminal epithelium of both the implantation and non-implantation sites at day 4.5 of pregnancy, following treatment with RU486. By days 5.5 and 6.5 of pregnancy, Calcitonin protein levels were similar in both the implantation and non-implantation sites of the RU486-treated animals relative to the control pregnant animals (Graph 7.9A; Figure 7.7A-F; Figure 7.13A-F; Table 7.3).

In the subepithelial stroma, Calcitonin levels in the implantation sites were significantly lower in the RU486-treated animals relative to the control pregnant animals at day 4.5 of; significantly higher in

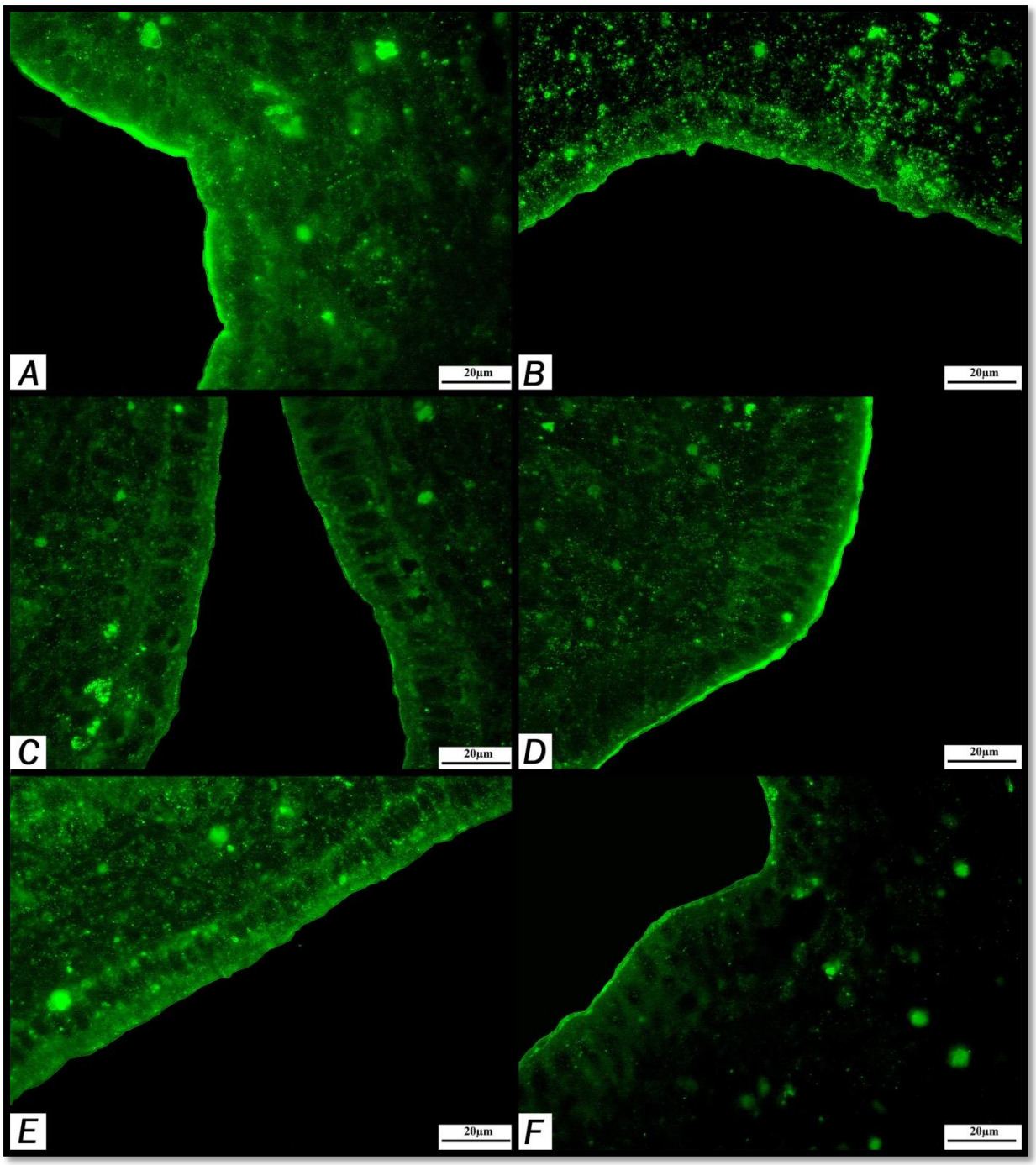


Figure 7.5 Immunofluorescent images illustrating Muc-1 protein localisation in the luminal epithelium and the subepithelial stroma of the implantation and non-implantation sites in the uteri of control pregnant rats. A: Implantation site at day 4.5 of pregnancy, **B:** Non-implantation site at day 4.5 of pregnancy, **C:** Implantation site at day 5.5 of pregnancy, **D:** Non-implantation site at day 5.5 of pregnancy, **E:** Implantation site at day 6.5 of pregnancy, **F:** Non-implantation site at day 6.5 of pregnancy. Scale = 20µm.

the RU486-treated animals at day 5.5 of pregnancy relative to the control pregnant animals; and then significantly lower again in the RU486-treated animals relative to the control pregnant animals by day 6.5 of pregnancy (Graph 7.9B; Figure 7.7A, C and E; Figure 7.13A, C and E; Table 7.3). Calcitonin protein levels in the non-implantation sites were similar in the RU486-treated animals, relative to the control pregnant animals at all three days of pregnancy (Graph 7.9B; Figure 7.7B, D and F; Figure 7.13B, D and F; Table 7.3).

Calcitonin protein levels in the glandular epithelium were significantly higher in the implantation sites of the control pregnant animals at day 4.5 of pregnancy, relative to the RU486-treated animals. No difference was noted between the non-implantation sites at this day of pregnancy (Graph 7.9C; Figure 7.8A and B; Figure 7.14A and B; Table 7.3). At day 5.5 of pregnancy, Calcitonin protein levels decreased significantly in both the implantation and non-implantation sites in the control pregnant animals, whereas RU486 inhibited this significant decrease in protein levels (Graph 7.9C; Figure 7.8C and D; Figure 7.14C and D; Table 7.3). By day 6.5 of pregnancy, Calcitonin levels had increased in the control pregnant animals, while remaining constant in the RU486-treated animals (Graph 7.3C; Graph 7.6C), thus resulting in similar levels of Calcitonin protein in both the implantation and non-implantation sites of the RU486-treated animals relative to the control pregnant animals (Graph 7.9C; Figure 7.8E and F; Figure 7.14E and F; Table 7.3).

With regards to the glandular stroma, Calcitonin levels were not significantly affected by RU486 treatment, with the exception of in the implantation sites at day 5.5 of pregnancy, where protein levels were significantly increased as a result of RU486 (Graph 7.9D; Figure 7.8A-F; Figure 7.14A-F; Table 7.3).

In summary, the overall effect of RU486 on LIF protein expression was to inhibit the high levels of this protein expressed during normal pregnancy, at days 4.5 and 5.5 of pregnancy.

The effect of RU486 on Muc-1 protein expression was to inhibit the decrease in Muc-1 levels in both the implantation and non-implantation sites at day 5.5 of pregnancy, the day of blastocyst implantation.

RU486 did not exhibit such a marked effect on Calcitonin protein expression except in the glandular epithelium at day 5.5 of pregnancy where the normal significant decrease in Calcitonin levels was inhibited by RU486.

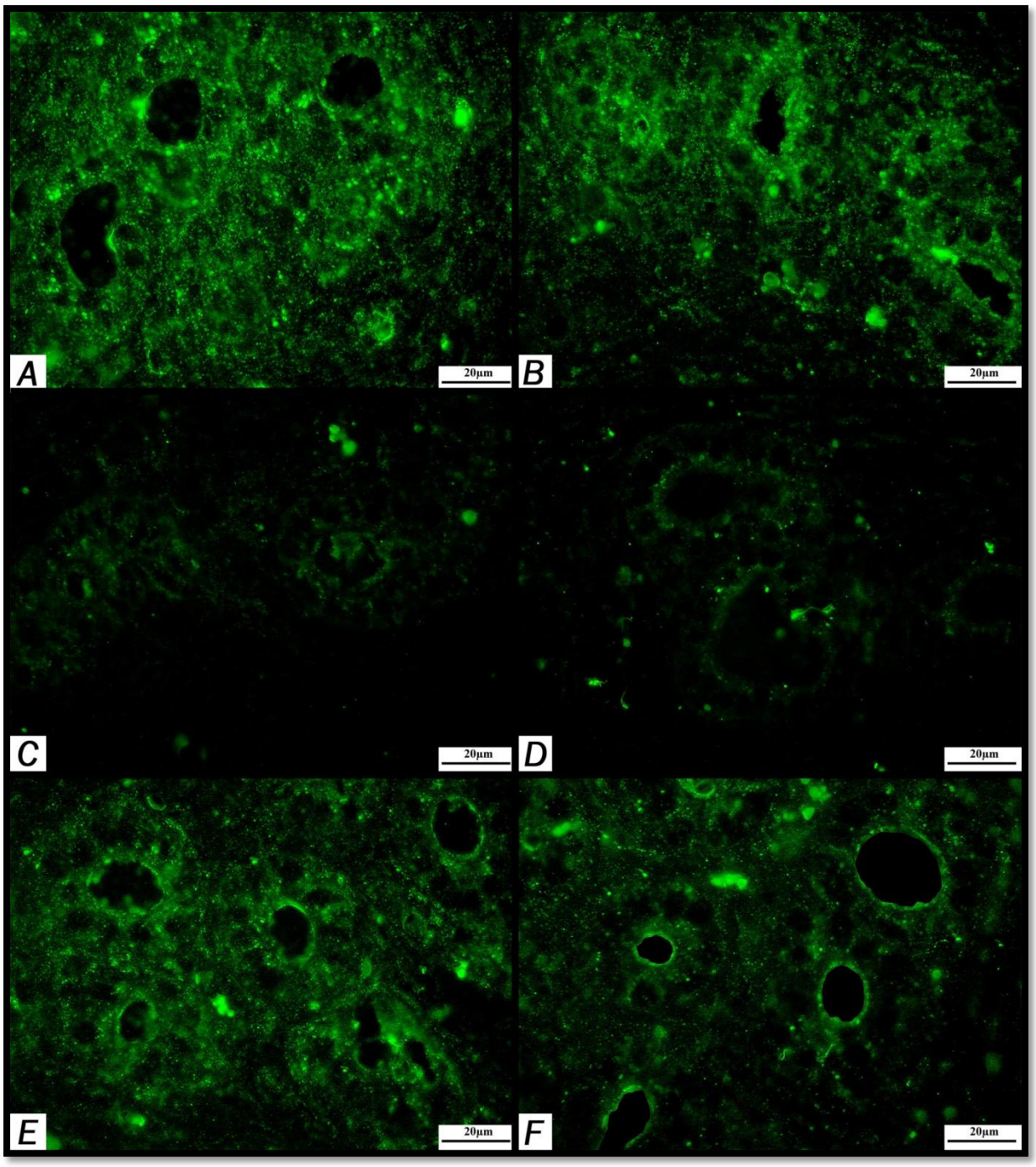
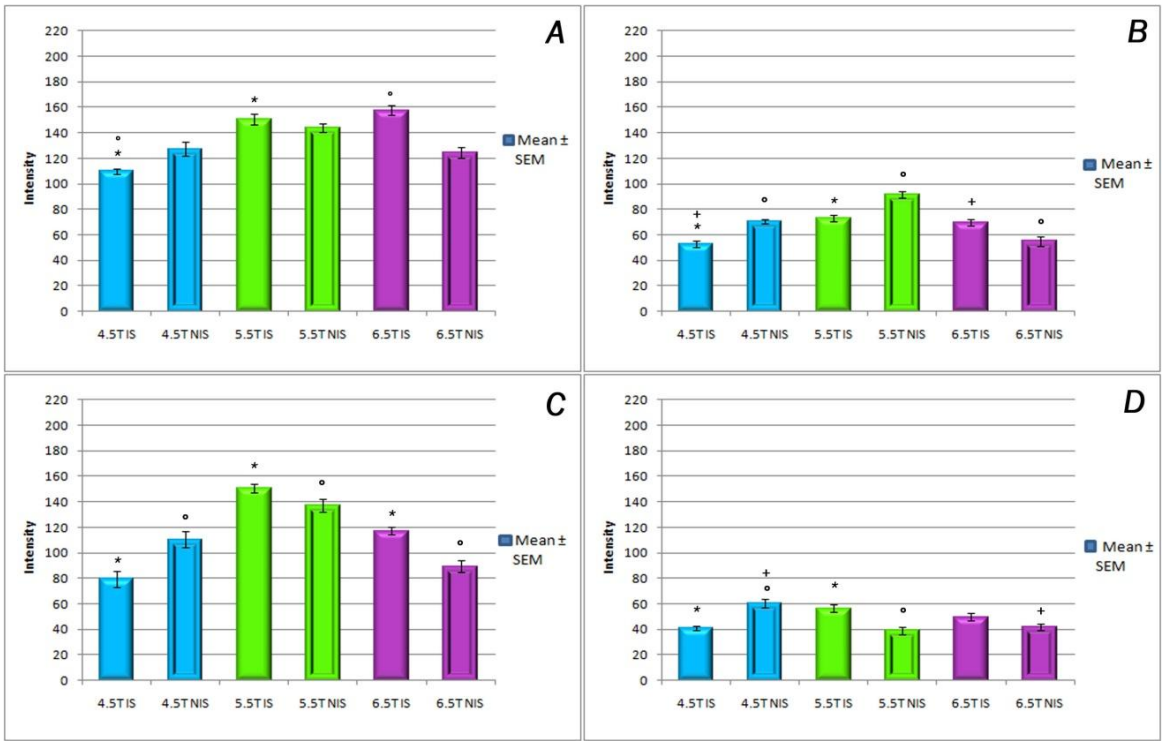
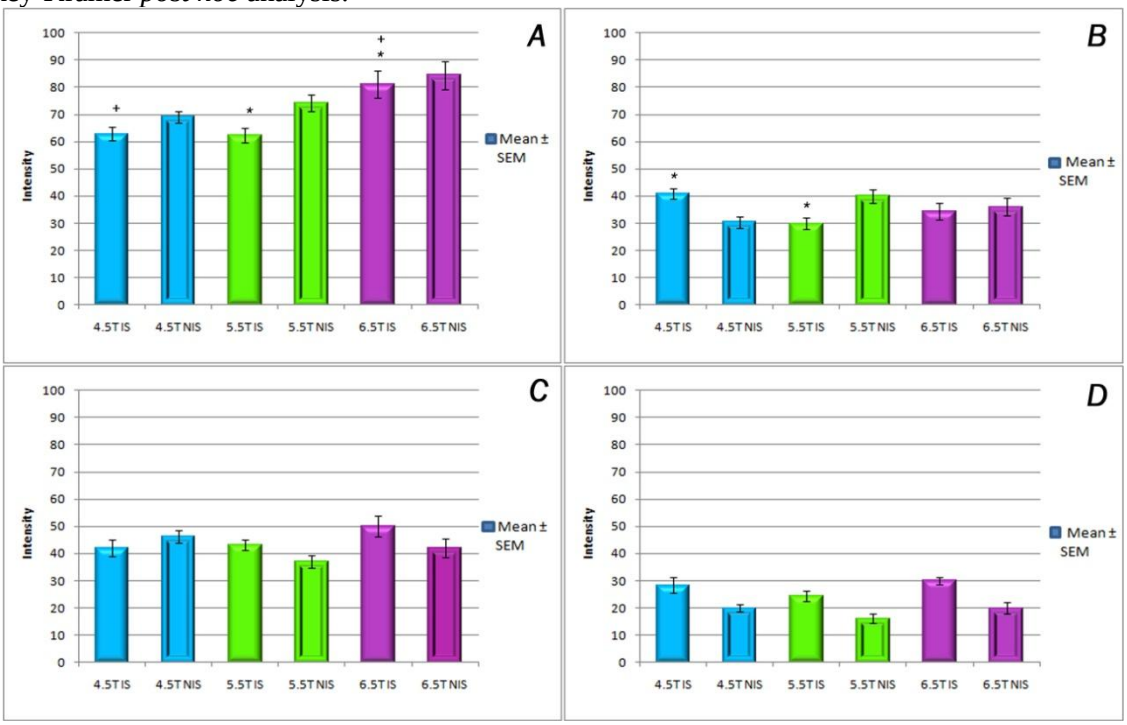


Figure 7.6 Immunofluorescent images illustrating Muc-1 protein localisation in the glandular epithelium and the glandular stroma of the implantation and non-implantation sites in the uteri of control pregnant rats. A: Implantation site at day 4.5 of pregnancy, **B:** Non-implantation site at day 4.5 of pregnancy, **C:** Implantation site at day 5.5 of pregnancy, **D:** Non-implantation site at day 5.5 of pregnancy, **E:** Implantation site at day 6.5 of pregnancy, **F:** Non-implantation site at day 6.5 of pregnancy. Scale = 20µm.



Graph 7.4 Graphical representation of the Mean ± SEM of LIF protein expression in the luminal epithelium (A), the subepithelial stroma (B), the glandular epithelium (C) and the glandular stroma (D) of the implantation (IS) and non-implantation (NIS) sites in day 4.5, day 5.5 and day 6.5 pregnant rat uteri treated with RU486 (T) at day 3.0 of pregnancy, as obtained from image analysis of fluorescent intensities. *, °, + = significantly different ($p \leq 0.05$) using the Tukey-Kramer *post hoc* analysis.



Graph 7.5 Graphical representation of the Mean ± SEM of Muc-1 protein expression in the luminal epithelium (A), the subepithelial stroma (B), the glandular epithelium (C) and the glandular stroma (D) of the implantation (IS) and non-implantation (NIS) sites in day 4.5, day 5.5 and day 6.5 pregnant rat uteri treated with RU486 (T) at day 3.0 of pregnancy, as obtained from image analysis of fluorescent intensities. *, + = significantly different ($p \leq 0.05$) using the Tukey-Kramer *post hoc* analysis.

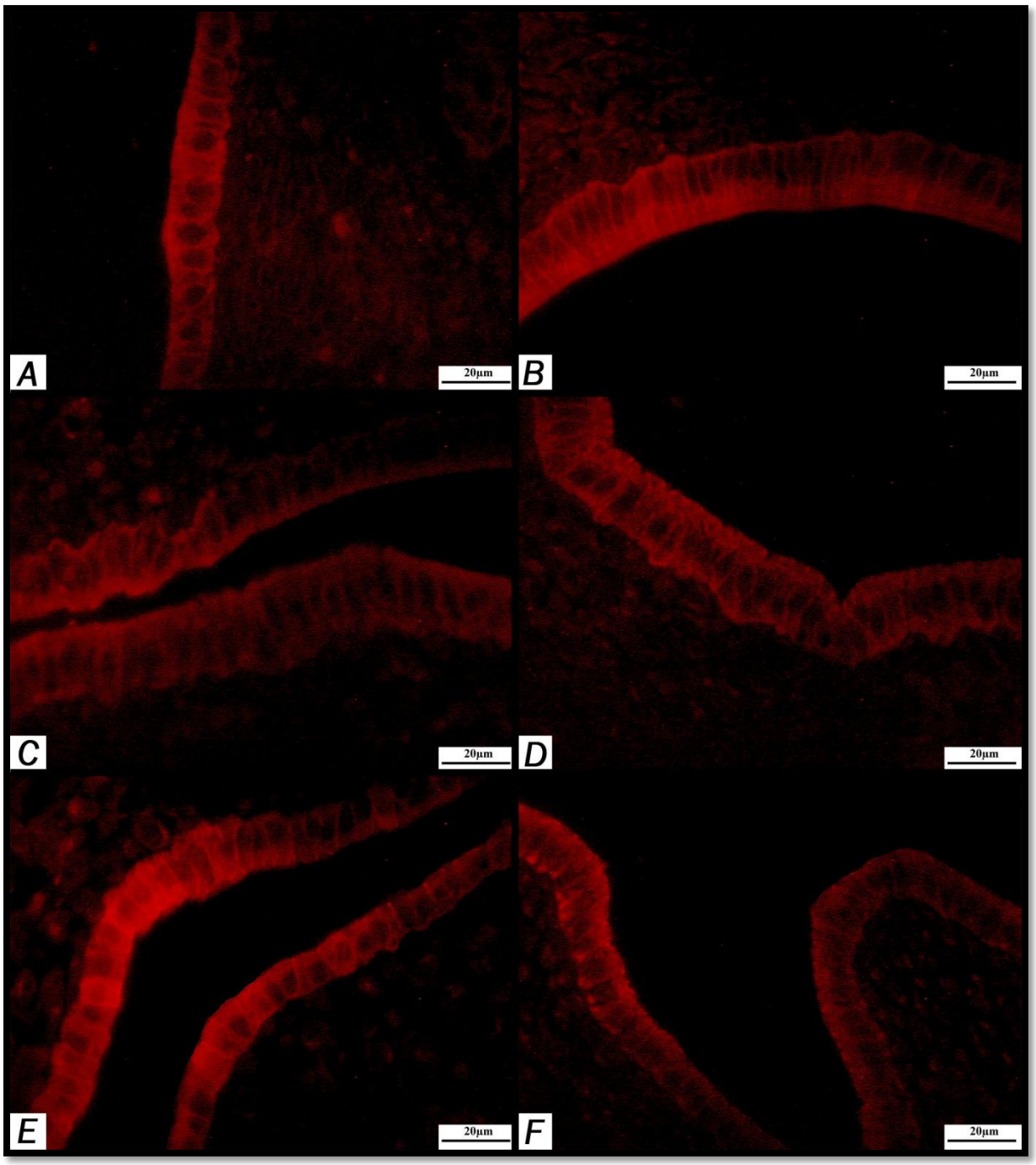
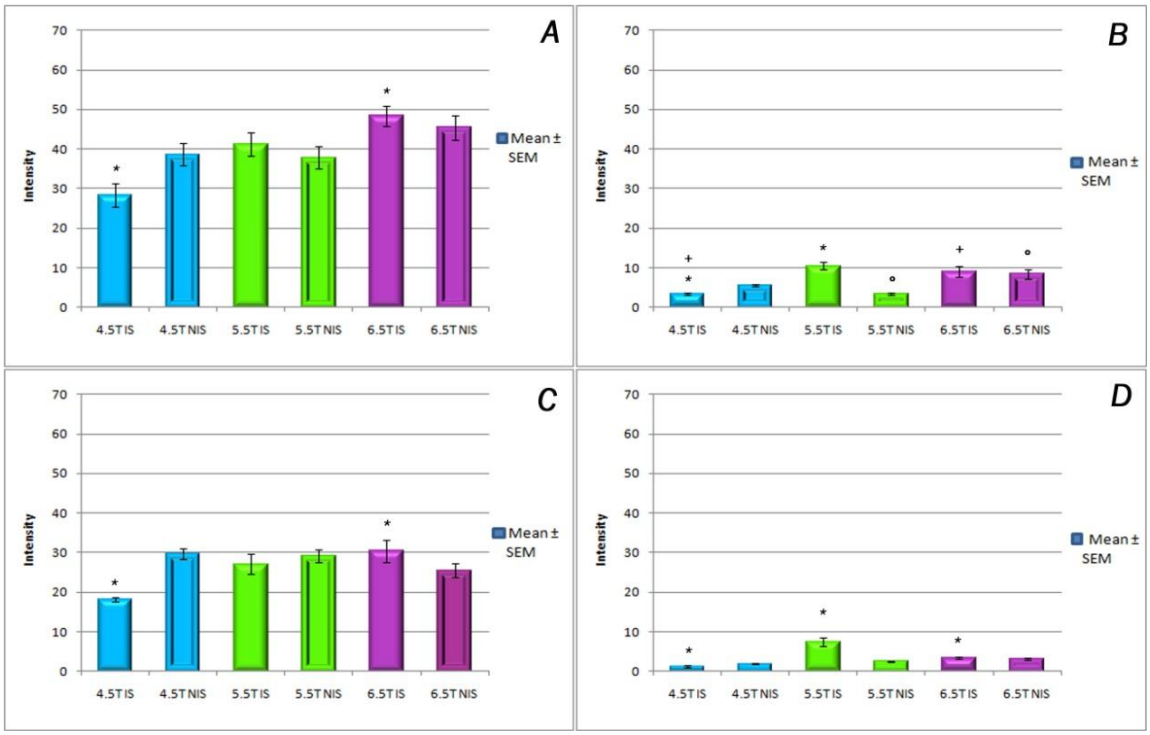
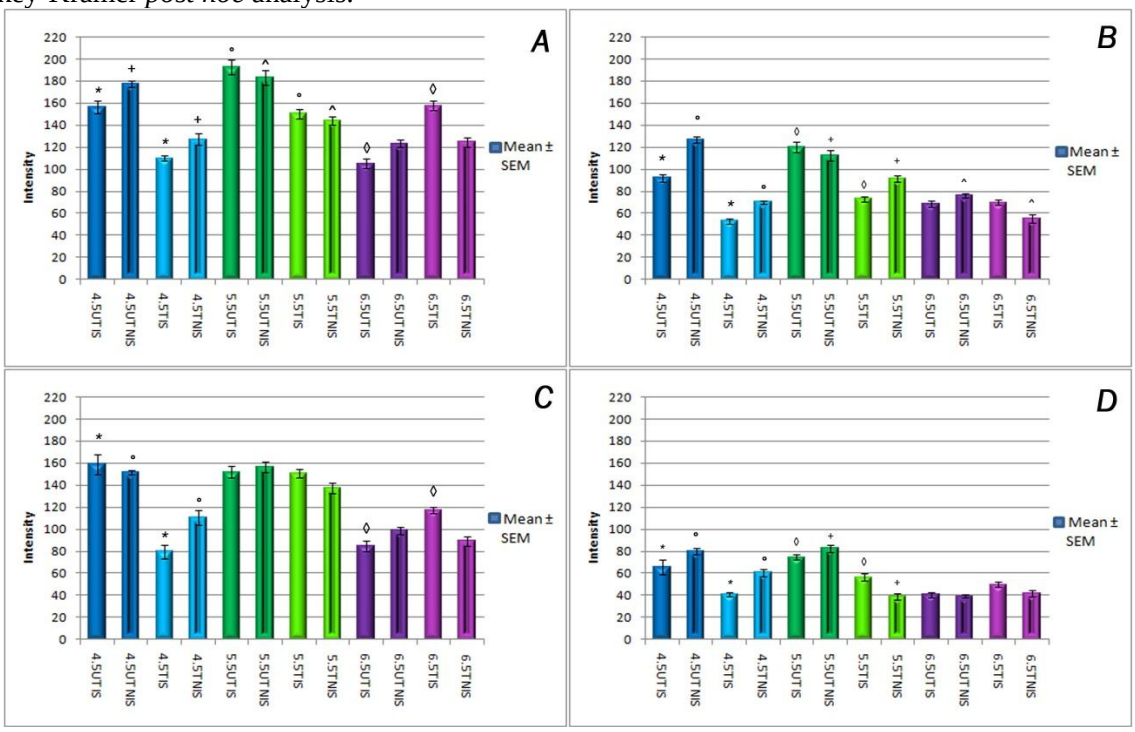


Figure 7.7 Immunofluorescent images illustrating Calcitonin protein localisation in the luminal epithelium and the subepithelial stroma of the implantation and non-implantation sites in the uteri of control pregnant rats. A: Implantation site at day 4.5 of pregnancy, **B:** Non-implantation site at day 4.5 of pregnancy, **C:** Implantation site at day 5.5 of pregnancy, **D:** Non-implantation site at day 5.5 of pregnancy, **E:** Implantation site at day 6.5 of pregnancy, **F:** Non-implantation site at day 6.5 of pregnancy. Scale = 20µm.



Graph 7.6 Graphical representation of the Mean ± SEM of Calcitonin protein expression in the luminal epithelium (A), the subepithelial stroma (B), the glandular epithelium (C) and the glandular stroma (D) of the implantation (IS) and non-implantation (NIS) sites in day 4.5, day 5.5 and day 6.5 pregnant rat uteri treated with RU486 (T) at day 3.0 of pregnancy, as obtained from image analysis of fluorescent intensities. *, ° = significantly different ($p \leq 0.05$) using the Tukey-Kramer *post hoc* analysis.



Graph 7.7 Graphical representation of the Mean ± SEM of LIF protein expression in the luminal epithelium (A), the subepithelial stroma (B), the glandular epithelium (C) and the glandular stroma (D) of the implantation (IS) and non-implantation (NIS) sites in day 4.5, day 5.5 and day 6.5 pregnant rat uteri treated with vehicle (UT) or RU486 (T) at day 3.0 of pregnancy, as obtained from image analysis of fluorescent intensities. *, °, +, ◊, ^ = significantly different ($p \leq 0.05$) using the Tukey-Kramer *post hoc* analysis.

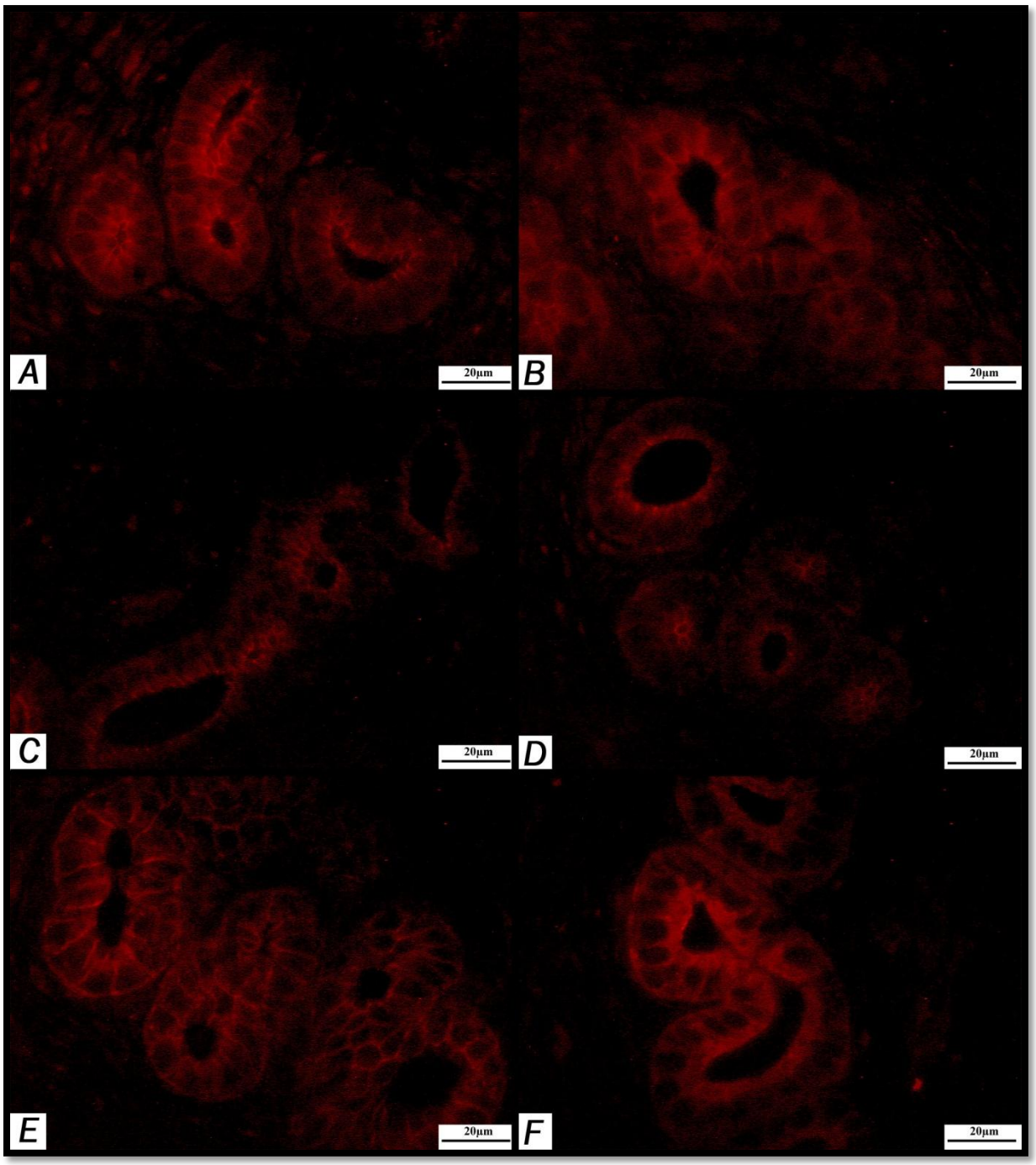
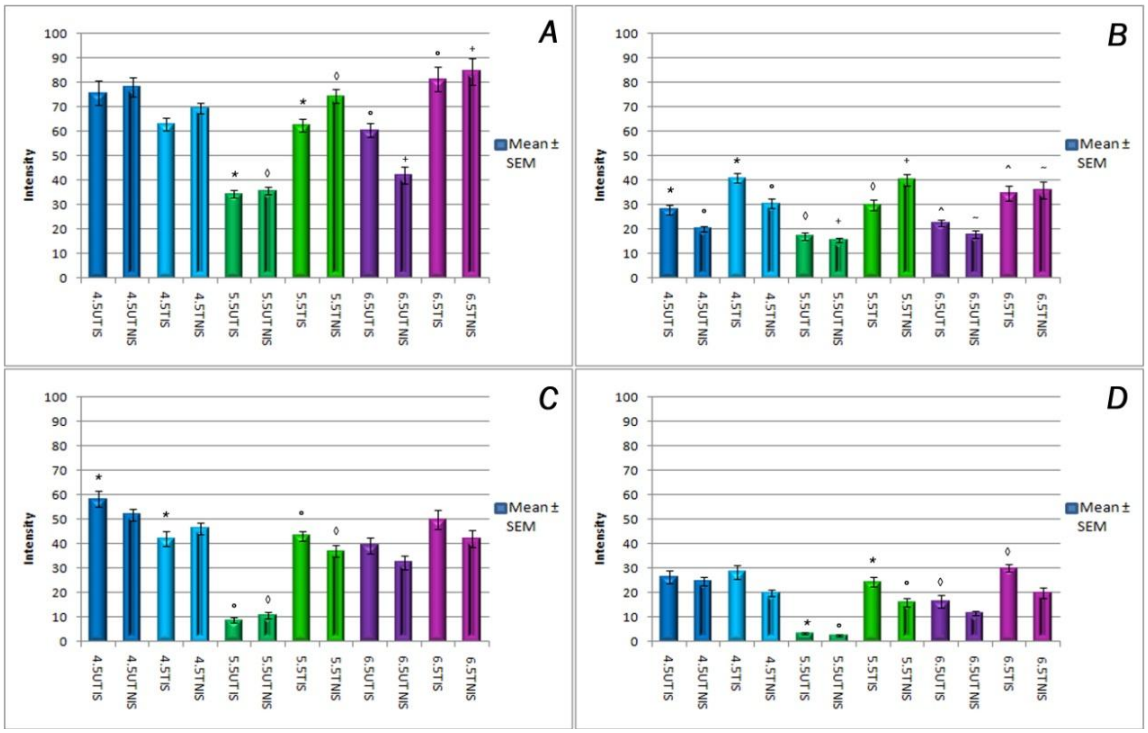
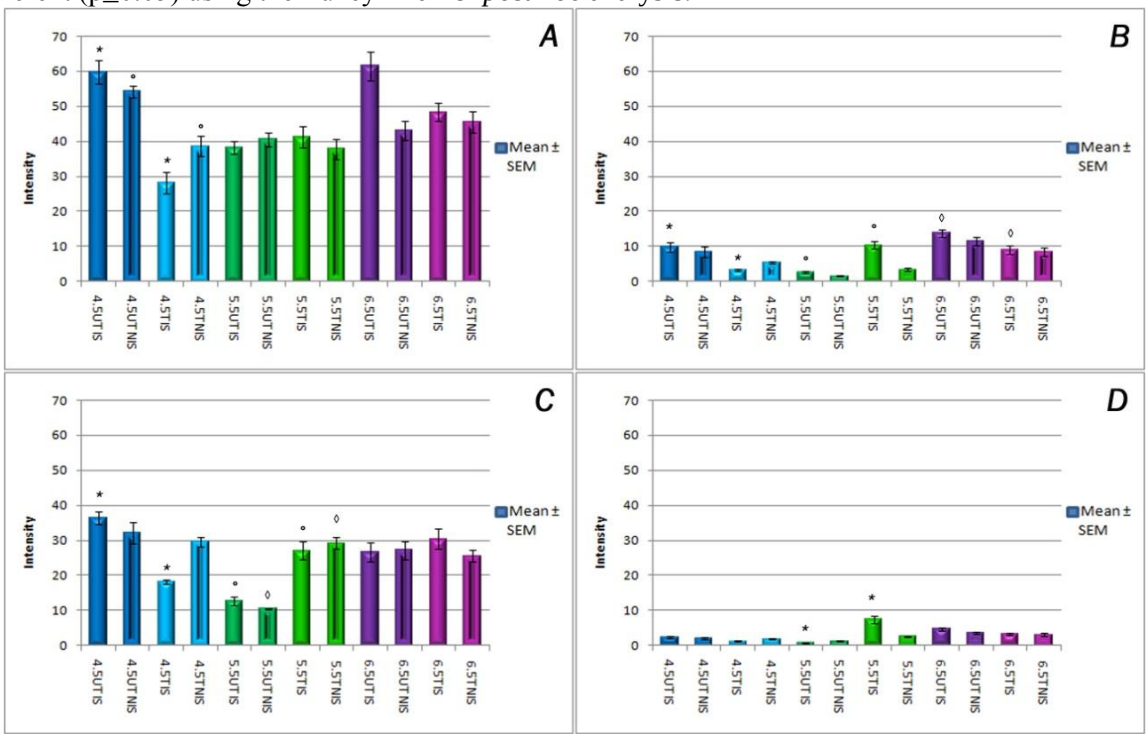


Figure 7.8 Immunofluorescent images illustrating Calcitonin protein localisation in the glandular epithelium and the glandular stroma of the implantation and non-implantation sites in the uteri of control pregnant rats. A: Implantation site at day 4.5 of pregnancy, **B:** Non-implantation site at day 4.5 of pregnancy, **C:** Implantation site at day 5.5 of pregnancy, **D:** Non-implantation site at day 5.5 of pregnancy, **E:** Implantation site at day 6.5 of pregnancy, **F:** Non-implantation site at day 6.5 of pregnancy. Scale = 20µm.



Graph 7.8 Graphical representation of the Mean ± SEM of Muc-1 protein expression in the luminal epithelium (A), the subepithelial stroma (B), the glandular epithelium (C) and the glandular stroma (D) of the implantation (IS) and non-implantation (NIS) sites in day 4.5, day 5.5 and day 6.5 pregnant rat uteri treated with vehicle (UT) or RU486 (T) at day 3.0 of pregnancy, as obtained from image analysis of fluorescent intensities. *, °, +, ◊, ^,~ = significantly different ($p \leq 0.05$) using the Tukey-Kramer *post hoc* analysis.



Graph 7.9 Graphical representation of the Mean ± SEM of Calcitonin protein expression in the luminal epithelium (A), the subepithelial stroma (B), the glandular epithelium (C) and the glandular stroma (D) of the implantation (IS) and non-implantation (NIS) sites in day 4.5, day 5.5 and day 6.5 pregnant rat uteri treated with vehicle (UT) or RU486 (T) at day 3.0 of pregnancy, as obtained from image analysis of fluorescent intensities. *, °, +, ◊ = significantly different ($p \leq 0.05$) using the Tukey-Kramer *post hoc* analysis.

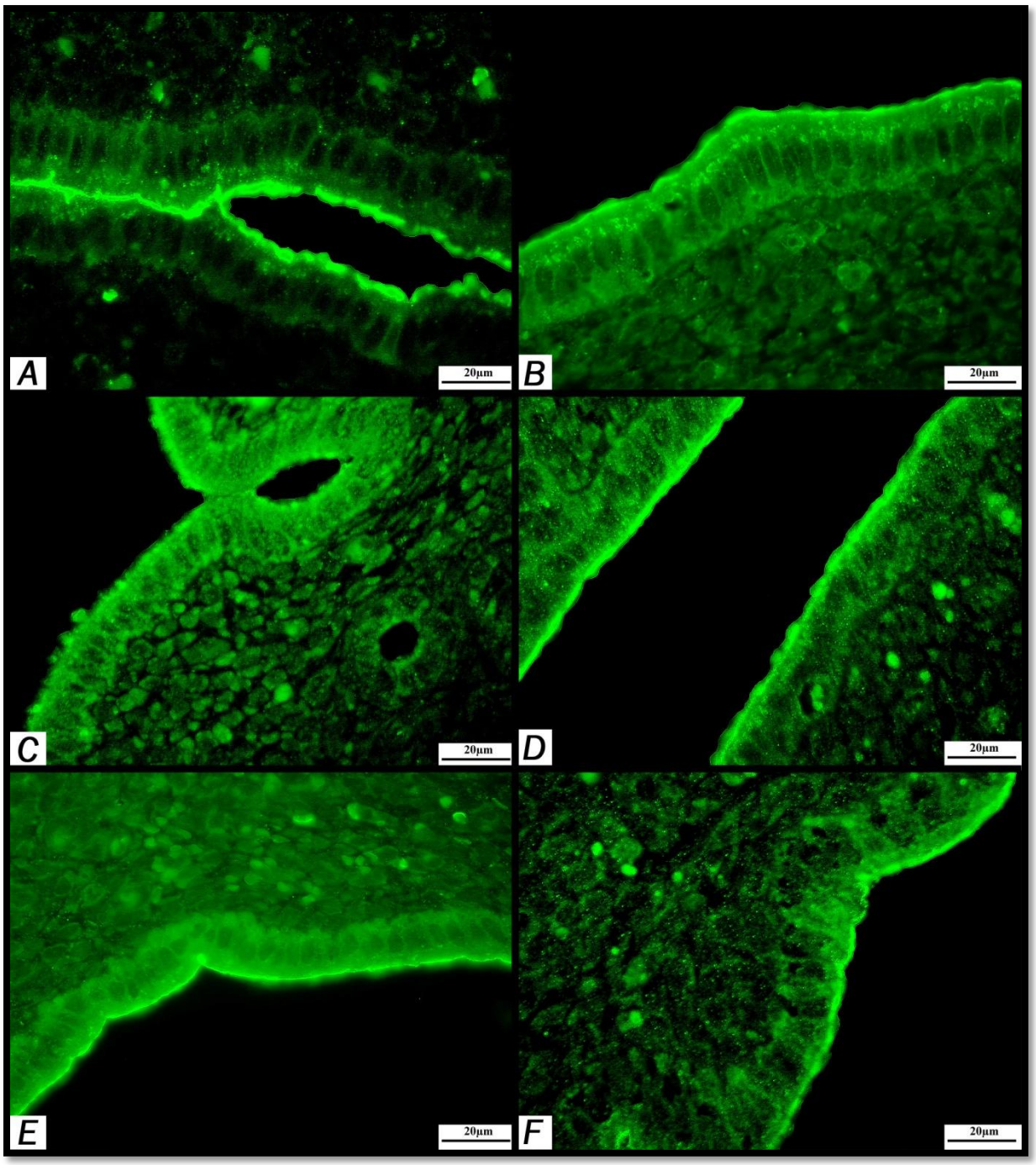


Figure 7.9 Immunofluorescent images illustrating LIF protein localisation in the luminal epithelium and the subepithelial stroma of implantation and non-implantation sites in the uteri of RU486-treated pregnant rats. A: Implantation site at day 4.5 of pregnancy, **B:** Non-implantation site at day 4.5 of pregnancy, **C:** Implantation site at day 5.5 of pregnancy, **D:** Non-implantation site at day 5.5 of pregnancy, **E:** Implantation site at day 6.5 of pregnancy, **F:** Non-implantation site at day 6.5 of pregnancy. Scale = 20µm.

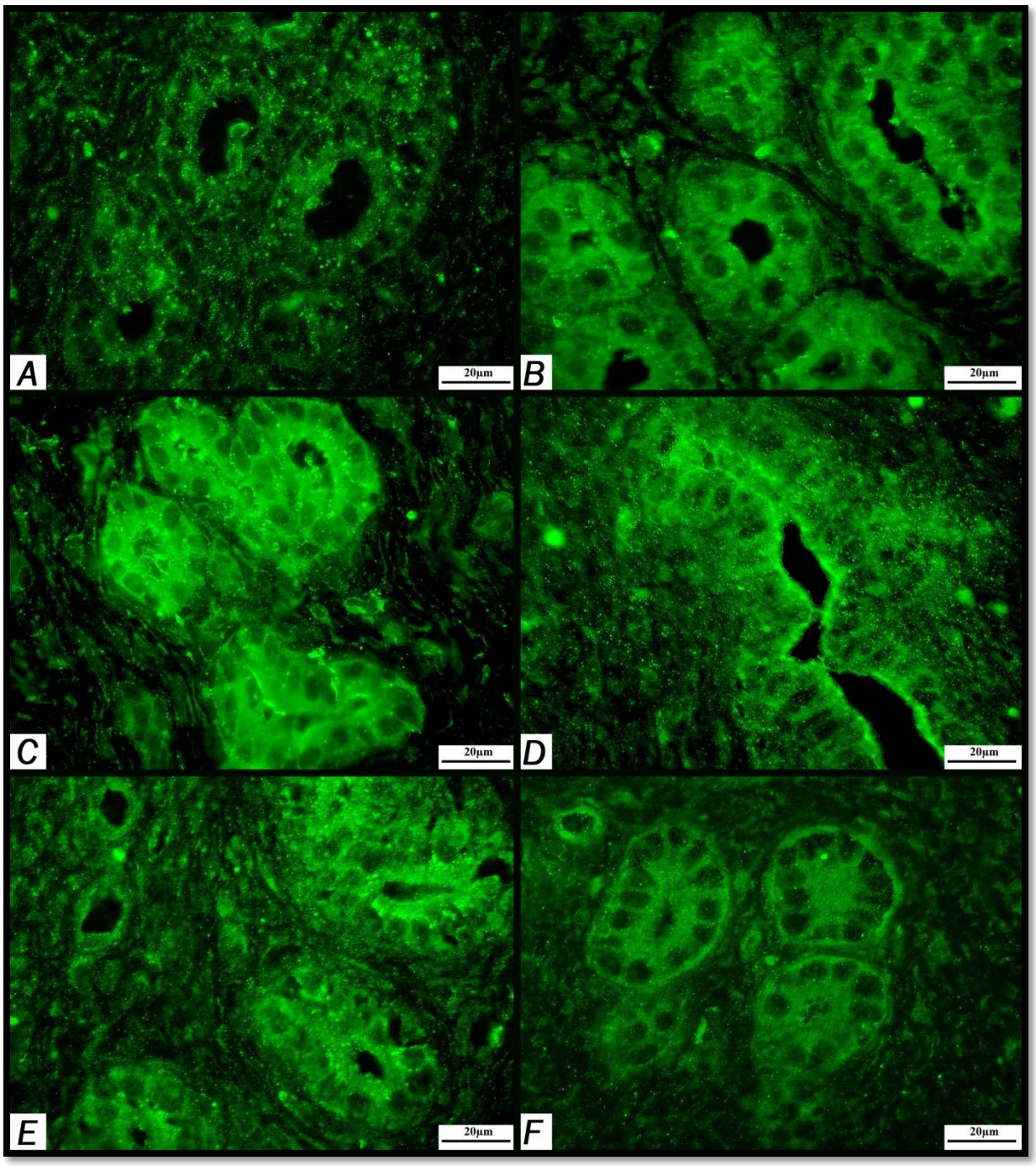


Figure 7.10 Immunofluorescent images illustrating LIF protein localisation in the glandular stroma and the glandular stroma of the implantation and non-implantation sites in the uteri of RU486-treated pregnant rats. A: Implantation site at day 4.5 of pregnancy, **B:** Non-implantation site at day 4.5 of pregnancy, **C:** Implantation site at day 5.5 of pregnancy, **D:** Non-implantation site at day 5.5 of pregnancy, **E:** Implantation site at day 6.5 of pregnancy, **F:** Non-implantation site at day 6.5 of pregnancy. Scale = 20µm.

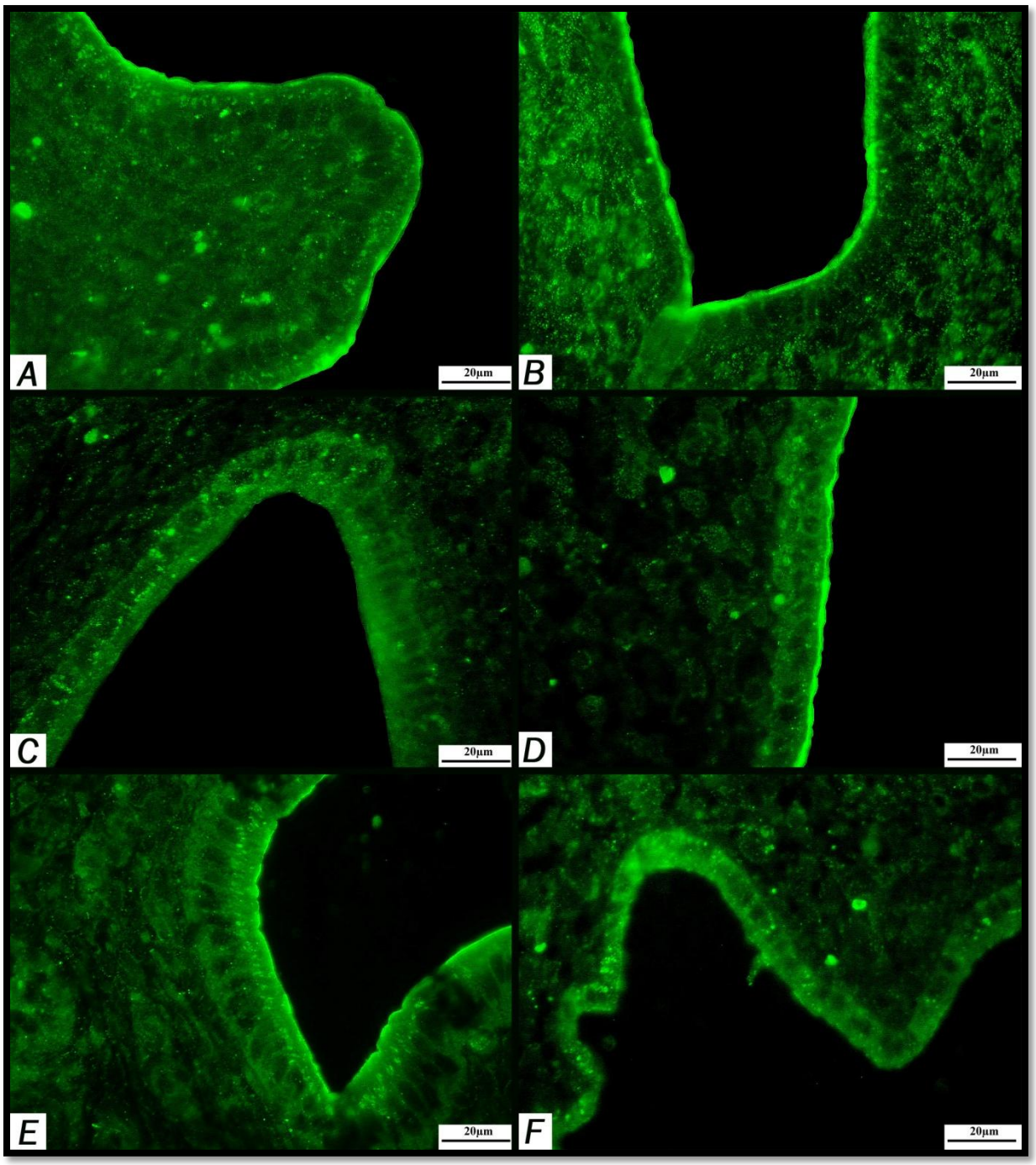


Figure 7.11 Immunofluorescent images illustrating Muc-1 protein localisation in the luminal epithelium and the subepithelial stroma of the implantation and non-implantation sites in the uteri of RU486-treated pregnant rats. A: Implantation site at day 4.5 of pregnancy, **B:** Non-implantation site at day 4.5 of pregnancy, **C:** Implantation site at day 5.5 of pregnancy, **D:** Non-implantation site at day 5.5 of pregnancy, **E:** Implantation site at day 6.5 of pregnancy, **F:** Non-implantation site at day 6.5 of pregnancy. Scale = 20µm.

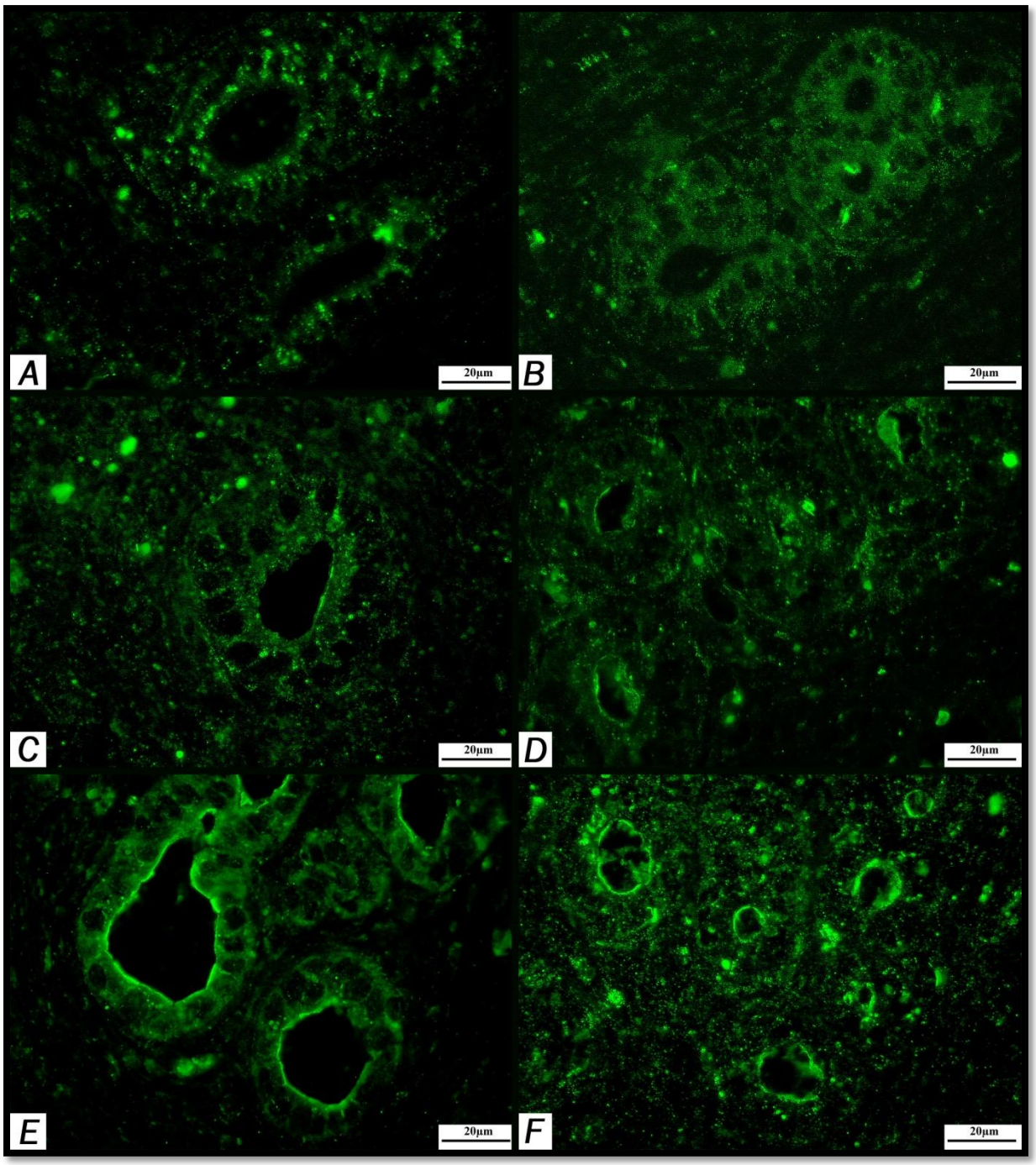


Figure 7.12 Immunofluorescent images illustrating Muc-1 protein localisation in the glandular epithelium and the glandular stroma of the implantation and non-implantation sites in the uteri of RU486-treated pregnant rats. A: Implantation site at day 4.5 of pregnancy, **B:** Non-implantation site at day 4.5 of pregnancy, **C:** Implantation site at day 5.5 of pregnancy, **D:** Non-implantation site at day 5.5 of pregnancy, **E:** Implantation site at day 6.5 of pregnancy, **F:** Non-implantation site at day 6.5 of pregnancy. Scale = 20µm.

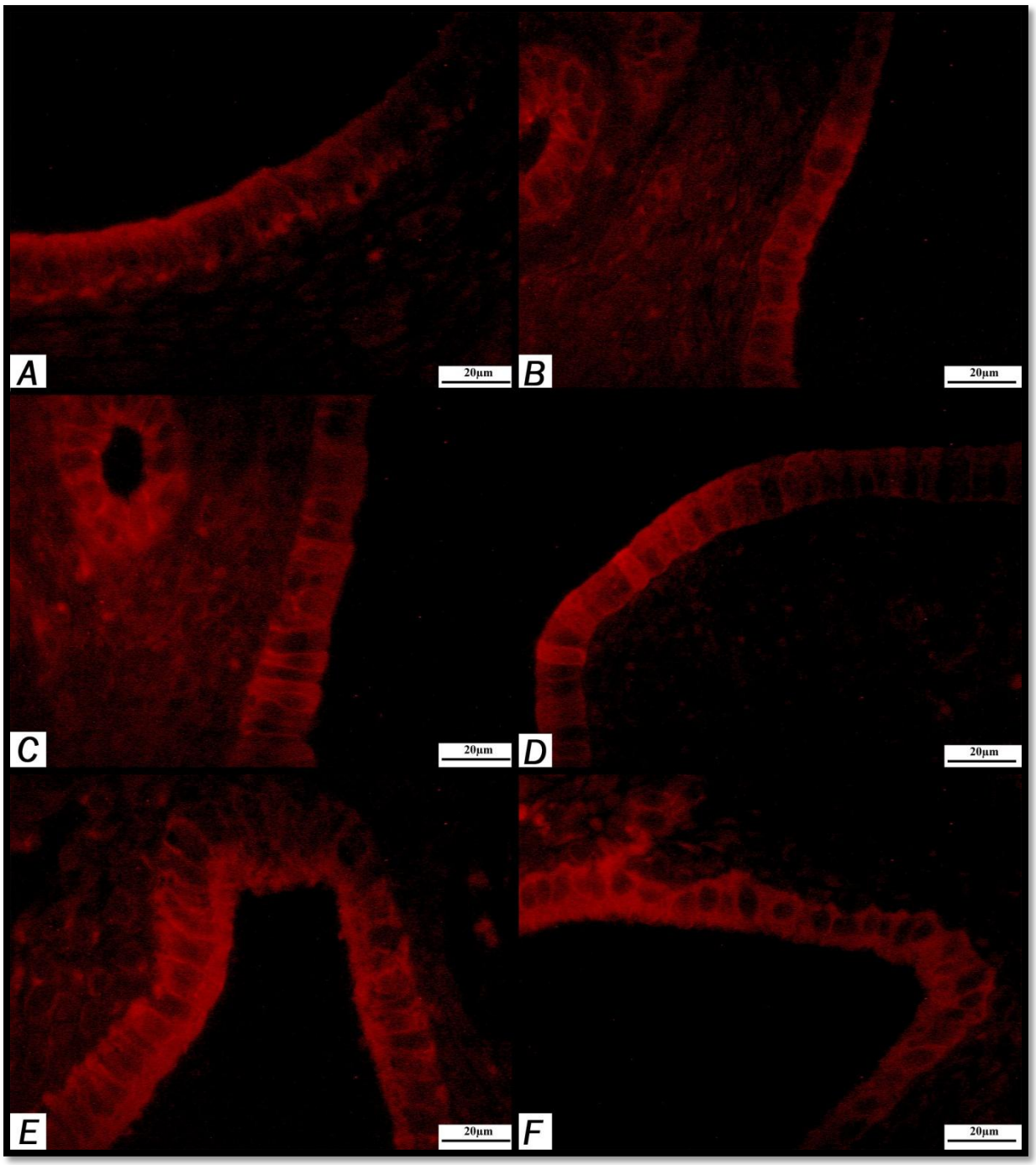


Figure 7.13 Immunofluorescent images illustrating Calcitonin protein localisation in the luminal epithelium and the subepithelial stroma of the implantation and non-implantation sites in the uteri of RU486-treated pregnant rats. A: Implantation site at day 4.5 of pregnancy, **B:** Non-implantation site at day 4.5 of pregnancy, **C:** Implantation site at day 5.5 of pregnancy, **D:** Non-implantation site at day 5.5 of pregnancy, **E:** Implantation site at day 6.5 of pregnancy, **F:** Non-implantation site at day 6.5 of pregnancy. Scale = 20µm.

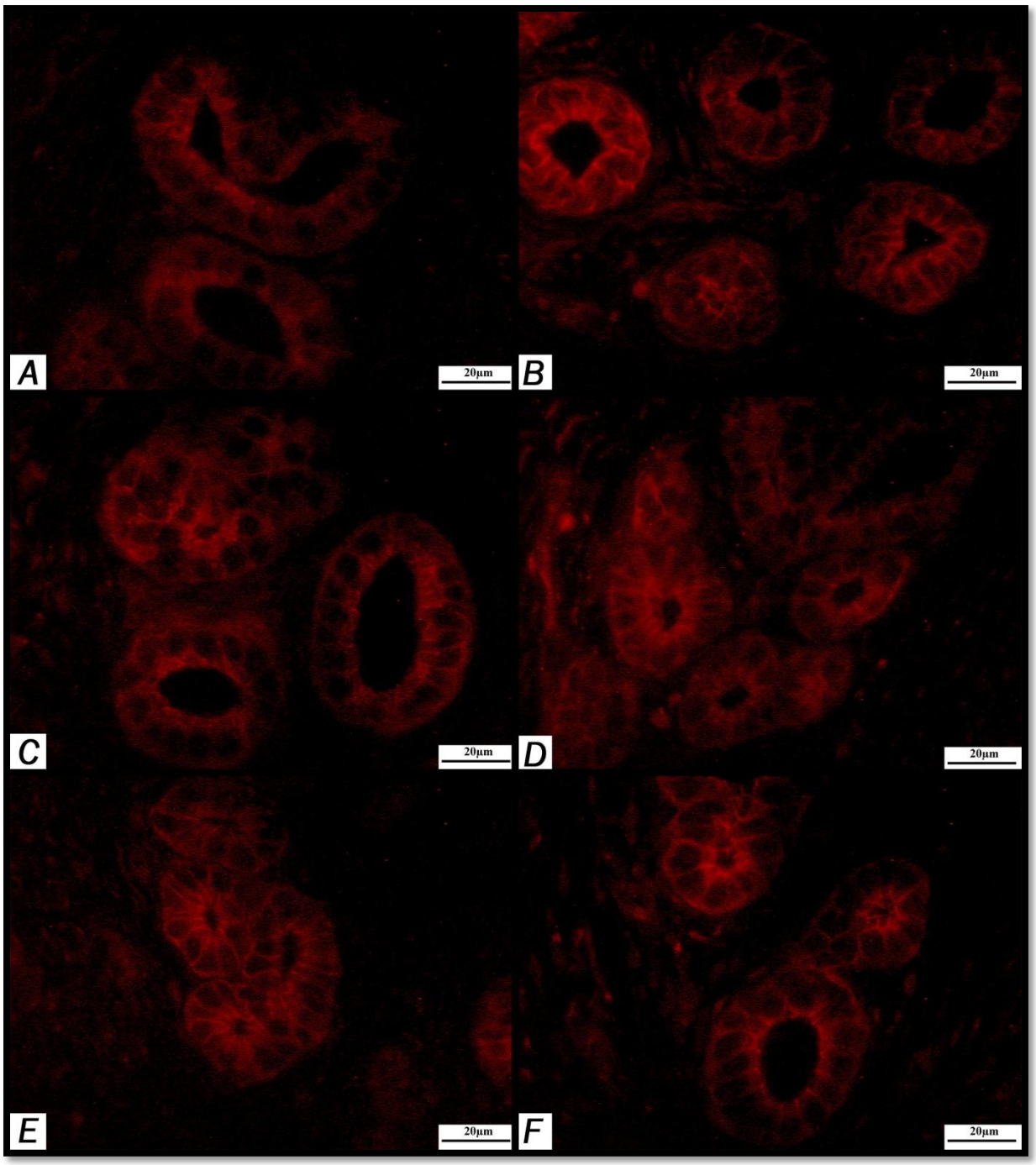


Figure 7.14 Immunofluorescent images illustrating Calcitonin protein localisation in the glandular epithelium and the glandular stroma of the implantation and non-implantation sites in the uteri of RU486-treated pregnant rats. A: Implantation site at day 4.5 of pregnancy, **B:** Non-implantation site at day 4.5 of pregnancy, **C:** Implantation site at day 5.5 of pregnancy, **D:** Non-implantation site at day 5.5 of pregnancy, **E:** Implantation site at day 6.5 of pregnancy, **F:** Non-implantation site at day 6.5 of pregnancy. Scale = 20µm.

7.2.2 The Effects of RU846 on Gene Expression of the Endometrial Biomarkers in the Rat Uterus during Early Pregnancy

The effect of RU486 on the expression of the endometrial biomarkers, LIF, Muc-1 and Calcitonin, gene expression in the implantation and non-implantation sites of the rat uterus at days 5.5 and 6.5 of pregnancy was analysed by relative quantification reverse transcriptase real-time qPCR. Only transcription on days 5.5 and 6.5 of pregnancy were analysed in the present study, as it was considered that these two days are the most important with regards to the implantation process since implantation and invasion occur on these days respectively. These genes have been identified within the endometrium as endometrial biomarkers, whose expression pattern can help with endometrial dating during early pregnancy. As implantation occurs at day 5.5 of pregnancy in the implantation sites this group was chosen as the calibrator sample and it follows that that all results are compared relative to this group.

7.2.2.1 Relative quantification (RQ) analysis of LIF, Muc-1 and Calcitonin gene expression in the control pregnant animals

In the control pregnant animals at day 5.5 of pregnancy, LIF gene expression was up-regulated by 3.5-fold in the non-implantation sites relative to the implantation sites (Graph 7.10; Table 7.4A). Consistent with immunofluorescence staining results, LIF gene expression was down-regulated by day 6.5 of pregnancy by 9.1-fold in the implantation sites and 6.2-fold in the non-implantation sites respectively (Graph 7.10; Table 7.4A). The LIF gene was expressed in greater amounts within the non-implantation sites at both days of pregnancy (Graph 7.10; Table 7.4A).

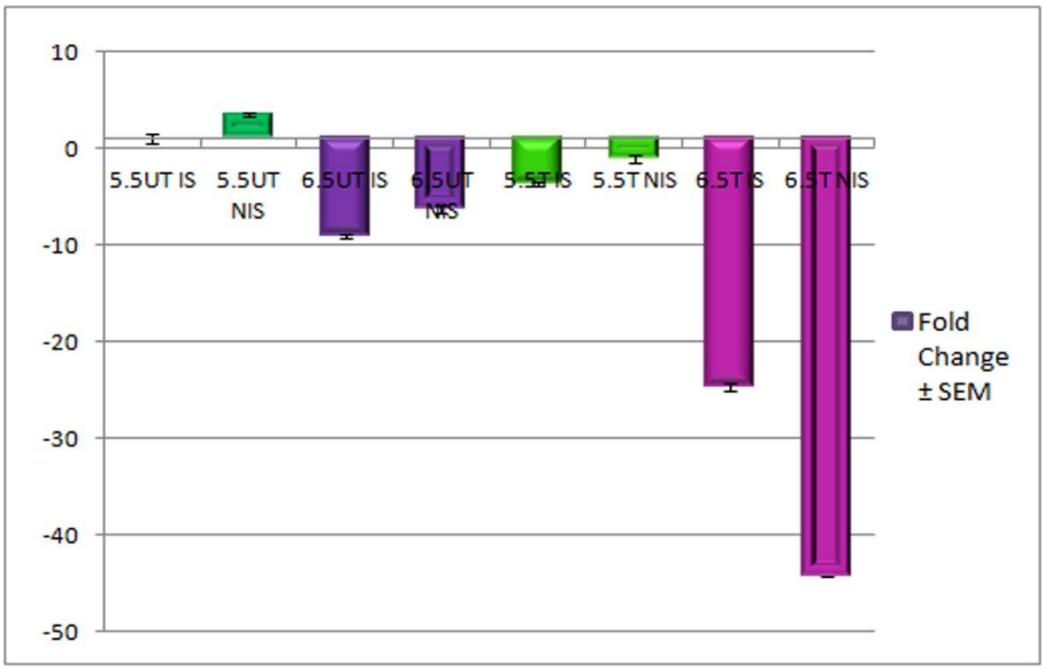
Muc-1 gene expression was higher in the non-implantation sites (2.3-fold) relative to the implantation sites at day 5.5 of pregnancy (Graph 7.11; Table 7.4B). By day 6.5 of pregnancy, Muc-1 gene expression was fairly similar (1.3-fold decrease) in the implantation sites relative to the calibrator, whereas it was up-regulated 2.2-fold in the non-implantation sites at this day of pregnancy (Graph 7.11; Table 7.4B). As is the case with LIF gene expression, Muc-1 levels were higher in the non-implantation sites relative to the implantation site at both days of pregnancy (Graph 7.11; Table 7.4B).

Calcitonin gene expression at day 5.5 of pregnancy was 2.3-fold higher in the non-implantation sites relative to the implantation sites (Graph 7.12; Table 7.4C). At day 6.5 of pregnancy, Calcitonin gene expression had decreased by 2-fold in the implantation sites and 2.1-fold in the non-implantation sites relative to the calibrator sample (Graph 7.12; Table 7.4C). Thus, at day 5.5 of pregnancy, Calcitonin gene levels were higher in the non-implantation sites, whereas at day 6.5 of pregnancy levels were fairly similar in both the implantation and non-implantation sites (Graph 7.12; Table 7.4C).

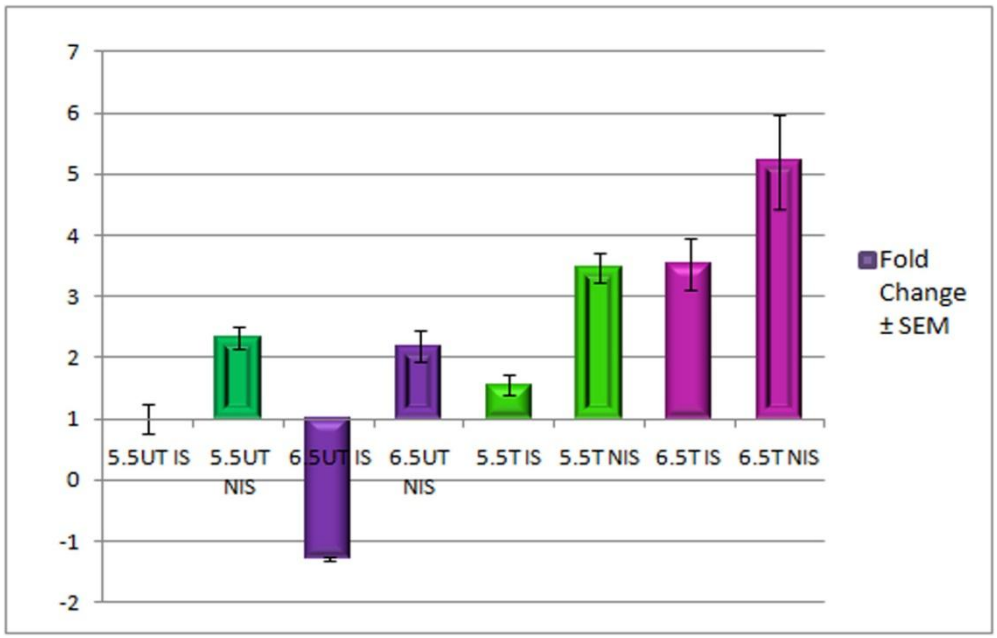
Table 7.4 RQ analysis of LIF, Muc-1 and Calcitonin gene expression in the implantation (IS) and non-implantation (NIS) sites at day 5.5 and 6.5 of pregnancy in the control pregnant (UT) and RU486-treated (T) animals. A fold change of 2 or more represents a significant difference in gene expression.

A: LIF Gene Expression								
Day of Pregnancy	**Avg. C_T**	**SEM**	**ΔC_T**	**SEM**	**$\Delta\Delta C_T$**	**$2^{-\Delta\Delta Ct}$**	**$Log_{10}(2^{-\Delta\Delta Ct})$**	**Fold Change ($2^{\Delta\Delta Ct}$)**
B-actin *	19.87	0.77	-	-	-	-	-	-
5.5UT IS **	29.31	1.21	9.44	0.44	0	1	0	1
5.5UT NIS	27.52	0.94	7.65	0.16	-1.79	3.46	0.54	3.46
6.5UT IS	32.50	0.98	12.62	0.21	3.19	0.11	-0.96	-9.10
6.5UT NIS	31.96	1.18	12.08	0.41	2.64	0.16	-0.80	-6.25
5.5T IS	31.21	1.01	11.34	0.24	1.90	0.27	-0.57	-3.74
5.5T NIS	29.46	1.20	9.58	0.43	0.15	0.90	-0.04	-1.11
6.5T IS	33.94	1.16	14.07	0.39	4.63	0.04	-1.39	-24.74
6.5T NIS	34.78	0.83	14.91	0.05	5.47	0.02	-1.65	-44.33
B: Muc-1 Gene Expression								
Day of Pregnancy	**Avg. C_T**	**SEM**	**ΔC_T**	**SEM**	**$\Delta\Delta C_T$**	**$2^{-\Delta\Delta Ct}$**	**$Log_{10}(2^{-\Delta\Delta Ct})$**	**Fold Change ($2^{\Delta\Delta Ct}$)**
B-actin *	19.87	0.77	-	-	-	-	-	-
5.5UT IS **	28.29	1.01	8.42	0.24	0	1	0	1
5.5UT NIS	27.08	0.95	7.20	0.17	-1.22	2.32	0.37	2.32
6.5UT IS	28.65	0.81	8.77	0.03	0.36	0.78	-0.11	-1.28
6.5UT NIS	27.16	1.03	7.29	0.25	-1.13	2.19	0.34	2.19
5.5T IS	27.65	0.94	7.78	0.17	-0.64	1.56	0.19	1.56
5.5T NIS	26.50	1.02	6.62	0.24	-1.80	3.47	0.54	3.47
6.5T IS	26.48	1.20	6.60	0.42	-1.82	3.52	0.55	3.52
6.5T NIS	25.91	1.54	6.03	0.77	-2.38	5.21	0.72	5.21
C: Calcitonin Gene Expression								
Day of Pregnancy	**Avg. C_T**	**SEM**	**ΔC_T**	**SEM**	**$\Delta\Delta C_T$**	**$2^{-\Delta\Delta Ct}$**	**$Log_{10}(2^{-\Delta\Delta Ct})$**	**Fold Change ($2^{\Delta\Delta Ct}$)**
B-actin *	19.87	0.77	-	-	-	-	-	-
5.5UT IS **	30.30	1.25	10.43	0.48	0	1	0	1
5.5UT NIS	29.12	1.16	9.25	0.38	-1.18	2.27	0.36	2.26
6.5UT IS	31.30	1.48	11.42	0.70	1.00	0.50	-0.30	-2.00
6.5UT NIS	31.33	1.32	11.46	0.55	1.04	0.49	-0.31	-2.05
5.5T IS	30.84	1.50	10.97	0.73	0.55	0.69	-0.16	-1.46
5.5T NIS	29.50	1.53	9.63	0.76	-0.80	1.74	0.24	1.74
6.5T IS	28.99	1.25	9.11	0.48	-1.31	2.48	0.40	2.48
6.5T NIS	27.72	0.91	7.85	0.14	-2.58	5.97	0.78	5.97

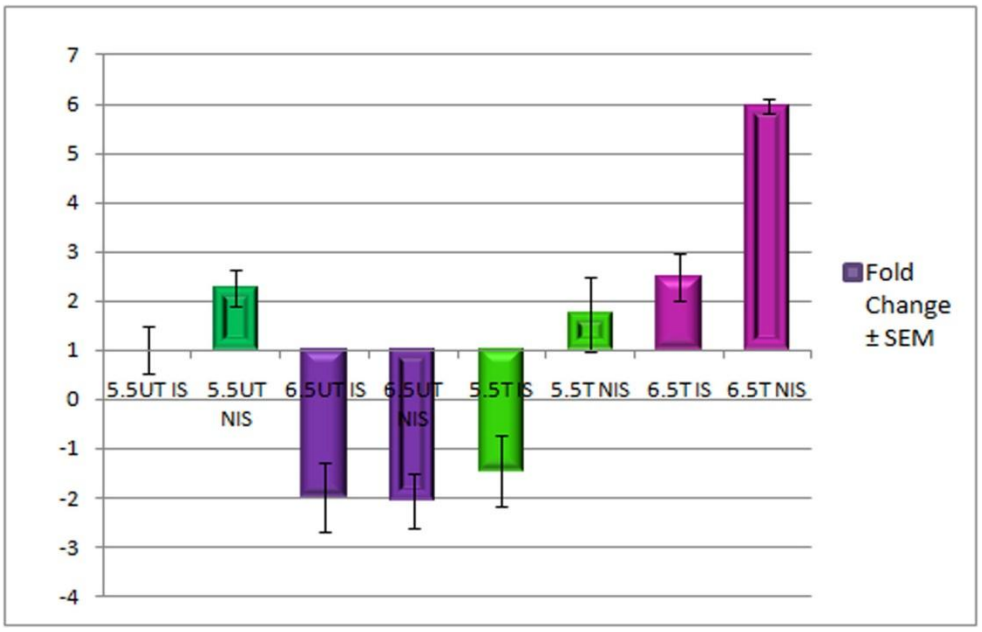
UT - untreated, **T** - treated, **IS** - implantation site, **NIS** - non-implantation site, **C_T** - threshold cycle, **SEM** - standard error of the mean, ***** - endogenous control, ****** - calibrator sample. **ΔC_T** = C_T (Target) - C_T (Endogenous control). **$\Delta\Delta C_T$** = ΔC_T (Target) - ΔC_T (Calibrator).



Graph 7.10 Graphical representation of LIF gene expression as compared to day 5.5 in the control pregnant animals, the calibrator sample. The data is expressed as the Fold Change ± SEM.
UT – untreated, **T** – treated, **IS** – implantation site, **NIS** – non-implantation site.



Graph 7.11 Graphical representation of Muc-1 gene expression as compared to day 5.5 in the control pregnant animals, the calibrator sample. The data is expressed as the Fold Change ± SEM.
UT – untreated, **T** – treated, **IS** – implantation site, **NIS** – non-implantation site.



Graph 7.12 Graphical representation of Calcitonin gene expression as compared to day 5.5 in the control pregnant animals, the calibrator sample. The data is expressed as the Fold Change ± SEM. **UT** – untreated, **T** – treated, **IS** – implantation site, **NIS** – non-implantation site.

7.2.2.2 Relative quantification (RQ) analysis of the effects of RU486 on LIF, Muc-1 and Calcitonin gene expression

Following treatment with RU486, LIF gene expression was down-regulated 3.7-fold in the implantation sites and remained similar (decrease of 1.1-fold) in the non-implantation sites at day 5.5 of pregnancy, relative to the calibrator sample (Graph 7.10; Table 7.4A). Overall, in the non-implantation sites LIF gene expression was decreased by 3.6-fold. By day 6.5 of pregnancy, RU486 administration resulted in a 24.8-fold decrease in the implantation sites and a 44.3-fold decrease in the non-implantation sites respectively, relative to the calibrator sample (Graph 7.10; Table 7.4A).

Muc-1 gene expression was fairly similar in the implantation sites at day 5.5 of pregnancy following treatment with RU486 (1.6-fold increase), whereas in the non-implantation sites it was up-regulated by 3.5-fold (Graph 7.11; Table 7.4B). By day 6.5 of pregnancy, Muc-1 gene expression was 3.5-fold higher in the implantation sites and 5.2-fold higher in the non-implantation sites respectively, relative to the calibrator sample (Graph 7.11; Table 7.4B). RU486 resulted in a 4.6-fold increase in Muc-1 gene expression in the implantation sites and a 2.4-fold increase in the non-implantation sites at day 6.5 of pregnancy (Graph 7.11; Table 7.4B).

Calcitonin gene expression was also fairly similar in the implantation sites at day 5.5 of pregnancy after treatment with RU486 (1.5-fold decrease), whereas it was up-regulated slightly by 1.7-fold in the

non-implantation sites relative to the calibrator sample (Graph 7.12; Table 7.4C). By day 6.5 of pregnancy, Calcitonin gene expression increased in the RU486-treated animals and was 2.5-fold higher in the implantation sites and 6-fold higher in the non-implantation sites relative to the calibrator sample (Graph 7.12; Table 7.4C). Overall, there was a 5-fold increase and a 12.4-fold increase in the implantation and non-implantation sites respectively at day 6.5 of pregnancy, as a result of RU486 administration (Graph 7.12; Table 7.4C).

In summary, RU486 had an overall inhibitory effect on LIF gene expression at day 5.5 and 6.5 of pregnancy. In contrast, Muc-1 gene expression was increased at day 5.5 and 6.5 of pregnancy by RU486 administration. Calcitonin gene expression was decreased initially at day 5.5 of pregnancy as a consequence of RU486 treatment and then increased at day 6.5 of pregnancy.

7.3 DISCUSSION

7.3.1 The Effects of RU486 on Selected Endometrial Biomarkers of Receptivity during Early Pregnancy

7.3.1.1 The spatiotemporal expression pattern of LIF in the rat uterus during early pregnancy and the effects of RU486 on this expression

Leukaemia Inhibitory Factor (LIF) is one cytokine which appears to be critically involved in implantation and embryonic development. The importance of LIF to blastocyst implantation has been demonstrated in both humans and mice (Stewart *et al.*, 1992; Laird *et al.*, 1997).

In the current study, LIF protein expression was analysed in the luminal and glandular epithelium as well as in the subepithelial stroma and that surrounding the glandular compartment. Immunofluorescence results from the control pregnant animals in this study concur with previous studies on LIF protein expression in the endometrium in the lead up to blastocyst implantation (Bhatt *et al.*, 1991; Yang *et al.*, 1996). The present study clearly demonstrated that LIF protein levels peaked at around day 5.5 of pregnancy, the day of blastocyst implantation. This increase was followed by a marked decrease in LIF levels by day 6.5 of pregnancy, observed in both the implantation and non-implantation sites. In the RT-qPCR analysis of the present study, LIF mRNA levels decreased by 9.13-fold in the implantation sites and 6.23-fold in the non-implantation sites, with the progression of pregnancy through to day 6.5. These results demonstrate an overall decrease in LIF mRNA levels in the control pregnant animals as pregnancy progresses from day 5.5 to day 6.5, in agreement with the immunofluorescence results in the current study.

In a study on the mouse endometrium, a second burst of LIF expression was observed by *in situ* hybridisation, at day 4 of pregnancy (they day of blastocyst implantation in mice) (Bhatt *et al.*, 1991). Subsequent to implantation of the blastocyst, LIF expression declined and remained at low levels throughout the remainder of the gestation period (Bhatt *et al.*, 1991). This increase in LIF expression around the time of blastocyst implantation and subsequent decline in LIF levels has also been described in pseudopregnant mice, indicating that LIF is maternally controlled rather than induced by a signal originating from the blastocyst (Bhatt *et al.*, 1991; Shen and Leder, 1992). In the Bhatt *et al.* (1991) study, LIF expression was observed to be highest in the glandular epithelium with lower levels in the luminal epithelium and lower still in the stromal compartments. The results from the current study differ from this finding, as levels were highest in the luminal epithelium at all three days of pregnancy, followed by the glandular epithelium and finally the stromal compartment. A possible reason for this discrepancy may relate to the focus on protein levels in the different endometrial

compartments in the present study, whereas mRNA levels were studied in the mouse (Bhatt *et al.*, 1991). Alternatively, LIF protein has been reported to be stored within the extracellular matrix, this possibly accounting for the described discrepancy in mRNA and protein levels. Since in the mouse endometrium, LIFR and gp130 are highly expressed in the luminal epithelium (Ni *et al.*, 2002), it can be suggested that the high levels of LIF protein in the present study is due to LIF bound to its receptors at this stage of pregnancy.

In cultured endometrial stromal cells, PDGF has been reported to be a potent inducer of LIF expression in a concentration- and time-dependent manner (Arici *et al.*, 1995). Were this regulation of LIF by PDGF to occur within the endometrium during early pregnancy then it is possible that the observed decrease in LIF expression in the control pregnant animals subsequent to blastocyst implantation, can be attributed to the reduction in PDGF expression seen at this stage of pregnancy, as described in Chapter 6. Further research is needed to better elucidate this possible control of LIF expression by this growth factor during early pregnancy.

Interestingly, in the present study, LIF protein levels increased significantly only in the luminal epithelium and subepithelial stromal compartments of the implantation sites with the progression of pregnancy from day 4.5 to day 5.5. Even though LIF expression is likely maternally controlled (see above), it nevertheless plays an important role in preimplantation development (Bhatt *et al.*, 1991; Shen and Leder, 1992; Mitchell *et al.*, 1994). Both LIF and its receptors have been described in the embryo as well as the endometrium (Kojima *et al.*, 1994; Nichols *et al.*, 1996; Ding *et al.*, 2008), suggesting a possible occurrence of auto-paracrine cross-talk between the two tissues. In the mouse endometrium, it is postulated that LIF derived from the luminal epithelium acts in a paracrine manner on the blastocyst and/or as an autocrine regulator of endometrial epithelium, to allow for blastocyst implantation (Stewart *et al.*, 1992). In addition, LIF increases the number of embryos developing to the blastocyst stage *in vitro* and leads to enhanced pregnancy and viability rates when transferred to pseudopregnant recipients (Mitchell *et al.*, 2002). Thus, it is possible that this increase in LIF expression around the implantation sites at day 5.5 of pregnancy reported in the present study is as a direct result of this cross-talk between the embryo and the endometrium.

This spatiotemporal expression of LIF and LIFR during early pregnancy has been described in various species; including, the mouse (Bhatt *et al.*, 1991), rabbit (Lei *et al.*, 2004), sheep (Vogiagis *et al.*, 1997), mink (Song *et al.*, 1998), skunk (Hirzel *et al.*, 1999; Passavant *et al.*, 2000), pig (Modric *et al.*, 2000), monkey (Yue *et al.*, 2000) and human (Charnock-Jones *et al.*, 1994; Cullinan *et al.*, 1996; Tsai *et al.*, 2000).

In the mouse uterus, LIF expression appears to be under the control of the ovarian hormone oestrogen as the two peaks of LIF expression observed in the lead-up to blastocyst implantation coincide with physiologically elevated levels of oestrogen (Bhatt *et al.*, 1991). In addition LIF expression is induced by an injection of oestrogen in ovariectomised mice and is not affected by progesterone, suggesting a strong oestrogenic effect (Bhatt *et al.*, 1991; Stewart and Cullinan, 1997; Chen *et al.*, 2000). In the ovariectomised mouse endometrium, LIF is also able to replace the nidatory oestrogen stimulus required for initiation of implantation as well as decidualisation of the stromal cells (Chen *et al.*, 2000). In the rabbit, LIF expression appears to be under the control of the ovarian hormone progesterone (Yang *et al.*, 1996; Lei *et al.*, 2004) as LIF and LIFR expression levels in the uterine epithelium are higher in oestrous, the stage of the oestrous cycle characterised by a progesterone surge (Spornitz *et al.*, 1999), when compared to the non-oestrous animals. LIF and LIFR levels were also shown to constantly increase after ovulation, supporting the idea that progesterone regulates LIF and LIFR expression in the rabbit endometrium as maternal progesterone levels increase following ovulation (Dugré *et al.*, 1989; Lei *et al.*, 2004).

In humans, LIF also appears to be under the control of progesterone as maximal LIF protein and mRNA expression is observed in the luminal and glandular epithelium during the postovulatory or secretory phase, a period when the endometrium is under the influence of progesterone (Charnock-Jones *et al.*, 1994; Cullinan *et al.*, 1996). LIF protein and mRNA is expressed at low levels in the glandular epithelial and stromal compartments during the proliferative phase of the menstrual cycle, when progesterone levels are low (Arici *et al.*, 1995; Yang *et al.*, 1996). In support of this, treatment with the PR antagonist RU486 immediately postovulation, reduced the glandular localisation of LIF around the time of blastocyst implantation (Danielsson *et al.*, 1997). In ovariectomised ewes, treatment with oestradiol alone resulted in lower levels of LIF when compared with animals treated with oestrogen and progesterone (Vogiagis *et al.*, 1997). Thus, in species in which no nidatory oestrogen surge is present, progesterone appears to be the dominant hormone at implantation and may regulate LIF expression.

In the present study, a single dose of the PRM, RU486 at day 3.0 of pregnancy significantly lowered levels of LIF protein in the luminal epithelial, decidual, glandular epithelial and glandular stromal compartments in both the implantation and non-implantation sites at day 4.5 of pregnancy. By day 5.5 of pregnancy in the RU486-treated animals, LIF protein levels in both the implantation and non-implantation sites had increased significantly from that observed at day 4.5 of pregnancy. LIF protein levels in the RU486-treated animals were still observed to be significantly lower than normal LIF protein levels in the pregnant animals, except in the glandular compartment. By day 6.5 of pregnancy, LIF protein levels in the control pregnant animals were shown to decrease significantly from that observed at day 5.5 of pregnancy. This decrease in LIF expression was inhibited in the RU486-treated

animals. Thus, RU486 was demonstrated to have an overall inhibitory effect on LIF mRNA levels in both the implantation and non-implantation sites at days 4.5 and 5.5 of pregnancy, whereas RU486 levels were higher at day 6.5 of pregnancy. In contrast to these results, LIF mRNA levels were observed to be decreased in both the implantation and non-implantation sites at days 5.5 and 6.5 of pregnancy due to RU486 administration. LIF mRNA levels were reduced at day 6.5 of pregnancy relative to day 5.5, whereas protein levels did not change much except for a reduction in the glandular epithelium. This discrepancy may pertain to the use of whole tissue homogenates in the RT-qPCR portion of the present study, so diluting any effect RU486 may have on LIF mRNA expression within a single endometrial compartment. It is possible that the decrease in LIF protein expression observed in the glandular epithelium is sufficient to result in an overall decrease in LIF mRNA levels. Alternatively, LIF protein levels within the myometrium were not analysed and as this endometrial portion is quite large, any decrease in LIF mRNA levels within this compartment would lead to an overall decrease in LIF mRNA expression within the endometrium.

Yang *et al.* (1996) demonstrated that LIF protein in the mouse uterus is directly or indirectly under the control of the maternal hormone oestrogen as LIF production in ovariectomised mice was stimulated by oestrogen administration. Progesterone was observed to have no additive effect when the ovariectomised mice were treated with both oestrogen and progesterone (Yang *et al.*, 1996). These findings are in agreement with the high levels of LIF mRNA and protein seen in unmated mice during the pro-oestrous and oestrous sages of the oestrous cycle, when the level of maternal oestrogen is high (Shen and Leder, 1992; Yang *et al.*, 1996).

In the present study, RU486 inhibited LIF expression around the time of blastocyst implantation where LIF levels are high in the control pregnant animals. Due to the antiprogestin qualities of RU486, it is tempting to suggest that these results indicate a role for progesterone in the regulation of LIF. A more likely explanation, however, is that animals treated with RU486 generally display characteristics of a hormonally under-stimulated uterus, reflective of that observed in ovariectomised animals. It has been previously reported that RU486 not only exhibits an antiprogestin effect within the endometrium, but an anti-oestrogen effect as well. RU486 has been shown to block oestrogen binding with over 80% efficiency relative to that of the pure oestrogen blocker ICI 164382 (McDonnell and Goldman, 1994). Thus, the decrease in LIF expression observed as a result of RU486 administration could be attributed to the decrease in oestrogen effects. This partial blockage of oestrogen action by RU486, resulting in some oestrogen binding and subsequent oestrogenic effects on the endometrium, could also explain why LIF levels were still high in the treated animals.

Despite all the evidence indicating the importance of LIF during implantation, it is not yet clear how LIF specifically functions in relation to the implantation process. LIFR is expressed in both oocytes

and blastocysts as well as in human pre-implantation embryos, suggesting that the blastocyst may be one target of this cytokine (van Eijk *et al.*, 1996). In the presence of LIF, trophoblast cultures have been shown to differentiate toward a more anchoring phenotype (Lass *et al.*, 2001), which has lead researchers to suggest a possible regulatory function for LIF on embryonic implantation by direct modulation of trophoblast differentiation (Nachtigall *et al.*, 1996). It has also been suggested that LIF mediates interactions between the endometrial leukocytes and the trophoblasts and may also control angiogenesis in the placental villi (Sharkey *et al.*, 1999). In mice, LIF has been shown to have an effect on the leukocyte populations in the preimplantation uterus as LIF knockout mice displayed decreased macrophage and increased natural killer (NK) cell subpopulations, which may contribute to the infertility seen in LIF knockout mice (Schofield and Kimber, 2005).

The decrease in LIF expression described in this study, as a direct consequence of RU486 administration, may be one of the mechanisms through which RU486 is able to successfully inhibit blastocyst implantation and subsequent pregnancy.

7.3.1.2 The spatiotemporal expression pattern of Muc-1 in the rat uterus during early pregnancy and the effects RU486 has on this expression

Muc-1 is a highly glycosylated mucin expressed on the uterine epithelial cell surface as part of the glycocalyx. It has been suggested that this mucin acts as a barrier to implantation and plays a crucial role in the defining of a receptive endometrium (Hey *et al.*, 1994). In this instance, in order to allow the close apposition of the blastocyst with the endometrium to facilitate successful implantation, the Muc-1 anti-adhesive barrier must be removed from the luminal surface (Surveyor *et al.*, 1995; Hild-Petito *et al.*, 1996).

The changes in the immunofluorescence pattern of Muc-1 during early pregnancy as demonstrated by the present study concur with previous findings in the mouse and pig endometrium; these demonstrated that Muc-1 is almost completely lost in both the luminal and glandular epithelium around the time of blastocyst implantation (Surveyor *et al.*, 1995; Bowen *et al.*, 1997). However, the findings of the present study appear to differ from a previous study in the rat endometrium, which reported this decrease of Muc-1 protein expression only in the luminal epithelium and not the glandular epithelium around the time of blastocyst implantation (DeSouza *et al.*, 1998), although the antibodies used in both studies were localised to the cytoplasmic tail of the Muc-1 protein. The antibody in the DeSouza *et al.* (1998) study was, however, pre-treated with *N*-ethylmaleimide (NEM) to reduce peptide interactions with tissue sections via disulfide cross-linking. This alteration was not carried out in the present study and in addition, there was a difference in timing. DeSouza *et al.*

(1998) determined Muc-1 levels at day 5 of pregnancy (day 1 designated day of sperm in vaginal smear), whereas in the present study levels were determined at days 4.5, 5.5 and 6.5 of pregnancy (day 0.5 designated as day of sperm in vaginal smear). Even so, in the present study, Muc-1 levels at day 4.5 of pregnancy were still moderate and did not exhibit the marked decrease in the luminal epithelium as reported by De Souza *et al.* (1998).

Were Muc-1 to function as a barrier to implantation, then the most important decrease in Muc-1 expression would certainly be the loss demonstrated in the apical portion of the luminal epithelial cells. In many species such as the mouse (Surveyor *et al.*, 1995), sheep (Johnson *et al.*, 2001), rabbit (Hoffman *et al.*, 1998) and pig (Bowen *et al.*, 1997), Muc-1 disappears on the day of initial attachment of the blastocyst to the luminal epithelium. In both the DeSouza *et al.* (1998) study and the present study, this loss of Muc-1 was reported in the luminal epithelium. These results are in agreement with the study on Muc-1 localisation by Isaacs and Murphy (2003) who, at an ultrastructural level, described the loss of early pregnancy associated Muc-1 from the apical surface of the uterine epithelial cells as occurring on day 6 of pregnancy, this being the day of blastocyst implantation.

In the rat study by DeSouza *et al.* (1998) and the mouse study by Surveyor *et al.* (1995), Muc-1 protein levels were not shown to increase again until at least day 8 in rats and day 6 in mice. This led them to suggest that Muc-1 does not play a role in the return of the unreceptive state of the uterus directly after blastocyst implantation (Surveyor *et al.*, 1995; DeSouza *et al.*, 1998). However, by day 6.5 of pregnancy in the present study, Muc-1 protein levels in the luminal epithelium of the implantation sites had increased to a similar level to that seen at day 4.5 of pregnancy. While Muc-1 protein levels had begun to increase in the glandular epithelium, levels were still lower than that seen at day 4.5 of pregnancy. It is possible that in the rat endometrium, the re-establishment of Muc-1 protein expression in the luminal epithelium plays a role in the restoration of the endometrium to an unreceptive state, following the window of receptivity. This is emphasised by the return of Muc-1 expression being more pronounced in the luminal epithelium, so lending more credibility to this suggestion, particularly as this is the first site of attachment. Moreover, it then follows that this site should be the first region to lose its receptive state. The presence of continued high progesterone levels throughout the rest of pregnancy, suggests that another factor/s besides progesterone and oestrogen levels are responsible for this increase in Muc-1 expression, as progesterone has previously been shown to antagonise the stimulatory effect oestrogen has on Muc-1 expression (Surveyor *et al.*, 1995). Further, the simultaneous change in Muc-1 expression within both the implantation and non-implantation sites with the progression of pregnancy, suggests that the blastocyst does not necessarily regulate Muc-1 expression. In support of this statement, unilateral ligation of a uterine horn does not prevent Muc-1 loss around the time of blastocyst implantation (DeSouza *et al.*, 1998).

In the present study, Muc-1 mRNA levels remained similar in both the implantation and non-implantation sites from day 5.5 to day 6.5 of pregnancy, in contrast to the increase demonstrated in Muc-1 protein levels at these days of pregnancy. This lack of increase in mRNA expression can be attributed to the utilisation of whole tissue homogenates in the RT-qPCR portion of the present study, resulting in dilution of expression patterns in the different endometrial compartments. Immunofluorescence staining demonstrated that the highest increase in Muc-1 protein levels occurred in the luminal and glandular epithelial compartments, while low levels of Muc-1 protein were maintained in the stromal compartments. As the stromal compartments make up the majority of the endometrium, it can be postulated that the lack of a considerable increase in the stromal compartments dilutes the increase observed in the epithelial compartments. In addition, the myometrium makes up a large portion of the endometrium as well, thus if levels are low in the myometrium, this would further dilute the increase observed in the epithelial compartments. *In situ* hybridisation studies would clarify the spatiotemporal expression pattern of Muc-1 mRNA.

In the rabbit, baboon and human endometrium, Muc-1 expression is regulated by the ovarian hormone progesterone (Hey *et al.*, 1994; Hild-Petito *et al.*, 1996; Hoffman *et al.*, 1998). In rabbits, Muc-1 reduction at the time of blastocyst attachment is restricted to the implantation sites, whereas a high level of Muc-1 is maintained within the non-implantation sites. It was thus hypothesised that Muc-1 down-regulation occurs via a local signal, probably produced by the blastocyst (Hoffman *et al.*, 1998). In humans, Muc-1 protein and mRNA levels increase during the implantation window, in contrast to findings in other animals, inclusive of the present study (Meseguer *et al.*, 2001). However, it must be mentioned that at the adhesion phase, the embryo induces a paracrine enzymatic cleavage of endometrial epithelial Muc-1 at the implantation sites, and it has thus been suggested that Muc-1 acts as an endometrial anti-adhesive molecule that is locally removed by the human blastocyst at the time of adhesion (Hoffman *et al.*, 1998; Meseguer *et al.*, 2001).

In contrast, in the mouse and rat endometrium Muc-1 expression is down-regulated in response to progesterone stimulation (Surveyor *et al.*, 1995; DeSouza *et al.*, 1998). Braga and Gendler (1993) demonstrated that Muc-1 expression in the uterus is high when serum concentrations of oestrogen are elevated and its expression is repressed by high levels of progesterone. In ovariectomised mice, oestrogen stimulated Muc-1 expression, whereas progesterone antagonised this increase by oestrogen (Surveyor *et al.*, 1995). This increase in Muc-1 expression was also antagonised by the anti-oestrogen ICI 164 384, indicating that the oestrogen regulation of Muc-1 is mediated by the ER (Dutt *et al.*, 1986). In support of Muc-1 regulation by steroid hormones and not the presence of the preimplantation blastocyst, unilateral ligation of a uterine horn did not prevent the loss of Muc-1 at day 5 of pregnancy (DeSouza *et al.*, 1998).

The antiprogestin RU486 did not appear to have a marked effect on Muc-1 protein levels as levels were stable in the RU486-treated animals with the progression of pregnancy from day 4.5 through to day 5.5, with levels similar to those observed in the control pregnant animals at day 4.5 of pregnancy, prior to the decrease in Muc-1 localisation. However, this lack of change in Muc-1 protein expression in the RU486-treated animals resulted in significantly higher levels in the RU486- treated animals at day 5.5 of pregnancy relative to the control pregnant animals, due to the loss of Muc-1 localisation around the time of blastocyst implantation during early pregnancy. By day 6.5 of pregnancy, the increase in Muc-1 protein levels in the control pregnant animals was not sufficient for levels to be similar to that in the RU486-treated animals. This was reflected in the mRNA analysis in that Muc-1 expression levels were higher in the implantation and non-implantation sites of the RU486-treated animals relative to the control pregnant animals.

It has been previously reported that the decrease in Muc-1 expression within the endometrium around the time of implantation is due to the antagonistic effect progesterone has on oestrogen stimulation of Muc-1 expression (Surveyor *et al.*, 1995). This control of Muc-1 expression by progesterone would account for the lack of reduction in Muc-1 expression as a consequence of RU486 administration at day 3.0 of pregnancy, as binding of RU486 to PR translates into lack of progesterone effects on the endometrium. As oestrogen is reported to have a stimulatory effect on Muc-1 expression, it is tempting to suggest that unopposed oestrogen action within the RU486-treated endometrium is responsible for the high levels of Muc-1 expression demonstrated in this study. However, RU486 has been reported to bind to the ER (Chwalisz *et al.*, 1995), thus resulting in an anti-oestrogenic effect on the endometrium in addition to the antiprogestin effect due to binding of RU486 to PR. RU486 has demonstrated an over 80% efficacy in its ability to reduce oestrogen action when compared to the pure anti-oestrogen ICI 164382 (McDonnell and Goldman, 1994). These data led to the formulation of the hypothesis that the stimulation of Muc-1 expression in the endometrium is not controlled by oestrogen alone.

In support of this hypothesis, in ovariectomised mice, control animals lacking hormonal replacement injections demonstrated the highest level of Muc-1 protein expression in both the luminal and glandular epithelium, when compared to those given oestrogen and progesterone combinations (Braga and Gendler, 1993). In this report Braga and Gendler (1993) suggest that oestrogen is not the regulatory factor in Muc-1 expression, but rather that increased progesterone results in a decrease in Muc-1 expression. When combined, these data suggest that the endometrium expresses Muc-1 at a basal level that is unaltered by oestrogen, and the modulation of expression in the uterus of Muc-1 seems to be via down-regulation by progesterone during early pregnancy. Zhou *et al.* (1998) indicated that ER does not directly regulate the murine Muc-1 gene promoter, suggesting that any control of Muc-1 gene expression mediated by oestrogen is likely to be indirect.

Interestingly, protein analysis results for Muc-1 expression after hormone replacement do not correlate with the RNA data; the highest mRNA levels were observed in oestrogen-treated animals, while highest protein levels associated with the epithelium were observed in the control animals (Braga and Gendler, 1993). This may account for the inconsistency observed in the mRNA analysis with the present study, as despite Muc-1 mRNA levels being higher in the RU486-treated animals at day 5.5 of pregnancy relative to the control pregnant animals; the difference was not as considerable as demonstrated in Muc-1 protein levels by immunofluorescence staining. However, by day 6.5 of pregnancy, Muc-1 mRNA levels were almost 4.5-fold higher in the implantation sites and 2.5-fold higher in the non-implantation sites in the RU486-treated animals relative to the control pregnant animals. If Muc-1 mRNA is regulated by oestrogen, as suggested by Braga and Gendler (1993), then this expression pattern of Muc-1 mRNA in the RU486-treated animals at day 5.5 of pregnancy may be due to a resultant lack of oestrogen stimulation, following RU486 binding to ER as described above. By day 6.5 of pregnancy in the RU486-treated animals, the increase in Muc-1 mRNA expression can be attributed to an increase in oestrogen signalling due to the fairly limited half-life of RU486 and the subsequent binding of oestrogen to its receptor as RU486 is released and metabolised.

This inhibition of the loss of the anti-adhesive mucin, Muc-1, as a result of RU486 administration at day 3.0 of pregnancy translates into a maintenance of the barrier to implantation and attenuation of a portion of the induction process of uterine receptivity necessary to ensure successful blastocyst implantation and subsequent pregnancy. Thus, this adhesiveness of the endometrium as a direct result of RU486 may be the mechanism through which RU486 successfully prevents pregnancy when used as a postcoital contraceptive.

7.3.1.3 The spatiotemporal expression pattern of Calcitonin in the rat uterus during early pregnancy and the effects RU486 has on this expression

While the role of Calcitonin in the regulation of calcium levels in bone and kidney is well established (for a review see Austin and Heath, 1981), in the endometrium, the mechanism of action of Calcitonin during blastocyst implantation remains unclear. The importance of this 32-amino acid peptide hormone has been demonstrated as antisense oligodeoxynucleotides (ODNs) specifically targeted against Calcitonin mRNA reduced the number of implanted blastocysts (Zhu *et al.*, 1998b).

In the current study, a significant decrease in Calcitonin protein levels was demonstrated in the implantation and non-implantation sites as pregnancy progressed from day 4.5 to day 5. This is consistent with previous studies in the rat (Ding *et al.*, 1994) in which Calcitonin immunofluorescence staining was detectable on day 3, became intense at day 4 and then diminished on day 5 of pregnancy,

with weak immunofluorescence staining reported on day 6 of pregnancy (sperm in vaginal smear designated day 1 of pregnancy). This increase in Calcitonin expression around the window of receptivity has also been described in the mouse (Wang *et al.*, 1998), baboon (Kumar *et al.*, 2003) and human endometrium (Kumar *et al.*, 1998). By day 6.5 of pregnancy, Calcitonin levels in both the implantation and non-implantation sites in the current study were increased. This increase in Calcitonin protein expression is inconsistent with previous reports (Ding *et al.*, 1994; Zhu *et al.*, 1998a). Ding *et al.* (1994) suggest that once Calcitonin protein levels decrease at day 6 of pregnancy, this peptide hormone is no longer expressed within the endometrium as they reported a lack of Calcitonin expression at both day 10 and day 15 of pregnancy. A possible explanation for this difference may be that levels were not analysed at day 7 (6.5 of pregnancy), as in the present study and thus, any increase in Calcitonin was overlooked by Ding *et al.* (1994) and Zhu *et al.* (1998a). It is possible that subsequent to the increase in Calcitonin at day 6.5 of pregnancy, Calcitonin levels decrease again, so that by day 10 and 15 of pregnancy no Calcitonin protein is expressed within the pregnant rat uterus. Expression of Calcitonin mRNA was, however, decreased in both the implantation and non-implantation sites with the progression of pregnancy from day 5.5 to day 6.5, this in contrast to the immunolocalisation pattern described in the present research. Ding *et al.* (1994) reported no significant immunofluorescence staining in the stroma or the myometrium during early pregnancy, consistent with the low levels of Calcitonin in the stromal compartments, as reported in the present study. In addition, using *in situ* hybridisation, Zhu *et al.* (1998a) demonstrated a lack of Calcitonin mRNA expression in the luminal epithelium, the stromal compartments and the myometrium. Altogether, these data suggest that the decrease in Calcitonin mRNA expression described with the progression of pregnancy from day 5.5 to day 6.5 may be as a result of dilution effects due to the use of whole tissue homogenates in the RT-qPCR portion of this study.

In the present research, immunolocalisation of Calcitonin was demonstrated in both the luminal and glandular epithelium with levels higher in the luminal epithelium in both the implantation and non-implantation sites at all three days of pregnancy. These results are inconsistent with previous reports on Calcitonin localisation during early pregnancy, which state that Calcitonin expression is restricted to the glandular epithelium during early pregnancy (Ding *et al.*, 1994; Zhu *et al.*, 1998a). Using *in situ* hybridisation, Zhu *et al.* (1998a) demonstrated a restricted localisation of Calcitonin gene expression to the glandular epithelium with no detection observed in the luminal epithelium, the stroma or the myometrium, suggesting that these cells are the actual site of Calcitonin synthesis (Zhu *et al.*, 1998a). Zhu *et al.* (1998a) described a significant amount of Calcitonin in the luminal secretions of the pregnant rat between days 4-5 of pregnancy. Thus, it is possible that while Calcitonin is synthesised in the glandular epithelium (Ding *et al.*, 1994; Zhu *et al.*, 1998a), it acts on the luminal epithelium in a paracrine manner and is released into the lumen around the time of blastocyst implantation. This hypothesis can provide an explanation for the high levels of Calcitonin protein immunolocalisation

observed within the luminal epithelial cells in the current study. In 1998, Zhu, Bagchi and Bagchi hypothesised that the Calcitonin secreted by the glandular cells may act on the luminal epithelium to regulate embryo attachment by inducing junction disassembly, redistribution of the junctional proteins and opening of the tight junction barrier in the uterine epithelial cells and thus promote invasion by the trophoblast cells of the implanting blastocyst (Zhu *et al.*, 1998b). In support of this hypothesis, Li *et al.* (2002) demonstrated a decrease in the calcium-dependent cell adhesion glycoprotein, E-cadherin. In addition, they described a decrease in E-cadherin expression in the epithelial cells of pregnant rats as a result of exogenous Calcitonin and proposed that the adherens junctions are reorganised as a result of this down-regulation of E-cadherin by Calcitonin, thus playing a crucial role in blastocyst implantation (Li *et al.*, 2002).

In addition to the possible role for Calcitonin in trophoblast invasion, Ding *et al.* (1994) postulated that, since one of the major roles of Calcitonin is to modulate calcium levels within target cells, this secretion of Calcitonin by the glands may act in a paracrine manner to control the level of calcium within the endometrium, thus protecting the implanting blastocyst from the effects of hypercalcaemia. In support of this hypothesis, Wang *et al.* (1998) described Calcitonin receptor, CR-1a, mRNA expression in pre-implantation embryos that increased when uterine expression of Calcitonin commences, suggesting a role for Calcitonin in peri-implantation embryo development by increasing intracellular Ca^{2+} concentrations, which in turn accelerates blastocyst differentiation.

Ding *et al.* (1994) also suggested that an additional role for Calcitonin in the endometrium during early pregnancy may be to prevent accidental triggering of myocontraction, as the release of calcium elevates the plasma ion concentration, resulting in smooth muscle contraction (Ding *et al.*, 1994). Another possible role for Calcitonin within the endometrium during early pregnancy is as a factor controlling early embryonic differentiation. LeBlanc and Brick (1981) reported a role for Calcitonin in cell aggregation during early embryogenesis and that, due to its hypocalcaemic properties, this peptide hormone may influence cell adhesion. This led Ding *et al.* (1994) to speculate that Calcitonin may have a role in the early stages of development, in addition to its regulatory role in calcium metabolism.

Calcitonin has previously been demonstrated to be under the control of the ovarian hormone progesterone as progesterone increased the expression of Calcitonin 20-fold in the ovariectomised rat endometrium and also, Calcitonin temporal expression in the pseudopregnant rat followed a similar pattern to that in the normal pregnant rat (Ding *et al.*, 1994; Zhu *et al.*, 1998a). In the ER knockout (ERKO) uterus, PR was able to induce Calcitonin expression, indicating that the basal level of PR is able to regulate the expression of the progesterone-dependent genes, even despite a lack of PR mRNA and protein induction by oestrogen (Curtis *et al.*, 1999). Thus, the partial progesterone blocker,

RU486, could have an effect on Calcitonin expression resulting in a loss of the critical functions of Calcitonin as described above. This could be one of the mechanisms through which RU486 exacts its effect on the endometrium in inhibiting blastocyst implantation and subsequent pregnancy.

In the present study, RU486 significantly decreased Calcitonin levels at day 4.5 of pregnancy. These results are consistent with a previous study in which RU486 was reported to abolish Calcitonin protein expression within 24 hours (Ding *et al.*, 1994), as well as Calcitonin mRNA levels in day 4 pregnant uteri (Zhu *et al.*, 1998a). In pseudopregnant rats, this decrease in Calcitonin protein expression was also observed as a direct result of RU486 administration within 16 h of treatment (Zhu *et al.*, 1998a). Combined, these results confirm the role of progesterone in Calcitonin regulation during early pregnancy. In the RU486-treated animals, Calcitonin expression was not completely abolished as described by Ding *et al.* (1994) and Zhu *et al.* (1998a). A possible explanation is that by day 4.5 of pregnancy in the current study, RU486 had been acting on the endometrium for 36 hours and thus, due to its 4 h half-life, progesterone signalling may be returning and thus be able to induce an increase in Calcitonin expression. At day 5.5 of pregnancy, Calcitonin protein levels in the control pregnant animals decreased significantly; however, levels in the RU486-treated animals began to increase or remained fairly similar in the different endometrial compartments, resulting in higher levels of Calcitonin in all the endometrial compartments of the implantation and non-implantation sites, with the exception of the luminal epithelium of the RU486-treated animals. Calcitonin mRNA levels, however, were not significantly different between the control pregnant and RU486-treated animals at day 5.5 of pregnancy. Again, this inconsistency can be attributed to dilution of expression levels as a consequence of the use of whole tissue homogenates. As pregnancy progressed from day 5.5 to day 6.5, Calcitonin mRNA expression increased in the RU486-treated animals, most likely as a result of the half-life of RU486, as described above.

It has been proposed that the high levels of Calcitonin expression in the rat endometrium prior to implantation is necessary for the priming of the endometrium for blastocyst implantation and possibly plays a role in early development of the embryo (Ding *et al.*, 1994; Zhu *et al.*, 1998b). Zhu *et al.* (1998b) described a dramatic reduction in the number of implanted blastocysts as a result of the administration of an antisense ODN targeted against Calcitonin. Combined with the decrease in Calcitonin expression as a direct consequence of RU486 administration, it can be postulated that this decrease in Calcitonin expression is one of the mechanisms through which RU486 exacts its anti-implantation effect on the endometrium, thus making it a successful emergency contraceptive.

CHAPTER 8

GENERAL DISCUSSION

8.1 The Use of RU486 as an Emergency Contraceptive

The controversial abortion drug, RU486, has recently been identified as a more successful emergency contraceptive regime than those currently in use, with better efficiency, longer action and fewer side-effects (Glasier *et al.*, 1992; Webb *et al.*, 1992; World health organisation task force on postovulatory methods of fertility regulation, 1998; World health organisation task force on postovulatory methods of fertility regulation, 1999; Jin *et al.*, 2005). Despite its proven efficiency as a highly effective emergency contraceptive, RU486 is only currently available for this use in a few countries, due to its status as an abortion drug (Chabbert-Buffet *et al.*, 2008).

While RU486 was previously thought to merely function as a potent progesterone (PR) and glucocorticoid receptor (GR) antagonist (Baulieu, 1991; Sarkar, 2002), recent studies have, nevertheless, indicated a weak binding affinity for the ER (Jeng *et al.*, 1993; Chwalisz *et al.*, 1995; Dibbs *et al.*, 1995). In the human, when compared to the pure anti-oestrogen ICI 164382, RU486 was able to block oestrogen action with over 80% efficacy, by effectively blocking PR-A-dependent regulation of ER action (McDonnell and Goldman, 1994).

During early pregnancy, the specific priming of the endometrium in preparation for the implantation of a viable blastocyst is under the control of the ovarian hormones, oestrogen and progesterone (Psychoyos, 1970;1973;1986). These hormones act on the different endometrial compartments to initiate a vital series of events, to establish the 'window of receptivity', a narrow range of time during which a blastocyst is able to successfully implant (Psychoyos, 1986). Although the main hormone acting on the endometrium during the early stages of pregnancy is progesterone (Psychoyos, 1970; Adams *et al.*, 2004; Murphy, 2004), oestrogen priming of the endometrium is necessary for progesterone action as oestrogen increases the expression of PRs in most target cells (Milgrom *et al.*, 1973; Tibbetts *et al.*, 1998; Tan *et al.*, 1999).

These data, combined with the ability of RU486 to bind with high affinity to PR and with a weaker affinity to ER, suggests that the ability of this drug to inhibit blastocyst implantation and subsequent pregnancy is through the disruption of the actions of the ovarian hormones. In this regards, despite the numerous studies on RU486 in the past, the exact effects RU486 has on the endometrium as a consequence of its anti-progestin and anti-oestrogen actions during early pregnancy has yet to be elucidated. The current study thus investigated the effects of RU486 at a cellular and molecular level,

on the priming of the endometrium leading up to the window of implantation and the period inclusive of early pregnancy.

8.2 The Effects of RU486 on the Cellular Responses of Early Pregnancy

The priming of the endometrium by the ovarian hormone progesterone is evident in the plasma membrane transformation of early pregnancy. This early pregnancy process is necessary to ensure endometrial receptivity to the implanting blastocyst (for a review see Murphy, 2004; Wang and Dey, 2006). In the current study, the administration of RU486 effectively inhibited or reduced the transformation of the endometrial cells into a receptive state, suggesting that when used as a postcoital contraceptive, this drug maintains the endometrium in an unreceptive state, thus preventing blastocyst implantation and subsequent pregnancy.

One of the most striking observations in the current study is the marked increase in apoptotic activity observed in the epithelial cells of the RU486-treated animals. This RU486-induced increase in apoptosis has previously been reported in rabbits (Rotello *et al.*, 1992) and rhesus monkeys (Sengupta *et al.*, 2003), and is attributed to the loss of progesterone signalling as a consequence of RU486 binding to PR, as progesterone is known to suppress endometrial apoptosis (Rotello *et al.*, 1992).

8.3 The Effects of RU486 on the Progesterone Receptor

During early pregnancy, PR levels are increased markedly in the lead up to blastocyst implantation, possibly to ensure proper priming of the endometrium by progesterone and the subsequent establishment of the window of receptivity. Treatment with RU486 at day 3.0 of pregnancy resulted in a significant decrease in PR levels at all three days of pregnancy. The decrease in PR levels can be attributed to the anti-oestrogenic effect of RU486 on the endometrium, as oestrogen is known to increase PR levels, whereas progesterone decreases PR levels (Milgrom *et al.*, 1973; Tibbetts *et al.*, 1998; Tan *et al.*, 1999). RU486 was not able to completely block the expression of PR during early pregnancy, suggesting that the anti-oestrogen effect of RU486 does not entirely attenuate oestrogen action. This could also be as a direct result of the limited, 4h, half-life of RU486 in the rat endometrium (Mahajan and London, 1997; Sitruk-Ware and Spitz, 2003), as once RU486 begins to metabolise, both progesterone and oestrogen will regain access to their respective receptors and thus exact their effects on the endometrium. The metabolism of RU486 and subsequent binding of the ovarian hormones to their receptors may account for the lack of complete loss of PR expression, described in the current study, from day 4.5 of pregnancy onwards, 36 hours after RU486 administration, as well as the increase in PR levels with the progression of pregnancy in the RU486-treated animals.

This decrease in PR expression as a consequence of RU486 administration is similar to the decrease observed in ovariectomised animals without hormonal replacement (Parczyk *et al.*, 1997; Tibbetts *et al.*, 1998). When combined, these data suggest that RU486 results in a more ahormonally stimulated PR expression pattern when administered during early pregnancy.

8.4 Bax/Bcl-2 is Not the Pathway Regulating the RU486-Induced Increase in Apoptosis Observed in the Rat Endometrium

Ultrastructural analysis in the present study, indicated a marked increase in epithelial apoptosis following treatment with RU486, in agreement with previous reports in the rabbit (Rotello *et al.*, 1992) and the rhesus monkey (Sengupta *et al.*, 2003). As the apoptosis pathway-related molecules, Bax and Bcl-2, have previously been reported to be important during the apoptosis that occurs in the endometrium during the menstrual and oestrous cycles as well as that which occurs during early pregnancy (Akcali *et al.*, 1996; Critchley *et al.*, 1999; Dai *et al.*, 2000; Akcali *et al.*, 2003; Mendoza-Rodríguez *et al.*, 2003), this led to the investigation of the possibility of the involvement of the Bax and Bcl-2 pathway in the increase in apoptosis described in the endometrial epithelia as a result of RU486 administration.

The present study indicated an overall anti-apoptotic Bax/Bcl-2 ratio in the RU486-treated animals, suggesting that this pathway is not responsible for the RU486-induced increase in apoptosis. Previous studies have indicated that the Fas/FasL pathway is also not the pathway responsible for this increase in apoptosis as a consequence of RU486 administration.

It is suggested here, that further studies on the splice variants of the Bcl-2 family protein, Bcl-X, would be beneficial to ascertain whether this pathway is responsible for the described increase in apoptosis, as progesterone has been shown to decrease apoptosis by increasing the Bcl-X_L/Bcl-X_S ratio in an endometrial cell line (Pecci *et al.*, 1997).

8.5 The Effects of RU486 on Selected Angiogenesis Pathway-related Growth Factors

During early pregnancy, angiogenesis, the formation of new blood vessels arising from pre-existing ones (Folkman and Shing, 1992), is necessary to ensure establishment of the vascular network and thus the maternal contribution to the future placenta (Shweiki *et al.*, 1993), vital for nourishment to ensure successful blastocyst implantation and development. The angiogenesis events of early pregnancy are regulated by different angiogenic factors; including, VEGF, bFGF and PDGF (Ferriani *et al.*, 1993; Smith, 1995; Torry and Torry, 1997; Rogers and Gargett, 1998; Weston and Rogers, 2000).

VEGF expression has been reported to coincide with increased vascular permeability indicative of the first vascular event of early pregnancy, suggesting a role for this growth factor during this process (Ma *et al.*, 2001). RU486 significantly decreased VEGF expression in the endometrium, in addition to inhibiting the increase in vascular permeability crucial for the establishment of early pregnancy, as evident by the Pontamine Sky blue reaction (Scholtz *et al.*, 2008).

The second vascular event of implantation, increased endothelial cell proliferation and migration, occurs around the time of blastocyst implantation (Goodger and Rogers, 1993). This increase in endothelial cell proliferation is suggested to be regulated by the ovarian hormone progesterone, as a significant increase in endothelial cell proliferation prior to implantation coincides with increasing plasma progesterone concentrations (Goodger and Rogers, 1993). It thus follows that the antiprogestin activity of RU486 would block this increase in vasculature necessary for blastocyst survival, resulting in early pregnancy failure.

The knowledge that angiogenesis is regulated the angiogenic factors; including, VEGF, bFGF and PDGF, suggests that RU486 may inhibit angiogenesis by blocking the expression of one or more of these factors. In the present study, RU486 was demonstrated to inhibit the increased VEGF and bFGF expression levels associated with day 5.5 of pregnancy, the day of blastocyst implantation. The simultaneous increase in VEGF and bFGF expression levels in both the implantation and non-implantation sites coincides with the increase in angiogenesis of early pregnancy, suggesting a synergistic role for these growth factors in the initiation of the vascular events of early pregnancy. Both *in vitro* and *in vivo* studies have indicated that bFGF is likely to play an important role in triggering VEGF-induced angiogenesis and/or up-regulating VEGF-induced angiogenesis once it is initiated (Pepper *et al.*, 1992; Goto *et al.*, 1993; Asahara *et al.*, 1995; Mandriota and Pepper, 1997).

PDGF levels increased significantly in the implantation sites of the control pregnant animals at day 5.5 of pregnancy, suggesting possible regulation of this growth factor by the implanting blastocyst. In the present study, the most significant effect of RU486 on PDGF expression was an inhibition of the marked increase in PDGF expression in the implantation sites at the time of blastocyst implantation. The spatiotemporal expression pattern of PDGF, as described in the present study, led to the formulation of the hypothesis that the increase in endothelial cell proliferation observed specifically in the implantation sites around the time of blastocyst implantation (Goodger and Rogers, 1993) is regulated by the increase in PDGF expression demonstrated here, within the implantation sites at the same stage of pregnancy.

When combined, these results suggest that VEGF and bFGF play a vital role in the initiation of angiogenesis within the endometrium during early pregnancy, whereas PDGF has a regulatory role in

the initiation of the increase in endothelial cell proliferation observed specifically in the implantation sites around the time of blastocyst implantation. The inhibition of the angiogenic pathway-related growth factors and subsequent vascular events may account for the inability of the RU486-treated endometrium to sustain pregnancy, thus providing an additional mechanism through which RU486 successfully ensures early pregnancy failure.

8.6 The Effects of RU486 on Selected Endometrial Biomarkers of Receptivity during Early Pregnancy

One of the major contributing factors to unsuccessful implantation, in both assisted reproduction and normal pregnancy, is failure of the blastocyst to implant during the narrow range of time, the 'window of receptivity' (Cavagna and Mantese, 2003). The assessment of possible implantation biomarkers of uterine receptivity as a means to improve implantation rates in both natural and assisted reproduction as well as to establish efficient contraceptives is an important area of research (Dey *et al.*, 2004; Achache and Revel, 2006). A few endometrial biomarkers have previously been described; including, LIF, Muc-1 and Calcitonin. As these three endometrial biomarkers are known to be vital to the establishment of uterine receptivity and subsequent blastocyst implantation (Stewart *et al.*, 1992; Aplin, 1997; Zhu *et al.*, 1998b), the effect of RU486 on these biomarkers around the time of blastocyst implantation was established.

RU486 was noted here to significantly lower the normally high levels of both LIF and Calcitonin in the endometrial compartments during early pregnancy. The exact function of these endometrial biomarkers in relation to the implantation process is yet to be established, despite the evidence indicating their importance during early pregnancy (Stewart *et al.*, 1992; Zhu *et al.*, 1998b). It is thus not possible to comment on the exact effect this RU486 derived decrease in LIF and Calcitonin expression may have on the implantation process. However, LIF null mice displayed viable blastocysts that were unable to implant or develop (Stewart *et al.*, 1992), suggesting that a decrease in the normally high levels of LIF in early pregnancy may result in the inability of the circulating blastocyst to implant in the uterine wall. Moreover, antisense oligonucleotides targeted against Calcitonin led to a marked decrease in the number of implantation sites (Zhu *et al.*, 1998b).

Alternatively, the decrease in Muc-1 expression around the time of blastocyst implantation in normal pregnancy was inhibited by RU486 administration. The anti-adhesive properties of Muc-1 is thought to establish its function as a barrier to implantation (Hey *et al.*, 1994; Isaacs and Murphy, 2003). As a result, in order for the blastocyst to be able to come into close apposition with the maternal tissue and establish cell-cell adhesions in preparation for implantation into the uterine wall, this Muc-1 barrier must be removed (Aplin *et al.*, 1994). The inhibition of this loss of the Muc-1 barrier during early pregnancy, due to RU486 administration, may account for the lack of blastocyst implantation in the

RU486-treated animals, suggesting a possible reason for the efficiency of RU486 as an emergency/postcoital contraceptive.

These data combined suggest that this inhibition of implantation and subsequent pregnancy may be the mechanism/one of the mechanisms through which RU486 exacts its anti-pregnancy effect within the endometrium.

8.7 The Hormonally Under-stimulated Endometrium of RU486-Treated Animals

Throughout the current study, the cellular and molecular changes that occur within the rat endometrium as a result of RU486 administration are reflected in the ovariectomy model lacking hormonal replacement. These results led to the formulation of the hypothesis that RU486 results in a more hormonally under-stimulated endometrium rather than an endometrium with unopposed oestrogen action (Scholtz *et al.*, 2008). In support of this, RU486 has been reported to bind to the ER, albeit weakly (Jeng *et al.*, 1993; Chwalisz *et al.*, 1995; Dibbs *et al.*, 1995), and when compared to the pure anti-oestrogen ICI 164382, presents an over 80% efficacy in its ability to block oestrogen action (McDonnell and Goldman, 1994).

The success of RU486 as a postcoital contraceptive can be explained by any of the above mentioned changes in pathways and molecules. The results from the present study suggest that RU486 acts via a variety of different mechanisms to exact its anti-implantation and anti-pregnancy effects. This is possibly as a result of the number of different pathways and molecules affected by this emergency contraceptive regime that accounts for its high success rate and efficiency.